Faculty of Science.

Development of Laterally Extended Two Dimensional Polymers for Applications in Solar Cells

Abdulraheem Safar Ali Almalki

November 2015

A thesis submitted to the University of Sheffield in partial fulfilment of the requirements for the degree of Doctor of Philosophy

Department Of Chemistry

Declaration

This thesis is submitted for the degree of doctorate of philosophy (PhD) at the University of Sheffield, having been submitted for no other degree. It records the research carried out at the University of Sheffield from October 2011 to July 2015. It is entirely my original work, unless where referenced.

Signed:…………………………………………………….

Date:…………………………………………………………

Abstract

The aim of this project is to synthesise laterally extended conjugated polymers based on quinoxaline and pyrene derivatives that can be used in solar cell applications. These materials should show high charge mobility, efficiency, stability and high flexibility. Unlike organic materials, inorganic compounds have a high cost of manufacturing and are difficult to process. This led scientists to develop organic semiconducting materials, which are easier to process and cheaper than inorganic compounds. In 2000, Alan J. Heeger, Alan G. MacDiarmid and Hideki Shirakawa received the Nobel Prize for the discovery and development of conductive polymers. The field of organic photovoltaics has developed rapidly recently. Organic based solar cells have some drawbacks, such as phase separation between the donor and the acceptor in the active layer, which can lower the efficiency of these devices. One promising solution to this problem is to synthesise donor–acceptor materials and control their morphology at the molecular level.

This thesis describes the preparation of novel conjugated polymers that possess 6,7,15,16-tetrakis(2-hexyldecyloxy)-2,11-di(thiophen-2-yl)quinoxalino[2',3':9,10]phenanthro[4,5-abc]phenazine as laterally extended repeat unit which was polymerised with various donors such as carbazole units to produce **P1**, fluorene units to produce **P2** and thiophene to produce **P3**. Incorporation of the 6,7,15,16-tetra(2-hexyldecyloxy)-quinoxalino[2',3':9,10]phenanthro[4,5-abc]phenazine repeat unit in polymers **P1**-**P3** did not show the expected donor-acceptor intramolecular charge transfer along the polymer backbone of these polymers as all polymers displayed wide energy band gaps. The hexyldecyloxy-substituents on the [2',3':9,10]phenanthro[4,5-abc]phenazine repeat units were therefore replaced with the less electron donating 3-pentyl-undecyl substituents in order to gauge the effects of such substitution on the electronic properties of the resulting materials. Polymers **P4**-**P6** which incorporated 6,7,15,16-tetra(3-pentyl-undecyl)-quinoxalino [2',3':9,10]phenanthro [4,5-abc]phenazine repeat units and respectively carbazole units, fluorene units and thiophene units were prepared in order to investigate their electronic properties. These polymers had indeed lower energy band gaps than corresponding polymers **P1**-**P3**, however, their absorption of light in the visible spectrum was not extensive enough for the use of these polymers in organic-based solar cells. Investigation on the use of these laterally

extended 6,7,15,16-tetra(substituted)-quinoxalino[2',3':9,10]phenanthro[4,5-abc]phenazine units as electron donors rather than electron acceptors were investigated in this work. Polymers incorporating these units flanked by thienyl units together with a series of alternating benzothiadiazole acceptors units were prepared. These series of polymers **P7-P12** have narrower energy band gaps (wider absorption in the visible spectrum) than those of **P1**-**P6**. The nature of substituents on the 6,7,15,16-tetra(substituted)-quinoxalino[2',3':9,10]phenanthro[4,5-abc]phenazine repeat units in these polymers affects the electronic properties of these materials. The structural, optical and electronic properties of these polymers are discussed in this work.

Acknowledgements

First of all I would like to thank my parents, my wife, brothers and my children for encouraging and supporting me. I am also greatly indebted to my supervisor Dr. Ahmed Iraqi for his continuous support, encouragement, and the help in course of writing this thesis. I would like to acknowledge all members of our group for a most productive collaboration and for helpful suggestions regarding the work. Also, I particularly would like to thank Robert Hanson for his kindness, patient and his great contribution of training me on GPC.

I would like to express my thanks and appreciation to the Ministry of Higher Education for sponsoring my study and funding this project.

Table of Figure

Glossary of abbreviations and terms

A

Acetone-d6	Deuterated acetone
Alq$_3$	tris(8-hydroxyquinolinato)aluminum

B

bs	Broad singlet (NMR)
br	Broad Multplet (NMR)

C

CB	Conduction band
CV	Cyclic voltammetry

D

d	Doublet (NMR)
dd	Doublet doublet (NMR)
DFT	Density functional theory
DMF	N,N-dimethylformamide
DMSO	Dimethyl sulfoxide
DCM	Dichloromethane
DP	Degree of polymerisation
DSC	Differential Scanning Calorimetry

E

E	Energy /J or /eV
E$_g$	Energy gap
EL	Electroluminescence
Ep$_a$	Potential of peak anodic current (from CV)
Ep$_c$	Potential of peak cathodic current (from CV)
EtOH	Ethanol
EtOAc	Ethyl Acetate
Et$_2$O	Diethyl ether
eV	Electron volt

F

Fc	Ferrocene
FT-IR	Fourier Transform Infra-Red spectroscopy
FET	Field-Effect Transistor

G

GPC	Gel Permeation Chromatography

H

HOMO	Highest Occupied Molecular Orbital
HPLC	High Pressure Liquid Chromatography

I

IR	Infra-Red spectroscopy
ITO	Indium Tin Oxide
ITN	Isothianaphthene

K

L

LED	Light-Emitting Diode
LUMO	Lowest Unoccupied Molecular Orbital
λ_{max}	Wavelength of maximum absorption

M

m	Multiplet (NMR)
Mn	Number average molecular weight
Mw	Weight average molecular weight
M.p.	Melting point
N	
NMR	Nuclear Magnetic Resonance
NBS	N-Bromosuccinimide
O	
OLED	Organic light emitting diode
OPV	Organic photovoltaic
P	
PCBM	6,6'-Phenyl-C61-butyric acid methyl ester
PCE	Power conversion efficiency
PD	Polydispersity Index
P(o-tol)$_3$	Tri-ortho-tolylphosphine
PPh$_3$	Triphenylphosphine
Pd$_2$(dba)$_3$	Tris(dibenzylidene acetone) palladium (0)
PPV	Poly(*para*-phenylene vinylene)
PPP	Polyparaphenylene
Pd(dppf)Cl$_2$	[1,1'-Bis(diphenylphosphino)ferrocene] dichloropalladium(II)
PSC	Polymer solar cell
P3HT	Poly(3-hexylthiophene)
S	
s	Singlet (NMR)
T	
Tg	Polymer glass-transition temperature
TGA	Thermogravimetric Analysis
THF	Tetrahydrofuran
TLC	Thin Layer Chromatography
t	Triplet (NMR)
U	
UV/Vis	Ultraviolet/visible absorption spectroscopy
V	
V	Volt
VB	Valence band

1 Chapter 1: Introduction

1.1 Conjugated polymers

1.1.1 Overview of conjugated polymers

In the mid-1970s, Heeger, MacDiarmid and Shirakawa discovered the electrical conductivity of conjugated polymers.[1] Since then, extensive works have been published on the topic.[2] However, the efficiency of this conductivity was low. The first polymers discovered to have such a property were polyacetylene and sulphur nitride (**Figure 1-1**). This property came from delocalisation of the π bonds along the polymer chain when, for example, polyacetylene is oxidatively doped.[2] This doping with AsF_5 increased the conductivity of polyacetylene by as much as 300 times.[3-4] This process allows for the dissociation of solitons into free carriers.[5]

Polyacetylene   Poly(sulphur nitride)
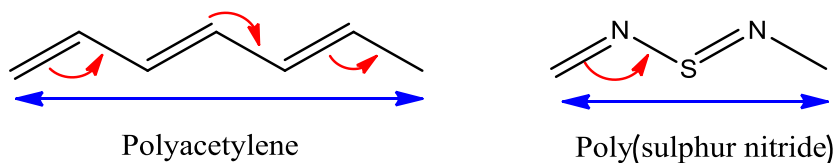
Figure 1-1: Conjugated polymers

This discovery has motivated scientists to do more investigations on these materials, especially as the demand for electronic devices has been growing considerably in the last 20 years. Studying the structure, mechanism and properties of these materials is greatly important in terms of conductivity and also to have a better understanding of the urgent need for a sustainable energy solution.

1.1.2 Electronic structure of conjugated polymers

A conjugated structure in chemical compounds means delocalised electrons in chemical materials with alternating single and double bonds. The electronic properties of semiconducting materials originate from the π (double) bonds.[1,6] Poly-acetylene is the first example of a semiconducting polymer (**Figure 1-2**). The delocalisation of π electrons along

the polymer chains fills the π bands which are known as the highest occupied molecular orbital (HOMO), while the empty π^* band is called the lowest unoccupied molecular orbital (LUMO).[7] Therefore, the π electrons are excited from HOMO to LUMO level and the difference between these two levels is called a 'band gap' which dominates the properties of the semiconducting polymers.[8-9]

$$\longleftarrow \text{ Charge moves along the chain } \longrightarrow$$
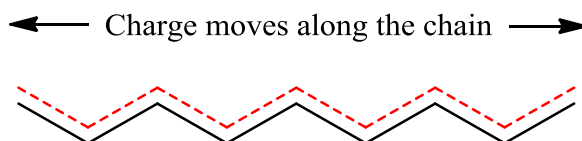
Figure 1-2: Fully delocalsed π electrons along the polymer chain

Doping of polymers is required as conjugated polymers are not conductive materials in their neutral state.[10-11] The doping can be carried out by either an oxidation or reduction process which allows a radical anion or cation to be generated and form a polaron.[12-13] A bipolaron can also be generated along the polymer chain as a result of further oxidation.[14] This allows charges to move along the polymer chains.[15]

1.2 Synthetic strategies of conjugated polymers

The design of conjugated polymer materials relies on alternating single and double bonds (unsaturated bonds), particularly in aromatic molecules (**Figure 1-3**). In order to synthesise these materials, scholars often use chemical[16] or electrochemical[17] methods. The electrochemical method can be described as an electrical potential that is applied to a monomer solution to generate a radical ion which is used to initiate the polymerisation.[18] On the other hand, the chemical route is a well established method which broadly aligns with the synthetic procedures of organic reactions. In addition, transition-metal-catalysed reactions are powerful tools especially for carbon - carbon bonds formations (**Figure 1-4**).[19]

double bonds
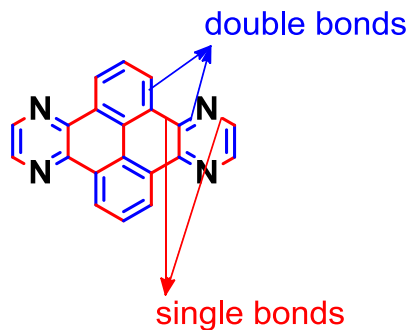
single bonds

Figure 1-3: Single and double bonds in aromatic molecules

R-R'

M(0)

R-X

Catalytic cycle

Reductive
elimination

Oxidative addition

^RM
R'

$^R M_X$

M'-X

R-'M'
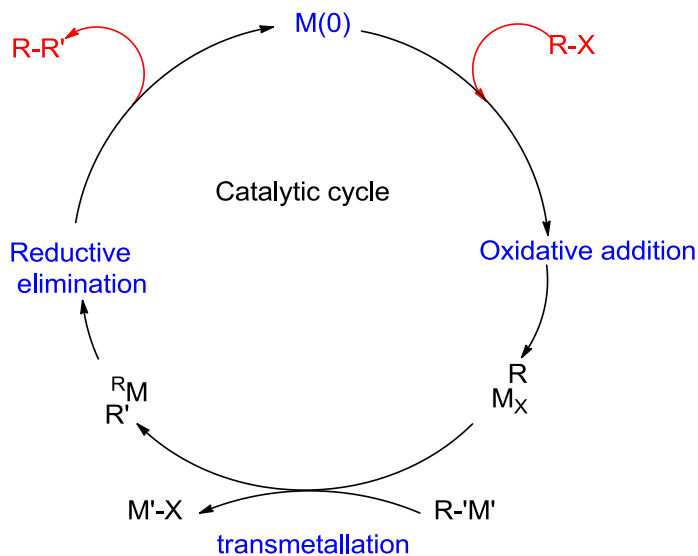
transmetallation

Figure 1-4 Producing conjugated polymers by transition-metal-catalysed reactions

As can be seen in **Figure 1-4**, following oxidative addition and a transmetallation step followed by a reductive elimination, result in carbon – carbon bond formation. There are many routes available to synthesise conjugated polymers. These strategies will be discussed below.

1.2.1 Electrochemical synthesis

The first polymer produced by this method was polypyrrole, which is stable, flexible and has a high conductivity. Therefore, this method has been commonly used to prepare a wide range of conductive materials. An example of electrochemical synthesis is anodic polymerisation, which is a widely used technique. This involves an electrical potential which is applied to a solution of monomers leading to an oxidative reaction. The polymerisation occurs on the electrode (anode) and polymers coating the anode (**Figure 1-5**).[20]
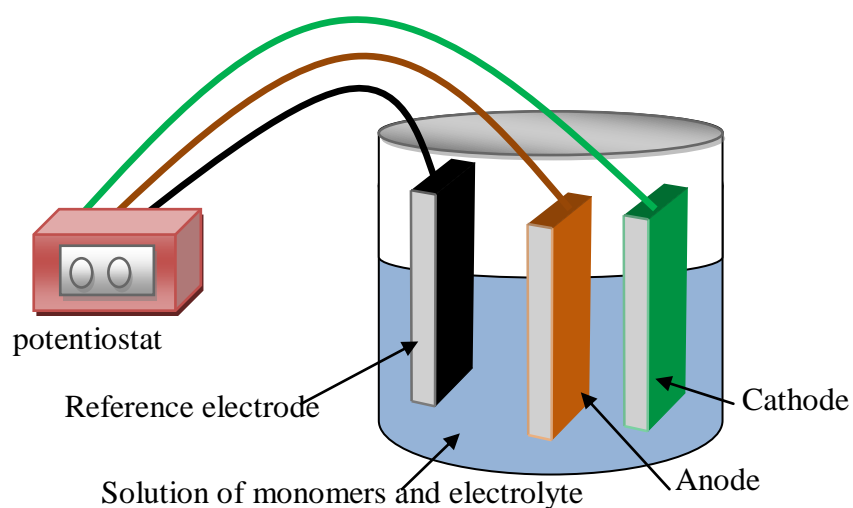
Figure 1-5: Polymerisation by electrochemical route

1.2.2 Kumada cross coupling

The Kumada coupling is a useful technique to form carbon-carbon bonds via the reaction of an organic halide with Grignard reagent.[21] Nickel or Palladium are usually utilised as transition metal catalysts in this reaction which was developed in 1972. The direct coupling of Grignard reagents is the advantage of this reaction which leads to a significant reduction in the number of reaction steps (**Figure 1-6**).
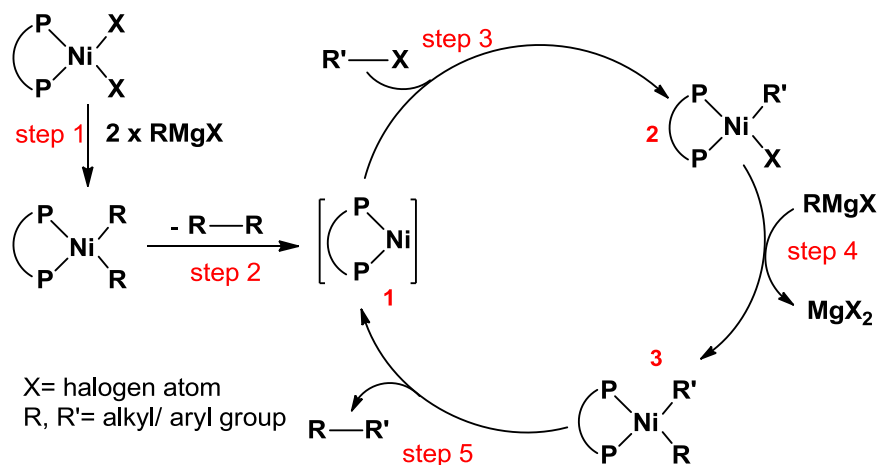
Figure 1-6: Kumada cross-coupling route

1.2.3 Suzuki coupling

Suzuki coupling involves palladium catalysed cross-coupling between aryl boronic ester or acid derivatives with aryl halides in the presence of mineral bases.[22] As there has been a lot of work devoted to improving the catalyst systems, many types of functional groups can be tolerated in this reaction;[23] for instance, alkyls, alkynyls and alkenyls (**Figure 1-7**).

$$Ar-X + Ar'-B(OH)_2 \longrightarrow Ar-Ar' + X-B(OH)_2$$

NaOR = base as Na_2CO_3
Ar, Ar' = aryl group
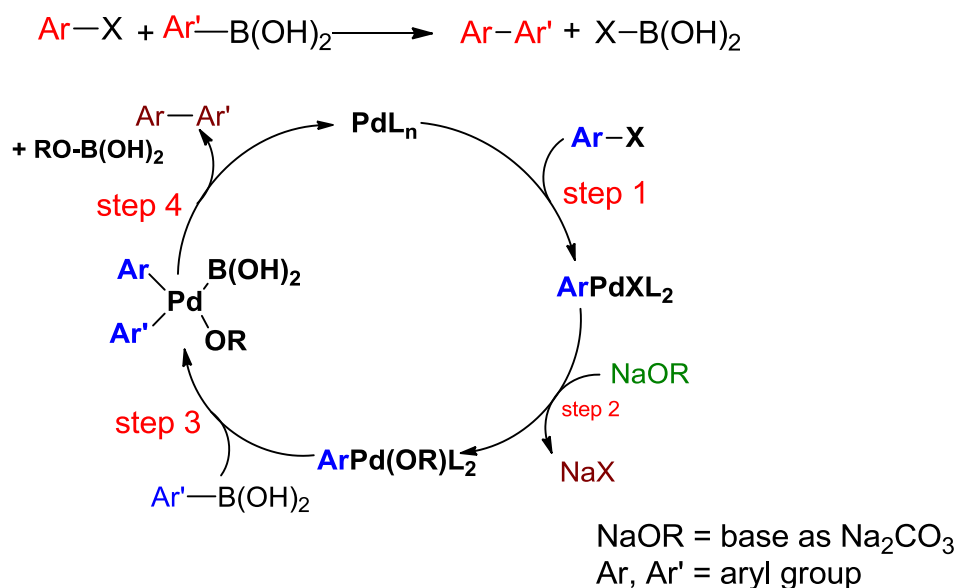
Figure 1-7 Suzuki cross-coupling route

1.2.4 Stille type cross coupling

In these reactions, functional monomers comprising halo- and/or organo-tin- functionalities are used, with few limitations on the R-groups.[24,25] The disadvantages of this reaction include low polarity of the tin molecules utilised which are less soluble in water. In addition, the toxicity involved with Sn chemistry is a major drawback. As organo-tin derivatives are used instead of Grignard-derivatives, the Stille cross-coupling reactions are similar to Kumada type reactions (**Figure 1-8**).
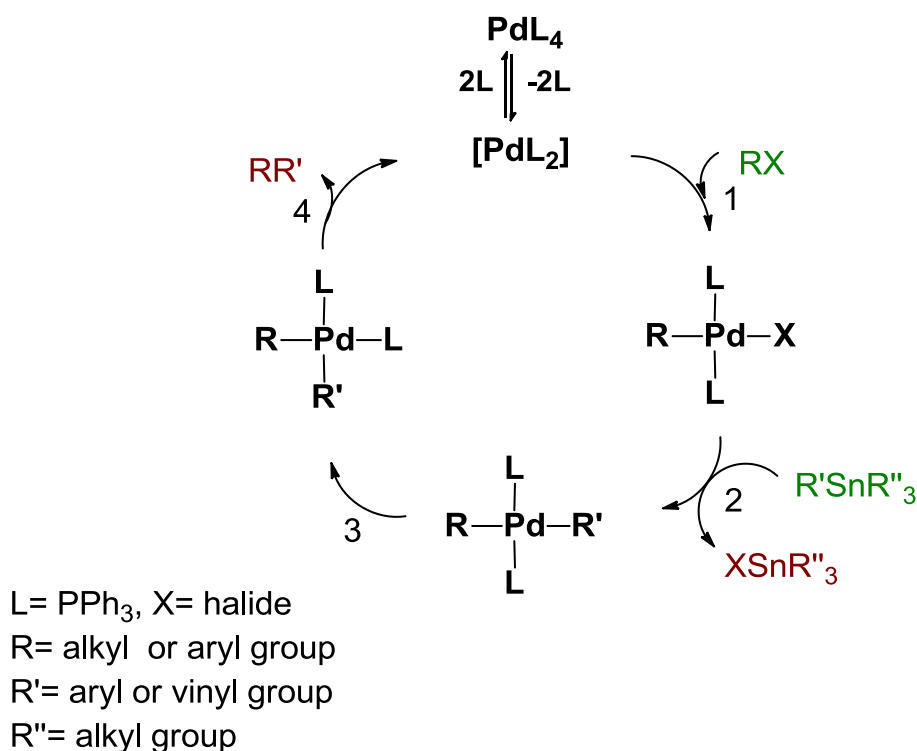
Figure 1-8: Stille type cross-coupling

Before studying the physical field of conjugated polymers, some fundamental aspects need to be clarified, namely, the basic physical properties of conjugated polymers. These include the excitation states, which appear after electrons are excited by light and move to a high energy level.

1.3 Fundamental of excitation in conjugated polymers

1.3.1 Polaron

A polaron is an electron (radical anion) or hole (radical cation) or electronic excitation, which is gathered to a lattice distortion.[26] This definition is applied particularly to non-degenerate ground state polymers such as polyacetylene and PPV.[27-28] These polymers have conjugated systems in which more charges can be produced by doping from electrodes or photoexcitation. The HOMO-LUMO gap is a result of Lattice distortion which causes localised electronic states. This phenomenon is known as polaron states (**Figure 1-9**).
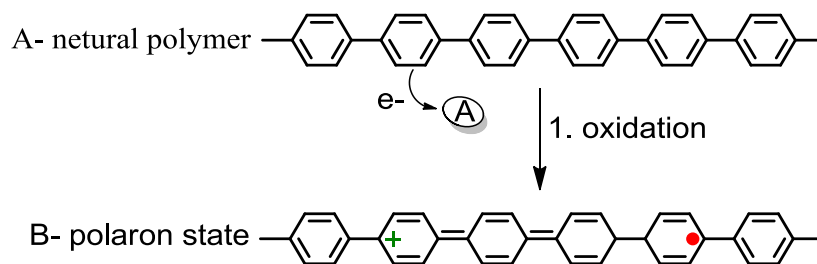
Figure 1-9: Polaron

1.3.2 Bipolaron

A pair of charges such as dianion or dication species are known as bipolarons, which are similar to polarons.[29] Unlike the polaron, the localised electronic transitions of bipolaron move away from the HOMO-LUMO levels (**Figure 1-10**).[30]
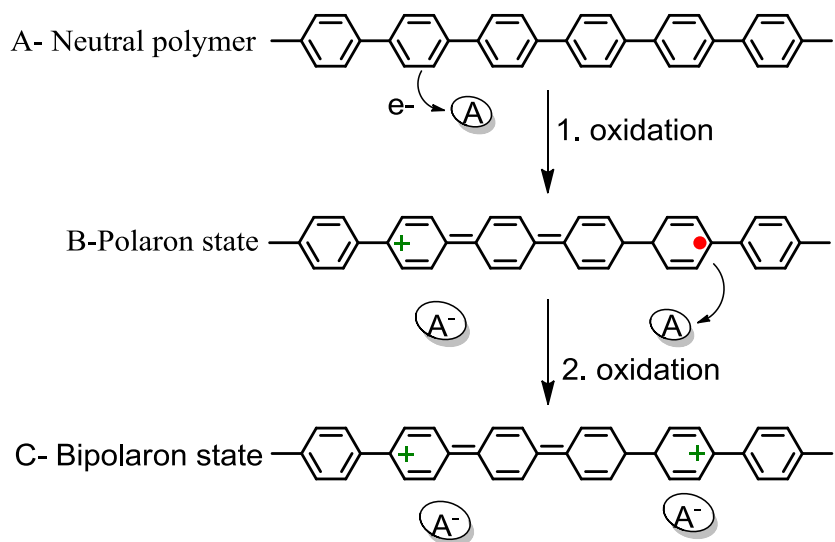
Figure 1-10: Bipolaron

1.3.3 Excitons

Excitons are electron-hole pairs that resulted from photoexcitation. As they are associated with photoluminescence, they attract more attention. Excitons can be either singlet or triplet excited states in molecular organic photophysics. Exciton decay may occur radiatively (photoluminescence) or non-radiatively with the release of vibrational energy and heat. The typical lifetime of an exciton is a few hundred picoseconds (**Figure 1-11**).
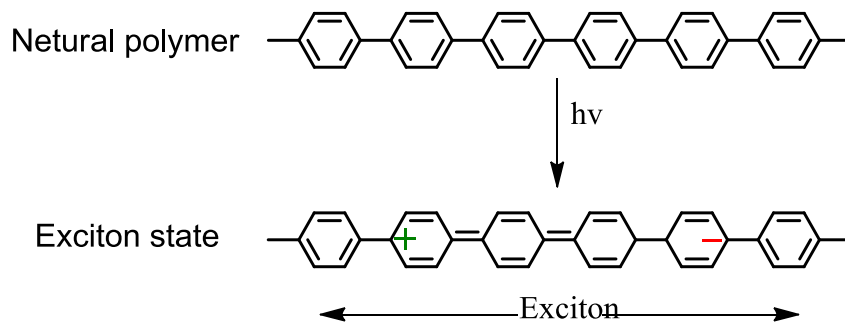
Figure 1-11: Exciton

1.4 Properties of semiconducting polymers

1.4.1 Transport of charge in conducting polymers

Even though it has been established that bipolarons and solitons are formed from charge carriers, the exact mechanism underlying the process still needs to be explored. In this regard, tracking the path of the charge carriers through the polymer proves to be the task that is actually difficult. Polymers are extremely complicated as they contain both amorphous and crystalline portions. Moreover, the movement between and along the polymer chains should be considered. Similarly, the complicated interfaces formed due to several phases also needs consideration. Influence of temperature, doping, frequency and magnetism have been investigated on the above mentioned phenomenon and it has been found that several different conduction mechanisms are being utilised. Transport of charge carriers between soliton, bipolaron or polaron or between restricted sites serves as the major underlying mechanism.

1.4.2 Stability of conducting polymers

The stability of the polymers is a very important feature which ensures that the polymer can work and be safely stored for a long time. In terms of stability, we can distinguish between two types, extrinsic and intrinsic.[6] The extrinsic stability is affected by the external environment such that water, peroxide and oxygen can attack the charged site of a polymer. To solve such a problem, the polymer can be protected by a stable coating, which can then tolerate hard conditions.

In contrast, degradation can occur for the polymers over time even in appropriate circumstances such as being dry and oxygen-free. This can be interpreted by the intrinsic instability of the polymers which is originally the thermodynamic stability of the polymers[31]. The irreversible chemical reaction causes the intrinsic instability between the dopant counter ions or the π-system of a neutral chain and the charged sites of the polymers. That can lead to the production of an sp^3 carbon which breaks the conjugation system. The thermally-driven mechanism produced by intrinsic instability can cause the polymer to lose its dopant. As a result of charge sites becoming unstable, the conformational changes in the polymer backbone appear. For example, alkyl substituted

polythiophenes show the instability of the alkyl chain which leads to the conformational changes in the backbone of the polymer.[32]

1.5 Application of conjugated polymers

The discovery of the conductive properties of conjugated polymers has changed the way scientists think. In particular, after 1980, huge and intensive works have been published, of which some results are already being applied in industry in the area of electronic devices; for instance, polymer solid-state condensers and polymer lithium-ion secondary batteries.[15] Other suggested applications of conjugated polymers include switching devices, antistatic agents, electroluminescent devices, electrochromic devices, laser devices, gas-sensors, biosensors, transparent conducting films, electromagnetic shielding materials, piezoelectric devices, field effect transistors, photo-recording media, actuators, bimorph cells, molecular devices, conductive soldering materials, solar cells, schottky diodes, and nonlinear optical devices.[33-34-35-36] The conducting polymers absorb low frequency radiation which may become an electromagnetic shielding or as parts of solar cells and semiconductors. Devices designed to transmit information by means of photons now incorporate polymeric materials with the appropriate structures.

1.5.1 Existing solar cell technologies

The conventional sources of energy that are used worldwide is coal, oil and nuclear power. These technologies have negative environmental impacts, so that alternative sources of energy are urgently needed. Solar cells can solve part of this problem by using the existing solar cell technologies (**Figure 1-12**). In this project, the concern is about developing new organic thin film systems only. However, silicon based solar cells have afforded the highest efficiency when compared to organic based solar cells. The history of inorganic solar cells has begun since along time ago and remained as a scientific phenomenon untill the 1960s which was the first time that silicon solar cells were used in practice.[37] Since then, many works have been done and published in this field, and recently we have two types of silicon solar cells, single and multi crystal solar cells (**Figure 1-12**).[38] These two types, particularly the second one, make up more than 80% of alternative sources of energy.[37] The high cost of processability and of production are the main limitations of this technology.[37,39] As our

interest is in the field of organic solar cells, the following parts will discuss relevant issues in this field.
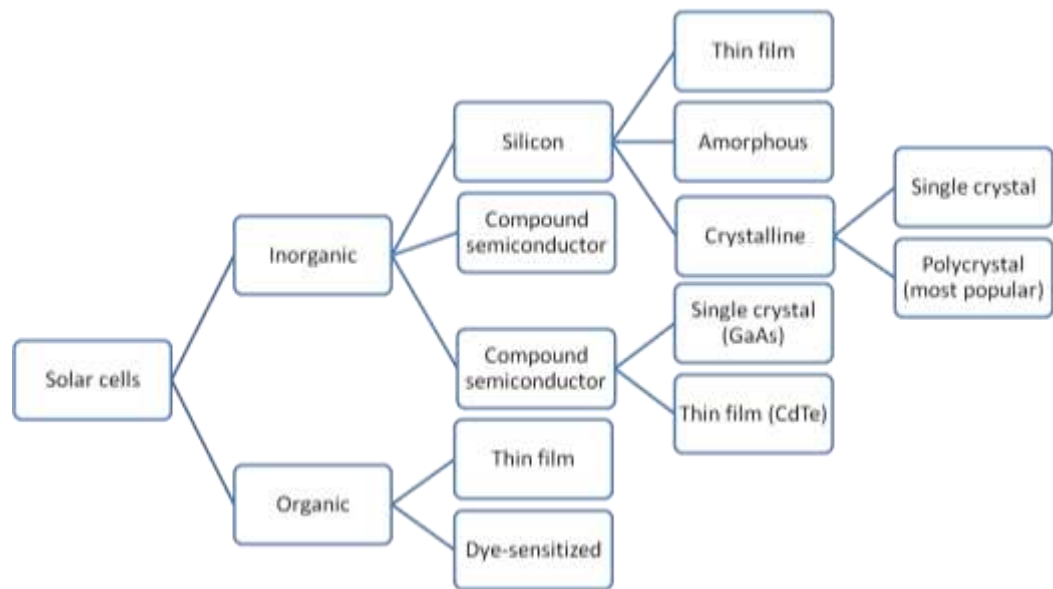
Figure 1-12 The existing solar cells technologies

1.5.1.1 Organic photovoltaic cells

Since harvesting energy from sunlight by solar cells is very important[16], the acceleration in the development of organic photovoltaic cells has increased considerably as a rival technology to the established silicon based technology. It can be clearly seen that organic photovoltaics offer a low thermal budget, flexible substrates, solution processing, low cost and a quite high speed of processing. The lifetime and efficiency are so far the major drawbacks of organic photovoltaics compared to the inorganic photovoltaics based cells.[40] In the period from 1980 to 1990, the efficiency of organic was very low and devices had a short lifetime.[17] However, this has changed and both lifetime and efficiency of organic photovoltaic cells have improved significantly with an estimated operational lifetime of twenty thousand hours and efficiencies of around 11%.[41] In addition, organic photovoltaic cells have advantages of better operation at low light compared with inorganic photovoltaics. In the last decade, extensive studies on these materials have been published in the field of synthesising polymers which can absorb light with wavelengths above 600

nm.[42-41] **Figure 1-13** shows both the spectrum from irradiation of sunlight, and the part of the spectrum which is absorbed by normal silicon solar cells.
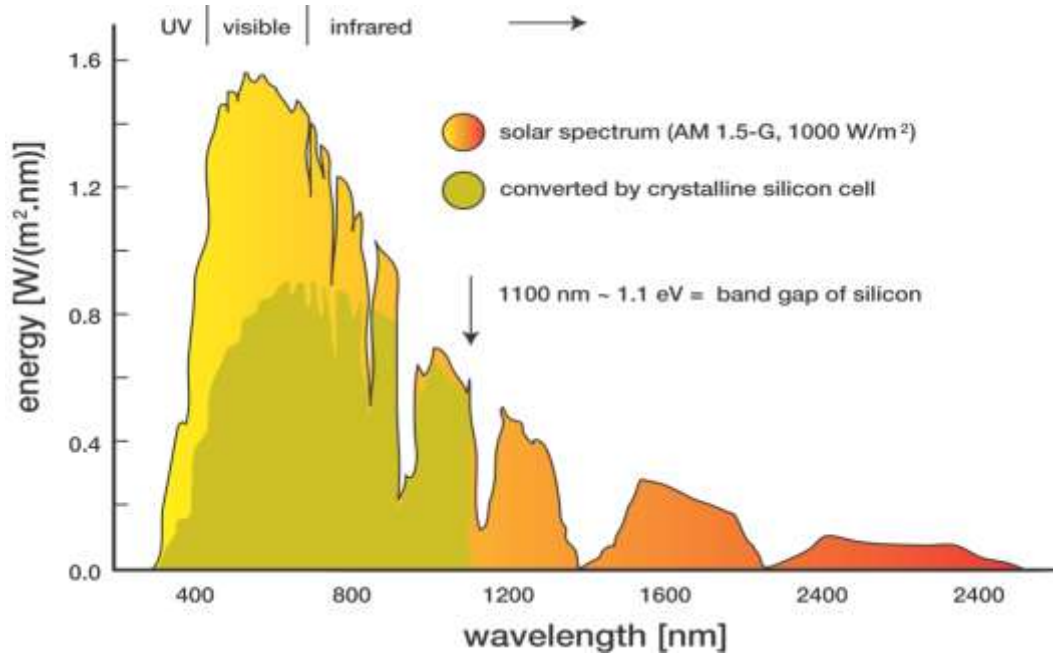
Figure 1-13: The solar irradiation spectrum. (2015), The solar irradiation spectrum [ONLINE]. Available at:http://solarcellcentral.com/limits_page.html [Accessed 12 May 15].

The type of polymers that need to be synthesised should have efficiencies that are higher than 10% and which can be done by using lower bandgap polymers with a high open circuit voltage (V_{oc}). Furthermore, an increase in power conversion efficiency depends on current density in devices which occurs due to the absorption of the acceptor beyond the band gap of the donor. The value of the V_{oc} is linked to the difference between the HOMO of the donor and the LUMO of the acceptor; V_{oc} increases by increasing this difference.[18] Therefore, to increase the V_{oc} and thus the efficiency of the device, new low band gap polymers which absorb light at longer wavelengths must be developed.[43]

1.5.1.2 Bulk heterojunction

Bulk heterojunction design appeared as a result of the fact that other designs of photovolatiac devices did not work well in terms of charge carrier separation and transport. The bulk heterojunction cell overcomes these problems, by having a bulk volume that

consists of a blend of donor and acceptor segments (**Figure 1-14**).[22] Therefore, excitons have less distance to approach the donor and the acceptor interface, and the charge separation takes place throughout the photoactive layer (**Figure 1-15**). The balance between electronic transport and optical absorption relies on the ratio of fullerence and polymer in the blend. Spectroscopic studies show that in devices with high band gap polymers, the charge generation is at maximum between a polymer:fullerene ratio of 4:1 to 1:1.
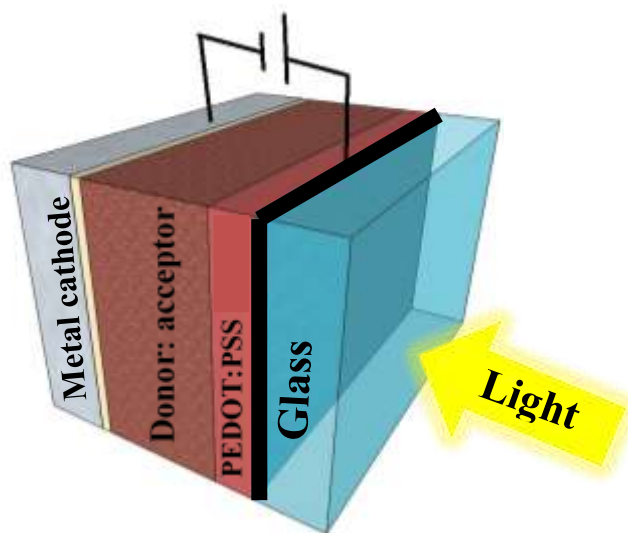
Figure 1-14: Bulk heterojunction solar cells

In the case of bulk heterojunction devices involving APFO-3 **Figure 1-16**, the mobility of electrons can be increased by raising the concentration of PCBM in the blend. In contrast, in a low band gap polymer, the hole mobility decreases when increasing the acceptor fraction. To improve the hole transport, the electron mobility in PCBM should be higher than that of the hole transport in the blend.[23]
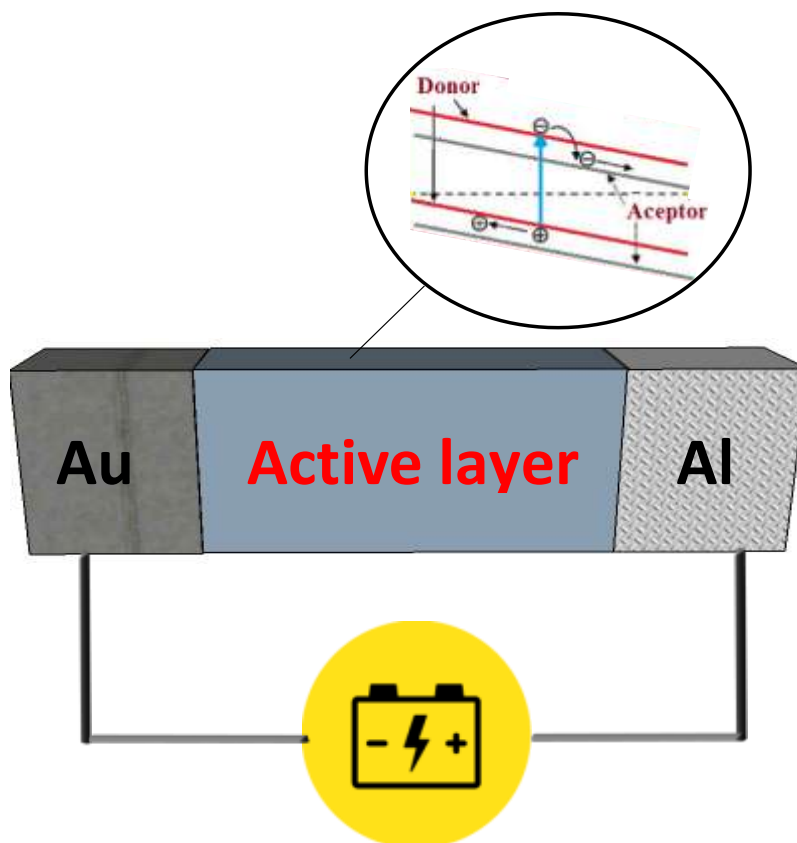
Figure 1-15: Schematic of a bulk heterojunction device
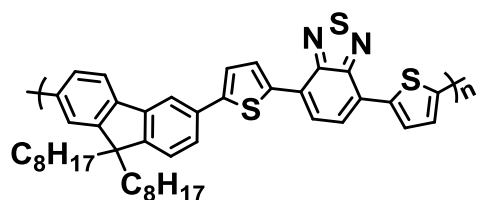
Figure 1-16 Structure of APFO-3

Figure 1-14 shows the bulk heterojunction photovoltaic device structure. This device is composed of a transparent conductive oxide as positive electrode (anode) which is basically made from indium-tin-oxide ITO coated glass or plastic. The active layer, containing the conjugated polymer and fullerene blend, is coated on top of this anode. This layer is usually known as a bulk heterojunction. As the top negative electrode (cathode), which is a metal layer, aluminium, calcium and gold are proven to be good candidates for this role. The LiF

is an interfacial layer located between the polymer and metal.[24] In terms of selecting materials for the anode and cathode, they must have the appropriate properties in order to maximise the potential for the device. These should include a suitable work function in order to move "electron holes" without any major obstacle, expense and stability. ITO is usually utilised for the anode. The reasons for this are that it is transparent and relatively inert; it is however a source of oxygen and causes the slow oxidation of some polymers. Furthermore, ITO has a high work function, making it ideal for hole transport. The preferable cathode is a reflective one, which reflects any photons back through the transparent anode and hence gives better results, such as Ca and Al. These are easily evaporated onto the surface of the polymer, giving a thin coating. That is why the polymer has close contact with them.

1.5.1.3 The working principle of bulk heterojunction devices.

There are three steps that govern the process of converting light to electric current in the organic photovoltaic cells: absorption of light of by the active layer, which leads to the formation of the exciton (a combination of electron-hole pair) and this exciton diffuses randomly to the interface area between the donor and the acceptor.[44-45] In terms of conjugated polymers, the average diffusion length for the exciton is between 5 to 20 nm[46] and the life time for this formed exciton is about 300 picoseconds.[46-47] The second step involves the dissociation of the formed exciton into a free electron and hole by an electric field.[48] The last step is the transportation of these free charges toward the electrodes (**Figure 1-17**).[49]
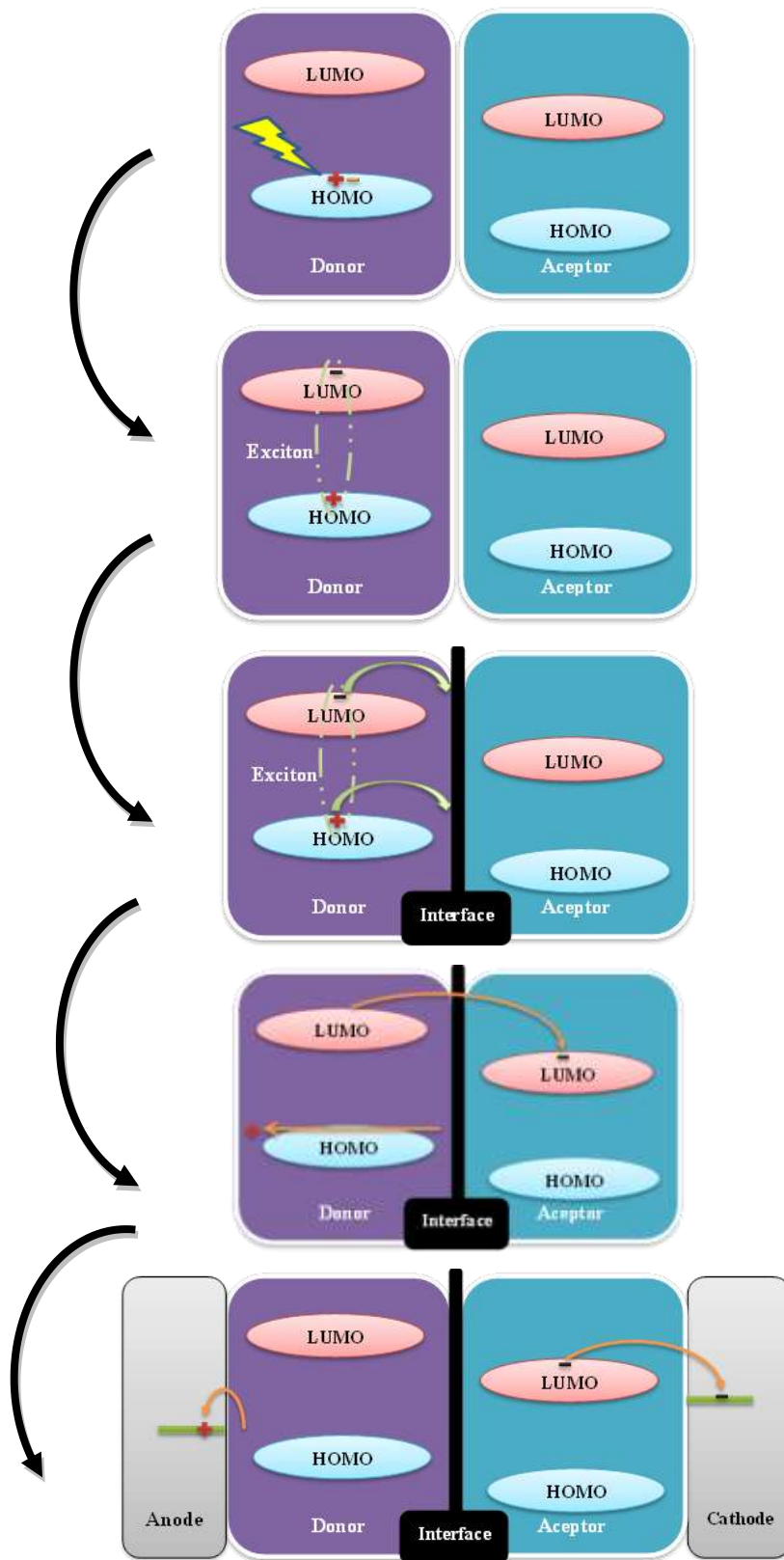
Figure 1-17 Operating mechanism of OPV

1.5.1.4 Polymer light-emitting diode

Electroluminescence occurs when an electrical current that passes through a material produces light emission; this is known as an optical and electrical phenomenon.[50] In terms of organic materials, this phenomenon was first reported for anthracence in 1960.[12] Further developments were achieved in 1987 by Ching W. Tang and Steve Van Slyke,[13] who demonstrated electroluminescence from a double layer structure. In their work, vapour deposition was used to fabricate a device utlilizing N,N'-diphenyl-N,N'-bis(3-methylphenyl)-1,1'-biphenyl-4,4'-diamine (TPD) as a hole transport layer, whereas emissive tri(8-hydroxquinolinato)aluminum (Alq_3) was used as the second layer. The devices used a mixture of magnesium-silver as the cathode and indium-tin oxide (ITO) as the anode (**Figure 1-18**). Extensive research has been reported on the performance of organic light emitting diodes (OLEDs). In 1990, Burroughes et al. obtained green light from a polyphenylene vinylene (PPV) based LED, which is known as a polymer-LED or PLED.[14-51]
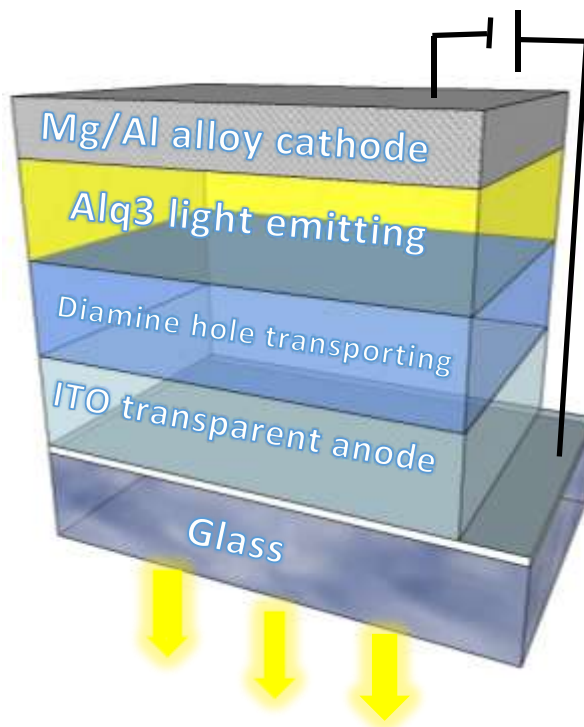
Figure 1-18: OLED structure

1.5.1.5 Organic field effect transistors

Organic-based field effect transistors (OFET), is one of the areas that has attracted scientists, and has seen significant improvement in the last two decades.[52a] Conjugated polymers as well as conjugated oligomers, are utilised for use in these organic electronic devices. More attention has been given to developing the circuitry that is utilised in disposable electronic devices.

In 1986, polythiophene was reported as the first polymer that was used in an OFET, which had a mobility of 10^{-5} $cm^2V^{-1}s^{-1}$.[53] Other polymers were discovered later on, which showed semiconducting properties such as oligomers of polyacenes which give highly efficient thin films such as TiPS pentacene which has a mobility greater than 1.0 $cm^2V^{-1}s^{-1}$.[54] Silicon has a charge mobility of 1500 $cm^2V^{-1}s^{-1}$, which is much better than that of organic based transistors, however, development of OFETs is directed towards the production of devices at much lower cost than silicon using solution processing technique.

The normal field effect transistors (FETs), made from single crystal silicon and germanium, are heavy and their fabrications are expensive as well as difficult. A FET is made up of a source, gate, drain, semiconducting material and insulating layer (**Figure 1-19**).
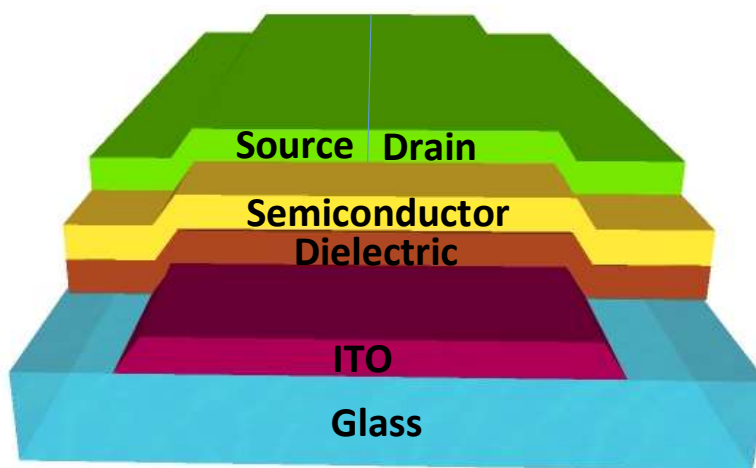
Figure 1-19: Organic field effect transistors structure

As a result of the insulating gate dielectric layer, the semiconducting material is separated from the gate electrode.[52b] Application of a potential difference across the source and drain electrodes will not result in current flowing through the device. However, if a voltage is applied there is firstly a build up of charge between the polymer layer and the insulating layer. As the potential difference is applied between the source and drain electrodes, the current will flow through the polymer and a dramatic increase can be seen in the charge carriers. There are two possible outputs as stated in the basic theory, firstly (0) which means no current flowing (OFF); or secondly, (1) which means there is current flowing (ON). Gold is a metal that has a high work function and is used as a drain and source electrode in OFETs. These properties are dependent on the semiconducting material used.[55] Various techniques can be used to deposit the organic layer; these include vacuum deposition, inkjet printing, thermal evaporation, photolithography, and line patterning.[55-56]

1.6 Efficiency of solar cells

Tang and his co-workers have reported in 1979 that OPV cells can be made by using donor–acceptor bilayer planar heterojunction.[57] These cells had on efficiency of power conversion of around 1%. Thereafter, C60 fullerene and its derivatives were the most effective breakthrough in the field of OPV. For instance, replacing n-type molecules in OPV cells with [6,6]-phenyl-C61-butyric acid methyl ester,[58] (PCBM) proved highly popular. This replacement was successful due to its high electron mobility as well as its strong electron affinity . As a consequence, the C60 fullerene and its derivatives have been used as standard n-type molecules in OPV cells. Heeger and his co-workers in the early 1990s had observed that extremely fast electron transfer process (around 50 to 100fs) between conjugated polymers and fullerene derivatives takes place. This result was also confirmed by Yoshino and his group.[59] Bulk heterojunction technology was first announced by Hiramoto et al, which worked in that the donor-acceptor materials mix together by co-evaporating under high vacuum conditions.[60] In 1995, the first bulk heterojunction device was efficiently produced by Heeger and his co-workers.[61] Since then, numerous works and materials have been produced to increase the efficiency of OPVs devices, whose efficiencies are reaching 10%. This makes this technology more promising for the future of organic solar cells.

1.7 Advanced development in the field of photovoltaic solar cells

As this field is very new, the acceleration of development has always been accompanied by new discoveries and innovations. Wudl has developed many PSC materials such as poly[2-methoxy-5-(2'-ethylhexyloxy)-p-phenylene . Yu and his group in 1995 achieved the first polymer to be used in solar cells with a high efficiency of 3%; this came from a polymer blend of poly(2-methoxy-5-(3',7'-dimethyloctyloxy)-p-phenylenevinylene) (MDMO-PPV).with PCBM (**Figure 1-20**).[62] However, this system had limitations such as the narrow light absorption range and low hole mobility. These drawbacks limit the efficiency of PPV-based blends.
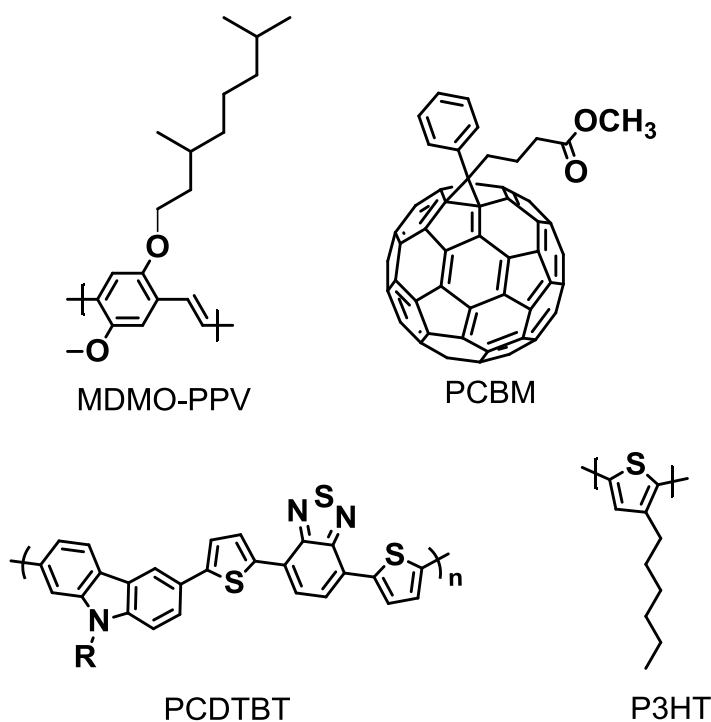
Figure 1-20: Chemical structure of some new classes of conductive polymers

In the 2000s, polythiophene derivatives such as poly(3-hexylthiophene) (P3HT)[63] became the standard materials for PSC due to their high hole mobility as well as the coverage of a wide range of light absorption.[63] Recently, [2,6-(4,4-bis-(2-ethylhexyl)-4H-cyclopenta[2,1-b;3,4-b']dithiophene)-alt-4,7-(2,1,3-benzothiadiazole)](PCPDTBT), **Figure 1-21** has become one of the high performance polymers with an efficiency of 3%; however, by adding alkane dithiol molecules, its efficiency increased to around 5.5%.[64] It has a low

band gap and also covers a wide range of light absorption to 900 nm. Another polymer gave 3.6% as efficiency for converting light,[65] which was developed later by Leclerc and his group, poly[N-9''-hepta-decanyl-2,7-carbazole-alt-5,5-(4',7'-di-2-thienyl-2',1',3'benzothiadiazole)] (PCDTBT), to give an efficiency of around 6.1%. This increment is due to incorporating titanium oxide (TiOx) as an optical layer.[43]

The most impressive work that has been made by Yu and his co-workers saw the development of one of the highest performance polymers so far, PCEs at around 7-8% efficiency. These polymers consist of thieno[3,4-b]-thiophene (TT) and benzodithiophene (BDT) alternating units (**Figure 1-21**).[66] More recently, many reports have been published indicating polymers with an efficiency of more than 7%.[67,68,69]
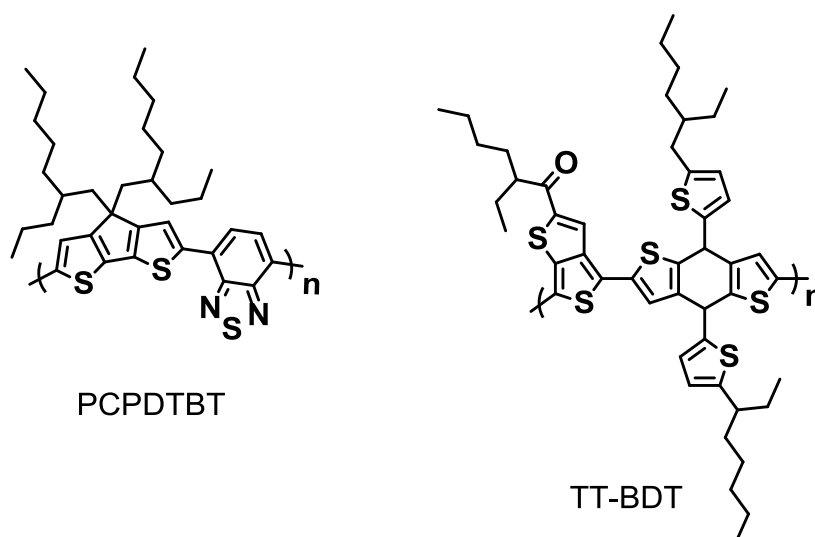
Figure 1-21 Structures of PCPDTBT and TT-BDT polymers

1.8 Structure of two-dimensional polymers

The search for two-dimensional polymers has been actively pursued by many scholars and researchers due to the demand for a renewable source of energy, which could meet the energy needs of the future.[70] Li et al. in 2004 mentioned the concept of two-dimensional (2-D) polymers. Since then, many published papers have focused on the 2-D nature of the side chains.[71-72] The 2-D structure for the polymer backbone could help increase the planarity of the polymers and hence increase the intramolecular charge transport along the polymer chain, which can give a 2-D polymer with high light absorption capacity.[73] It is worth

mentioning some examples of 2-D polymers, which include polythiophene derivatives (**Figure 1-22**).[74]
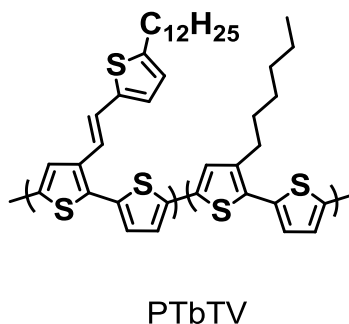
PTbTV

Figure 1-22. The chemical structure of PTbTV

The two-dimensional structure enhances the conjugation of the polymers laterally and hence improves their physical properties. Polymer PTbTV showed a broad absorption region from 350 nm to 650 nm and the hole mobility increased as a consequence of the 2-D structure.[75] There was also an improvement in device efficiency when PTbTV was combined with PCBM, reaching 3.2 % compared with P3HT, which achieved only 2.4 %. This could be attributed to the 2-D structure of this polymer.[71a]

1.8.1 Pyrene systems

Pyrene is one of the molecules that has been attracting scientists for many years mostly due to its optical properties.[76] This has led to pyrene being used in many fluorescence studies. The optical properties of pyrene come from the sensitivity of its structure to the surrounding environment.[77] Therefore pyrene can be used as a probe to report the hydrophilic and hydrophobic parts of its surrounding area.[78] A big challenge for organic molecules was to emit light in the blue region. This problem has been resolved by using pyrene derivatives.[79] This is because pyrene has very good electronic properties, and it was used as a monomer in a polymer light emitting diode [PLED]. Pyrene derivatives showed a very interesting result in PLED, which gave a high luminance of 40400 cd m^2 at 14 V with high external quantum efficiency (η_{ext}) of 5.2%.[80] The PLED is a reverse process to organic photovoltaic, therefore pyrene can be utilised in OPV systems as well. The pyrene system is also used in electron transfer systems as it has electron donating properties.[66b] These

properties make the pyrene system a perfect choice to be used in new donor acceptor polymers. There are many factors that play a significant role in terms of donor acceptor polymers. These include planarity of the polymer chain, which pyrene system exhibits as a group of fused aromatic rings that can enforce a planarity on the backbone of the polymer chain.[81] The delocalisation of π electrons along the polymer backbone can affect the bond length alternation. These factors can be controlled to get low band gap polymers and hence high efficiency.[82] It is worth noting that the pyrene system has many positions that can be functionalised to either increase the solubility by adding alkyl chains or extend the structure of the monomer. In summary, the aim of the project is to investigate whether pyrene derivatives can prove to be high efficiency materials in OPV devices.

1.8.2 Quinoxaline as an electron deficient group

Quinoxaline is a heterocyclic ring containing two nitrogen atoms that has been used widely in many fields. For example, it is used in antibiotics in pharmaceuticals,[83] and was also used against transportable tumours as an active agent.[84] In addition, quinoxaline has been used as an efficient organic semiconductor,[85] as well as in electroluminescent materials.[86] As this project concerns organic semiconductor materials, an example of quinoxaline that has been used in this field is given. The polymer poly[2,3-bis(3-octyloxyphenyl) quinoxaline-alt-thiophene] TQ1 (**Figure 1-23**) is one of the quinoxaline-based polymers that is well known and thoroughly studied because its features prompted it to be one of the top synthesised polymers used for semiconductor devices.[87] This is because it has an efficiency of around 6% in OPV devices with a fill factor of nearly 0.64 and open-circuit voltage (V_{oc}) of about 0.91 V. The optical band gap for this polymer is 1.7 eV and it has a deep highest occupied molecular orbital (HOMO) energy level.[88]
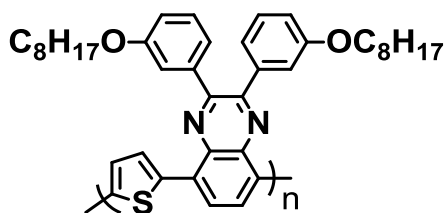
Figure 1-23. The chemical structure of TQ1

1.8.3 The effect of side chains on the polymer properties

There are many factors that could play crucial roles in controlling the properties of polymers.[89-90-91] One factor is linked to the type of alkyl chain attached to the donor or acceptor repeat units, which modifies the solubility of the target polymer.[92] Another factor is the effect of the alkyl or alkoxy chain on the polymer properties.[93] Moreover, the position of these alkyl or alkoxy chains could alter the polymer properties and hence increase or decrease the efficiency of electronic devices.

1.8.4 Linear or branched alkyl chains

The alkyl chains are an important element that could influence some properties of conjugated polymers. It is believed that they increase the solubility of target polymers and make them easier to process and also they can increase the molecular weight of the desired polymers.[94] There are both linear and branched alkyl chains, where the linear alkyl chains are less effective than their branched counterparts for enhancing the solubility of the target polymers.[95] However, an oversized branched alkyl chain will influence the π-π interaction. As a result, the π-π stacking distance will be increased and hence the carrier mobility will be reduced.[96]

1.8.5 Alkoxy and alkyl chains

The influence of either alkyl or alkoxy chains on the target polymers is important as the alkoxy chain is richer in electrons than the alkyl chain and can donate them to the conjugated π system. This could increase the HOMO energy level and hence decrease the band gap.[97] For example, the benzo[1,2-*b*:3,4-*b*]dithiophene, BDT, unit which has the alkyl side chain replaced by an alkoxy side chain resulted in a decrease in the HOMO level by 0.1 eV.[98]

1.8.6 The position of the side chain and its influence on polymer properties

The position of the side chain is interesting because it plays an important role in controlling the performance of the polymer in photovoltaic devices.[99] For example, the polymers PDTSTTz-3 and PDTSTTz-4 have dithiophenesilole as a donor and thiazolothiazole as an

acceptor unit (**Figure 1-24**). The difference between these two polymers is in the position of the alkyl chain, where PDTSTTz-4 has a higher hole mobility than PDTSTTz-3.[100] This could be attributed to the position of the side chain of PDTSTTz-4 increasing the planarity of the backbone of the polymers and hence a better efficiency can be obtained, PCE = 5.88 %, for PDTSTTz-4 compared with a PCE of 5.59 % for PDTSTTz-3.[100]
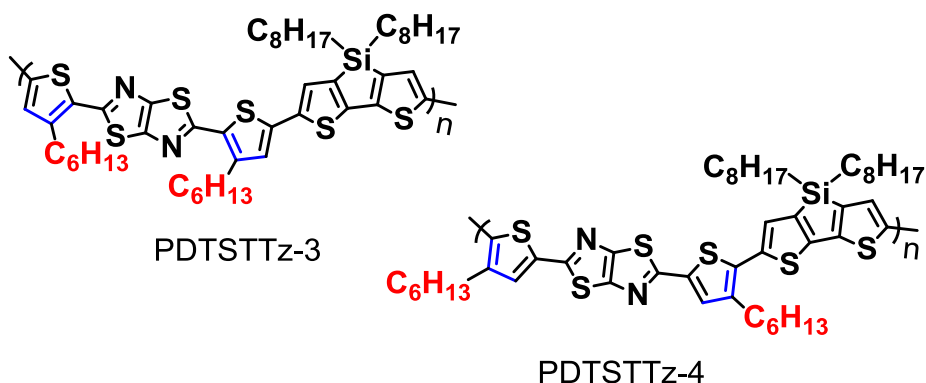
Figure 1-24. The chemical structures of PDTSTTz-3 and PDTSTTz-4

The photovoltaic properties could also depend on the distance of the branched alkyl chain from the main chain. It is worth mentioning that DPPTT-T C1, C2 and C3 are polymers with the same chemical structure (**Figure 1-25**); however, there are either one (C1), two (C2) or three (C3) carbons between the main chain and the branched alkyl chain. Therefore, the distance between the main chain and the branched alkyl chain varies, with C1 closer to the main chain whereas C2 and C3 are further away from the main chain. As a consequence, the DPPTT-T with one carbon distance between the main chain and the branched alkyl chain is blue shifted as well as having a lower hole mobility compared with the DPPTT-T with C2 and C3.[101] This could be ascribed to the large branched alkyl chain decreasing the hole mobility as the interaction of the polymer backbone decreases. However, the longer distance between the main chain and the alkyl chain could reduce the negative effect of the alkyl chain on the polymer backbone interaction. The PCE efficiency of these polymers is in solar cell devices using PCBM as an acceptor 5.9 % for C1, 7.3 % for C2 and 6.9 % for C3.[101]
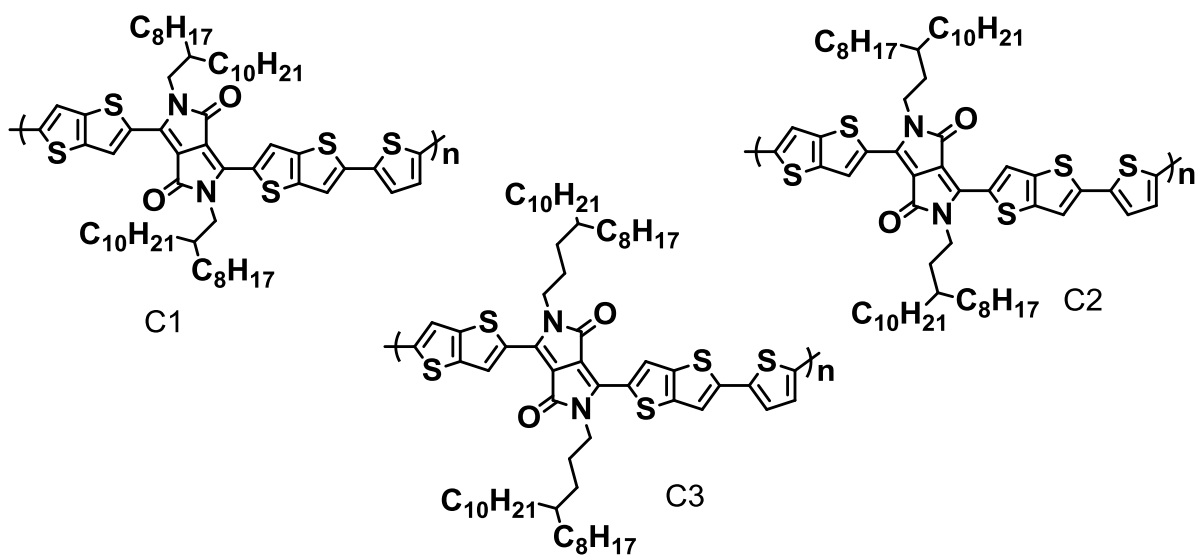
Figure 1-25 Chemical structures of DPPTT-T C1, C2 and C3

1.9 Characterisation of OPV devices and material requirements for optimal performance

An extensive amount of optimisation is required to produce highly efficient organic solar cells. Optimisation of polymer:fullerene weight ratios, annealing solvent, casting temperature and the addition of additives have shown to be effective methods in increasing the efficiency of devices. Over the last ten years, the efficiency and lifetime of organic solar cells have increased dramatically now exceeding 10% and 10 years respectively.[33] Previous literature has shown that the theoretical limited to power conversion efficiency for a bulk heterojunction organic solar cell is 23%.[102] Extensive research into organic solar cells has shown that a series of criteria needs to be fulfilled in order to achieve high efficiencies.[103] These conditions are discussed later. The power conversion efficiency (PCE) is the most important parameter as it takes into account each individual factor and gives the overall efficiency of the device. The PCE is a measurement of how much incident light is converted into electrical energy. The formula for the PCE is given below.

$$PCE = \frac{J_{SC} \; V_{OC} \; FF}{p_{light}}$$

Where J_{sc} is the short-circuit current of the cell, V_{oc} its open-circuit voltage, FF its fill-factor and P_{light} the incident light flux.

1.9.1 Open-Circuit Voltage (V_{oc})

The energy level difference between the HOMO of the donor polymer and the LUMO of the acceptor fullerene is tightly correlated with the V_{oc}.[104] According to the literature, maximum V_{oc} would be seen in polymers that have low-lying HOMO levels. However, continually lowering the HOMO level will have a negative impact on photovoltaic devices as this will result in a wider band gap. A minimum energy difference of ~0.3eV between the LUMO of the donor and acceptor is required to promote efficient exciton dissociation. The minimum LUMO level of the donor polymer would be close to −3.9 eV when $PC_{61}BM$ is utilised as an acceptor as this has a LUMO level of −4.2 eV. A compromise has to be reached as to the level of the HOMO of the polymer so it allows a decent value of the V_{oc} from the PV cell at the same time as having a low enough band gap to provide a good J_{sc} value from the PV device. The origin of V_{oc} is still under debate even though latest information describes that a collection of other elements determine the V_{oc} in addition to the HOMO level of the polymer.[105] Moreover, the morphology of the active layer, interchain distances and bulkiness of side chains have a considerable effect on the V_{oc}.[106]

1.9.2 Short-Circuit Current (J_{sc}).

The amount of excitons formed during the process of solar illumination determines the theoretical upper limit for J_{sc} of any excitonic solar cell. In an ideal situation, the absorption of the active layer should be well-matched to the solar spectrum so that it can increase the number of excitons produced. The donor polymer plays the role of the main light absorber because $PC_{61}BM$ has a low absorption in the visible and near-IR region. It is known that, approximately 70% of the sunlight energy is distributed in the wavelength area between 380 and 900 nm.[103] As a result, the ideal polymer has to have a strong and broad absorption in this area which can only be possible if the polymer has a band gap between 1.4-1.5 eV.

A narrower band gap polymer is capable of absorbing more light which would raise the J_{sc}. However, any increase in the HOMO level of the donor polymer (if we assume that the LUMO level is -3.9 eV with $PC_{61}BM$ as an acceptor)[107] would lower the band gap and reduce the V_{oc}. It is evident that a PCE of more than 10% can be achieved by using an ideal polymer that has an optimal band gap of 1.5 eV and also a HOMO level of approximately -5.4 eV.[103] The experimental J_{sc} derived from a polymer solar cell is usually less than the theoretical J_{sc} owing to loss mechanisms such as monomolecular or bimolecular recombination that take place during charge generation, charge transportation and extraction.[108] Optimisation of the active layer and polymer can help alleviate these losses. More specifically, high charge carrier mobilities, a controlled active layer morphology and high molecular weights help improve the experimental J_{sc}.[103]

1.9.3 Fill Factor (FF)

From the perspective of a semiconductor photovoltaic device, two factors are required to achieve high FF. These are a small series of resistance (R_s) and a large shunt resistance (R_{sh}).[109] The aforementioned elements R_s and R_{sh} are considerably influenced by the morphology of the polymer/fullerene blend. The favourable charge separation and charge transportation can be achieved by optimizing the morphology of the active layer. Thus, leading to a higher FF. For future application and commercialisation of organic solar cells some requirements need to be considered. These include high PCE, long term stability of polymer solar cells and solution processability. These can be achieved by designing polymers that have high molecular weights, high hole mobility, good solubility and HOMO and LUMO levels around -5.4 and -3.9 eV respectively. Furthermore, optimal device morphology is necessary.[103,110]

2   Chapter 2: Aims of the project

The demand for alternative energy will increase in the coming decades as the global usage of fossil energy has reached the peak of production. Solar energy is one of the best clean energy sources. It has the potential to meet the world's demand for energy indefinitely. There are many processes that can be used to convert solar energy into electrical energy. One of these is the use of organic based solar cells, in which organic materials are used to harvest light which is then converted into electricity. This field has been extensively investigated and many organic compounds have given promising results. Examples of promising organic materials are carbazole-based polymers, benzothiadiazole-based polymers and quinoxaline-based polymers. There is also some interest in the structure of these materials, which are based on either one-dimensional or two-dimensional conjugated systems. In particular, one-dimensional-based polymers have been studied extensively. Two-dimensional-based polymers have been less explored and have been attracting a lot of interest in this field recently.

The main objective of this project is to prepare a series of light-harvesting copolymers based on laterally extended 2-D structures. The project will focus on pyrene-functionalised-quinoxaline polymers. These polymers will be synthesised and their physical properties characterised. Pyrene is a planar molecule and has a high hole mobility.[111] Moreover, quinoxaline is a good acceptor because it has multiple nitrogen atoms which should pull electronic density towards them.[112] Incorporating a large and planar molecule, such as pyrene, between two units of quinoxaline should extend the conjugation length in the lateral direction. The improved planarity should result in strong interchain stacking which will increase the area of absorption and improve charge carrier mobility.[113] The chemical and physical properties of pyrene derivatives can be chemically tailored to ensure they function as ideal p-type materials in organic photovoltaic (OPV) devices. The final polymers will be synthesised in two general stages, the synthesis of monomers followed by the synthesis of the polymers.

The target monomers **8** and **10** are based on pyrene condensed with quinoxaline bearing hexyldecyloxy side chains. These are attached to ensure the final polymer has an acceptable

level of solubility (**Scheme 2-1**).The shape of monomers **8** and **10** which have a laterally extended electronic conjugations (6 aromatic fused rings) is expected to help extend the conjugation, which should increase the number of intermolecular interactions in the final polymers. It will also introduce electron-withdrawing nitrogen atoms which should make pyrene-quinoxaline a good accepting unit. Indeed quinoxaline based units are most commonly used as electron-acceptor units in donor-acceptor low band gap conjugated polymers and a number of such system are known. [94,114] The solubilising groups that are attached to the monomers should increase the solubility of the final polymers (**Scheme 2-1**). Monomers **15** and **17** which have alkyl substituents rather than alkoxy substituents will also be prepared in order to increase the electron-accepting properties (**Scheme 2-1**).

R= O-C$_{16}$H$_{33}$ = 8   R= O-C$_{16}$H$_{33}$ = 10

or   or

R=C$_{16}$H$_{33}$ = 15   R=C$_{16}$H$_{33}$ = 17
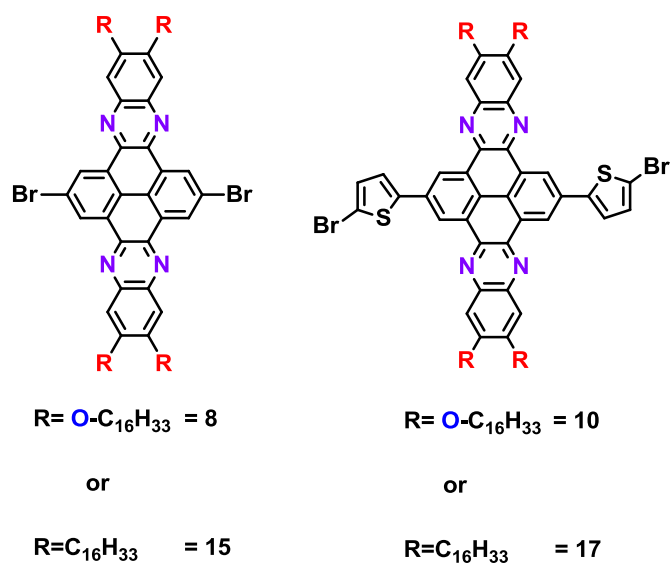
Scheme 2-1 The chemical structure of the target monomers **8**, **10**, **15** and **17**

A series of polymers will be prepared *via* Stille or Suzuki coupling reactions associating monomers **8**, **10**, **15** and **17** as potential electron-accepting repeat units and electron-donating units such as carbazole, fluorene and 2,2'-bithiophene units in order to obtain polymers with low energy band gaps for photovoltaic applications (**Scheme 2-2**)

Monomers **8**, **10**, **15** and **17** will also be investigated as electron-donating units in alternating copolymers associating strong electron-accepting units such as benzothiadiazole units in order to produce new series of low energy band gap polymers (polymers **P7**-**P12**, **Scheme 2-2**).
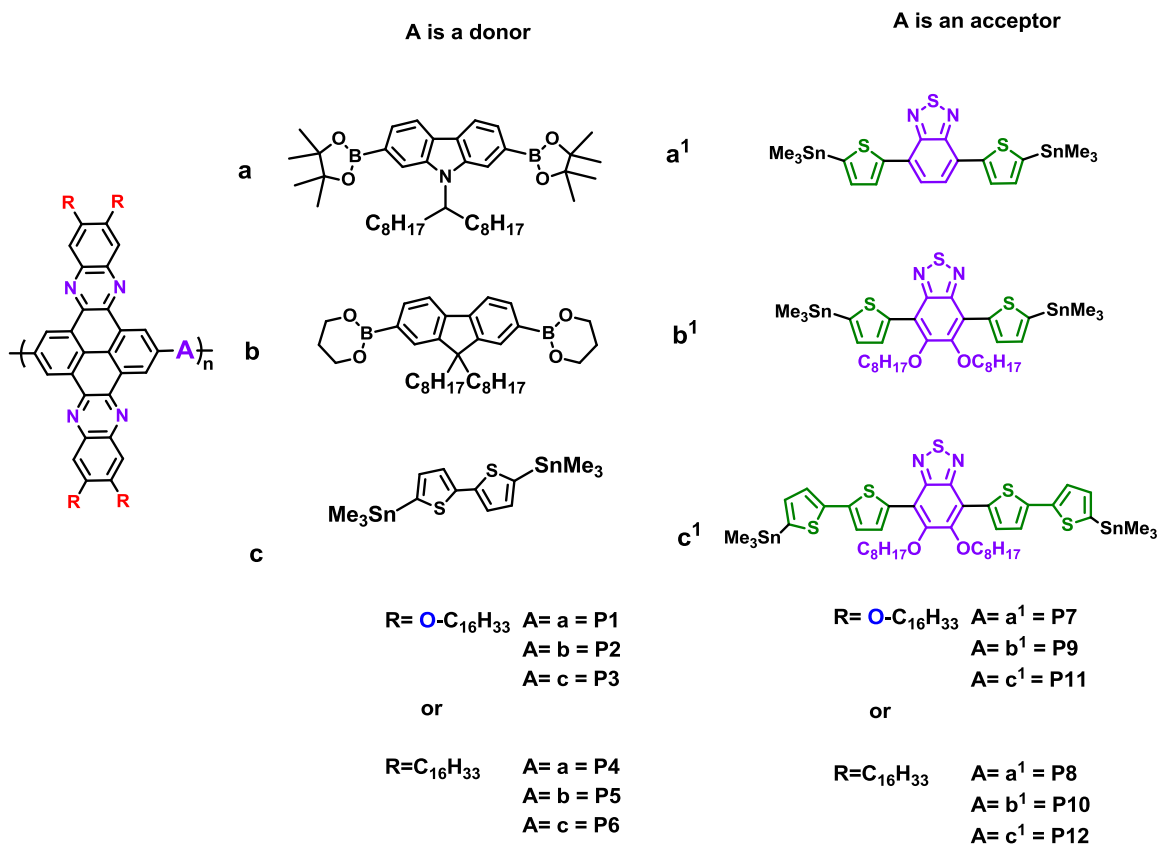
Scheme 2-2 Targeted polymers **P1** to **P12**

Various techniques will be used to examine both the monomers and polymers. The monomer will be analysed using ^{1}H and ^{13}C NMR, mass spectrometry, matrix assisted laser desorption ionisation–time-of-flight (MALDI–TOF) spectrometry, elemental analysis, IR spectroscopy and melting point analysis. These techniques will determine the structure of the monomers and give an indication as to their purity. The number-average and weight-average molecular weight of the polymers will be estimated using gel permeation chromatography. This is very important as the chain length of polymers is known to affect

the photophysical, electronic and morphological properties of these systems when applied as active layers in solar cell devices. The thermal stability of the polymers will be determined using thermogravimetric analysis. The absorption spectra will be used to determine the extent of conjugation in the polymers and estimate their optical band gap. Cyclic voltammetry (CV) will be used to measure the HOMO and LUMO levels of the polymers. This will give an indication about their oxidative stability and the amount of D-A character the polymers possess. All of these methods can increase the understanding of the properties of the polymers and will assess their suitability for applications as donor materials in BHJ solar cells.

3 Chapter 3 Experimental procedures

3.1 Materials

All chemical materials and solvents were purchased from commercial sources and used as received unless stated. Grubbs solvent purification system was the supplier for the dry solvents used such as chloroform, toluene, DMF, THF, and hexane. In terms of the preparation and polymerisation of monomers, inert gases, either nitrogen or argon, were used unless otherwise stated. Some monomers were prepared in the Iraqi group and used without further purification; these included 3,6-difluoro-9-(heptadecan-9-yl)-2,7-bis(4,4,5,5-tetramethyl-1,3,2-dioxaborolan-2-yl)-9H-carbazole, which was prepared by Hunan Yi and used for polymers **P1** and **P4**. 9,9-Dioctylfluorene-2,7-diboronic acid bis(1,3-propanediol) ester was bought from Sigma Aldrich and used as received for polymers **P2** and **P5**. Benzothiadiazole-4,7-bis(boronic acid pinacol ester was also purchased from Sigma Aldrich and used for preparing polymer **P7**. 5,5'-Bis(trimethylstannyl)-2,2'-bithiophene was prepared by A. Murad of the Iraqi group and used for preparing polymers **P3** and **P6**. 5,6-Bis(octyloxy)-4,7-bis(5-(trimethylstannyl)thiophen-2-yl)benzo[c][1,2,5]thiadiazole was also prepared by S. Alesae and utilised for preparing polymers **P9** and **P10**.

3.2 General procedure

3.2.1 Melting points

The Gallenkamp Melting Point Apparatus was used to perform the melting points for all of the solid monomers prepared throughout this project.

3.2.2 Mass spectral analysis

The Mass spectrometry technique was performed on the Perkin Elmer Turbomass Mass Spectrometer, which is equipped with autosystem XL GC and autosampler. Mass spectra for all of the monomers were recorded through electron ionisation (EI) or chemical ionisation (CI) methods.

3.2.3 Infra red absorption spectra (IR)

The Perkin Elmer Spectrum 100 FT-IR Spectrometer was used to record the IR absorption spectra for all of the intermediate molecules (**2**) to (**29**).

3.2.4 NMR spectra

The process of NMR spectroscopy was conducted on Bruker Avance 400 (400 MHz) and Avance 250 (250 MHz) NMR spectrometers at 22 ^{0}C in DMSO-d_6 or chloroform-d_1 for monomer and intermediate compounds. For the polymers, NMR spectroscopy was performed on a Bruker 500 (500 MHz) NMR spectrometer at 100 ^{0}C in 1,1,2,2-tetrachloroethane-d_2. The coupling constant is measured in the form of Hertz (Hz) while chemical shifts are stated in parts per million (ppm). The abbreviations given below are used to represent the NMR multiplicities: broad singlet (br), singlet (s), doublet-doublet (dd), doublet (d), triplet (t), and multiplet (m). The Top Spin 3.0 program was used to study the spectra.

3.2.5 Gel permeation chromatography analysis (GPC)

A GPC system was used to measure the molecular weight of the polymers. The GPC system comprised a Viscotec GPC max Model, two polymer labs PLgel 5 μm Mixed-C (300 mm × 7.5 mm) column and a guard (50 mm × 7.5 mm), and Water 410 differential Refractometer detector. A flow rate of 1 cm^3/min was used and 1,2,4-trichlorobenzene was utilised as the eluent. The polymer samples were developed as solution in 1,2,4-trichlorobenzene (5 mg in 2 cm^3) and the measurements for it were performed at 140 ^{0}C. The GPC was adjusted using a set of polystyrene narrow standards. The separation of the polymer molecules is reliant on the hydrodynamic volume in which small polymer molecules enter the pore of the polystyrene (stationary stage) which leads to an increase in the retention time whereas bigger polymer molecules travel much quicker in the column, resulting in lesser retention time. But, the GPC measurements tend to be incorrect due to the inflexible structure of the target polymers in this project. When compared with the reported molecular weight, the actual molecular weight of this kind of polymers could be three times bigger. This is due to the inflexible structure of the polymers which will also result in an increase in their retention time.

3.2.6 UV-Visible absorption spectroscopy

A Specord S 600 UV-Vis diode array spectrometer was used to perform UV-visible absorption spectra. Absorption of copolymers was done in chloroform solution through rectangular quartz-cuvettes (light path length =10 mm). The temperature was moderate through rectangular quartz-cuvettes (light path length =10 mm). Moreover, thin layers of copolymers for UV-visible absorption spectra analysis were conducted by dip coating quartz plates to nearly 1 mg cm^{-3} of chloroform solution. They were kept in open air at a suitable temperature in order to dry in the air.

3.2.7 Cyclic voltammetry (CV)

A Princeton Applied Research Model 263A Potentiostat/Galvanostat was used to measure the cyclic voltammograms. These measurements were carried out within an inert argon atmosphere of around 25 ± 2 ^{0}C. For the electrolyte solution, around 10 mL of tetrabutylammonium perchlorate in dry acetonitrile solution (0.1 M) was used. There are three electrodes in this system, beginning with Ag/Ag$^+$ reference electrode. This is a silver wire that is placed in a solution of silver nitrate (0.01 mol L^{-1}). The second electrode comprises of a platinum working electrode having a 2 mm smooth platinum diameter 3.14 $\times 10^{-2}$ cm^2. The platinum wire counter electrode is the third type of electrode. Through drop casting of around 1.0 mm^3 of polymer solution of chloroform, the polymer solid thin film was formed. This was dried in the air at room temperature. As per the suggestions of IUPAC, ferrocene was used as a reference redox system because its ionisation potential under vacuum (-4.80 eV) is known. Furthermore, it is also known that the oxidation occurs at 0.083 eV against a Ag/Ag$^+$ reference electrode. The HOMO and LUMO energy levels are calculated using the following equations $E_{(HOMO)}$=-(E_{ox}-0.083)+4.8 and $E_{(LUMO)}$=-(E_{re}-0.083)+4.8 respectively.

3.2.8 Thermogravimetric analysis (TGA)

A Perkin Elmer TGA-7 Thermogravimetric Analyser collected the TGA curves. The scan rate was 10 ^{0}C per minute within an inert nitrogen atmosphere. The sample mass was between 8-10 mg.

3.2.9 Elemental analysis

A Perkin Elmer 2400 CHN elemental analyser was used to perform the elemental analyses of CHN and the Schoniger oxygen flask combustion method was used to carry our elemental analysis of anions like halides and sulphur. The elemental analysis was used to study all the intermediate products, polymers and monomers. It was observed through the elemental analysis of the target polymers that the calculated values and the found values were different from each other. This was due to the fact that the sample was not entirely broken down into simpler components when it was burnt during an excess of oxygen, meaning some of the sample converted into char form.

3.2.10 High pressure liquid chromatography (HPLC)

This method was utilised since the usual purification methods like recrystallisation and column chromatography were not able to purify the crude product 2,11-bis(5-bromothiophen-2-yl)-6,7,15,16-tetrakis   (2-hexyldecyloxy)-5,8-dihydroquinoxalino [2',3':9,10]phenanthro[4,5-abc]phenazine (**10**). Initially, Waters LCT (ES) was used to perform the LC-MS analyses so that the mixtures could be identified. Following this, the technique HPLC was employed in which the method of purification was developed on a system which included a Waters 2487 Dual λ Absorbance Detector, Waters 2690 Separation Module, and a reversed-phase HPLC column Altima HP C18 HL 5μ (length 150 mm, ID 4.6 mm). After a period of 20 minutes, the solvent system included 80 to 100% THF in water and the flow rate was 1 cm^3 min^{-1}. A preparative HPLC system including a Varian Automatic Fraction Collector, Varian ProStar (two pumps, UV-Vis Detector), and a reversed-phase HPLC column Altima HP C18 HL 5μ (length 150 mm, ID 22 mm) was used to perform the process of purification. The samples were first made as solutions in THF (100 mg cm^{-3}), following which 0.475 mL of the sample solution was injected every time. In this mobile phase, the flow rate was (20 cm^3 min^{-1}). The elution system (mobile phase) included water (A) and THF (B). The gradient used was 60 % B for a duration of 33 minutes, followed by 60 % to 95 % B for 1 min, and then 95 % B for a period of 6 minutes. After this, from 95 % to 60 % B for 1 min, and lastly 60 % B for 9 minutes. For each injection, the total time duration was 50 minutes. The collection of pure compound was done between 21 to 29 minutes.

3.3 Synthesis of monomers

3.3.1 Purifying pyrene over Raney Nickel (1)

Sulphur contaminants were removed from the pyrene by washing pyrene (21.00 g, 104 mmol) in ethyl acetate (250 mL) with a Raney-Nickel alloy (10.00 g). The mixture was stirred for 48 hours. Once complete, the alloy was filtered off and the solution was evaporated to give 20.00 g of yellow crystal pyrene (1).

3.3.2 Pyrene-4,5,9,10-tetraone (2)
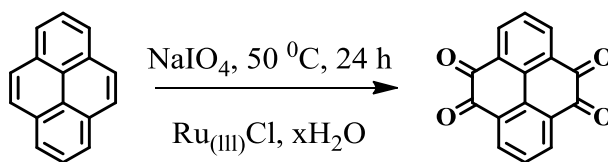
The modified Julius Rebek's reaction was used to prepare monomer (2).[115] To a solution of pyrene (1) (6.06 g, 30.3 mmol) in dichloromethane (DCM) (120 mL) and acetonitrile (CH_3CN) (120 mL) were added sodium periodate ($NaIO_4$) (52.40 g, 245.3 mmol), H_2O (150 mL), and $RuCl_3:xH_2O$ (0.27 g, 3.6 mmol). The dark brown suspension formed was kept at 30-40 ^{0}C for 30 hours. The mixture was then added into 200 mL of water which was then filtered to separate the solid contents. This gave a green organic phase. The dark green organic phase was washed with water (500 mL). The aqueous phase from the previous stage was continually extracted with small portions of CH_2Cl_2 (~50 mL) until the organic phase was colourless. At this stage, the organic phases were combined and the solvent removed under reduced pressure to give a dark green solid. A number of different fractions were identified through thin layer chromatography (TLC) which was carried out in ethyl acetate-hexane (2:5; v/v) mixture. However, isolation of these component fractions was not performed. Instead, the product was purified *via* recrystallization with m-xylene to give bright orange crystals of (2), yield (1.71 g, 6.50 mmol, 22 %). ^{1}H NMR (400 MHz, DMSO-d$_6$) δ_H/ppm: 8.33 (d, 4H, J=7.6), 7.74 (t, 2H, J=7.7). ^{13}C NMR: N/A due to low solubility; Anal.Calcd. for $C_{16}H_6O_4$: C, 73.29; H, 2.31; Found: C, 72.08; H, 2.21%); M.p,

349-351 ºC, lit (350 ^{0}C)[115] ; FT-IR (ATR): (cm^{-1}) 3066, 1703, 1672, 1558, 1449, 1420, 1334, 1272, 1173, 1102, 1053, 1000, 960, 908, 805, 761; Mass (EI$^+$): (m/z) 262 (M$^{+\bullet}$).

3.3.3 2,7-Dibromopyrene-4,5,9,10-tetraone (3)
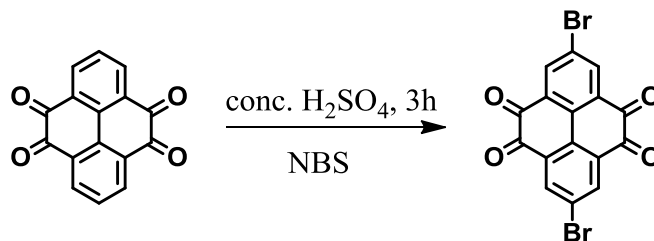
2,7-Dibromopyrene-4,5,9,10-tetraone (**3**) was prepared according to a modified procedure of Kawano *et al.*[116] Pyrene-4,5,9,10-tetraone (**2**) (0.50 g, 1.9 mmol) was dissolved in concentrated H_2SO_4 (13 mL). N-bromosuccinimide (NBS) (1.40 g, 7.9 mmol) was added slowly to the mixture at room temperature. The mixture was stirred for an additional hour and then poured into ice-water; forming a precipitate. The precipitate was filtered and washed with deionised water. The crude product was heated, as a suspension, in methanol, filtered, and heated again in diethyl ether and filtered. The residue was finally then refluxed in dichloromethane (DCM), filtered and dried overnight. 2,7-Dibromopyrene-4,5,9,10-tetraone (**3**) was obtained as a white powder in a yield of (0.45 g, 1.07 mmol, 56 %). ^{1}H NMR (400 MHz, $C_2D_2Cl_4$, 100 ^{0}C) δ_H/ppm: 8.54 (s, 4H). ^{13}C NMR N/A low solubility; Anal.Calcd. for $C_{16}H_6O_4Br_2$: C, 45.75; H, 0.96; Br, 38.05 Found: C, 45.80; H, 0.93; Br, 37.82: M.P. 380 ^{0}C ; FT-IR (ATR): (cm^{-1}) 3077, 1710, 1690, 1680, 1577, 1547, 1459, 1420, 1394, 1278, 1259, 1253, 1120, 1087, 1005, 941, 924, 800, 724, 712, 642; Mass (EI$^+$): (m/z) 418. 420. 422 (M$^{+\bullet}$).

3.3.4 2-Hexyl-1-bromodecane (4)
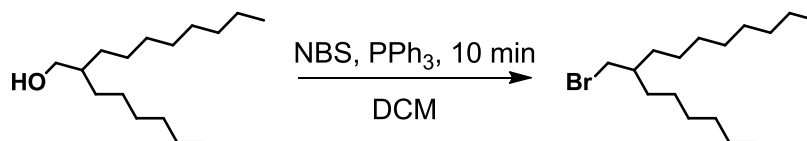
2-Hexyl-1-bromodecane (**4**) was prepared by using the modified procedure of Lee *et al.*[117] To a solution of 2-hexyldecan-1-ol (24.2 g, 100 mmol) in DCM (1 L) were added triphenylphosphine (PPh$_3$) (31.5 g, 120 mmol) and NBS (21.4 g, 120 mmol). The solution was stirred for 10 minutes at room temperature. The organic phase was then washed with an aqueous saturated NaHCO$_3$ solution (200 mL) and dried with MgSO$_4$. The solvent was removed under reduced pressure. Column chromatography with pure hexane was used to purify the crude product. The obtained residue was dried in vacuum to give 2-hexyl-1-bromodecane (**4**) as a colourless liquid in a yield of (29.8 g, 98 mmol, 98 %). ^{1}H NMR (400 MHz, CDCl$_3$) δ_H/ppm: 3.46 (d, 2H, J = 4.6 Hz), 1.61-1.57 (m, 1H), 1.26-1.43 (m, 24H), 0.90 (t, 6H, J = 4.24 Hz). ^{13}C NMR (400 MHz, CDCl$_3$) δ_C/ppm: 39.7, 39.5, 32.5, 31.9, 31.8, 29.8, 29.5, 29.4, 29.3, 26.5, 22.6, 14.0; (Anal.Calcd. for C$_{16}$H$_{33}$Br: C, 62.94; H, 10.89; Br, 26.17;. Found: C, 63.23; H, 11.56; Br, 27.00. FT-IR (ATR): (cm^{-1}) 2957, 2926, 2855, 1459, 1378, 1338, 1233, 652, 576. Mass (EI$^+$): (m/z) 304, 306, 308 (M$^{+\bullet}$).

3.3.5 1,2-Bis(2-hexyldecyloxy)benzene (5)
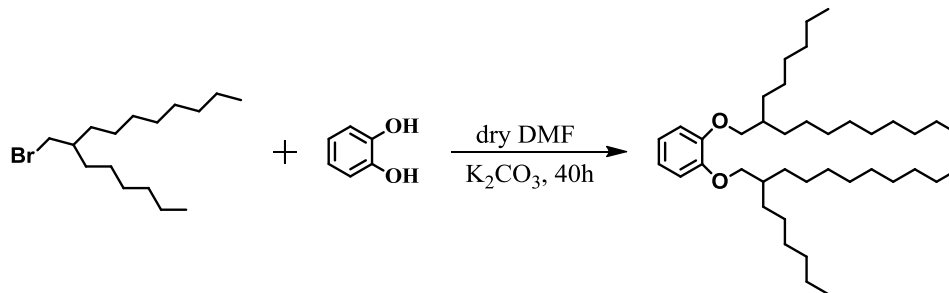
1,2-Bis(2-hexyldecyloxy)benzene (**5**) was synthesised using a modified procedure of Zhang *et al.*[118] To a solution of catechol (3.34 g, 30.0 mmol) in dry DMF (16 mL), were added 2-hexyl-1-bromodecane (**4**) (21.3 g, 67.0 mmol) and K$_2$CO$_3$ (12.7 g, 90.0 mmol). The mixture was left to stir under an inert gas at 100 ^{0}C for 48 hours. The progress of the reaction was monitored by thin layer chromatography. After cooling the mixture to room temperature, the reaction was quenched with water (100 mL). The organic phase was separated, and the aqueous phase was extracted with DCM. The combined organic phase was dried over MgSO$_4$. After filtration, the mixture was concentrated under *vacuum*. Column chromatography with a gradient eluent system (pure hexane followed by hexane:ethyl acetate (30:1 v/v)) was used to purify the crude product. The product (**5**) was obtained as a colourless liquid, yield (6.00 g, 10.2 mmol, 34 %). ^{1}H NMR (400 MHz, CDCl$_3$) δ_H/ppm: 6.89 (s, 4H), 3.86 (d, 4H, J=5.6 Hz), 1.82 (m, 2H), 1.26 (m, 48H), 0.87 (t, 12H, J=4.5 Hz). ^{13}C NMR (400 MHz, CDCl$_3$) δ_C/ppm: 149.6, 120.8, 113.9, 71.9, 38.2, 31.9, 31.3, 30.15, 29.8, 29.6, 29.4, 26.9, 22.7, 14.1 ; (Anal.Calcd. for C$_{38}$H$_{70}$O$_2$: C, 80.65; H, 12.18;. Found: C,80.82; H,12.71. FT-IR (ATR): (cm^{-1}) 3050, 2955, 2925, 2855,1593, 1506, 1467, 1378, 1381, 1254, 1223, 911, 752. Mass (EI$^+$): (m/z) 559 (M$^{+\bullet}$).

3.3.6 1,2-Dinitro-4,5-bis(2-hexyldecyloxy)benzene (6)
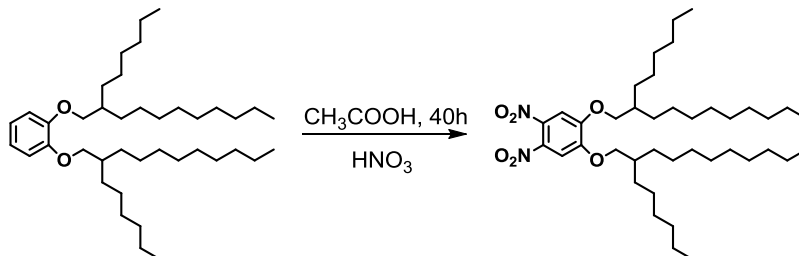
1.2-Dinitro-4,5-bis(2-hexyldecyloxy)benzene (**6**) was prepared using the procedure outlined by Sessler *et al.*[119] To a solution of 1,2-bis(2-hexyldecyloxy)benzene (**5**) (0.70 g, 1.2 mmol) in DCM (8 mL) was added acetic acid (9 mL). The solution was cooled down to 6 °C and HNO_3 (65 %, 1 mL) was added dropwise. The reaction mixture was left to react at room temperature for 1 hour. The reaction mixture was cooled to 6 °C, and the flask was charged with fuming nitric acid (3 mL). The reaction was stirred for 40 hours, over the course of which time a yellow solid precipitated. On completion, the reaction mixture was poured onto ice resulting in the formation of more yellow precipitate. The mixture was then extracted with two portions of DCM (2×300 mL). The organic layers were combined and washed with water, sat. with $NaHCO_3$ (aq), brine, and dried over $MgSO_4$. Evaporation of the solvent gave the crude product 1,2-dinitro-4,5-bis(2-hexyldecyloxy)benzene (**6**) as a transparent yellow liquid, yield (0.69 g, 1.0 mmol, 86 %). ^1H NMR (400 MHz, $CDCl_3$) δ_H/ppm: 7.29 (s, 2H), 3.97 (d, 4H, J= 5.3 Hz), 1.85 (m, 2H), 1.26 (m, 48H), 0.89 (t, 12H, J= 4.2 Hz). ^{13}C NMR (400 MHz, $CDCl_3$) δ_C/ppm: 152.1, 136.4, 107.5, 72.5, 37.8, 31.9, 31.8, 31.2, 30.1, 29.6, 29.3, 26.8, 22.6, 14.1; (Anal.Calcd. for $C_{38}H_{68}N_2O_4$: C, 70.69; H, 10.72; N, 4.14. Found: C, 69.98; H, 11.07; N, 4.30. FT-IR (ATR): (cm^{-1}) 3072, 2955, 2926, 2855,1590, 1537, 1466, 1370, 1353, 1336, 1284, 1223, 911, 752. Mass (EI$^+$): (m/z) 648 (M$^{+\bullet}$).

3.3.7 2,11-Dibromo-6,7,15,16-tetrakis(2-hexyldecyloxy)quinoxalino [2',3':9,10]phenanthro[4,5-abc]phenazine (8)
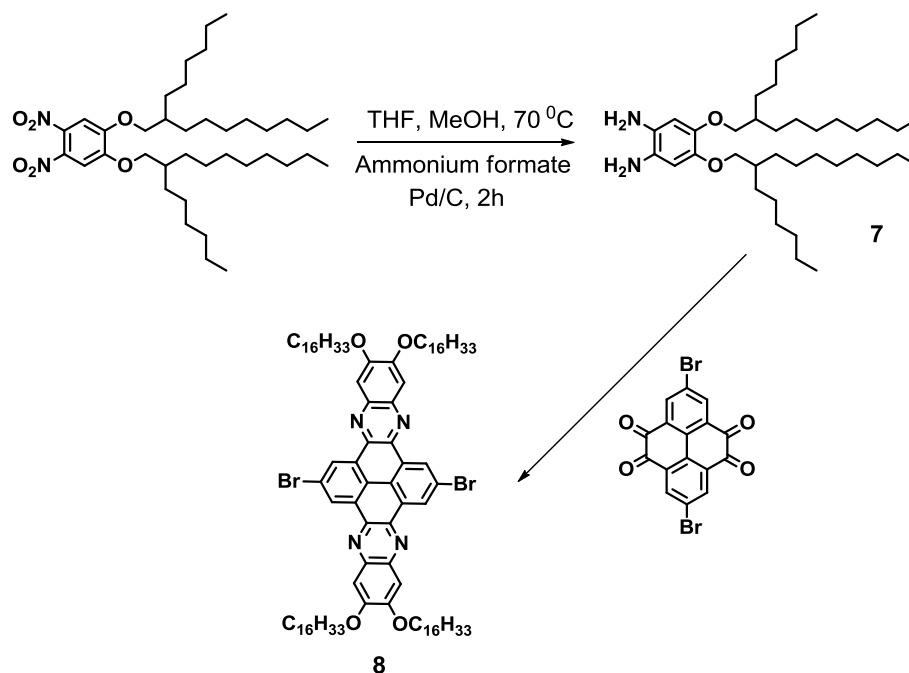
The preparation of 2,11-dibromo-6,7,15,16-tetrakis(2-hexyldecyloxy)quinoxalino [2',3':9,10]phenanthro[4,5-abc]phenazine (**8**) proceeded *via* two steps. The unstable 1,2-Diamino-4,5-bis(2-hexyldecyloxy)benzene (**7**) was produced initially; then was used directly, without purification, to produce (**8**). The intermediate compound (**7**) was prepared using a modified method outlined by MacLachlan.[120] To a solution of 1,2-dinitro-4,5-bis(2-hexyldecyloxy)benzene (**6**) (1.00 g, 1.6 mmol) in a mixture of methanol (40 mL) and THF (20 mL) were added 10% of Pd/C (0.10 g) and ammonium formate (0.82 g, 0.01 mmol). The mixture was left to stir under inert gas for 10 minutes at room temperature. The mixture was then heated to 70 ^{0}C for 2 hours until the solution became clear and colourless. After cooling down to room temperature, the catalyst was removed by filtration through a Schlenk frit, to yield a colourless filtrate. The solvent was removed under *vacuum*. Degassed water and chloroform were added to the flask, and the product was extracted into the chloroform under nitrogen. The chloroform was removed under *vacuum* to yield the green oily air-sensitive compound 1,2-diamino-4,5-bis(2-hexyldecyloxy)benzene (**7**) in the yield (0.20 g, 0.3 mmol, 23%). 2,11-Dibromo-6,7,15,16-tetrakis(2-hexyldecyloxy) quinoxalino[2',3':9,10] phenanthro [4,5 -abc]phenazine (**8**) was synthesised using a

modified method outlined by Harris *et al.*[121] 1,2-Diamino-4,5-bis(2-hexyldecyloxy)benzene (**7**) (2.51 g, 4.1 mmol) was added to a solution of 2,7-dibromopyrene-4,5,9,10-tetraone (**3**) (0.71g, 1.6 mmol) in toluene (50 mL) under argon, in a flame-dried schlenk flask. The solution was stirred for 24 hours under reflux (120 °C). The solvent was removed *in vacuo* to yield a dirty orange solid. The product was purified *via* column chromatography using hexane and toluene (2:1; v/v) as the eluent. The pure product was obtained as an orange solid. This was recrystallised from ethanol to give the pure product (**8**) in a yield of (1.71 g, 1.1 mmol, 67 %). ^{1}H NMR (400 MHz, CDCl$_3$) δ_H/ppm: 9.51(s, 4H), 7.52 (s, 4H), 4.17 (d, 8H, J=5.0 Hz), 2.00 (m, 4H), 1.26 (m, 96H), 0.92 (t, 24H, J=7.0 Hz). ^{13}C NMR (400 MHz, CDCl$_3$) δ_C/ppm: 154.3, 140.3, 138.2, 130.9, 127.6, 123.5 122.4, 106.1, 71.8, 37.9, 32.2, 31.9, 31.4, 30.7, 30.2, 29.9, 29.8, 29.7, 29.4, 29.1, 27.0, 26.9, 22.8, 22.7, 14.1; (Anal.Calcd. for C$_{92}$H$_{140}$Br$_2$N$_4$O$_4$: C, 72.41; H, 9.25; Br, 10.47; N, 3.67; O, 4.19;. Found: C, 73.01; H, 9.11; Br, 10.98; N, 3.82. M.p, 172-174 ºC. FT-IR (ATR): (cm^{-1}) 3070, 2955, 2924, 2854, 2730, 1796, 1625, 1584, 1529, 1466, 1395, 1377, 1353, 1316, 1208, 1166, 1124, 1096, 985, 914, 889, 729. Mass (MALDI-TOF): (m/z) 1523, 1525, 1527 (M$^{+\bullet}$).

3.3.8 6,7,15,16-Tetrakis(2-hexyldecyloxy)-2,11-di(thiophen -2-yl) quinoxalino[2',3':9,10]phenanthro[4,5-abc]phenazine (9)
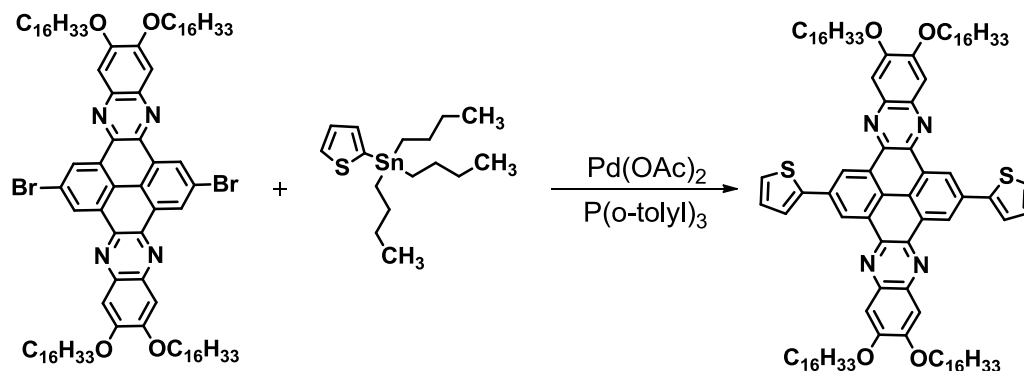
6,7,15,16-Tetrakis(2-hexyldecyloxy)-2,11-di(thiophen-2-yl) quinoxaline [2',3':9,10] phenanthro [4,5-abc]phenazine (**9**) was synthesised from a modified procedure outlined by Helgesen *et al.*[122] To a solution of 2,11-dibromo-6,7,15,16-tetrakis(2-hexyldecyloxy) quinoxalino [2',3':9,10]phenanthro[4,5-abc]phenazine (**8**) (1.49 g, 0.9 mmol), palladium acetate (2.0 mg, 0.1 mmol) and tri-o-tolylphsophine (122 mg, 0.4 mmol) in dry toluene (15

mL) was added 2-tributylstannylthiophene (1.0 mL, 1.17 g, 0.3 mmol). The reaction mixture was heated under an argon atmosphere for reflux for 72 hours. Upon completion, the resulting product was concentrated *in vacuo*. Gradient column chromatography (hexane followed by hexane:chloroform (2:1 v/v)) was used as the eluent. The solid was recrystallised from ethanol to give the pure product (**9**) as an orange powder in a yield of (1.45 g, 0.9 mmol, 96 %). ^{1}H NMR (400 MHz, CDCl$_3$) δ_H/ppm: 9.56 (s, 4H), 7.80 (s, 4H), 7.49 (d, 2H, J=5.4 Hz), 7.39 (d, 2H, J=5.5 Hz), 7.18 (t, 2H, J=3.6 Hz), 4.14 (d, 8H, J=5.0), 2.02 (m, 4H), 1.28 (m, 96H), 0.87 (t, 24H, J=6.7 Hz). ^{13}C NMR (400 MHz, CDCl$_3$) δ_C/ppm: 153.7, 144.7, 140.0, 139.5, 132.6, 129.9, 128.0, 125.0, 124.6, 124.1, 121.9, 106.4, 71.7, 38.1, 32.0, 31.5, 31.2, 29.9, 29.8, 29.5, 29.2, 27.0, 23.2, 22.8, 22.7, 14.2; (Anal.Calcd. for C$_{100}$H$_{146}$N$_4$O$_4$S$_2$: C, 78.38; H, 9.60; N, 3.66; O, 4.18; S, 4.18; Found: C, 78.38; H, 9.60; N, 3.66; S, 4.18. M.p, 188-190 ºC. FT-IR (ATR): (cm^{-1}) 3070, 2953, 2917, 2850, 2730, 2117, 1610, 1521, 1565, 1453, 1405, 1330, 1208, 1166, 1124, 1096, 985, 914. Mass (MOLDI-TOF): (m/z) 1532 (M$^{+\bullet}$).

3.3.9 2,11-Bis(5-bromothiophen-2-yl)-6,7,15,16-tetrakis (2-hexyldecyloxy)-5,8-dihydroquinoxalino[2',3':9,10]phenanthro [4,5-abc]phenazine (10)
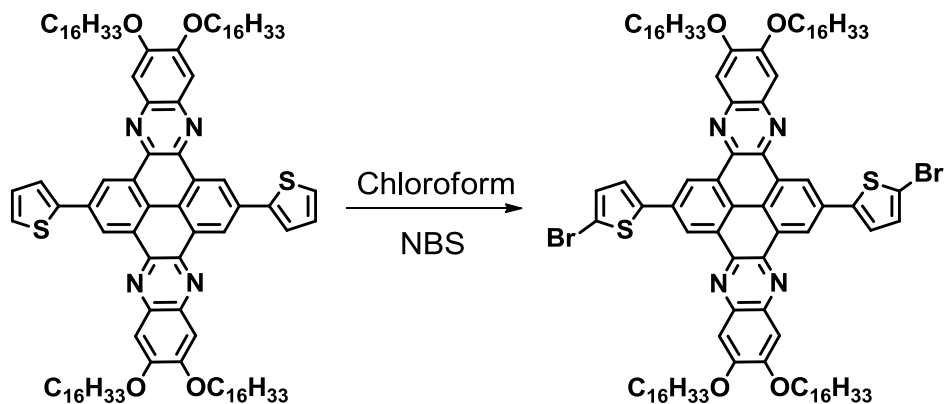
The preparation of 2,11-bis(5-bromothiophen-2-yl)-6,7,15,16-tetrakis (hexadecyloxy) quinoxalino[2',3':9,10]phenanthro[4,5-abc]phenazine (**10**) followed a modified procedure outlined by Qin *et al.*[123] To a solution of 6,7,15,16-tetrakis(2-hexyldecyloxy)-2,11-di(thiophen-2-yl) quinoxalino[2',3':9,10]phenanthro[4,5-abc]phenazine (**9**) (0.71 g, 0.4 mmol) in dried chloroform (40 mL) was added NBS (0.17 g, 0.9 mmol) in one portion. The mixture was stirred for 72 hours in the dark. The solvent was removed under reduced pressure. This product could not be purified using either column chromatography or recrystallisation. Therefore, preparative HPLC was employed in which the method of purification was developed on a system which included a Waters 2487 Dual λ Absorbance Detector, Waters 2690 Separation Module, and a reversed-phase HPLC column Altima HP C18 HL 5μ (length 150 mm, ID 4.6 mm). After a period of 20 minutes, the solvent system included 80 to 100% THF in water and the flow rate was 1 cm^3 min^{-1}. A preparative HPLC system including a Varian Automatic Fraction Collector, Varian ProStar (two pumps, UV-Vis Detector), and a reversed-phase HPLC column Altima HP C18 HL 5μ (length 150 mm, ID 22 mm) was used to perform the process of purification. The samples were first made as solutions in THF (100 mg cm^{-3}), following which 0.475 mL of the sample solution was injected every time. In this mobile phase, the flow rate was 20 cm^3 min^{-1}. The elution system (mobile phase) included water (A) and THF (B). The gradient used was 60 % B for

a duration of 33 minutes, followed by 60 % to 95 % B for 1 min, and then 95 % B for a period of 6 minutes. After this, from 95 % to 60 % B for 1 min, and lastly 60 % B for 9 minutes. For each injection, the total time duration was 50 minutes. The collection of pure compound was done between 21 to 29 minutes. The product was obtained as a yellow solid (0.70 g, 0.4 mmol, 90%). ^{1}H NMR (400 MHz, CDCl$_3$) δ_H/ppm: 8.92 (s, 4H), 7.24 (s, 4H), 7.03 (m, 4H), 4.17 (d, 8H, J=5.0 Hz), 2.05 (m, 4H), 1.26 (m, 96H), 0.95 (t, 24H, J=5.8 Hz). ^{13}C NMR (400 MHz, CDCl$_3$) δ_C/ppm: 154.3, 145.2, 141.4, 140.9, 133.1, 130.8, 129.1, 126.3, 125.3, 124.5, 122.9, 106.5, 71.9, 38.1, 32.0, 31.6, 31.2, 29.9, 29.8, 29.6, 29.2, 27.3, 23.1, 22.9, 22.4, 14.1; (Anal.Calcd. for C$_{100}$H$_{154}$Br$_2$N$_4$O$_4$S$_2$: C, 70.64; H, 9.13; Br, 9.40; N, 3.30; S, 3.77; Found: C, 70.12; H, 10.13; Br, 9.59; N, 2.99; S, 3.75. M.p, 196-198 ºC. FT-IR (ATR): (cm^{-1}) 3070, 2953, 2917, 2850, 2730, 2117, 1610, 1521, 1565, 1453, 1405, 1330, 1208, 1166, 1124, 1096, 985, 914, 891, 729. Mass (MALDI-TOF): (m/z) 1686, 1688, 1690 (M$^{+\bullet}$).

3.3.10 1,2-Dibromo-4,5-dinitrobenzene (11)
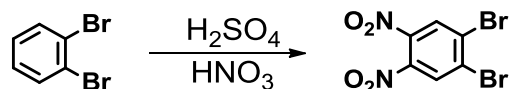
The preparation of 1,2-dibromo-4,5-dinitrobenzene (**11**) involved using a modified method outlined by Frode and co-workers.[124] 1,2-Dibromobenzene (70.8 g, 0.3 mol) was added dropwise over 20 min to an ice-cold, stirred mixture of nitric acid (100%, 200 mL, 4.8 mol) and sulphuric acid (98%, 150 mL, 27.0 mol). The solution was heated up to 150 ^{0}C for 10 hours, cooled and poured into ice-water. The solid slowly precipitated over 48 hours, and then was filtered off and washed with water three times. The crude product was recrystallised from ethanol:acetic acid (8:2; v/v) to give 1,2-dibromo-4,5-dinitrobenzene (**11**) as a pale yellow solid in a yield of (32.5 g, 0.1 mol, 33% yield). ^{1}H NMR (400 MHz, CDCl$_3$) δ_H/ppm: 8.20 (s, 2H); ^{13}C NMR (400 MHz, CDCl$_3$) δ_C/ppm: 129.5, 130.7, and 141.3. Anal.Calcd for C$_6$H$_2$Br$_2$N$_2$O$_4$: C, 22.11; H, 0.62; Br, 49.04; N, 8.60. Found: C, 22.10; H, 0.64; Br, 50.04; N, 8.59. M.p. 159-161 °C, lit (160-161 ^{0}C)[125]. FT-IR (cm^{-1}): 3099,

2522, 2159, 2024, 1977, 1579, 1524, 1453, 1353, 1330, 1240, 1164, 1112, 1083, 899, 884, 852, 771, 752, 739, 678, 667, 613; Mass (EI$^+$): (m/z) 323.8, 325.8, 327.8 (M$^{+\bullet}$).

3.3.113-Pentyl undec-1-yne (12)
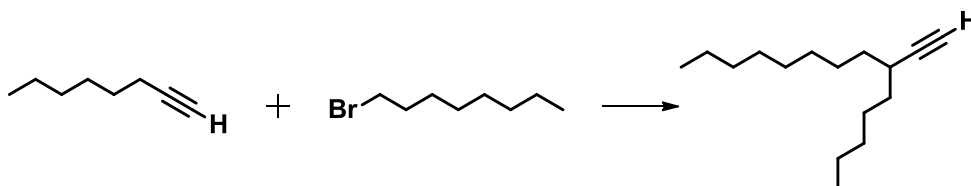
The production of 3-pentylundec-1-yne (**12**) followed the modified method outlined by Ding and co-workers.[126] In a 500 mL flask purged with argon, was added dry hexane (220 mL) and 1-octyne (32.4 g, 0.2 mol). Then n-BuLi (2.5M in hexane, 194 mL, 0.4 mol) was added dropwise at -78 ^{0}C in a dry ice/acetone bath. After stirring at -78 ^{0}C for 30 min, the solution was warmed up to -42 ^{0}C using an acetonitrile/dry ice bath for 1 hour. Freshly distilled 1-bromooctane (38.0 g, 0.2 mol) was added and the mixture was allowed to slowly warm up to room temperature overnight. The reaction was cooled using an ice-water bath. Once cool, HCl (6 M, 220 mL) was slowly added to quench the reaction. The organic phase was separated and washed with deionised water, and dried over MgSO$_4$. The product (**12**) was purified by vacuum distillation to give a pale yellow oil in a yield of (24.6 g, 0.1 mol, 40 %). ^{1}H NMR (400 MHz, CDCl$_3$) δ_H/ppm: 2.32 (m, 1H), 2.05 (d, 1H, J=2.4 Hz), 1.61–1.22 (m, 22H), 0.90 (m, 6H); ^{13}C NMR (400 MHz, CDCl$_3$) δ_C/ppm: 88.3, 68.8, 34.9. 34.9, 31.8, 31.7, 31.5, 29.7, 29.5, 29.3, 28.3, 27.2, 26.9, 22.6, 22.5, 14.1; Anal.Calcd. for C$_{16}$H$_{30}$: C, 86.40; H, 13.60. Found: C, 86.41; H, 13.59. FT-IR (cm^{-1}): 3313, 2926, 2871, 2858, 2730, 2671, 2112, 2028, 1639, 1466, 1378, 1342, 1302, 1239, 1120, 1100, 1076, 967, 891, 723, 627. Mass (EI$^+$): (m/z) 222.2 (M$^{+\bullet}$).

3.3.12 1,2-Dinitro-4,5-bis(3-pentylundec-1-yn-1-yl)benzene (13)
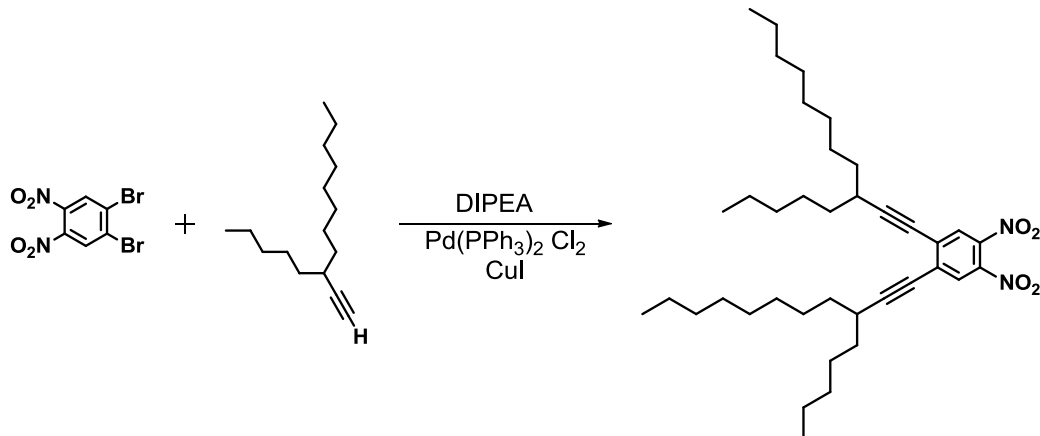
1,2-Dinitro-4,5-bis(3-pentylundec-1-yn-1-yl)benzene (**13**) was synthesised using a modified method of Chi and co-workers.[127] 1,2-Dibromo-4,5-dinitrobenzene (**11**) (2.1 g, 6.5 mmol), Pd(PPh$_3$)Cl$_2$ (227 mg, 0.3 mmol) and CuI (123 mg, 0.6 mmol) were added into a flask under the protection of an inert nitrogen atmosphere. DIPEA (4.2 g, 32.4 mmol) was then added followed by a solution of 3-pentyl undec-1-yne (**12**) (6.8 g, 16.2 mmol) in THF (25 mL, dry and oxygen free). The reaction mixture was then stirred at reflux overnight. Upon completion, the reaction was cooled to room temperature. The reaction was quenched *via* addition of a saturated solution of ammonium chloride. The reaction mixture was then extracted with ethyl acetate (EA) (3 x 50 mL), washed with deionised water (3 x 50 mL) and dried over MgSO$_4$. The solvent was removed *in vacuo* and the product purified *via* silica gel column chromatograph using a gradient eluent system (hexane: toluene 150: 1 to 50: 1) to give the pure target product (**13**) as an orange oil in a yield of (2.80 g, 4.5 mmol, 71 %). ^{1}H NMR (400 MHz, CDCl$_3$) δ_H/ppm: 8.87 (s, 2H), 2.61 (m, 2H), 1.62–1.23 (m, 44H), 0.89 (m, 12H); ^{13}C NMR (400 MHz, CDCl$_3$) δ_C/ppm: 140.6, 131.8, 128.1, 106.0, 34.7, 34.7, 32.9, 31.8, 31.7, 29.7, 29.5, 29.3, 27.5, 27.2, 22.6, 22.5, 14.0; Anal.Calcd for C$_{38}$H$_{60}$N$_2$O$_4$: C, 74.96; H, 9.93; N, 4.60. Found: C, 74.3; H, 10.2; N, 4.50. FT-IR (cm^{-1}): 3167, 3104, 3079, 3048, 2956, 2928, 2856, 2729, 2670, 2381, 2222, 2029, 1795, 1617, 1595, 1543, 1466, 1358, 1241, 1219, 1198, 1143, 1119, 1095, 1076, 1040, 973, 906, 849, 831, 779, 755, 724, 660 ; Mass (EI$^+$): (m/z) 609 (M$^{+\bullet}$)

3.3.13 2,11-Dibromo-6,7,15,16-tetrakis (3-pentyl undecyl) quinoxalino [2`,3`:9,10] phenanthro [4,5-abc] phenazine (15)
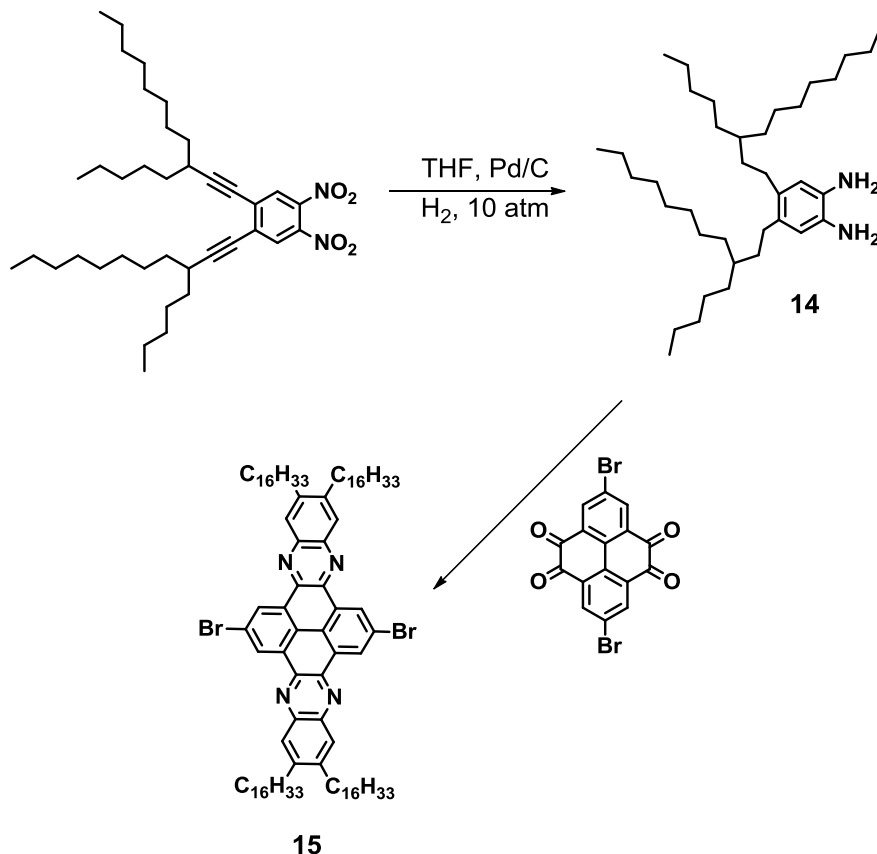
The preparation of 2,11-Dibromo-6,7,15,16-tetrakis (3-pentyl undecyl) quinoxalino [2`,3`:9,10] phenanthro [4,5-abc] phenazine (**15**) proceeded through two steps. The unstable 4,5-bis(3-pentylundecyl)benzene-1,2-diamine (**14**) was produced initially. This was then used directly to produce (**15**). 1,2-Dinitro-4,5-bis(3-pentylundec-1-yn-1-yl)benzene (**13**) (2.50 g, 4.1 mmol) was hydrogenated in anhydrous THF (40 mL) in the presence of 10% Pd/C (0.4 g) under a hydrogen atmosphere (10 atm). The reaction was filtered under an inert atmosphere. The filtrate was concentrated *in vacuo* to give 4,5-bis(3-pentylundecyl)benzene-1,2-diamine (**14**) as a green liquid in a yield of (2.19 g, 4.3 mmol, 96 %). As the product is unstable, no further purification was undertaken and the product was reacted directly into the next step. The preparation of 2,11-dibromo-6,7,15,16-tetrakis (3-pentyl undecyl) quinoxalino [2`,3`:9,10] phenanthro [4,5-abc] phenazine (**15**) was conducted using a modified method outlined by Harris *et al.*[121] 4,5-Bis(3-

pentylundecyl)benzene-1,2-diamine (**14**) (2.52 g, 4.5 mmol) was added to a solution of 2,7-dibromopyrene-4,5,9,10-tetraone (**3**) (0.76 g, 1.8 mmol) in toluene (50 mL) under argon, in a flame-dried schlenk flask. The solution refluxed (120 °C) for 24 hours. The solvent was removed *in vacuo* and the crude material purified *via* column chromatography using hexane:toluene (8:2; v/v) as the eluent. The still crude material was purified again, *via* recrystallisation with ethanol to give (**15**) in a yield of (2.43 g, 1.6 mmol, 92 %). ^{1}H NMR (400 MHz, CDCl$_3$) δ_H/ppm: 9.54 (s, 4H), 7.98 (s, 4H), 2.73 (t, 8H, J=8.0 Hz), 1.69 (t, 8H), 1.45–1.21 (m, 92H), 0.90 (t, 24H, J=6.1 Hz); ^{13}C NMR (400 MHz, CDCl$_3$): δ_C/ppm 145.6, 140.9, 139.6, 130.4, 128.8, 127.2, 123.9, 122.8, 38.0, 34.7, 33.7, 33.6, 32.5, 32.0, 30.3, 30.1, 29.8, 29.5, 26.9, 26.5, 22.8, 22.7, 14.2, 14.1; Anal.Calcd for C$_{92}$H$_{140}$Br$_2$N$_4$: C, 75.58; H, 9.65; N, 3.83; Br, 10.93. Found: C, 75.75; H, 9.53; N, 3.87; Br, 11.19. M.p. 209-211°C. FT-IR (cm^{-1}): 3078, 2955, 2924, 2854, 2729, 1797, 1623, 1585, 1528, 1466, 1395, 1377, 1353, 1316, 1208, 1166, 1124, 1096, 985, 914, 888, 797, 749, 729, 721, 623; Mass: (m/z) (MALDI-TOF) 1460, 1462, 1464 (M$^{+\bullet}$).

3.3.14 6,7,15,16-Tetrakis (3-pentyl undecyl) -2,11-di(thiophen-2-yl) quinoxalino[2',3':9,10]phenanthro[4,5-abc]phenazine (16)
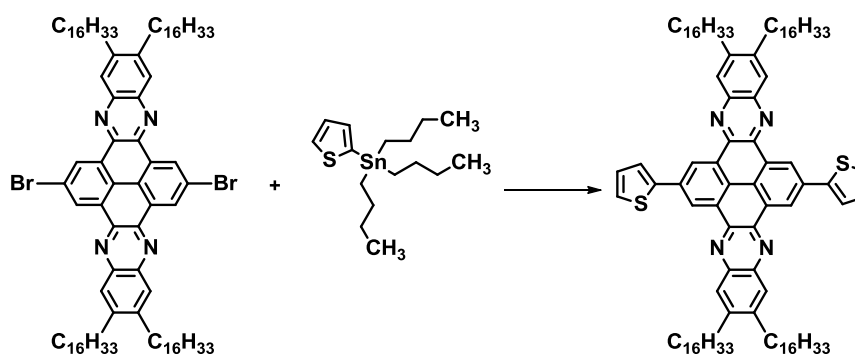
6,7,15,16-Tetrakis (3-pentyl undecyl) -2,11-di(thiophen-2-yl) quinoxalino[2',3':9,10] phenanthro[4,5-abc]phenazine (**16**) was synthesised from a modified procedure outlined by Helgesen and colleges.[122] To a solution of 2,11-dibromo-6,7,15,16-tetrakis (3-pentyl undecyl) quinoxalino [2`,3`:9,10] phenanthro [4,5-abc] phenazine (**15**) (1.50 g, 1.1 mmol), palladium acetate (22 mg, 0.1 mmol) and tri-o-tolylphsophine (121 mg, 0.4 mmol) in dry

toluene (15 mL) was added 2-tributylstannylthiophene (1.00 mL, 1.17 g, 0.3 mmol). The reaction mixture was heated to reflux for 72 hour under an argon atmosphere. The resulting product was concentrated *in vacuo*. Gradient silica gel column chromatography (hexane followed by hexane:chloroform (2:1; v/v)) was used as the eluent. The solid product was recrystallised from ethanol to give a pure orange product (**16**) in the yield of (1.42 g, 0.9 mmol, 91 %). ^{1}H NMR (400 MHz, CDCl$_3$) δ_H/ppm: 9.35 (s, 4H), 7.76 (s, 4H), 7.74 (dd, 2H, J$_1$= 4.9 Hz, J$_2$=1.1 Hz), 7.47 (dd, 2H, J$_1$=5.0 Hz, J$_2$=1.0 Hz), 7.22 (t, 2H, J=4.1 Hz), 2.59 (t, 8H, J=8.2 Hz), 1.75 (t, 8H), 1.55-1.30 (br, 92H), 0.97 (t, 24H); ^{13}C NMR (400 MHz, CDCl$_3$) δ_C/ppm: 144.9, 144.5, 141.0, 140.8, 133.0, 129.5, 128.1, 127.3, 125.2, 125.1, 124.4, 123.1, 38.2, 34.8, 33.7, 32.0, 30.4, 30.1, 29.9, 29.5, 26.9, 26.6, 22.9, 22.7, 14.3, 14.1; Anal.Calcd for C$_{100}$H$_{146}$N$_4$S$_2$: C, 81.80; H, 10.02; N, 3.82. Found: C, 81.92; H, 9.77; N, 3.89; M.p. 233-235 °C. FT-IR (cm^{-1}): 3070, 2953, 2917, 2850, 1610, 1521, 1465, 1453, 1405, 1375, 1330, 1269, 1165, 1132, 1096, 985, 914, 878, 790, 745, 721, 623; Mass: (m/z) (MALDI-TOF) 1468.1(M$^{+\bullet}$).

3.3.15 2,11-Bis(5-bromothiophen-2-yl)-6,7,15,16- tetrakis (3-pentyl undecyl) quinoxalino [2',3':9,10]phenanthro[4,5-abc]phenazine (17)
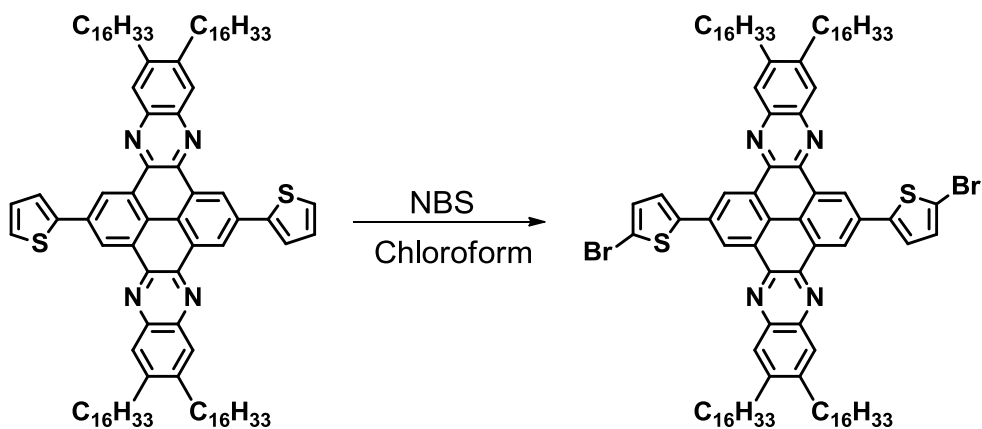
The preparation of 2,11-bis(5-bromothiophen-2-yl)-6,7,15,16- tetrakis (3-pentyl undecyl) quinoxalino [2',3':9,10]phenanthro[4,5-abc]phenazine (**17**) followed a modified procedure

outlined by Qin *et al.*[123] To a solution of 6,7,15,16-tetrakis (3-pentyl undecyl)-2,11-di(thiophen-2-yl) quinoxalino[2',3':9,10]phenanthro[4,5-abc]phenazine (**16**) (1.14 g, 0.7 mmol) in dried chloroform (40 mL) was added NBS (303 mg, 1.7 mmol) in one portion. The mixture was stirred for 72 hour in the dark. The solvent was removed *in vacuo*. The crude material was purified *via* silica gel column chromatography using hexane:toluene (7:3; v/v) as the eluent. The still crude material was then recrystallisation from ethanol to yield (**17**) as a yellow solid in a yield of (1.1 g, 0.6 mmol, 87%). ^{1}H NMR (400 MHz, CDCl$_3$) δ_H/ppm: 8.92 (s, 4H), 7.70 (s, 4H), 7.28 (d, 2H, J=3.6 Hz), 7.04 (d, 2H, J=3.7 Hz), 2.63 (t, 8H, J=8.0 Hz), 1.75 (t, 8H), 1.55-1.30 (m, 92H), 0.96 (t, 24H, J= 5.1 Hz); ^{13}C NMR (400 MHz, CDCl$_3$) δ_C/ppm: 145.5, 144.8, 140.6, 140.2, 131.4, 130.8, 129.1, 127.1, 124.4, 123.9, 121.7, 111.8, 38.3, 34.8, 33.8, 33.7, 32.6, 32.0, 30.4, 30.1, 29.9, 29.6, 27.0, 26.6, 22.9, 22.8, 14.3, 14.2; Anal.Calcd for C$_{100}$H$_{144}$Br$_2$N$_4$S$_2$: C, 73.86; H, 8.93; Br, 9.83; N, 3.45; Found: C, 73.94; H, 8.94; N, 3.55; Br, 10.21. M.p. 272-274 °C. FT-IR (cm^{-1}): 3070, 2954, 2920, 2851, 1609, 1519, 1445, 1404, 1376, 1353, 1332, 1264, 1220, 1192, 1134, 1096, 975, 891, 788; Mass: (m/z) (MALDI-TOF) 1625.9, 1627.9, 1629.9 (M$^{+\bullet}$).

3.3.16 4,7-Dibromo-2,1,3-benzothiadiazole (18)
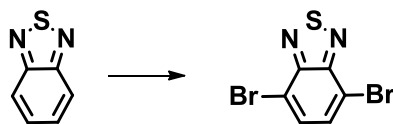
4,7-Dibromobenzo[c][1,2,5]thiadiazole (**18**) was prepared using a modified method outlined by Zoombelt *et al.*[128] A mixture of 2,1,3-benzothiadiazole (10 g, 0.07 mmol) in hydrobromic acid HBr (48 %, 10 mL, 0.2 mol) was flushed with nitrogen and heated to 100 °C. The reaction mixture was charged with Br$_2$ (11 mL, 0.2 mmol) in dropwise manner over 1 hour. Upon complete addition, a further portion of aq. HBr (48 %, 50 mL, 0.9 mol) was added and the mixture was left to stir at 120 ^{0}C for 3 hours. On completion, the reaction mixture was filtered, while still hot, and the precipitate was thoroughly washed with deionised water. More precipitation occurred while the filtrate was cooling down. Thus, the precipitate was filtered off again and washed with further portions of deionised

water. The remaining bromine was destroyed by pouring the filtrate into a solution of sodium thiosulphate ($Na_2S_2O_3$) (10 % w/w). The crude product was recrystallised from ethanol twice. The still crude material was recrystallised again from a hexane:chloroform (1:2; v/v) mixture to give pure product (**18**) as off-white needles crystals in a yield of (21.04 g, 72.1 mmol, 97 %).^{1}H NMR (400 MHz, $CDCl_3$) δ_H/ppm: 7.76 (s, 2H). ^{13}C NMR (400 MHz, $CDCl_3$) δ_C/ppm: 152.9, 132.3, 113.9. FT-IR (ATR): (cm-1) 3079, 3045, 1650, 1587, 1498, 1475, 1375, 1309, 1272, 1183, 1121, 1080, 1019, 934, 873, 842, 824, 793, 743, 730, 705, 686, 656, 632, 615, 585. M.p. 186 – 187 °C, (lit, 189-190 [0]C)[129] FT-IR (cm^{-1}) 3070, 3047, 1858, 1475, 1309, 1183, 934, 829, 823, 873, 730. Anal.Calcd for $C_6H_2Br_2N_2S$: C, 24.51; H, 0.69; N, 9.53; Br, 54.36. Found: C, 23.45; H, 0.69; N, 10.39; Br, 53.41. Mass (EI^+): (m/z) 292, 294, 296 ($M^{+\bullet}$).

3.3.17 4,7-Di(thiophen-2-yl)benzo[c][1,2,5]thiadiazole (19)
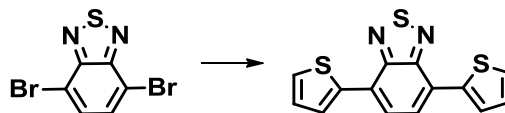
4,7-Di(thiophen-2-yl)benzo[c][1,2,5]thiadiazole (**19**) was prepared using a modified procedure outlined by Palama and co-workers.[130] A mixture of 4,7-dibromo-2,1,3-benzothiadiazole (**18**) (5 g, 17.0 mmol) and 2-(tributylstannyl)thiophene (13 mL, 37.6 mmol) was placed under an inert atmosphere of Ar. Dry toluene (50 mL) was then added. The resulting solution was degassed again. Palladium acetate (0.30 g, 1.3 mmol) and tri-o-tolylphosphine (1.65 g, 5.4 mmol) were then added. The reaction mixture was degassed again, heated to 110 °C and left overnight. The reaction was cooled to room temperature and the solvent was removed *in vacuo*. Dry column chromatography with a mixture of DCM and hexane (1:1; v/v) was used to purify the crude product. The still crude product was recrystallised from (ethanol:toluene, 9:1 v/v) to yield pure 4,7-di(thiophen-2-yl)benzo[c][1,2,5]thiadiazole (**19**) as a red solid in a yield of (4.23 g, 14.1 mmol, 82 %). ^{1}H NMR (400 MHz, $CDCl_3$) δ_H/ppm: 8.13 (d, 2H, J = 3.6 Hz); 7.89 (s, 2H); 7.48 (d, 2H, J = 5.0 Hz); 7.23 (dd, 2H, J_1=4.8 Hz, J_2=3.8 Hz). ^{13}C NMR $CDCl_3$ δ_C/ppm: 152.6, 139.3,

128.0, 127.5, 126.8, 125.9, 125.7. M.p. 123-124 °C, (lit, 123-125 ^{0}C)[131] FT-IR (cm^{-1}) 3093, 3019, 1857, 1661, 1480, 1215, 1072, 823, 817. Anal.Calcd for $C_{14}H_8N_2S_3$: C, 42.65; H, 2.05; N, 7.11; S, 8.13. Found: C, 42.47; H, 1.72; N, 6.97; S, 10.22. Mass (EI+): (m/z) 300.0 (M$^{+\bullet}$).

3.3.18 4,7-Bis(5-(trimethylstannyl)thiophen-2-yl)benzo [c] [1,2,5] thiadiazole (20)
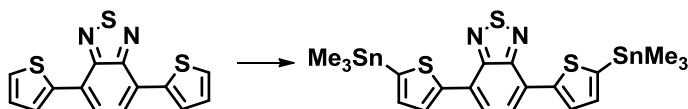
The synthesis of 4,7-bis(5-(trimethylstannyl)thiophen-2-yl)benzo[c][1,2,5] thiadiazole (**20**) was performed according to a modified procedure outlined by Reichmanis and co-workers.[132] 2,2,6,6-Tetramethylpiperdine (1.4 mL, 1.21 g, 8.6 mmol, 2.6 eq) was dissolved into dry THF (20 mL) under an inert atmosphere. The solution was cooled to -78°C and n-Butyllithium (3.4 mL, 2.5 M solution in hexane, 2.35 g, 8.6 mmol, 2.6 eq.) was added into the solution rapidly. The resulting solution was stirred at -78 °C for 30 min. The solution was then warmed to room temperature and stirred for 10 min to afford lithium 2,2,6,6-tetramethylpiperidide (LTMP). The solution was cooled to -78 °C and 4,7-di(thiophen-2-yl)benzo[c][1,2,5]thiadiazole (**19**) (1.0 g, 3.3 mmol, 1.0 eq) in THF (15 mL) was added in a dropwise manner. During this time the colourless solution turned purple. On complete addition, the resulting solution was stirred at -78 °C for 45 min. Trimethyltin chloride (8.3 mL, 1.0 M solution in THF, 8.3 mmol, 2.5 eq) was then added in a dropwise manner. During this time the solution turned from purple to orange. The solution was then warmed to room temperature and was stirred for 12 hours. Brine (20 mL) was added and the mixture was extracted into CH_2Cl_2 (3 x 30 mL). The organic extracts were combined, washed with brine (3 x 60 mL) and dried over anhydrous $MgSO_4$. The $MgSO_4$ was removed *via* filtration and the solvent was removed *in vacuo*. The crude material was recrystallised from ethanol to give (**20**) as orange needle-like crystals in a yield of (1.29 g,

2.1 mmol, 90 %). ^{1}H NMR (400 MHz, CDCl$_3$) δ_H/ppm: 8.20 (d, 2H, J=3.4 Hz); 7.88 (s, 2H), 7.32 (d, 2H, J=3.4 Hz,); 0.45 (s, 18H). ^{13}C NMR (400 MHz, CDCl$_3$) δ_C/ppm: 152.6, 145.0, 140.2, 136.2, 135.9, 128.3, 125.8, -8.1. M.p. 170-171 [0]C. FT-IR (cm^{-1}) 3040, 2967, 2911, 1871, 1517, 1203, 1046, 946, 795, 761, 711, 536. Anal.Calcd for C$_{20}$H$_{24}$N$_2$S$_3$Sn$_2$, C, 38.37; H, 3.86; N, 4.47; S, 15.37; Sn, 37.92. found, , C, 38.42; H, 3.22; N, 4.51. Mass (EI[+]): (m/z) 626.0 (M[+•]).

3.3.19 1,2-Bis(octyloxy)benzene (21)
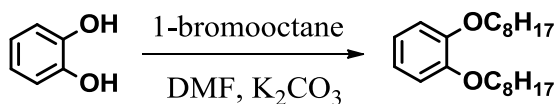
1,2-Bis(octyloxy)benzene (**21**),[118] was prepared according to a modified method outlined by Janssen and co-workers.[133] To a solution of 1,2-dihydroxybenzene (20.0 g, 181.7 mmol) in dry DMF (100 mL) were added K$_2$CO$_3$ (76.0 g, 5.0 mmol) and 1-bromooctane (80.5 g, 72 mL, 416.8 mol). The mixture was left to stir under an inert atmosphere for 48 hours at 100 [0]C. After cooling the mixture to room temperature, the reaction was quenched with water (100 mL). The organic phase was separated, and the aqueous phase was extracted with DCM (3 x 100 mL). The organic phases were combined and dried over MgSO$_4$. After filtration, the mixture was concentrated *in vacuo*. The crude product was recrystallised from ethanol to obtain the pure product (**21**) as needle like crystals in a yield of (47 g, 140.7 mmol, 78 %). ^{1}H NMR (250 MHz, CDCl$_3$) δ_H/ppm: 6.94 (s, 4H), 4.01 (t, 4H, J=6.7 Hz), 1.93-1.83 (m, 4H), 1.62-1.34 (m, 20H), 0.89 (t, 6H, J=6.8 Hz). ^{13}C NMR (250 MHz, CDCl$_3$) δ_C/ppm: 141.1, 119.9, 113.0, 69.3, 31.9, 29.5, 29.3, 26.1, 22.7, 14.1. M.p. 25-26 [0]C (lit, 24-25 [0]C)[134]. FT-IR (ATR): (cm^{-1}) 2953-2871, 2850, 1594, 1466 1454, 1387, 1255, 1120. Elemental Analysis (%) calculated for C$_{22}$H$_{38}$O$_2$: C, 78.99; H, 11.45. Found: C, 79.10; H, 10.95. Mass (EI[+]): (m/z) 334 (M[+•]).

3.3.201,2-Dinitro-4,5-bis(octyloxy)benzene (22)
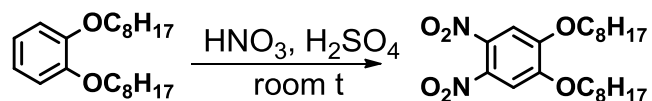
The preparation of 1,2-dinitro-4,5-bis(octyloxy)benzene (**22**) involved using a modified method outlined by Janssen and co-workers.[133] To a solution of 11,2-bis(octyloxy)benzene 3.3.3 (**21**) (10 g, 19.9 mmol) in CH_2Cl_2 (140 mL) was added acetic acid (140 mL). The solution was cooled to 6 °C and HNO_3 (65%, 20 mL) was added dropwise. The reaction mixture was left to react at room temperature for 1 hour. The mixture was the again cooled to 6 °C, and the flask was charged with a portion fuming nitric acid (50 mL). The reaction was stirred for 40 hours, over the course of which time a yellow solid precipitated. On completion, the reaction mixture was poured over ice resulting in the formation of more yellow precipitate. The mixture was then extracted with DCM (3×200 mL). All the organic layers were combined and washed with water, sat. $NaHCO_3$, brine and dried over $MgSO_4$. The solvent was removed *in vacuo* and the crude material was recrystallised from ethanol to yield (**22**) as a yellow solid in a yield of (34.2 g, 80.6 mmol, 90 %). ^{1}H NMR (250 MHz, $CDCl_3$) δ_H/ppm: 7.31 (s, 2H), 4.12 (t, J = 6.7 Hz, 4H), 1.96-1.82 (m, 4H), 1.56-1.22 (m, 20H), 0.90 (t, 6H, J=4.4 Hz). ^{13}C NMR (250 MHz, $CDCl_3$) δ_C/ppm: 152.8, 137.5, 108.9, 69.2 32.7, 30.1, 29.7, 26.8, 22.6, 14.0. M.p. 88-89 [0]C, (lit, 87-87.5 [0]C)[134]. FT-IR (ATR): (cm^{-1}) 3071, 2956, 2921, 2853, 2438, 2160, 2023, 1586, 1527, 1468, 1371, 1354, 1334, 1287, 1221, 1043, 992, 954, 905, 872, 827, 810, 750, 720. Elemental Analysis (%) calculated for $C_{22}H_{36}N_2O_2$: C, 62.42; H, 8.55; N, 6.60. Found: C, 63.32; H, 9.36; N, 5.50. Mass (EI^+): (m/z) 424 ($M^{+\bullet}$).

3.3.21 5,6-Bis(octyloxy)benzo[c][1,2,5]thiadiazole (24)
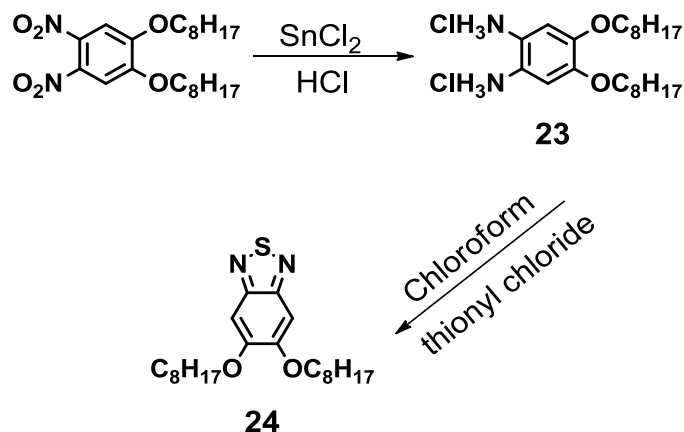
The preparation of 5,6-Bis(octyloxy)benzo[c][1,2,5]thiadiazole (**24**) proceeded through two steps. The unstable 4,5-Bis(octyloxy)benzene-1,2-diaminium chloride (**23**) was produced initially. This was then used directly to produce (**24**). The intermediate compound (**23**) was performed according to a modified method outlined by Janssen and co-workers.[133] To a solution of 11,2-dinitro-4,5-bis(octyloxy)benzene (**22**) (5.0 g, 11.8 mol) in ethanol (175 mL) were added Sn(II)Cl$_2$ (17.8 g, 9.4 mol) and conc.HCl (175 mL). The reaction was put under an inert atmosphere, heated to 85 °C and left overnight. The reaction mixture was then cooled to ambient temperature and filtered to obtain the product. The material was washed with methanol and water. The product was dried under a stream of nitrogen and used in the next step without further purification. The product (**23**) was a white solid obtained in a yield of (4.48 g, 10.2 mmol, 86 %). No further analysis could be done for this molecule due to degradation problems. As a result, 5,6-Bis(octyloxy)benzo[c][1,2,5] thiadiazole (**24**) was directly synthesised according to a modified method outlined by Janssen and co-workers.[133] A mixture of 4,5-bis(octyloxy)benzene-1,2-diaminium chloride (**23**) (4.4 g, 10.3 mmol), triethylamine (10.8 g, 15 mL, 107.6 mmol) and dry chloroform (25 mL) was placed in two neck round bottom flask under an inert atmosphere. Thionyl chloride (2.4 g, 20.7 mol, 1.51 mL) in dry chloroform (25 mL) was added slowly to the mixture. Upon complete addition, the mixture was refluxed overnight. The reaction mixture was poured in water (300 mL) and DCM (300 mL). The organic layer was washed with

water (5 x 300 mL) and dried over anhydrous MgSO$_4$. The solvent was removed *in vacuo* and the crude product was recrystallised from ethanol. The product (**24**) was obtained as an off white powder in a yield of (4.50 g, 11.4 mmol, 92 %). ^{1}H NMR (250 MHz, CDCl$_3$) δ_H/ppm: 7.14 (s, 2H), 4.10 (t, 4H, J = 6.5 Hz), 1.99-1.86 (m, 4H), 1.56-1.22 (m, 20H), 0.91 (t, 6H, J=4.4 Hz). ^{13}C NMR (250 MHz, CDCl$_3$) δ_C/ppm: 153.2, 151.4, 97.4, 68.1, 30.7, 30.1, 28.2. 27.7, 25.0, 22.6, 14.0. M.p. 100-101 [0]C, (lit, 97.1-97.5 [0]C)[134]. FT-IR (cm^{-1}): 3118, 3080 and 3052, 2950-2958, 1460, 1195 1065, 724. Elemental Analysis (%) calculated for C$_{22}$H$_{36}$N$_2$O$_2$S: C, 67.30; H, 9.24; N, 7.14. Found: C, 67.50; H, 8.65; N, 8.42. Mass (EI[+]): (m/z) 392 (M[+•]).

3.3.22 4,7-Dibromo-5,6-bis(octyloxy)benzo[c][1,2,5] thiadiazole (25)
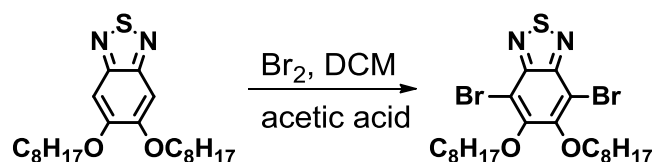
4,7-Dibromo-5,6-bis(octyloxy)benzo[c][1,2,5]thiadiazole (**25**), was prepared according to a modified method of Janssen and co-workers.[133] 5,6-Bis(octyloxy)benzo[c][1,2,5]thiadiazole (**24**) (10.0 g, 25.4 mmol) was dissolved in a mixture of DCM (380 mL) and acetic acid (180 mL). Bromine (28.5 g, 9.1 mL, 178.4 mol) was added to the mixture and stirred in the dark for 72 hours at room temperature. On completion, the mixture was quenched with deionised water (500 mL). The mixture was then extracted with DCM (2×300 mL). All the organic layers were combined and washed with water, sat. with NaHCO$_{3(aq)}$, brine and dried over MgSO$_4$. The solvent was removed *in vacuo* and the crude material purified *via* silica gel column chromatography using hexane:ethyl acetate (2:8; v/v) as the eluent. The still crude material was purified again *via* recrystallisation with ethanol to give the target product (**25**) as a white powder in a yield of (10.7 g, 19.6 mmol, 77 %). ^{1}H NMR (250 MHz, CDCl$_3$) δ_H/ppm: 4.17 (t, 4H, J = 6.6 Hz), 1.97-1.83 (m, 4H), 1.62-1.24 (m, 20H), 0.91 (t, 6H, J=4.4 Hz). ^{13}C NMR (250 MHz, CDCl$_3$) δ_C/ppm: 154.5, 150.3, 106.2, 58.5, 31.8, 30.27, 30.2, 29.4, 29.2, 25.9, 22.6, 18.4, 14.0. M.p. 44-46 [0]C, (lit, 44-45 [0]C)[134]. FT-IR (cm^{-1}): 2950-

2958, 1470, 1285, 1059, 797, 724. Elemental Analysis (%) calculated for $C_{22}H_{34}N_2O_2Br_2S$: C, 48.01; H, 6.23; Br, 29.04; N, 5.09; S, 5.82. Found: C, 47.89; H, 5.93; Br, 29.02; N, 7.42; S, 6.01. Mass (EI$^+$): (m/z) 548, 550, 552 (M$^{+\bullet}$).

3.3.23 5-Tri-methylstannyl-2,2-bithiophene (26)
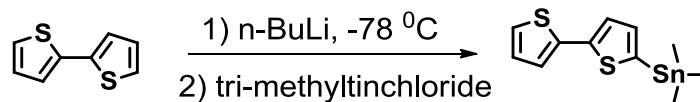
5-Trimethylstannyl-2,2-bithiophene (**26**) was synthesised according to a modified procedure outlined by Jakle and co-workers.[135] A solution of bithiophene (1.0 g, 6.01 mmol) in THF (40 mL) was placed under an inert atmosphere and cooled to -78 ^{0}C. n-BuLi (2.4 mL, 2.5 M in hexanes, 6.1mmol) was added dropwise and the reaction was left to stir at -78 ^{0}C for 30 minutes. To the reaction was added a solution of tri-methyltin chloride (6 mL, 1.0 M in THF, 1.2 g, 6.01 mmol). Once added the reaction was left to stir overnight at room temperature. On completion, the reaction mixture was quenched with cold water (20 mL) and the solvent removed *in vacuo*. The oily crude product was poured into hexane (100 mL) and filtered. The crude material was purified *via* silica gel column chromatography using a mixture of hexane and triethylamine (8:2; v/v) as the eluent. Product (**26**) was obtained as a colourless oil in a yield of (1.72 g, 5.2 mmol, 87 %). ^{1}H NMR (250 MHz, CDCl$_3$) δ_H/ppm 7.32 (d, 1H, J = 3.1 Hz); 7.23 − 7.19 (m, 2H); 7.11 (d, 1H, J = 3.4 Hz); 7.01 (dd , IH, J$_1$=5.1 Hz, J$_2$=3.6 Hz); 0.42 (s, 9H). ^{13}C NMR (250 MHz, CDCl$_3$) δ_C/ppm: 137.5, 137.4, 135.8, 135.7, 127.7, 125.2, 125.0, 124.3, -8.2. FT-IR (ATR): (cm^{-1}): 3106, 3070, 2981, 2914, 1644, 1495, 1413, 1300, 1282, 1206, 1195, 944, 816, 773, 691, 533. Elemental Analysis (%) calculated for $C_{11}H_{14}S_2Sn$: C, 40.15 ; H, 4.29; S, 19.49. Found : C, 39.89; H, 5.10; S, 18.97. Mass (EI$^+$): (m/z) 329 (M$^{+\bullet}$).

3.3.24 4,7-Di(2,2'-bithiophen-5-yl)-5,6-bis(octyloxy)benzo[c] [1,2,5] thiadiazole (27)
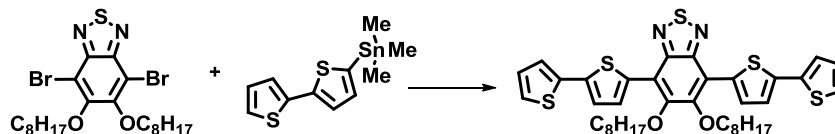
The synthesis of 4,7-di(2,2′-bithiophen-5-yl)-5,6-bis(octyloxy)benzo[c][1,2,5] thiadiazole (**27**) followed a modified method of Iraqi and co-workers.[136] 4,7-Dibromo-5,6-bis-octyloxy-benzo[1,2,5] thiadiazole (**25**) (1.0 g, 1.8 mmol), tri(o-tolyl)phosphine (75 mg, 0.2 mmol) and Pd(OAc)$_2$ (27 mg, 0.1 mmol) were added to a round bottom flask and placed under an inert atmosphere. Anhydrous toluene was added (50 mL) followed by 5,5'-bis(tri-methylstannyl)-2,2'-bithiophene (**26**) (1.8 g, 5.4 mmol). The reaction was degassed again and placed under an inert atmosphere. The mixture heated to 110 ^{0}C and allowed to react for 24 hours. Upon completion, the mixture was cooled to room temperature and water (100 mL) was added. The material was extracted with toluene (3 x 150 mL). The organic phases were combined, washed with brine and water and dried over MgSO$_4$. After filtration, the solvent was removed *in vacuo*. The product was purified *via* silica gel column chromatography using hexane and chloroform (5:1; v/v; gradient) as the eluent to yield (**27**) as pure orange crystals in a yield of (1.09 g, 1.5 mmol, 84 %). ^{1}H NMR (400 MHz, CDCl$_3$) δ_H/ppm: 8.52 (d, 2H, J = 4.0 Hz), 7.32 (dd, 4H, J$_1$= 5.0 Hz, J$_2$= 3.5 Hz), 7.29 (d, 2H, J = 3.9 Hz), 7.09 (dd, 2H, J$_1$= 5.1 Hz, J$_2$= 3.6 Hz), 4.19 (t, 4H, J = 7.0 Hz), 2.03 (m, 4H), 1.51-1.34 (m, 20H), 0.90 (t, 6H, J=6.8 Hz). ^{13}C NMR (400 MHz, CDCl$_3$) δ_C/ppm: 151.6, 150.8, 138.8, 137.6, 134.2, 131.6, 127.9, 124.6, 123.7, 123.5, 117.3, 74.5, 31.8, 30.4, 29.5, 29.3, 26.0, 22.7, 14.1. Mp. 89-91 °C. FT-IR (ATR): (cm^{-1}) 3010, 2961, 2830, 2210, 2029, 1601, 1503, 1453, 1419, 1407, 1388, 1366, 1335, 1272, 1209, 1186, 1079, 1037, 1021, 963, 928, 911, 887, 848, 819, 739, 719, 681, 642, 626. Elemental Analysis (%) calculated for C$_{38}$H$_{44}$N$_2$O$_5$S$_5$: C, 63.29; H, 6.15; N, 3.88; S, 22.23. Found: C, 62.11; H, 5.87; N 2.98; S, 21.68. Mass (EI$^+$): (m/z) 720 (M$^{+\bullet}$).

3.3.25 4,7-Bis(5'-bromo-2,2'-bithiophen-5-yl)-5,6-bis(octyloxy)benzo [c] [1,2,5] thiadiazole (28)
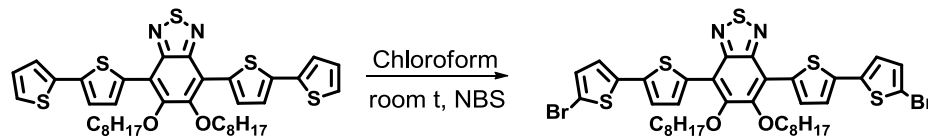
The synthesis of 4,7-bis(5′-bromo-2,2′-bithiophen-5-yl)-5,6-bis(octyloxy)benzo[c][1,2,5]thiadiazole (**28**) was performed using a modified method of Iraqi and co-workers.[136] To a solution of 4,7-di(2,2'-bithiophen-5-yl)-5,6-bis(octyloxy)benzo[c][1,2,5]thiadiazole (**27**) (0.98 g, 1.3 mmol) in dried chloroform (40 mL), was added NBS (0.4 g, 2.7 mmol) in one portion which was kept in the dark for 48 hours. Upon completion, the solvent was removed *in vacuo* to give an orange solid. Column chromatography with hexane and toluene (8:2; v/v) was used to purify the product. Precipitation of the product thus obtained was carried out in hot methanol that resulted in formation of dark red crystals in a yield of (0.9 g, 1.1 mmol, 82%). ^{1}H NMR (400 MHz, CDCl$_3$) δ_H/ppm: 8.51 (d, 2H, J=4.0 Hz); 7.25 (d, 2H, J=4.0 Hz); 7.04 (dd, 4H, J$_1$= 6.0 Hz, J$_2$= 3.8 Hz), 4.17 (t, 4H, J=7.0 Hz); 1.99 (m, 4H); 1.53-1.20 (m, 20H); 0.91 (t, 6H, J=6.8 Hz). ^{13}C NMR (400 MHz, CDCl$_3$) δ_C/ppm: 151.6, 150.6, 139.0, 137.7, 133.5, 131.6, 130.7, 123.7, 117.2, 111.2, 74.5, 31.8, 30.4, 29.5, 29.3, 26.0, 22.7, 14.1. FT-IR (ATR): (cm^{-1}) 3071, 2950,2920, 2870, 2851, 1723, 1555, 1462, 1262, 1281,1256, 1214, 1194, 1179, 1126, 1062, 1013, 998, 958, 937, 909, 851, 823, 753, 784, 723, 663, 603. Mp. 92-94 °C. Elemental Analysis (%) calculated for C$_{38}$H$_{42}$Br$_2$N$_2$O$_5$S$_5$: C, 51.93; H, 4,82; N, 3.19; S, 18.24. Found: C, 50.87; H, 5.51; N, 4.32; S, 18.04. Mass (EI$^+$): (m/z) 876, 878, 880 (M$^{+\bullet}$)

3.3.26 5,6-Bis(octyloxy)-4,7-bis(5'-(trimethylstannyl)-[2,2'-bithiophen] -5-yl)benzo[c][1,2,5]thiadiazole (29)
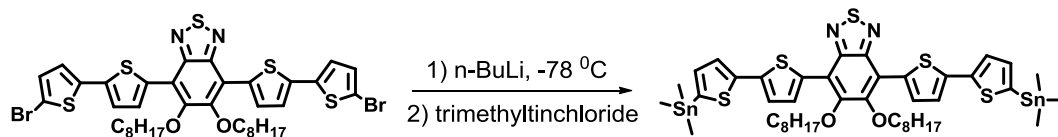
The synthesis of 5,6-bis(octyloxy)-4,7-bis(5′-(trimethylstannyl)-[2,2′-bithiophen]-5-yl)benzo[c][1,2,5] thiadiazole (**29**) was done according to a modified procedure by Jin *et al.*[100] 7-Bis(5'-bromo-2,2'-bithiophen-5-yl)-5,6-bis(octyloxy)benzo [c] [1,2,5] thiadiazole (**28**) (0.75 g, 1.1 mmol) was dissolved in dry THF (30 mL) under an inert argon atmosphere. The solution was cooled to -78 °C and n-BuLi (1.3 mL, 2.5 M in hexanes, 3.3 mmol) was added dropwise. After stirring for 5 hours at -78 °C, SnMe$_3$Cl (3.1 mL, 1M in hexanes, 3.1 mmol) was added dropwise. The reaction was stirred at -78 °C for 1 hour. Once this time had elapsed the reaction was warmed to room temperature and allowed to react overnight. The mixture was poured into H$_2$O (50 mL) and extracted with diethyl ether (3 x 50 mL). The organic layer was washed with H$_2$O (3 x 20 mL), dried over MgSO$_4$ and solvent removed *in vacuo* to give a thick red oil product (**29**) that was used without further purification in a yield of (0.82 g, 0.7 mmol, 75%). ^{1}H NMR (400 MHz, CDCl$_3$) δ_H/ppm: 8.51 (d, 2H, J=4.2 Hz); 7.42 (d, 2H, J=4.1 Hz), 7.31 (d, 2H, J=3.9 Hz), 7.16 (d, 2H, J= 3.8 Hz), 4.17 (t, 4H, J=7.0 Hz); 1.99 (m, 4H); 1.53-1.20 (m, 20H); 0.91 (t, 6H, J=6.7 Hz), 0.43 (s, 18H). ^{13}C NMR (400 MHz, CDCl$_3$) δ_C/ppm: 151.5, 150.8, 143.0, 139.0, 137.9, 136.0, 132.9, 131.6, 124.9, 123.4, 117.3, 77.3, 74.5, 31.8, 30.4, 29.6, 29.3, 26.0, 22.7, 14.1, -8.1. FT-IR (ATR): (cm^{-1}) 3071, 2954, 2924, 2850, 1465, 1414, 1378,1281, 1109, 944, 793, 770, 538. Elemental Analysis (%) calculated for C$_{44}$H$_{60}$N$_2$O$_2$S$_5$Sn$_2$: C, 50.49; H, 5.78; N, 2.68; S, 15.32. Found: C, 50.55; H, 5.73; N, 2.71; S, 14.71 .Mass (EI[+]); (m/z): 1048 (M[+•]).

3.4 Synthesis of polymers

3.4.1 Poly(9-(heptadecanyl)-9H-carbazole-2,7-diyl)-alt-di(thiophen-2-yl)-6,7,15,16-tetrakis[hexadecyloxy]-quinoxalino[2',3':9,10]phenanthro[4,5-*abc*]phenazine-2,11-diyl] (P1)
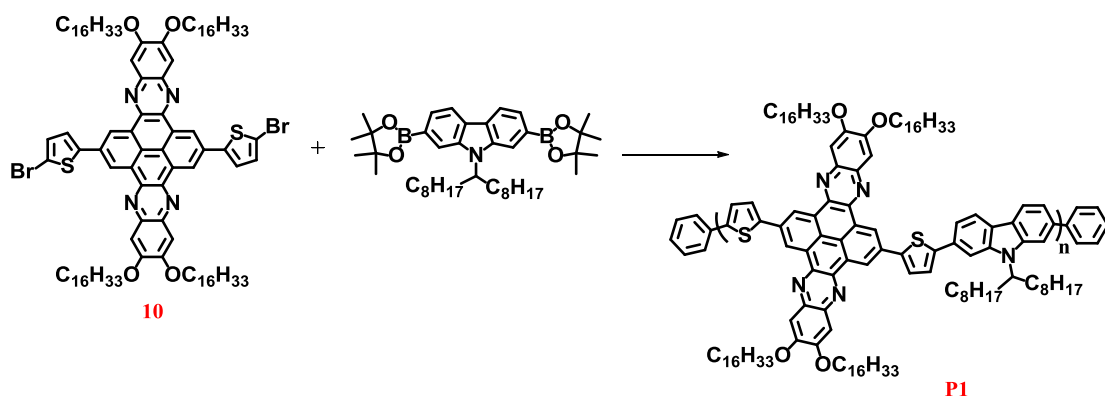
A mixture of 9-(heptadecan-9-yl)-2,7-bis(4,4,5,5-tetramethyl-1,3,2-dioxaborolan-2-yl)-9H-carbazole (46 mg, 0.07 mmol) and 2,11-bis(5-bromothiophen-2-yl)-6,7,15,16-tetrakis(hexadecyloxy)quinoxalino[2',3':9,10]phenanthro[4,5-abc]phenazine (120 mg, 0.07 mmol) in THF (4 mL) was degassed. To the mixture was added a saturated solution of $NaHCO_3$ (1 mL, previously degassed) under argon. $Pd(OAc)_2$ (3 mg, 0.01 mmol) and tri(o-tolyl)phosphine (7 mg, 0.02 mmol) were then added and the system was degassed and placed under argon. The reaction was heated to 90 ^{0}C. When any precipitate was observed the reaction was stopped and cooled to room temperature. Once cool, 5 mL of THF was added and the mixture was degassed and kept at 90 ^{0}C for a further 2 hours. Upon completion, the mixture was cooled to room temperature and bromobenzene (0.1 mL, 0.9 mmol) was added. The mixture was degassed and heated at 90 ^{0}C for 1 hour. Upon completion, the reaction was cooled to room temperature and phenylboronic acid (0.05 g, 0.4 mmol) was added to the mixture. The reaction was degassed and heated at 90 ^{0}C for 3 hours. The mixture was then cooled to room temperature and poured in $CHCl_3$ (200 mL) followed by ammonium hydroxide solution (28% in H_2O, 50 mL). The reaction was refluxed for 3 hours. The reaction was cooled to room temperature and the organic phase

was separated and washed with distilled water (3 x 100mL). The organic phase was then concentrated *in vacuo* (~40 mL) and precipitated in methanol-water (300 mL, 10:1, previously degassed). The precipitate was stirred overnight and filtered to obtain the crude solid. The crude solid was then cleaned *via* Soxhlet extraction using methanol, acetone, hexane and chloroform. The chloroform fraction was concentrated (~40 mL) and precipitated in methanol (300 mL). The precipitate was stirred overnight and filtered to obtain the polymer as a yellow solid. The yield of chloroform fraction was (121 mg, 88%). GPC (1,2,4-trichlorobenzene at 140 °C): M_n = 29,300, M_w = 67,800, PD = 2.31. Elemental analysis (%) calculated for $C_{131}H_{189}N_5O_4S_2$: C, 80.19; H, 9.71; N, 3.57; S, 3.27. Found: C, 77.30; H, 9.37; N, 3.41; S, 2.24. ^{1}H NMR (500 MHz, $C_2D_2Cl_4$, 100 ^{0}C) δ_H/ppm: 9.55 (br, 4H), 7.87 (s, 2H), 7.78 (d, 2H), 7.53 (m, 2H), 7.51 (s, 4H), 7.30 to 7.18 (br, 4H), 4.25 (br, 1H), 4.18 (br, 8H), 2.41 (br, 4H), 2.08 (br, 4H), 1.66 (br, 4H), 1.60-1.10 (br, 116H), 0.98-0.75 (br, 30H). λ_{max}(solution) nm = 471. λ_{max}(thin film) nm = 475.

3.4.2 Poly[9,9-dioctyl-9H-fluorene-2,7-diyl-alt-di(thiophen-2-yl)-6,7,15,16-tetrakis[hexadecyloxy] -quinoxalino[2',3':9,10] phenanthro[4,5-*abc*]phenazine-2,11-diyl] (P2)
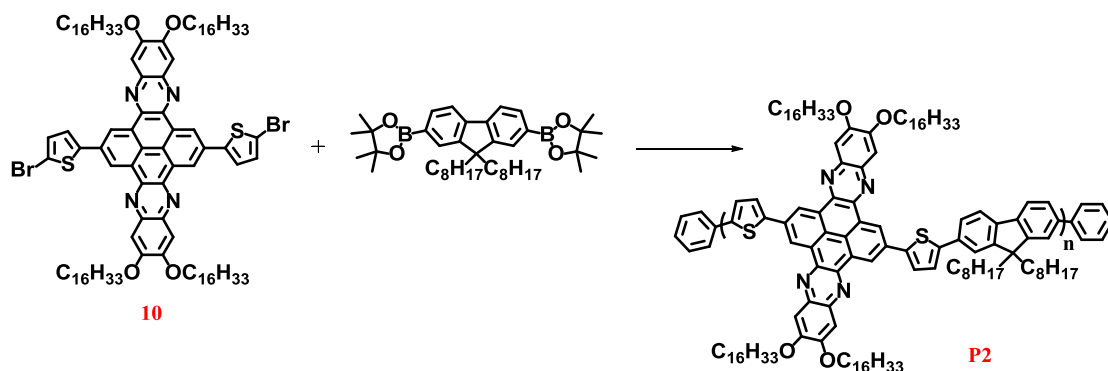
A mixture of 9,9-Dioctylfluorene-2,7-diboronic acid bis(1,3-propanediol) ester (46mg, 0.07 mmol) and 2,11-bis(5-bromothiophen-2-yl)-6,7,15,16-tetrakis(hexadecyloxy) quinoxalino[2',3':9,10]phenanthro[4,5-abc]phenazine (120 mg, 0.07 mmol) in THF (4 mL) was degassed. To the mixture was added a saturated solution of NaHCO$_3$ (1 mL, previously degassed) under argon. Pd(OAc)$_2$ (3 mg, 0.01 mmol) and tri(o-tolyl)phosphine (7 mg, 0.02

mmol) were then added and the system was degassed and placed under argon. The reaction was heated to 90 ^{0}C. When any precipitate was observed the reaction was stopped and cooled to room temperature. Once cool, 5 mL of THF was added and the mixture was degassed and kept at 90 ^{0}C for a further 2 hours. Upon completion, the mixture was cooled to room temperature and bromobenzene (0.1 mL, 0.9 mmol) was added. The mixture was degassed and heated at 90 ^{0}C for 1 hour. Upon completion, the reaction was cooled to room temperature and phenylboronic acid (0.05 g, 0.4 mmol) was added to the mixture. The reaction was degassed and heated at 90 ^{0}C for 3 hours. The mixture was then cooled to room temperature and poured in $CHCl_3$ (200 mL) followed by ammonium hydroxide solution (28% in H_2O, 50 mL). The reaction was refluxed for 3 hours. The reaction was cooled to room temperature and the organic phase was separated and washed with distilled water (3 x 100 mL). The organic phase was then concentrated *in vacuo* (~40 mL) and precipitated in methanol-water (300 mL, 10:1, previously degassed). The precipitate was stirred overnight and filtered to obtain the crude solid. The crude solid was then cleaned *via* Soxhlet extraction using methanol, acetone, hexane and chloroform. The chloroform fraction was concentrated (~40 mL) and precipitated in methanol (300 mL). The precipitate was stirred overnight and filtered to obtain the polymer as a orange solid. The yield of chloroform fraction was (126 mg, 92 % yield). GPC (1,2,4-trichlorobenzene at 140 ˚C): M_n = 15300, M_w = 50700, PD = 3.31. Elemental analysis (%) calculated for $C_{131}H_{188}N_4O_4S_2$: C, 80.81; H, 9.73; N, 2.88; S, 3.29. Found: C, 79.96; H, 9.50; N, 2.85; S, 2.19. ^{1}H NMR (500 MHz, $C_2D_2Cl_4$, 100 ^{0}C) δ_H/ppm: 9.54 (br, 4H), 7.88 (m, 2H), 7.71 (d, 2H), 7.60 (m, 2H), 7.52 (s, 4H), 7.24 to 7.41 (br, 4H), 4.18 (br, 8H), 2.18 (m, 4H), 2.00 (br, 4H), 1.69 (br, 4H), 1.60-1.11 (br, 116H), 1.00-0.78 (br, 30H). λ_{max}(solution) nm = 468. λ_{max}(thin film) nm = 470.

3.4.3 Poly [2,2'-bithiophen]-5,5'-diyl-alter-6,7,15,16- tetrakis (2-hexyl decyloxy)quinoxalino[2',3':9,10]phenanthro[4,5-abc]phenazine-2,11-diyl] (P3)
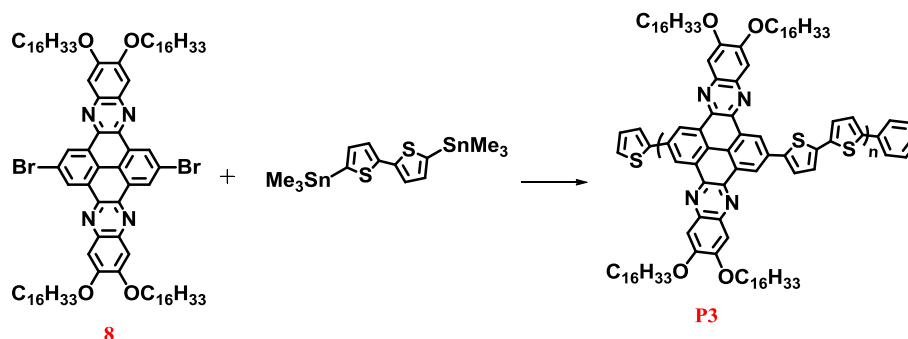
In a 100 mL one-neck round bottom flask was added 2,11-bis(5-bromothiophen-2-yl)-6,7,15,16-tetrakis(hexadecyloxy)quinoxalino[2',3':9,10]phenanthro [4,5-abc]phenazine (200 mg, 0.1 mmol) and 5,5'-bis(trimethylstannyl)-2,2'-bithiophene (64 mg, 0.1 mmol) and 8 mL of dry toluene were added under an inert argon atmosphere. $Pd_2(dba)_3$ (6 mg, 0.006 mmol) and tri-ortho-tolylphosphine (12 mg, 0.03 mmol) were added to the reaction. The system was degassed again and put under an argon atmosphere that was maintained for 20 minutes. Once this time had elapsed the temperature was raised to 110 ^{0}C for 24 hours. Upon completion, the reaction was cooled to room temperature. Dry toluene (5 mL) and bromobenzene (0.1 mL, 0.9 mmol) were added and the system was degassed and heated for one hour at 110 ^{0}C. Upon completion, the mixture was cooled to room temperature and 2-(tributylstannyl)thiophene (0.1 mL 0.4 mmol) was added. Again, the mixture was subjected to degassing and heated at 110 ^{0}C for three hours. The mixture was cooled to room temperature and poured in $CHCl_3$ (200 mL) followed by ammonium hydroxide solution (28% in H_2O, 50 mL). This mixture was stirred overnight. The organic phase was separated and washed with distilled water. It was concentrated *in vacuo* (~40 mL) and added to a degassed mixture of methanol-water (300 mL, 10:1, previously degassed). This mixture was stirred overnight and filtered to obtain the crude solid. The crude solid was cleaned *via* Soxhlet extraction using methanol, acetone, hexane, chloroform and chlorobenzene. The chloroform and chlorobenzene fractions were independently concentrated *in vacuo* (~40 mL) and precipitated in methanol (300 mL). These mixtures were stirred overnight and filtered to obtain the polymer as orange solids. The yield of chloroform fraction was (87

mg, 39% yield). GPC (1,2,4-trichlorobenzene at 140 ˚C): M_n = 9900, M_w = 16300, PD = 1.6. The yield of chlorobenzene fraction was (116.00 mg, 52.59% yield). GPC (1,2,4-trichlorobenzene at 140 ˚C): M_n = 21500, M_w = 29800, PD = 1.3. Elemental analysis (%) calculated for $C_{100}H_{146}N_4O_4S_2$: C, 78.38; H, 9.60; N, 3.66; O, 4.18; S, 4.18. Found: C, 80.40; H, 11.98; N, 2.68; S, 2.92. ^{1}H NMR (500 MHz, $C_2D_2Cl_4$, 100 ^{0}C) δ_H/ppm: 9.52 (br, 4H), 7.98 (br, 2H), 7.70 (s, 4H), 7.21 (br, 2H), 4.18 (br, 8H), 1.99 (m, 4H), 1.62-1.10 (br, 96H), 1.00-0.77 (24H). λ_{max}(solution) nm = 487. λ_{max}(thin film) nm = 489.

3.4.4 Poly (9-(heptadecanyl)-9H-carbazole-2,7-diyl)-alt-di(thiophen-2-yl)-6,7,15,16-tetrakis[3-pentylundecyl]-quinoxalino [2',3':9,10]phenanthro [4,5-abc]phenazine-2,11-diyl] (P4)
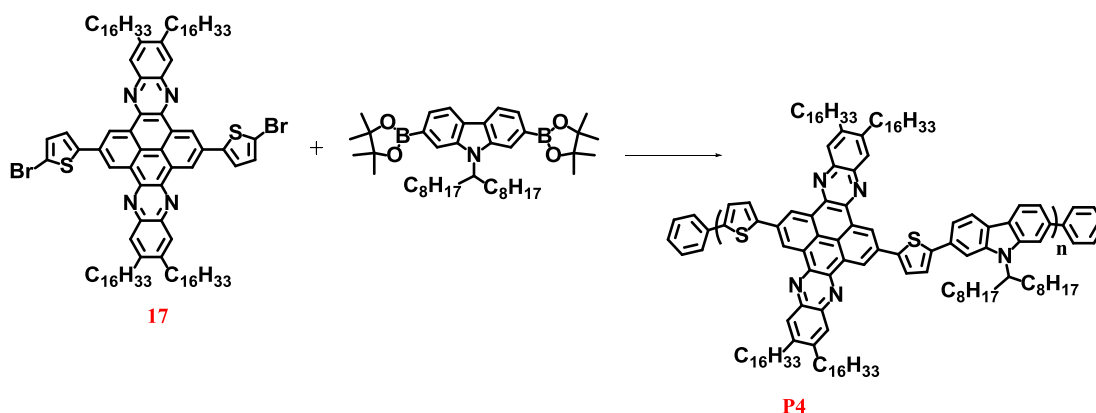
A mixture of 2,11-bis(5-bromothiophen-2-yl)-6,7,15,16- tetrakis (3-pentyl undecyl) quinoxalino [2',3':9,10]phenanthro[4,5-abc]phenazine (166 mg, 98.3 mmol) and 9-(heptadecan-9-yl)-2,7-bis(4,4,5,5-tetramethyl-1,3,2-dioxaborolan-2-yl)-9H-carbazole (64 mg, 98.3 mmol) in THF (6 mL) was degassed. To the mixture was added a saturated solution of NaHCO$_3$ (1.4 mL, previously degassed) under argon. Pd(OAc)$_2$ (3 mg, 0.01 mmol) and tri(o-tolyl)phosphine (7 mg, 0.02 mmol) were then added and the system was degassed and placed under argon. The reaction was heated to 90 ^{0}C. When any precipitate was observed the reaction was stopped and cooled to room temperature. Once cool, 5 mL of THF was added and the mixture was degassed and kept at 90 ^{0}C for a further 2 hours. Upon completion, the mixture was cooled to room temperature and bromobenzene (0.1 mL,

0.9 mmol) was added. The mixture was degassed and heated at 90 ^{0}C for 1 hour. Upon completion, the reaction was cooled to room temperature and phenylboronic acid (0.05 g, 0.4 mmol) was added to the mixture. The reaction was degassed and heated at 90 ^{0}C for 3 hours. The mixture was then cooled to room temperature and poured in $CHCl_3$ (200 mL) followed by ammonium hydroxide solution (28% in H_2O, 50 mL). The reaction was refluxed for 3 hours. The reaction was cooled to room temperature and the organic phase was separated and washed with distilled water (3 x 100 mL). The organic phase was then concentrated *in vacuo* (~40 mL) and precipitated in methanol-water (300 mL, 10:1, previously degassed). The precipitate was stirred overnight and filtered to obtain the crude solid. The crude solid was then cleaned *via* Soxhlet extraction using methanol, acetone, hexane and chloroform. The chloroform fraction was concentrated (~40 mL) and precipitated in methanol (300 mL). The precipitate was stirred overnight and filtered to obtain the polymer as a yellow solid. The yield of chloroform fraction was (124 mg, 75% yield). GPC (1,2,4-trichlorobenzene at 140 ˚C): M_n = 17800, M_w = 46000, PD = 2.5. Elemental analysis (%) calculated for $C_{129}H_{187}N_5S_2$: C, 82.76; H, 10.07; N, 3.74; S, 3.43. Found: C, 82.83; H, 9.62; N, 3.63; S, 2.97. ^{1}H NMR (500 MHz, $C_2D_2Cl_4$, 100 ^{0}C) δ_H/ppm: 9.55 (br, 4H), 8.17 (br, 2H), 7.90 (m, 4H), 7.58 (s, 4H), 7.16 (m, 4H), 4.25 (br, 1H), 2.91-2.76 (br, 12H), 1.80 (br, 8H), 1.59-1.13 (br, 116H), 1.05-0.79 (br, 30H). λ_{max}(solution) nm = 476. λ_{max}(thin film) nm = 487.

3.4.5 Poly (9,9-dioctyl)-9H-(fluorene-2,7-diyl)-alt-di(thiophen-2-yl)-6,7,15,16-tetrakis[3-pentylundecyl]–quinoxalino [2',3':9,10]phenanthro[4,5-abc]phenazine-2,11-diyl] (P5)
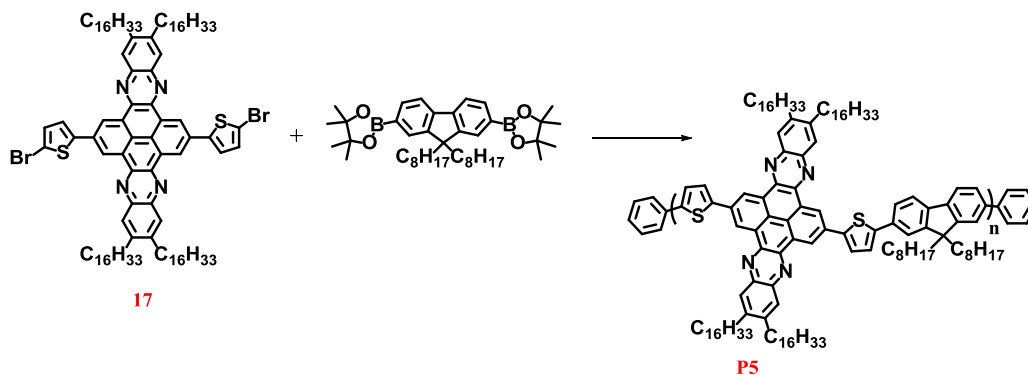
A mixture of 2,11-bis(5-bromothiophen-2-yl)-6,7,15,16- tetrakis (3-pentyl undecyl) quinoxalino [2',3':9,10]phenanthro[4,5-abc]phenazine (150 mg, 92.2 mmol) and 9,9-dioctylfluorene-2,7-diboronic acid bis(1,3-propanediol) ester (51 mg, 92.2 mmol) in THF (5 mL) was degassed. To the mixture was added a saturated solution of $NaHCO_3$ (1.2 mL, previously degassed) under argon. $Pd(OAc)_2$ (3 mg, 0.01 mmol) and tri(o-tolyl)phosphine (10 mg, 0.03 mmol) were then added and the system was degassed and placed under argon. The reaction was heated to 90 ^{0}C. When any precipitate was observed the reaction was stopped and cooled to room temperature. Once cool, 5 mL of THF was added and the mixture was degassed and kept at 90 ^{0}C for a further 2 hours. Upon completion, the mixture was cooled to room temperature and bromobenzene (0.1 mL, 0.9 mmol) was added. The mixture was degassed and heated at 90 ^{0}C for 1 hour. Upon completion, the reaction was cooled to room temperature and phenylboronic acid (0.05 g, 0.4 mmol) was added to the mixture. The reaction was degassed and heated at 90 ^{0}C for 3 hours. The mixture was then cooled to room temperature and poured in $CHCl_3$ (200 mL) followed by ammonium hydroxide solution (28% in H_2O, 50 mL). The reaction was refluxed for 3 hours. The reaction was cooled to room temperature and the organic phase was separated and washed with distilled water (3 x 100 mL). The organic phase was then concentrated *in vacuo* (~40 mL) and precipitated in methanol-water (300 mL, 10:1, previously degassed). The precipitate was stirred overnight and filtered to obtain the crude solid. The crude solid was

then cleaned *via* Soxhlet extraction using methanol, acetone, hexane and chloroform. The chloroform fraction was concentrated (~40 mL) and precipitated in methanol (300 mL). The precipitate was stirred overnight and filtered to obtain the polymer as a yellow solid. The yield of chloroform fraction was (111 mg, 67% yield). GPC (1,2,4-trichlorobenzene at 140 °C): M_n = 16800, M_w = 26500, PD = 1.5. Elemental analysis (%) calculated for $C_{129}H_{186}N_4S_2$: C, 83.43; H, 10.10; N, 3.02; S, 3.45. Found: C, 81.60; H, 9.63; N, 3.12; S, 3.21. ^{1}H NMR (500 MHz, $C_2D_2Cl_4$, 100 °C) δ_H/ppm: 9.56 (br, 4H), 8.10 (m, 2H), 7.81 (m, 2H), 7.65 (m, 2H), 7.53 (s, 4H), 7.21 (m, 4H), 2.78 (br, 4H), 2.22 (br, 8H), 1.85 (br, 8H), 1.51-1.12 (br, 116H), 1.08-0.76 (br, 30H). λ_{max}(solution) nm = 470. λ_{max}(thin film) nm = 482.

3.4.6 Poly [2,2'-bithiophen]-5,5'-diyl-alter-6,7,15,16- tetrakis [3-pentylundecyl]quinoxalino[2',3':9,10]phenanthro[4,5-abc]phenazine-2,11-diyl] (P6)
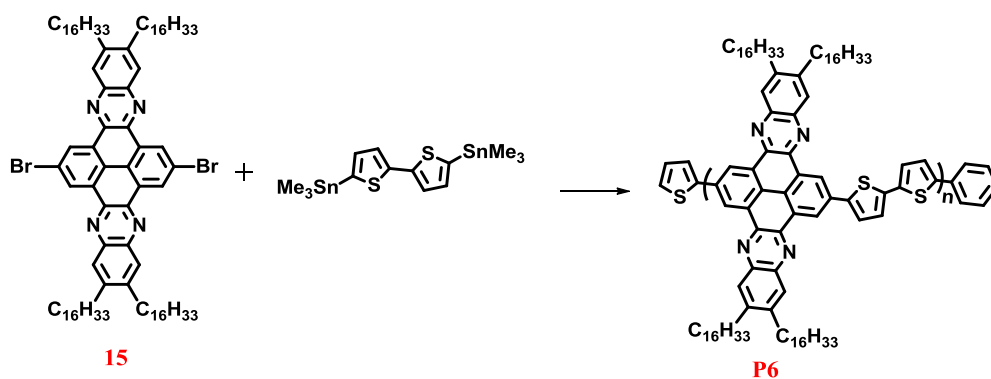
15   **P6**

In a 100 mL one-neck round bottom flask was added 2,11-dibromo-6,7,15,16-tetrakis(3-pentylundecyl)quinoxalino[2',3':9,10]phenanthro[4,5-abc] phenazine (150 mg, 0.1 mmol) and 5,5'-bis(trimethylstannyl)-2,2'-bithiophene (65 mg, 0.1 mmol) and 8 mL of dry toluene under an inert argon atmosphere. $Pd_2(dba)_3$ (5 mg, 0.005 mmol) and tri-ortho-tolylphosphine (9 mg, 0.03 mmol) were added to the reaction. The system was degassed again and put under an argon atmosphere that was maintained for 20 minutes. Once this time had elapsed the temperature was raised to 110 °C for 24 hours. Upon completion, the reaction was cooled to room temperature. Dry toluene (5 mL) and bromobenzene (0.1 mL,

0.9 mmol) were added and the system was degassed and heated for one hour at 110 ^{0}C. Upon completion, the mixture was cooled to room temperature and 2-(tributylstannyl)thiophene (0.1 mL 0.4 mmol) was added. Again, the mixture was subjected to degassing and heated at 110 ^{0}C for three hours. The mixture was cooled to room temperature and poured in CHCl$_3$ (200 mL) followed by ammonium hydroxide solution (28% in H$_2$O, 50 mL). This mixture was stirred overnight. The organic phase was separated and washed with distilled water. It was concentrated *in vacuo* (~40 mL) and added to a degassed mixture of methanol-water (300 mL, 10:1, previously degassed). This mixture was stirred overnight and filtered to obtain the crude solid. The crude solid was cleaned *via* Soxhlet extraction using methanol, acetone, hexane, chloroform and chlorobenzene. The chloroform and chlorobenzene fractions were independently concentrated *in vacuo* (~40 mL) and precipitated in methanol (300 mL). These mixtures were stirred overnight and filtered to obtain the polymer as orange solids. The yield of chloroform fraction was (40 mg, 23% yield). GPC (1,2,4-trichlorobenzene at 140 ˚C): M_n = 10,400, M_w = 11,500, PD = 1.1. The yield of chlorobenzene fraction was (80 mg, 45% yield). GPC (1,2,4-trichlorobenzene at 140 ˚C): M_n = 19,300, M_w = 28,500, PD = 1.4. Elemental analysis (%) calculated for C$_{100}$H$_{146}$N$_4$S$_2$: C, 81.80; H, 10.02; N, 3.82; S, 4.37. Found: C, 80.10; H, 11.32; N, 2.17; S, 2.76. ^{1}H NMR (500 MHz, C$_2$D$_2$Cl$_4$, 100 ^{0}C) δ_H/ppm: 9.50 (br, 4H), 7.92 (br, 8H), 2.78 (br, 8H), 1.54 (m, 8H), 1.26-1.18 (br, 92H), 0.84 (br, 24H). λ_{max}(solution) nm =500. λ_{max}(thin film) nm = 504.

3.4.7 Synthesis of Poly(6,7,15,16-tetrakis[hexadecyloxy]-quinoxalino [2',3':9,10]phenanthro[4,5-abc]phenazine-2,11-diyl]-alt-(4,7-dithiophen-2-yl)-2',1',3'-benzothiadiazole-5,5'-diyl] (P7)
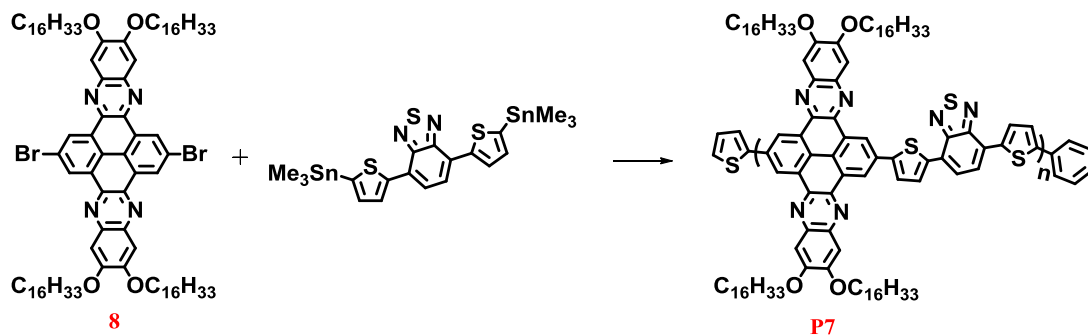
In a 100 mL one-neck round bottom flask was added 2,11-dibromo-6,7,15,16-tetrakis(2-hexyldecyloxy)quinoxalino[2',3':9,10]phenanthro [4, 5-abc]phenazine (200 mg, 130.0 mmol), 4,7-bis(5-(trimethylstannyl)thiophen-2-yl)benzo[c][1,2,5]thiadiazole (82 mg, 130.0 mmol) and 9 mL of dry toluene under an inert argon atmosphere. $Pd_2(dba)_3$ (6 mg, 0.006 mmol) and tri-ortho-tolylphosphine (12 mg, 0.03 mmol) were added to the reaction. The system was degassed again and put under an argon atmosphere that was maintained for 20 minutes. Once this time had elapsed the temperature was raised to 110 ^{0}C for 24 hours. Upon completion, the reaction was cooled to room temperature. Dry toluene (5 mL) and bromobenzene (0.1 mL, 0.9 mmol) were added and the system was degassed and heated for one hour at 110 ^{0}C. Upon completion, the mixture was cooled to room temperature and 2-(tributylstannyl)thiophene (0.1 mL 0.4 mmol) was added. Again, the mixture was subjected to degassing and heated at 110 ^{0}C for three hours. The mixture was cooled to room temperature and poured in $CHCl_3$ (200 mL) followed by ammonium hydroxide solution (28% in H_2O, 50 mL). This mixture was stirred overnight. The organic phase was separated and washed with distilled water. It was concentrated *in vacuo* (~40 mL) and added to a degassed mixture of methanol-water (300 mL, 10:1, previously degassed). This mixture was stirred overnight and filtered to obtain the crude solid. The crude solid was cleaned *via* Soxhlet extraction using methanol, acetone, hexane, chloroform and chlorobenzene. The chloroform and chlorobenzene fractions were independently concentrated *in vacuo* (~40

mL) and precipitated in methanol (300 mL). These mixtures were stirred overnight and filtered to obtain the polymer as purple solids. The yield of chloroform fraction was (52 mg, 26% yield). GPC (1,2,4-trichlorobenzene at 140 ˚C): M_n = 10500, M_w = 20200, PD = 1.9. The yield of the chlorobenzene fraction was (102 mg, 52% yield). GPC (1,2,4-trichlorobenzene at 140 ˚C): M_n = 14900, M_w = 25500, PD = 1.7. Elemental analysis (%) calculated for $C_{106}H_{148}N_6O_4S_3$: C, 76.39; H, 8.95; N, 5.04; S, 5.77. Found: C, 77.10; H, 10.03; N, 3.97; S, 4.53. ^{1}H NMR (500 MHz, $C_2D_2Cl_4$, 100 ^{0}C) δ_H/ppm: 8.31 (br, 2H), 7.95 (br, 4H), 7.87 (s, 2H), 7.31 (br, 4H), 7.13 (br, 2H), 4.18 (br, 8H), 2.00 (m, 4H), 1.70-1.15 (br, 96H), 0.98 (br, 24H). λ_{max}(solution) nm = 540. λ_{max}(thin film) nm = 620.

3.4.8 Poly(6,7,15,16-tetrakis[3-pentylundecyl]-quinoxalino [2',3':9,10]phenanthro[4,5-abc]phenazine-2,11-diyl]-alt-(4,7-dithiophen-2-yl)-2',1',3'-benzothiadiazole-5,5'-diyl] (P8)
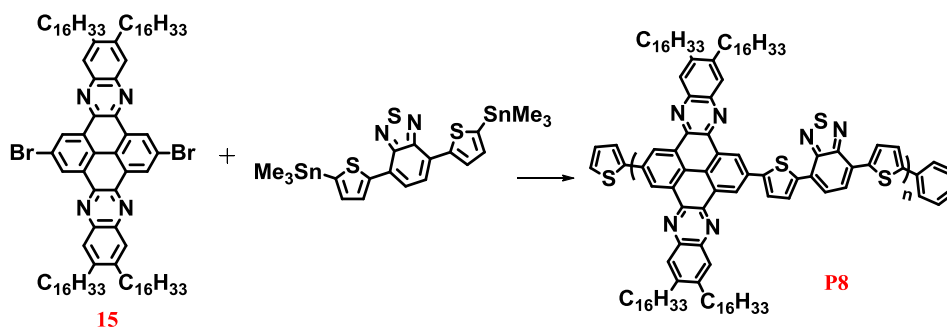
In a 100 mL one-neck round bottom flask was added 2,11-dibromo-6,7,15,16-tetrakis (3-pentyl undecyl) quinoxalino [2`,3`:9,10] phenanthro [4,5-abc] phenazine (150 mg, 102.8 mmol), 4,7-bis(5-(trimethylstannyl)thiophen-2-yl)benzo[c][1,2,5]thiadiazole (64 mg, 102.8 mmol) and 9 mL of dry toluene under an inert argon atmosphere. $Pd_2(dba)_3$ (5 mg, 0.005 mmol) and tri-ortho-tolylphosphine (9 mg, 0.03 mmol) were added to the reaction. The system was degassed again and put under an argon atmosphere that was maintained for 20 minutes. Once this time had elapsed the temperature was raised to 110 ^{0}C for 24 hours. Upon completion, the reaction was cooled to room temperature. Dry toluene (5 mL) and bromobenzene (0.1 mL, 0.9 mmol) were added and the system was degassed and heated for one hour at 110 ^{0}C. Upon completion, the mixture was cooled to room temperature and 2-

(tributylstannyl)thiophene (0.1 mL 0.4 mmol) was added. Again, the mixture was subjected to degassing and heated at 110 ^{0}C for three hours. The mixture was cooled to room temperature and poured in CHCl$_3$ (200 mL) followed by ammonium hydroxide solution (28% in H$_2$O, 50 mL). This mixture was stirred overnight. The organic phase was separated and washed with distilled water. It was concentrated *in vacuo* (~40 mL) and added to a degassed mixture of methanol-water (300 mL, 10:1, previously degassed). This mixture was stirred overnight and filtered to obtain the crude solid. The crude solid was cleaned *via* Soxhlet extraction using methanol, acetone, hexane, chloroform and chlorobenzene. The chloroform and chlorobenzene fractions were independently concentrated *in vacuo* (~40 mL) and precipitated in methanol (300 mL). These mixtures were stirred overnight and filtered to obtain the polymer as purple solids. The yield of chloroform fraction was (17mg, 9% yield). GPC (1,2,4-trichlorobenzene at 140 ˚C): M$_n$ = 9700, M$_w$ = 15520, PD = 1.6. The yield of chlorobenzene fraction was (109 mg, 60% yield). GPC (1,2,4-trichlorobenzene at 140 ˚C): M$_n$ = 16500, M$_w$ = 23200, PD = 1.4. Elemental analysis (%) calculated for C$_{106}$H$_{148}$N$_6$S$_3$: C, 79.44; H, 9.31; N, 5.24; S, 6.00. Found: C, 80.50; H, 10.60; N, 4.49; S, 5.04. ^{1}H NMR (500 MHz, C$_2$D$_2$Cl$_4$. 100 ^{0}C) δ_H/ppm: 9.30 (br, 4H), 7.80 (br, 2H), 7.49 (s, 2H), 7.36 (s, 4H), 7.15 (d, 2H), 2.70 (br, 8H), 1.92 (m, 8H), 1.70-1.15 (br, 92H), 0.99 (br, 24H). λ_{max}(solution) nm = 520. λ_{max}(thin film) nm = 610.

3.4.9 Poly 6,7,15,16-tetrakis(hexadecyloxy)quinoxalino [2',3':9,10] phenanthro[4,5-abc]phenazine-2,11-diyl-alt-(5,6-bis (octyloxy)-4,7-dithiophen-2-yl)benzo[1,2,5]thiadiazole-5,5-diyl] (P9)
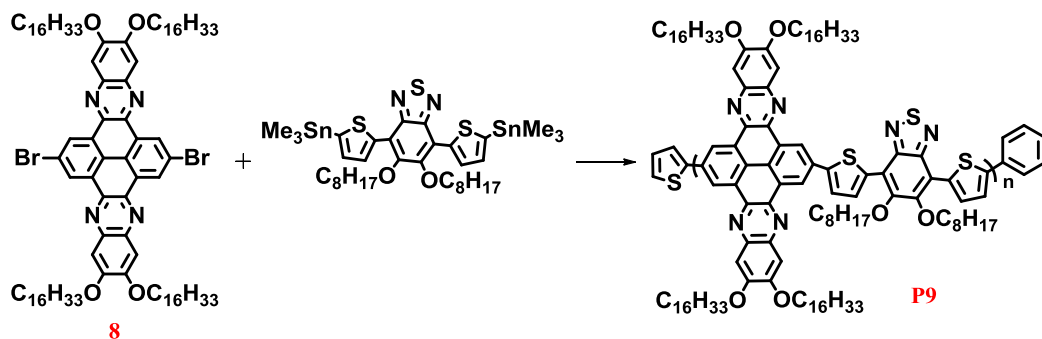
In a 100 mL one-neck round bottom flask was added 2,11-dibromo-6,7,15,16-tetrakis(2-hexyldecyloxy)quinoxalino[2',3':9,10]phenanthro [4, 5-abc]phenazine (200 mg, 0.1 mmol), 5,6-bis(octyloxy)-4,7-bis(5-(trimethylstannyl)thiophen-2-yl)benzo[c][1,2,5]thiadiazole (116 mg, 0.1 mmol) and 8 mL of dry toluene under an inert argon atmosphere. $Pd_2(dba)_3$ (6 mg, 0.006 mmol) and tri-ortho-tolylphosphine (12 mg, 0.03 mmol) were added to the reaction. The system was degassed again and put under an argon atmosphere that was maintained for 20 minutes. Once this time had elapsed the temperature was raised to 110 ^{0}C for 24 hours. Upon completion, the reaction was cooled to room temperature. Dry toluene (5 mL) and bromobenzene (0.1 mL, 0.9 mmol) were added and the system was degassed and heated for one hour at 110 ^{0}C. Upon completion, the mixture was cooled to room temperature and 2-(tributylstannyl)thiophene (0.1 mL 0.4 mmol) was added. Again, the mixture was subjected to degassing and heated at 110 ^{0}C for three hours. The mixture was cooled to room temperature and poured in $CHCl_3$ (200 mL) followed by ammonium hydroxide solution (28% in H_2O, 50 mL). This mixture was stirred overnight. The organic phase was separated and washed with distilled water. It was concentrated *in vacuo* (~40 mL) and added to a degassed mixture of methanol-water (300 mL, 10:1, previously degassed). This mixture was stirred overnight and filtered to obtain the crude solid. The crude solid was cleaned *via* Soxhlet extraction using methanol, acetone, hexane and toluene. The toluene fraction was concentrated *in vacuo* (~40 mL) and precipitated in methanol (300 mL). This mixture was

stirred overnight and filtered to obtain the polymer as dark red solids. The yield of toluene fraction was (55 mg, 21% yield). GPC (1,2,4-trichlorobenzene at 140 ˚C): M_n = 10100, M_w = 13200, PD = 1.3. Elemental analysis (%) calculated for $C_{122}H_{180}N_6O_6S_3$: C, 76.20; H, 9.43; N, 4.37; O, 4.99; S, 5.00. Found: C, 74.18; H, 9.03; N, 4.29; S, 4.38. ^{1}H NMR (500 MHz, $C_2D_2Cl_4$. 100 [0]C) δ_H/ppm: 9.98 (br, 4H), 8.58 (br, 2H), 7.87 (br, 4H), 7.52 (br, 2H), 4.31 (d, 8H), 4.22 (d, 4H), 2.11 (m, 4H), 2.00 (d, 4H), 1.69-1.11 (br, 116H), 0.97 (br, 30H). λ_{max}(solution) nm = 504. λ_{max}(thin film) nm = 520.

3.4.10 Poly 6,7,15,16-tetrakis(3-pentylundecyl)quinoxalino [2',3':9,10] phenanthro[4,5-abc]phenazine-2,11-diyl-alt-(5,6-bis(oc tyloxy)-4,7-dithiophen-2-yl)benzo[1,2,5]thiadiazole-5,5-diyl] (P10)
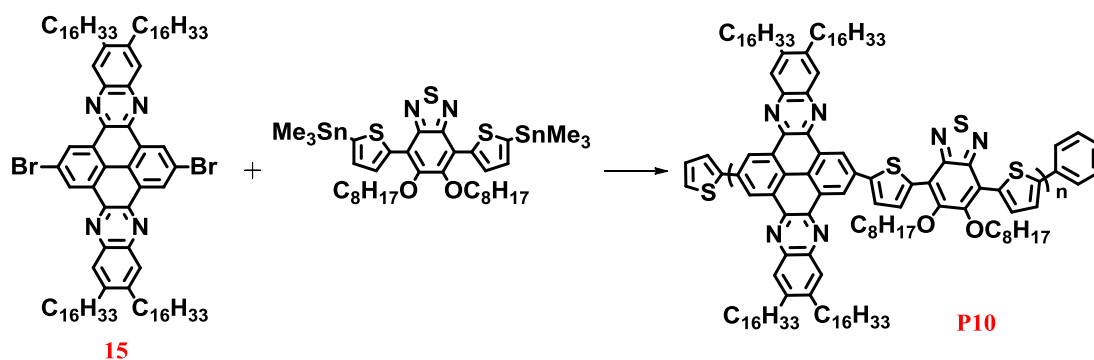
In a 100 mL one-neck round bottom flask was added 2,11-dibromo-6,7,15,16-tetrakis(3-pentylundecyl)quinoxalino[2',3':9,10]phenanthro [4, 5-abc]phenazine (200 mg, 0.1 mmol), 5,6-bis(octyloxy)-4,7-bis(5-(trimethylstannyl)thiophen-2-yl)benzo[c][1,2,5]thiadiazole (121 mg, 0.1 mmol) and 8 mL of dry toluene under an inert argon atmosphere. $Pd_2(dba)_3$ (6 mg, 0.006 mmol) and tri-ortho-tolylphosphine (12 mg, 0.03 mmol) were added to the reaction. The system was degassed again and put under an argon atmosphere that was maintained for 20 minutes. Once this time had elapsed the temperature was raised to 110 [0]C for 24 hours. Upon completion, the reaction was cooled to room temperature. Dry toluene (5 mL) and bromobenzene (0.1 mL, 0.9 mmol) were added and the system was degassed and heated for one hour at 110 [0]C. Upon completion, the mixture was cooled to room temperature and 2-(tributylstannyl)thiophene (0.1 mL 0.4 mmol) was added. Again, the mixture was subjected

to degassing and heated at 110 ^{0}C for three hours. The mixture was cooled to room temperature and poured in CHCl$_3$ (200 mL) followed by ammonium hydroxide solution (28% in H$_2$O, 50 mL). This mixture was stirred overnight. The organic phase was separated and washed with distilled water. It was concentrated *in vacuo* (~40 mL) and added to a degassed mixture of methanol-water (300 mL, 10:1, previously degassed). This mixture was stirred overnight and filtered to obtain the crude solid. The crude solid was cleaned *via* Soxhlet extraction using methanol, acetone, hexane and toluene. The toluene fraction was concentrated *in vacuo* (~40 mL) and precipitated in methanol (300 mL). This mixture was stirred overnight and filtered to obtain the polymer as dark red solids. The yield of toluene fraction was (40 mg, 15% yield). GPC (1,2,4-trichlorobenzene at 140 ˚C): M_n = 13300, M_w = 16300, PD = 1.2. Elemental analysis (%) calculated for C$_{122}$H$_{180}$N$_6$O$_2$S$_3$: C C, 78.82; H, 9.76; N, 4.52; O, 1.72; S, 5.17. Found: C, 74.02; H, 9.13; N, 3.88; S, 4.23. ^{1}H NMR (500 MHz, C$_2$D$_2$Cl$_4$, 100 ^{0}C) δ_H/ppm: 9.95 (s, 4H), 8.58 (d, 2H), 7.51 (s, 4H), 7.21 (d, 2H), 4.22 (m, 4H), 2.82 (br, 8H), 2.12 (br, 8H), 1.82 (d, 4H), 1.65-1.09 (br, 112H), 0.97 (br, 30H). λ_{max}(solution) nm = 500. λ_{max}(thin film) nm = 517.

3.4.11 Poly 6,7,15,16 tetrakis(hexadecyloxy)quinoxalino [2',3':9,10]phenanthro[4,5-abc]phenazine-2,11-diyl-alt-(5,6-bis(octyloxy)-4,7-di(2,2-bithiophen-5-yl)benzo[c][1,2,5]thiadiazole)-5,5-diyl] (P11)
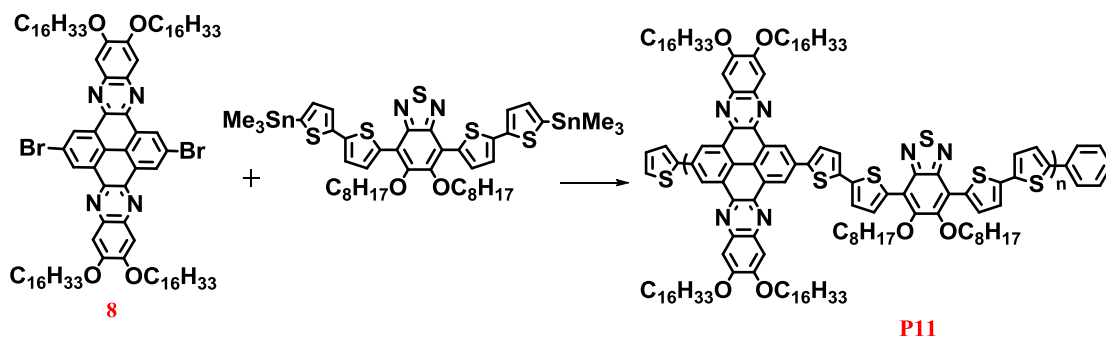
In a 100 mL one-neck round bottom flask was added 2,11-dibromo-6,7,15,16-tetrakis(2-hexyldecyloxy)quinoxalino [2',3':9,10]phenanthro[4, 5-abc]phenazine (150 mg, 0.09 mmol) ,5,6-bis(octyloxy)-4,7-bis(5'-(trimethylstannyl)-[2,2'-bithiophen]-5-yl)benzo[c][1,2,5] thiadiazole (103 mg, 0.09 mmol) and 6 mL of dry toluene were added under an inert argon atmosphere. $Pd_2(dba)_3$ (6 mg, 0.006 mmol) and tri-ortho-tolylphosphine (12 mg, 0.03 mmol) were added to the reaction. The system was degassed again and put under an argon atmosphere that was maintained for 20 minutes. Once this time had elapsed the temperature was raised to 110 ^{0}C for 24 hours. Upon completion, the reaction was cooled to room temperature. Dry toluene (5 mL) and bromobenzene (0.1 mL, 0.9 mmol) were added and the system was degassed and heated for one hour at 110 ^{0}C. Upon completion, the mixture was cooled to room temperature and 2-(tributylstannyl)thiophene (0.1 mL 0.4 mmol) was added. Again, the mixture was subjected to degassing and heated at 110 ^{0}C for three hours. The mixture was cooled to room temperature and poured in $CHCl_3$ (200 mL) followed by ammonium hydroxide solution (28% in H_2O, 50 mL). This mixture was stirred overnight. The organic phase was separated and washed with distilled water. It was concentrated *in vacuo* (~40 mL) and added to a degassed mixture of methanol-water (300 mL, 10:1, previously degassed). This mixture was stirred overnight and filtered to obtain the crude solid. The crude solid was cleaned *via* Soxhlet extraction using methanol, acetone, hexane,

toluene and chloroform. The chloroform fraction was concentrated *in vacuo* (~40 mL) and precipitated in methanol (300 mL). This mixture was stirred overnight and filtered to obtain the polymer as purple solids. The yield of chloroform fraction was (136 mg, 67% yield). GPC (1,2,4-trichlorobenzene at 140 ˚C): M_n = 11000, M_w = 16000, PD = 1.4. Elemental analysis (%) calculated for $C_{130}H_{184}N_6O_6S_5$: C, 74.81; H, 8.89; N, 4.03; O, 4.60; S, 7.68. Found: C, 76.69; H, 10.15; N, 3.21; S, 5.90. ^{1}H NMR (500 MHz, $C_2D_2Cl_4$, 100 ^{0}C) δ_H/ppm: 9.90 (br, 4H), 8.45 (br, 2H), 7.71 (d, 2H), 7.55 (d, 2H), 7.49 (br, 4H), 7.25 (br, 2H), 4.31-4.16 (br, 12H), 2.00 (m, 4H), 1.65 (d, 4H), 1.55-1.13 (br, 116), 0.90 (t, 30H). λ_{max}(solution) nm = 530. λ_{max}(thin film) nm = 605.

3.4.12 Poly 6,7,15,16 tetrakis(3 pentylundecyl)quinoxalino [2',3':9,10] phenanthro[4,5-abc]phenazine-2,11-diyl-alt-(5,6-bis (octyloxy)-4,7-di(2,2-bithiophen-5-yl)benzo[c][1,2,5]thiadiazole)-5,5-diyl] (P12)
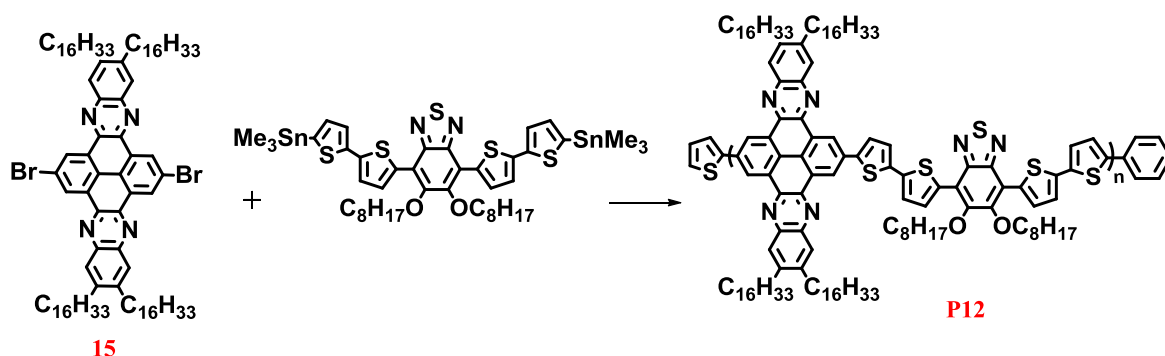
In a 100 mL one-neck round bottom flask was added 2,11-dibromo-6,7,15,16-tetrakis(3-pentyl undecyl)quinoxalino [2',3':9,10]phenanthro[4, 5-abc]phenazine (150 mg, 0.1 mmol), 5,6-bis(octyloxy)-4,7-bis(5'-(trimethylstannyl)-[2,2'-bithiophen]-5-yl)benzo[c][1,2,5] thiadiazole (90 mg, 0.1 mmol) and 6 mL of dry toluene were added under an inert argon atmosphere. $Pd_2(dba)_3$ (6 mg, 0.006 mmol) and tri-ortho-tolylphosphine (12 mg, 0.03 mmol) were added to the reaction. The system was degassed again and put under an argon atmosphere that was maintained for 20 minutes. Once this time had elapsed the temperature was raised to 110 ^{0}C for 24 hours. Upon completion, the reaction was cooled to room temperature. Dry toluene (5 mL) and bromobenzene (0.1 mL, 0.9 mmol) were added and the system was degassed and heated for one hour at 110 ^{0}C. Upon completion, the mixture

was cooled to room temperature and 2-(tributylstannyl)thiophene (0.1 mL 0.4 mmol) was added. Again, the mixture was subjected to degassing and heated at 110 ^{0}C for three hours. The mixture was cooled to room temperature and poured in $CHCl_3$ (200 mL) followed by ammonium hydroxide solution (28% in H_2O, 50 mL). This mixture was stirred overnight. The organic phase was separated and washed with distilled water. It was concentrated *in vacuo* (~40 mL) and added to a degassed mixture of methanol-water (300 mL, 10:1, previously degassed). This mixture was stirred overnight and filtered to obtain the crude solid. The crude solid was cleaned *via* Soxhlet extraction using methanol, acetone, hexane, toluene and chloroform. The chloroform fraction was concentrated *in vacuo* (~40 mL) and precipitated in methanol (300 mL). This mixture was stirred overnight and filtered to obtain the polymer as purple solids. The yield of chloroform fraction was (144mg, 70% yield). GPC (1,2,4-trichlorobenzene at 140 ˚C): M_n = 10000, M_w = 14000, PD = 1.4. Elemental analysis (%) calculated for $C_{130}H_{184}N_6O_2S_5$: C, 77.17; H, 9.17; N, 4.15; O, 1.58; S, 7.92. Found: C, 79.17; H, 10.47; N, 3.19; S, 6.94. ^{1}H NMR (500 MHz, $C_2D_2Cl_4$, 100 ^{0}C) δ_H/ppm: 9.88 (br, 4H), 8.40 (d, 2H), 7.89 (d, 2H), 7.75 (br, 4H), 7.25 (br, 4H), 4.21 (br, 4H), 2.93-2.16 (br, 12H), 1.80, (br, 8H), 1.70-1.10 (br, 112), 0.95 (t, 30H). λ_{max}(solution) nm = 528. λ_{max}(thin film) nm = 600.

4 Chapter 4: Synthesis of laterally extended two-dimensional quinoxaline based polymers with alternating electron donors

4.1 Introduction

The homopolymer P3HT has found widespread use in organic solar cells and efficiencies in excess of 5% have been achieved when blended with $PC_{70}BM$ and used in BHJ solar cells.[137] However, the limitations associated with the homopolymer P3HT mean that efficiencies have reached their limit. One of the limitations associated with P3HT is its large optical band gap and mismatch with the solar spectrum, which limits the light harvesting properties of the polymer.[138]

Previous literature has shown that when an electron-deficient monomer is copolymerised in an alternate fashion with an electron-rich monomer, in a so called donor-acceptor (D-A) approach, the resulting polymer possess a low optical band gap.[10] The low optical band gaps seen in these D-A polymers can be attributed to a portion of charge being transferred between the donor and acceptor units. This gives rise to an intramolecular charge transfer (ICT) band in the visible region of the incident electromagnetic spectrum. Modifying the donor and acceptor units can influence the polymers' light harvesting properties.[12]

Quinoxaline derivatives are one class of acceptor monomers used in the design of low band gap D-A conjugated polymers. Quinoxaline has attracted the attention of researchers due to the electron deficient *N*-heterocycle.[139] Alongside the quinoxaline derivatives, pyrene compounds can be incorporated between two quinoxaline molecules to build a two-dimensional structure, which could improve the physical properties of the D–A system.[71a] The design of extended two-dimensional polymers can improve the planarity of the resulting molecules which should increase the delocalisation of π-electrons. Furthermore, the improved planarity should also increase the number of π-π stacking interactions which should improve charge carrier mobility. The polymers shown in (**Scheme 4-1**) were targeted, and a series of monomers must be synthesised first.
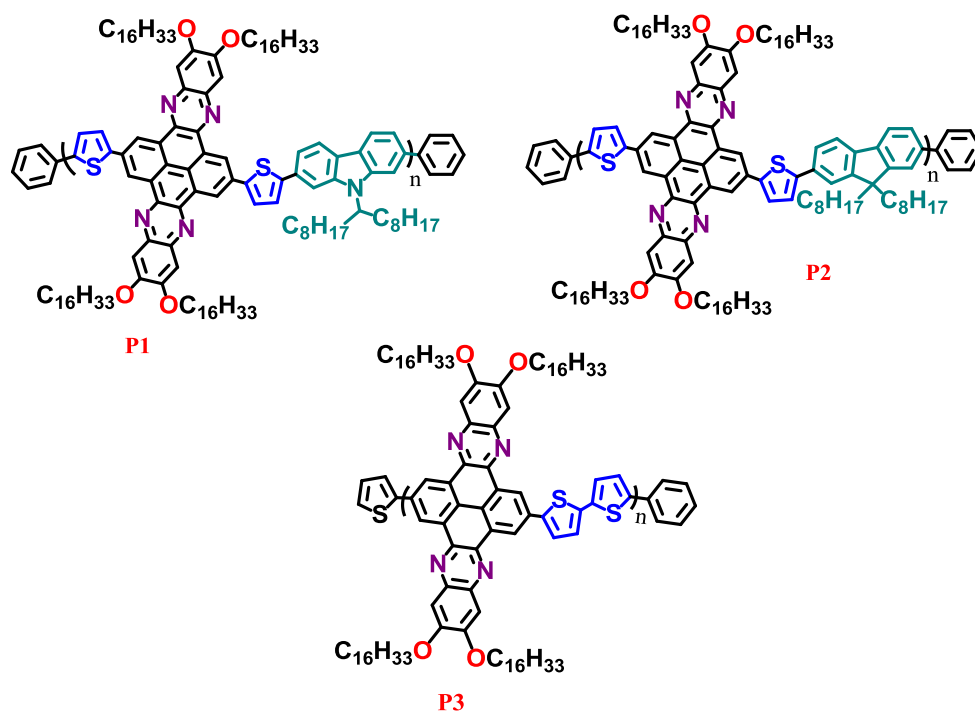
Scheme 4-1 The chemical structure of targeted polymers **P1**, **P2** and **P3**

P1 will use carbazole flanked by two thiophenyl groups as the donor-unit. Replacing the *9H*-carbon in fluorene with nitrogen forms the carbazole unit. The presence of a sp^2 hybridised nitrogen atom provides better electron donating properties to carbazole, relative to fluorene, leading to a more pronounced D-A alternate copolymer. Literature has shown that PCDTBT, a polymer that uses carbazole and benzothiadiazole as the donor and acceptor units, has efficiencies in excess of 6%.[111] The pyrene-quinoxaline acceptor unit designed in this thesis has multiple advantages over benzothiadiazole including improved solubility and a more planar structure. Thus, it is expected that polymers based on pyrene-quinoxaline-*alt*-carbazole will display efficiencies and properties that exceed those of PCDTBT.

Fluorene flanked by two thiophenyl units will be used as the donor-unit in **P2**. Fluorene is a highly planar molecule that has an extended conjugation across the two benzene rings. Previous polymers based on fluorene have shown high thermal stability and deep HOMO levels.[140] The solubility of fluorene based polymers can be improved by attaching solubilising chains at the *9*H-position of fluorene. This will allow the final polymer product to undergo solution processing; a benefit of organic solar cells.[141] Furthermore, the

properties of fluorene based copolymers can be tuned by introducing different substituents at the *9*H-poisition of fluorene.[142] The high hole mobilities displayed by fluorene-based copolymers in organic light emitting diodes should remain when the material is used in organic solar cells.[143]

P3 will use 2,2'-bithiophene as the donor-unit. Previous literature has shown that D-A conjugated polymers that incorporate dithiophene units into the polymer backbone have improved photophysical properties relative to polymers that incorporate six-membered rings.[144] Six-membered rings generate a large amount of steric hindrance. Replacing six-membered rings with the five-membered thiophene ring alleviates this steric strain resulting in a highly planar D-A copolymer that possesses a strong electron-delocalisation ability.[145] The improved electron delocalisation leads to improved orbital mixing. Consequently, thiophene is a strong electron donor. [144] Generally, stronger donor units causes the resulting polymer to exhibit a narrower optical band gap and a shallow LUMO level. Thus, when fabricated into photovoltaic devices the resulting device shows a high J_{sc} and a low V_{oc}.[146]

Attaching alkyl chains to the donor and acceptor units improves the solubility of the final monomers and of the resulting polymer. However, sometimes the alkyl chains are in close proximity to each other and the conjugated backbone twists to relieve this strain. This disrupts the planarity of the polymer backbone which limits the conjugation length resulting in a wide optical band gap. Previous literature has shown that inserting unfunctionalised thiophene or dithiophene spacers between the donor and acceptor units is an effective method of separating the donor and acceptor units,[136] thus, relieving any unwanted steric strain. An example of this is shown in **Scheme 4-2**.[147] Incorporating a thiophene spacer in PDTS-DTBTA improves the backbone planarity resulting in a low optical band gap polymer that demonstrates improved photovoltaic performance.[147]
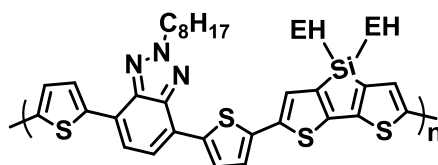
Scheme 4-2 The chemical structure of PDTS-DTBTA

4.2   Synthesis of monomers for polymers P1, P2 and P3

In order to prepare the polymers (**P1**), (**P2**), some monomers were needed. These include, 2,11-bis(5-bromothiophen-2-yl)-6,7,15,16-tetrakis (hexadecyloxy) quinoxalino [2',3':9,10] phenanthro [4,5-abc] phenazine (**10**), which was prepared successfully in nine steps (**Scheme 4-4**). Monomer 9-(heptadecan-9-yl)-2,7-bis(4,4,5,5-tetramethyl-1,3,2-dioxaborolan-2-yl)-9H-carbazole (**32**) was synthesised by Hunan Yi of the Iraqi group, (**Scheme 4-3**) and monomer 9,9-dioctylfluorene-2,7-diboronic acid bis(1,3-propanediol) ester (**33**) was bought from Sigma Aldrich (**Scheme 4-3**). For (**P3**) two monomers were needed, monomer 2,11-dibromo-6,7,15,16-tetrakis(2-hexyldecyloxy)quinoxalino [2',3':9,10]phenanthro[4,5-abc]phenazine (**8**) was synthesised successfully (**Scheme 4-3**) and monomer 5,5'-bis(trimethylstannyl)-2,2'-bithiophene (**34**) which was prepared by A. Murad of the Iraqi group (**Scheme 4-3**). The structure and the purity of these intermediate monomers were checked and examined by ^{1}H NMR, ^{13}C NMR, FT-IR, mass spectrometry, melting point and elemental analysis.
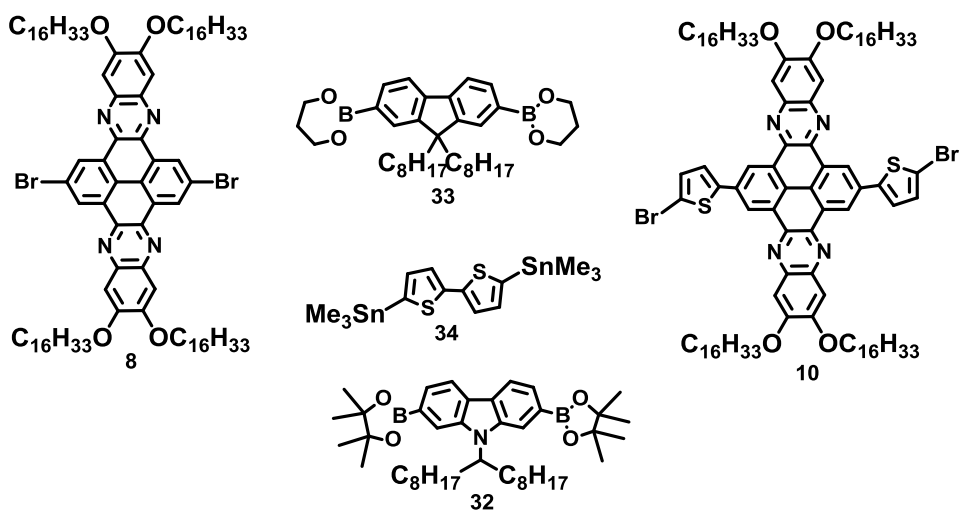
Scheme 4-3 monomers required for preparing **P1**, **P2** and **P3**

4.2.1 2,11-bis(5-bromothiophen-2-yl)-6,7,15,16-tetrakis (2-hexyldecyloxy)-5,8-dihydroquinoxalino[2',3':9,10]phenanthro[4,5-abc]phenazine (10)

Monomer (**10**) was prepared successfully in nine steps as shown in **Scheme 4-4**. The structure and the purity of these intermediate monomers were checked and examined by ^{1}H NMR, ^{13}C NMR, FT-IR, mass spectrometry, melting point and elemental analysis.
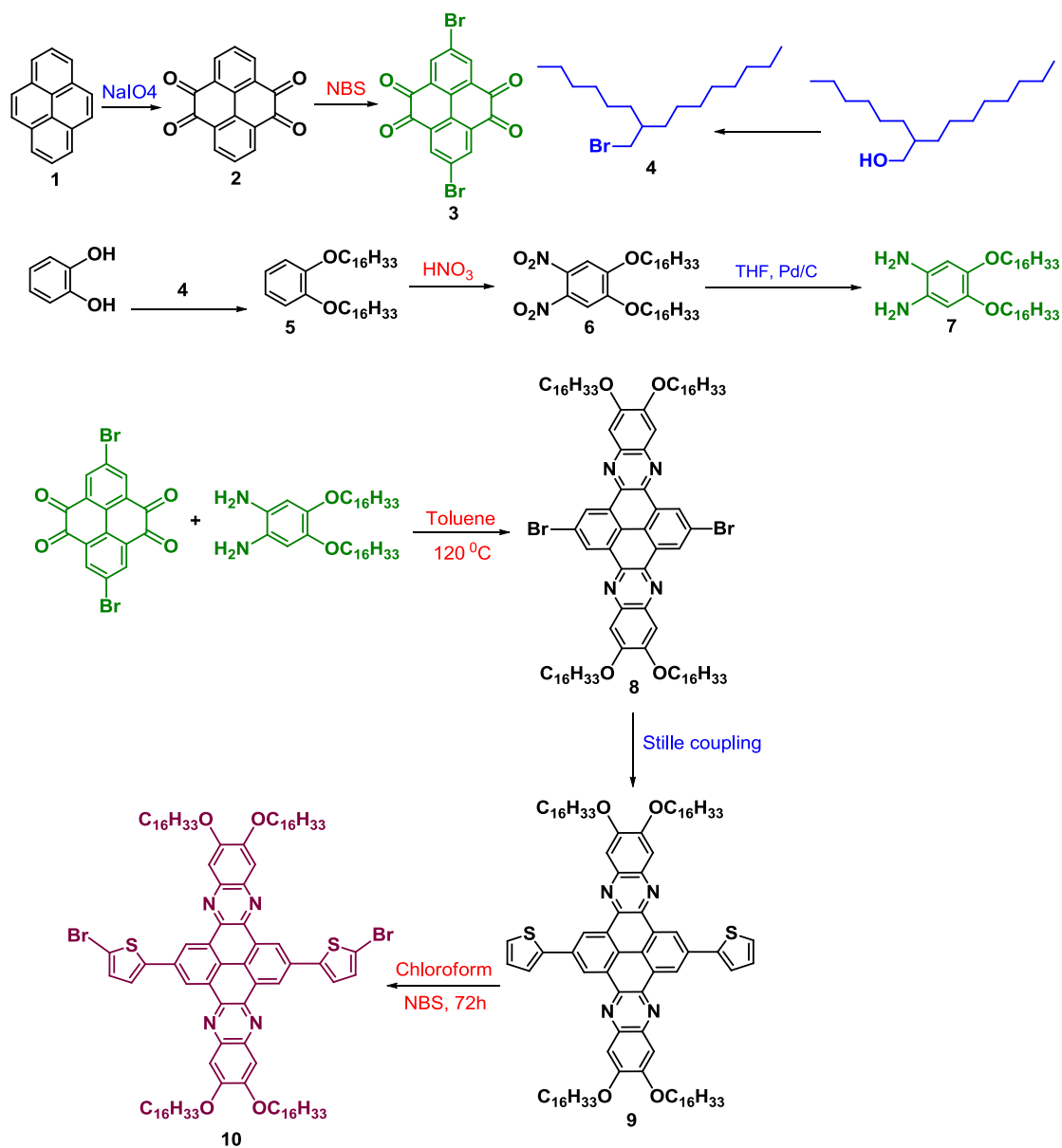
Scheme 4-4 The preparation route for (**10**)

Pyrene molecule (**1**) was treated with Raney nickel catalyst for 3 days to remove any traces of sulphur to give a purer product (yellow crystals). The modified Julius Rebek's reaction was used to prepare monomer (**2**).[148] In this reaction pyrene was oxidised in positions 4,5,9 and 10 by using sodium periodate (NaIO$_4$. 8 eq) as oxidiser and ruthenium (III) chloride (RuCl$_3$) as a catalyst. The mixture was left stirring vigorously at reflux for 30 hours. The crude product was recrystallised from m-xylene to give the pure product as bright orange crystals in 22% yield. The possible mechanism for this reaction involves converting ruthenium (III) chloride (RuCl$_3$) to ruthenium tetroxide (RuO$_4$) in the presence of sodium periodate (NaIO$_4$) and H$_2$O. The ruthenium tetroxide (RuO$_4$) reagent is a good oxidiser which can introduce the carbonyl group to positions 4,5,9 and 10 of the pyrene molecule (**1**).

^{1}H NMR, mass spectrometry, FT-IR, m.p and elemental analysis were used to characterise the product, which confirmed the structure of (**2**). The pyrene-4,5,9,10-tetraone (**2**) is a symmetrical molecule that has two proton environments. The doublet peak at 8.33 ppm is assigned to the hydrogens on carbons 1, 3, 6 and 8. In addition, the hydrogens on carbons 2 and 7 appeared as a triplet at 7.74 ppm in the ^{1}H NMR chart. The FT-IR is a perfect tool to analyse such a monomer, which has carbonyl peaks. These peaks occur in unique areas in the spectrum. Comparing the peaks of the starting materials with the product, many new stretching peaks appear at the central area, especially at 1672 cm^{-1}, which was assigned to the four carbonyl groups attached to the pyrene molecule. The mass of the molecular ion clearly shows a peak at m/z = 262 (M$^+$). As expected, the melting point is between 349 to 351 ^{0}C, which is in agreement with literature values.[115]

Pyrene-4,5,9,10-tetraone (**2**) was brominated using a N-bromsuccinimide (NBS) in concentrated sulphuric acid.[116] This is because the solubility of (**2**) is low, and hence, a strong solvent needs to be used. It is worth noting that the conjugation of this molecule is reduced to two rings only, which leads to a concentration of the electronic density at positions 2 and 7. In consequence, the bromine atoms are directed into positions 2 and 7 only.

This reaction is an electrophilic substitution in which N-bromsuccinimide (NBS) provide the bromine atom as a cation, which can replace the hydrogen on carbons at the positions 2 and 7.[149] The reaction was completed in 3 hours, wherein NBS was injected in portions over 2 hours to avoid overheating this reaction. It was stirred for 1 hour to make sure that the reaction was completed. Thereafter, the mixture was quenched in ice-water to precipitate (**3**) and eliminate H_2SO_4.

The purification of the product passed through many steps. First, the crude product was washed with boiling methanol, then filtered off and dried. The same procedure was repeated with diethyl ether and DCM solvents.

The structure of (**3**) was confirmed by using ^{1}H NMR, which shows a singlet peak at 8.54 ppm assigned for the hydrogens at positions 1, 3, 6 and 8. The FT-IR also confirmed the synthesis of the new compound by having a new peak at 642 cm^{-1}, which refers to the new C-Br bond. Mass spectrometry was also used, and it revealed peaks at 418, 420 and 422 (M^+), which were assigned to two isotopes ^{79}Br and ^{81}Br respectively. The ratio between these peaks 418, 420, and 422 (M^+) are 1:2:1.

As monomer (**3**) has very low solubility in common organic solvents, the need for attaching an alkyl chain is important; therefore, 2-hexyl-1-bromodecane (**4**) was prepared by using the modified procedure of Lee et al.[117] The resulting product was a colourless liquid. The reaction was convenient and easy to do, which took only 10 min, and was then washed with saturated H_2O with sodium carbonate and dried under rotary evaporation. The TLC in pure hexane indicated that the residue of the NBS and triphenyl phosphine were present; therefore, a column chromatography with pure hexane was used to purify 2-hexyl-1-bromodecane. The reaction mechanism, as suggested by Trippett which followed the S_N2 route.[150]

Characterisation of the product (**4**) confirmed its purity by ^{1}H NMR, mass spectrometry, and elemental analysis. The ^{1}H NMR spectra showed a doublet at 3.46 ppm assigned for the hydrogens on the carbon next to the oxygen. The mass spectra revealed the main integer masses at 304 and 306 (M^+) as expected. The ratio between these two integers is 1:1 which

is suitable for [79]Br and [81]Br isotopes. The elemental analysis for this monomer was also in agreement with the proposed structure.

As monomer (**3**) has a very low solubility in common organic solvents, the needs for attaching an alkyl chain is important; therefore, catechol and the alkyl bromide with the branched chain was used to form compound (**5**). This procedure was modified from Zhang et al.[118] In this reaction, DMF was used as a solvent, and potassium carbonate K_2CO_3 was utilised as a weak base. The alkyl bromide ($C_{16}H_{33}$-Br) was added in portions to push the reaction forward to the product. The reaction progress was followed by thin layer chromatography (TLC), which indicated the end of the reactions after 48 h.

The mechanism of this reaction follows an S_N2 nucleophilic substitution, which deprotonates the hydroxyl group by K_2CO_3 and can then work as a nucleophile and attack ($C_{16}H_{33}$-Br) to produce monomer (**5**) (**Scheme 4-5**).
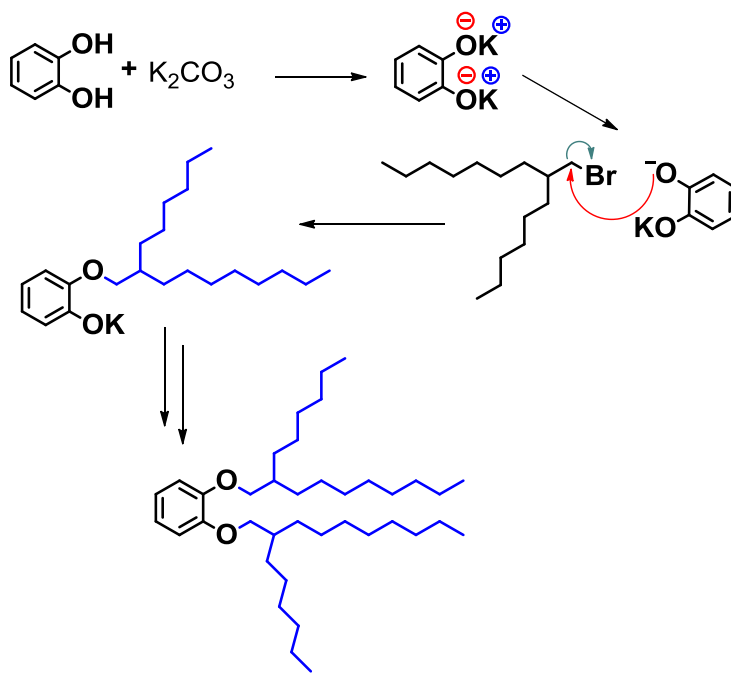
Scheme 4-5 The proposed scheme for producing (**5**)

Column chromatography was used in 2 steps to purify product (**5**). In the first step, pure hexane was used to elute the column to remove the residue of the excess alkyl bromide.

Secondly, a mixture of hexane and ethyl acetate (30:1; v/v) was used to collect monomer (**5**). ^{1}H NMR was used to assess the purity of the product, and a doublet appeared at 3.86 ppm, which is assigned for the hydrogens on the carbon next to the oxygen. Additionally, a singlet appeared at 6.89 ppm for the aromatic hydrogens.

Mass spectrometry of the pure product showed a main peak at m/z = 559 (M^{+}) as expected for the molecular ion. Elemental analysis also confirmed the purity of the product. FT-IR spectra also confirmed the alkylation of the catechol from the disappearance of the stretched peaks between 3100 to 3500 cm.$^{-1}$

To prepare 1,2 dinitro-4,5-bis(2-hexyldecyloxy)benzene (**6**), the Sessler procedure was followed,[119] which gave a good yield (85%) as a transparent oil form. The reaction was carried out under strong acidic conditions, in which nitric acid 68%, acetic acid, and nitric acid 100% were stirred, along with the starting materials (**5**). The mechanism of this reaction follows two steps; the first step produces the nitronium cation (NO$_2^{+}$), which in the second step attacks the benzene ring to introduce nitro group at meta positions of (**6**) **Scheme 4-6**.

As the reaction finished, it was washed with ice-water to remove the residue of the acids; next, it was washed with saturated distilled water with sodium hydrogen carbonate and brine solution to get rid of all the inorganic impurities. ^{1}H NMR was used to assess the purity and the formation of the monomer, and there was a doublet at 3.97 ppm assigned to the hydrogens on the carbon next to the oxygen. This doublet was de-shielded from 3.86 ppm in alkylated catechol to 3.97 ppm in this monomer.

The mass spectrum showed a main integral peak at m/z = 649 (M^{+}), as expected for such a molecule. The FT-IR confirmed the nitration of the product by showing new strong bands at 1570 and 1353 cm,$^{-1}$ which corresponded to the vibration of the nitro groups.
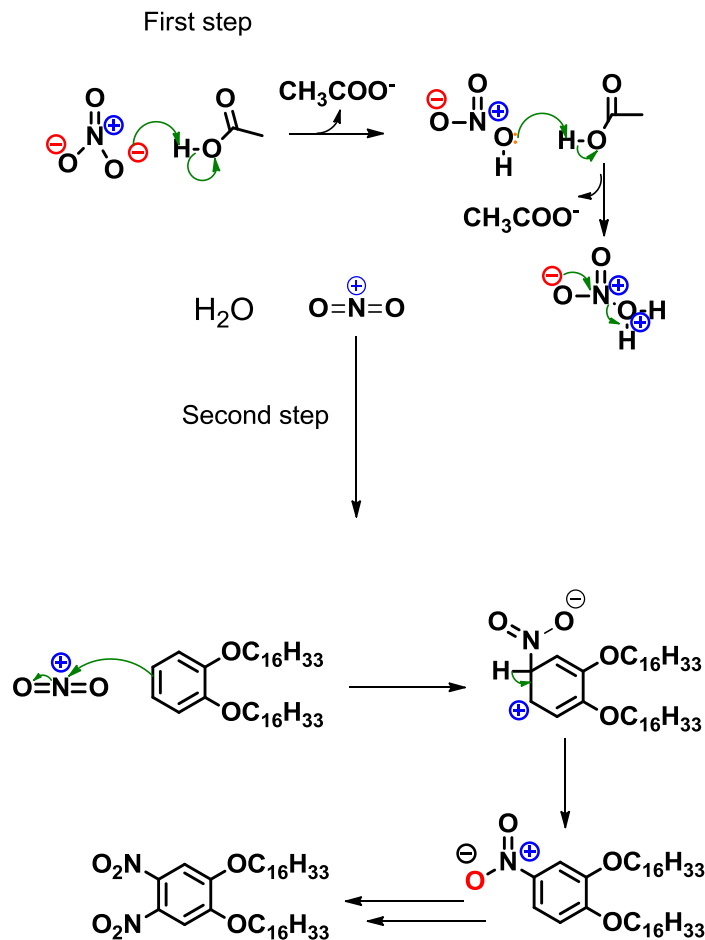
Scheme 4-6 The proposed scheme for preparing (**6**)

The preparation of 1,2-diamino-4,5-bis(2-hexyldecyloxy)benzene (**7**) was undertaken using a modified method of MacLachlan.[120] The reaction used the catalyst Pd/C and ammonium formate in a solvent mixture of methanol and THF and was refluxed for 2 hours. All the treatments of the product were done under inert gas in view of the high sensitivity of (**7**) to oxidation. This method allowed us to produce compound (**7**) in a pure form.

The reaction starts by decomposition of the ammonium formate in the presence of Pd/C to produce hydrogen, ammonia, and carbon dioxide. Then, hydrogen adsorbs on the surface of the Pd/C catalyst, which then would be ready for reducing the nitro groups to produce the nitroso compound. This compound reduces to hydroxylamine and then further proceeds to provide the amine group. As the product was an unstable and air-sensitive molecule, most of the characterisation could not be done.

The preparation of 2,11-dibromo-6,7,15,16-tetrakis(2-hexyldecyloxy) quinoxalino [2',3':9,10]phenanthro[4,5-abc]phenazine (**8**) was conducted using a modified method by Harris, et al..[121] In this reaction, the unstable 1,2-diamino-4,5-bis(2-hexyldecyloxy)benzene (**7**) was placed with the 2,7-dibromopyrene-4,5,9,10-tetraone (**3**) and heated to reflux for 12 hours. The purpose of this reaction is to form the quinoxaline by condensing the amino groups with the carbonyl groups. The mechanism of preparing (**8**) starts by a lone pair of the amino groups attacking the carbonyl to form the intermediate. Then, the amino attached to the pyrene in positions 4,5,9 and 10, during which a side product of H_2O was formed (**Scheme 4-7**).
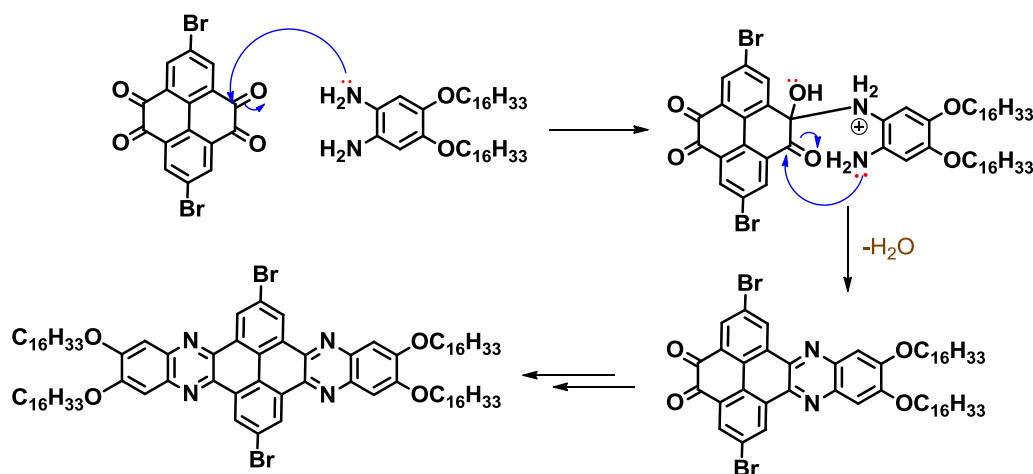
Scheme 4-7. The proposed scheme for producing (**8**)

The purification of this product was done by two techniques. Firstly, column chromatography was used with a mixture of hexane and toluene (2:1; v/v). TEA was also used with the eluent during the purification process. Secondly, the product was then recrystallised in ethanol to afford the product as an orange solid.

^{1}H NMR spectra confirmed the structure of (**8**). Four hydrogens gave a singlet at 9.51 ppm. This peak was tentatively assigned to the hydrogens in the quinoxaline rings. These hydrogens atoms are closest to the electron-withdrawing quinoxaline unit, which should deshield them. Consequently, it is expected the peak for these protons to be located further down-field relative to the protons on the pyrene ring. The singlet at 7.52 ppm was tentatively assigned to the hydrogens on the pyrene rings. A doublet at 4.17 ppm

corresponded to the hydrogens on the carbon next to the oxygen in the alkyl chain (**Figure 4-1**).
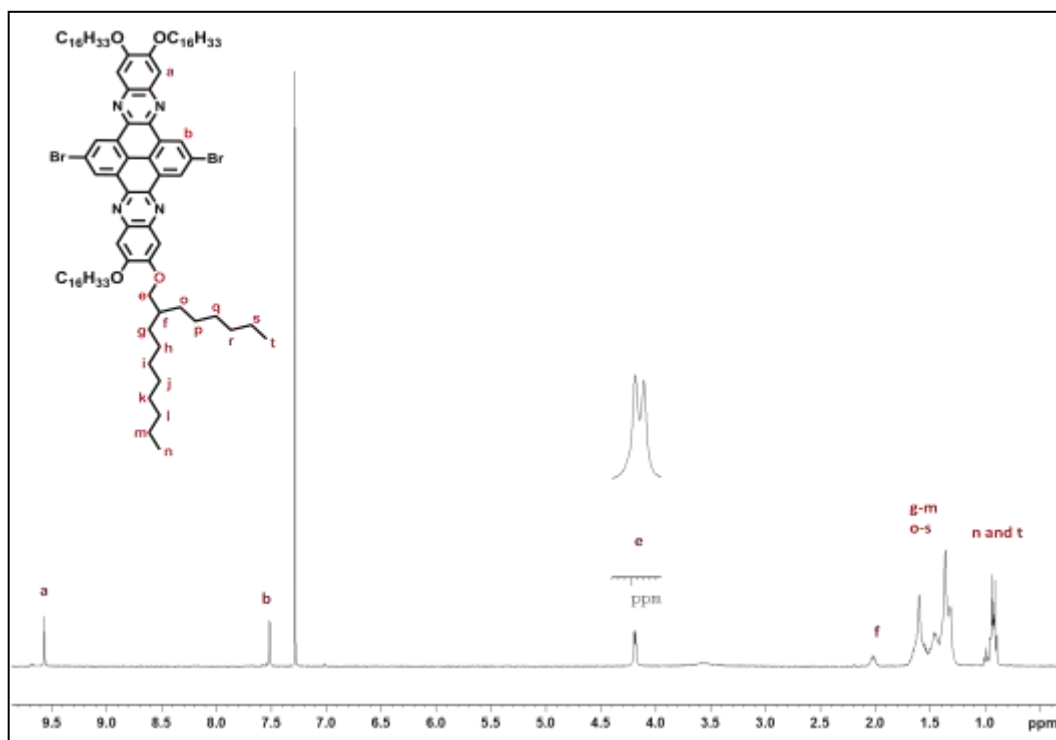
Figure 4-1: ^{1}H NMR for the monomer (**8**)

The mass spectra revealed main isotope peaks at m/z = 1523, 1525 and 1527 (M$^+$) which represented Br isotopes and the ratio between them was 1:2:1. The elemental analyses for this monomer were found to be in agreement with the theoretical calculation. The ^{13}CNMR showed eight peaks in the aromatic region from 154.3 to 106.1 ppm which corresponds well with the target structure of the product.

The 6,7,15,16-tetrakis(2-hexyldecyloxy)-2,11-di(thiophen-2-yl)quinoxaline [2',3':9,10] phenanthro [4,5-abc]phenazine (**9**) was synthesised from a modified procedure of Helgesen.[122] In this reaction, a Stille coupling method was conducted to introduce thiophene rings to the monomer (**8**). The reaction lasted for 72 hours under argon; toluene was used as a solvent with a mixture of catalysts palladium acetate [Pd(OAc)$_2$] and tri-o-tolylphosphine [P(o-tol)$_3$]. As this reaction is a type of Stille coupling method, one monomer must have a halogen, such as bromine, and the other one must have an

organostannyl group, such as 2-tri-butylstannyl thiophene. The proposed catalytic cycle for this reaction involves four steps: oxidative addition, transmetalation, isomerisation, and reductive elimination (**Scheme 4-8**).

Firstly, Pd(0) reacts with PPh₃ to form the catalytically active complex Pd (tol-o)₃P-Pd-P(o-tol)₃. Secondly, the monomer (**8**) reacts with Pd(P(o-tol)₃ to form complex [1]. Thirdly, complex [1] reacts with 2-tri-butylstannyl thiophene, the substitution of phosphine by 2-tri-butylstannyl thiophene, to give intermediate [2]. In addition, the nucleophilic attack of the Pd-coordinated bromine and electrophilic attack of Pd then react to give [3]. In summary, the coupling manufactured [4], and the catalyst was eliminated and the cycle restarted.
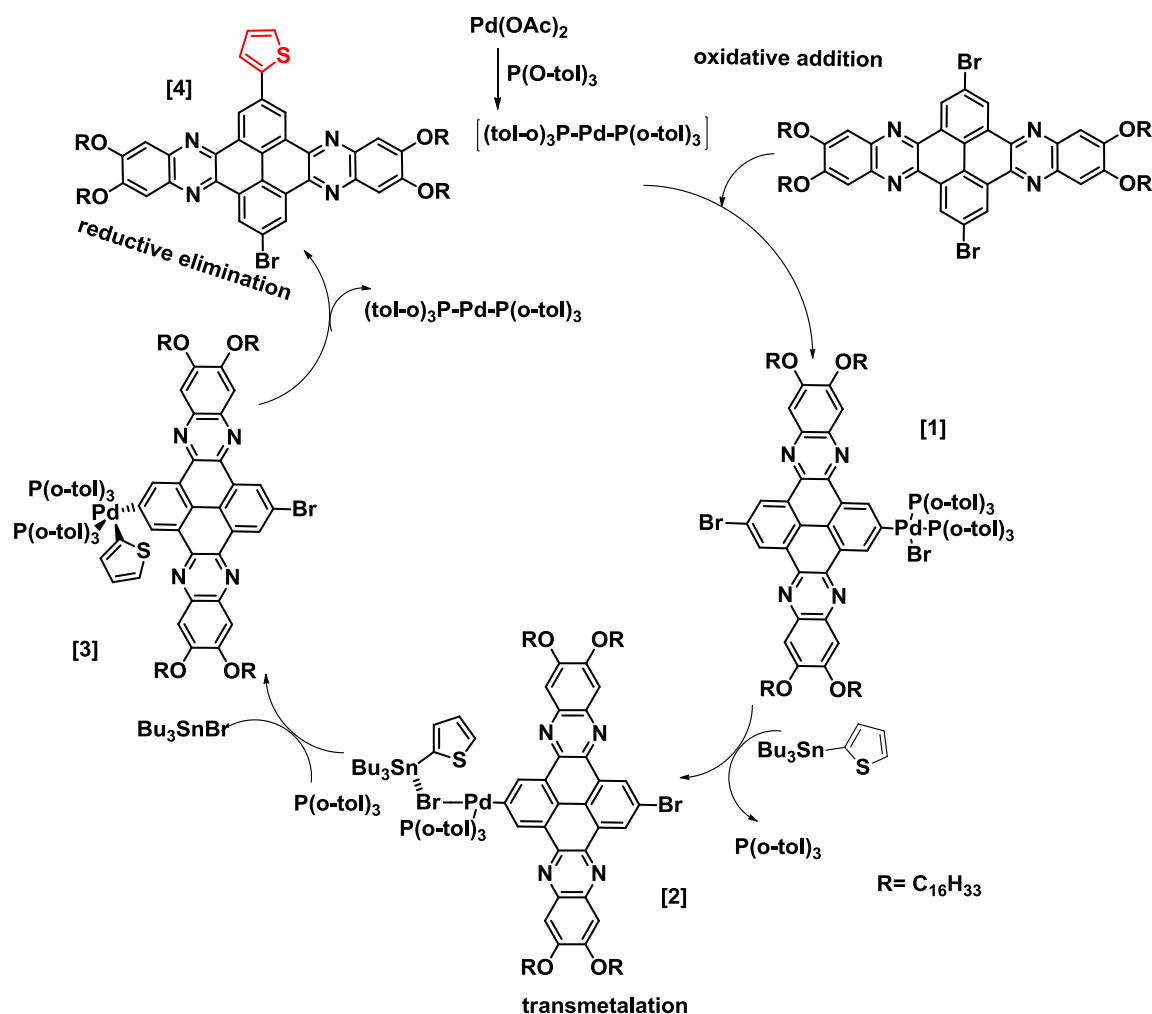
Scheme 4-8 The catalytic cycle for producing (**9**)

Two techniques were used to purify this monomer. Firstly, pure hexane was used as the eluent in column chromatography to remove residues of the 2-tributylstannyl thiophene, followed by a mixture of hexane and chloroform (2:1; v/v) to collect the product. Secondly, recrystallisation from ethanol was utilised to remove the remaining impurities.

The ^{1}H NMR spectra showed a singlet at 9.56 ppm which we tentatively ascribe to the hydrogens in the quinoxaline molecule. Reasons for this assignment have been explained previously. Another singlet was observed at 7.80 ppm, which may correspond to the hydrogen on the pyrene. There were three hydrogen environments assigned for the thiophene molecule: two doublets at 7.49, 7.43 ppm and one triplet at 7.18 ppm. The doublet peak at 4.14 ppm, corresponds to the hydrogens on the carbon next to the oxygen at the alkyl chain segments.

Further analyses were conducted to ensure the product was of sufficient purity before continuing with the synthesis. MALDI-TOF indicated the presence of a peak at m/z = 1532 (M$^+$), which corresponded to the mass of the molecular ion. Elemental analysis results were also in agreement with the proposed structure. The ^{13}C NMR also confirmed the purity of (**9**) by having 12 peaks in the aromatic region between 153.7 to 106.4 ppm, which corresponds well with the proposed structure of (**9**).

The preparation of 2,11-bis(5-bromothiophen-2-yl)-6,7,15,16-tetrakis (hexadecyloxy) quinoxalino[2',3':9,10]phenanthro[4,5-abc]phenazine (**10**) followed a modified procedure of Qin, et al.[123] The reaction was left for 72 hours at room temperature under an inert atmosphere and was covered with foil all of the time to prevent formation of bromine radicals. An excess of NBS (2.1 equivalent) was used to ensure that no trisbromine could occur. The yield was as high as 90%, which was similar to the reported literature value.[123]. The mechanism of this reaction follows an electrophilic substitution, in which the bromine of NBS was attacked by a thiophene double bond. This led the bromine to attach to the thiophene ring to produce the brominated ring (**Scheme 4-9**).
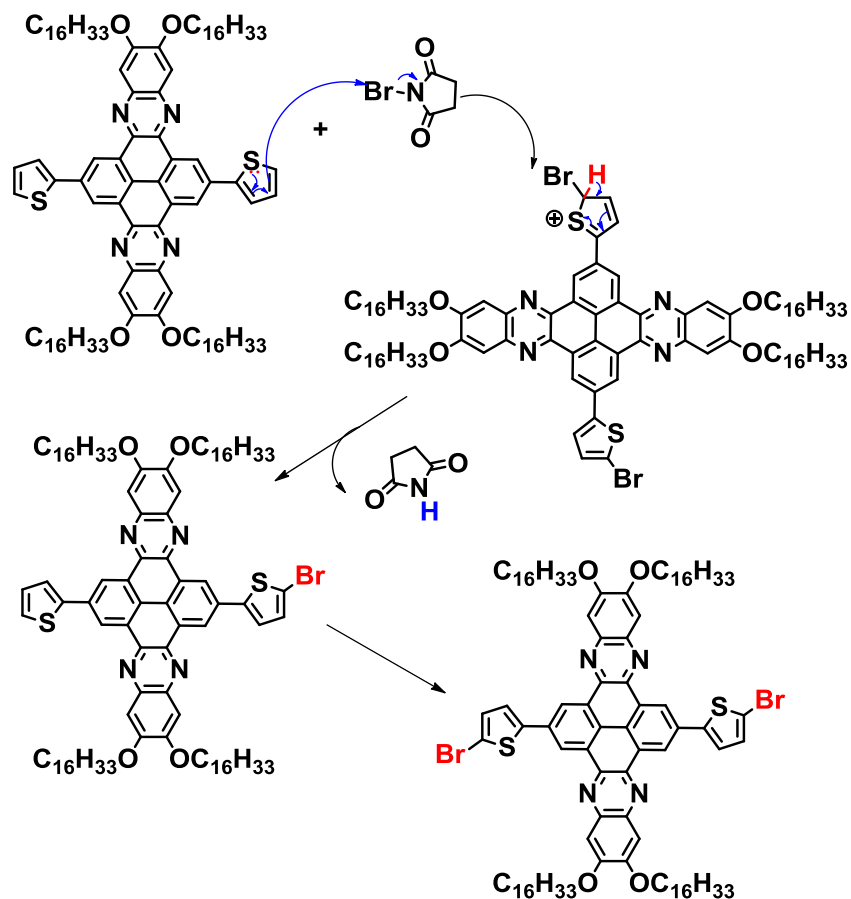
Scheme 4-9 The proposed scheme for producing (**10**)

The purification of this monomer encountered some problems due to contamination by impurities that could not be removed by either column chromatography or recrystallisation. At first, these impurities were thought to be consequences of the aggregation of this molecule, as the ^{1}H NMR gave strange peaks when it was done at different concentrations. While some peaks appeared to be doublets or singlets in low or high concentrations, the impurities' peaks still existed. This was the reason that we started to think of removing these peaks, as they were not a result of the aggregation; they were impurities (**Figure 4-2**).
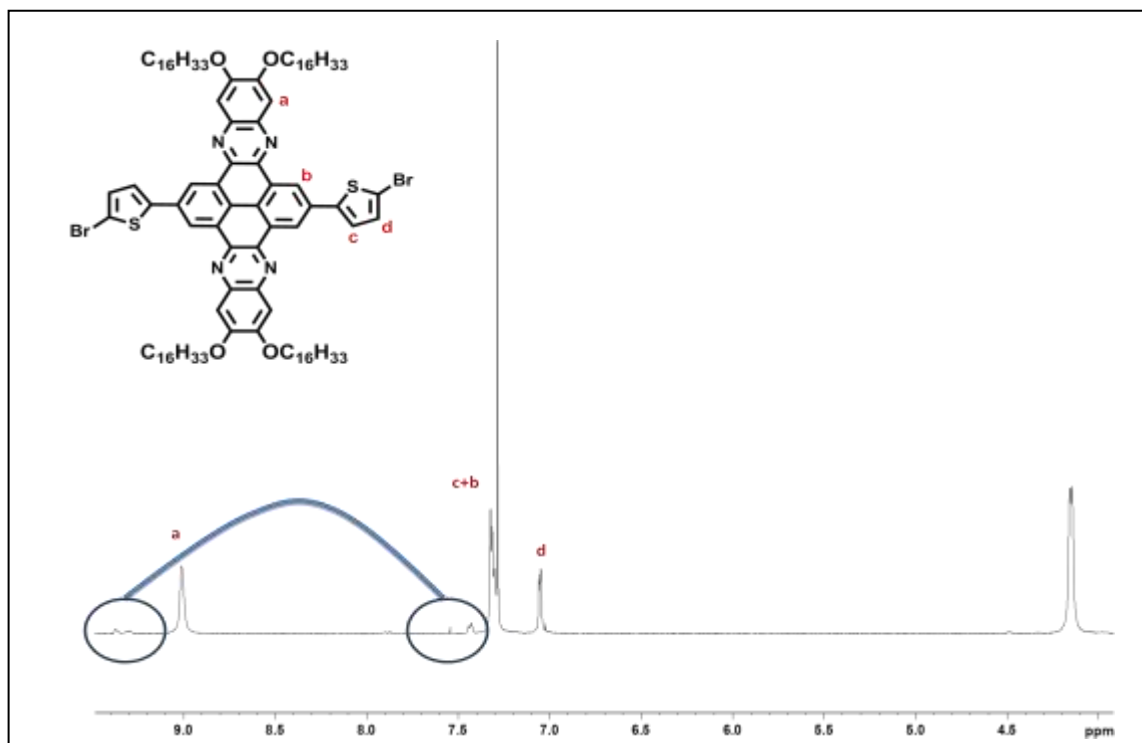
Figure 4-2: ^{1}H NMR for monomer (**10**) with the impurities.

Preparative high pressure liquid chromatography (HPLC) was then used as a technique to remove these impurities. After developing a method of removing these impurities (experimental chapter), the HPLC instrument was used to collect the pure monomer, which successfully removed these impurities. The ^{1}H NMR chart showed a singlet at 8.92 ppm, which was presumably assigned to the hydrogens in the quinoxaline parts at position a. A multiplet peak appeared at 7.24 ppm. This overlapped with the deuterated chloroform peak. We assign this multiplet to the hydrogens located on the pyrene (position b) and thiophene units (position c). There is also a multiplet peak that appeared at 7.03 ppm which is assigned to the hydrogens on the thiophene rings at position d. Another distinguished peak appeared at 4.17 ppm, which corresponded to the hydrogen on the carbon next to the oxygen in the alkyl chain (**Figure 4-3**).
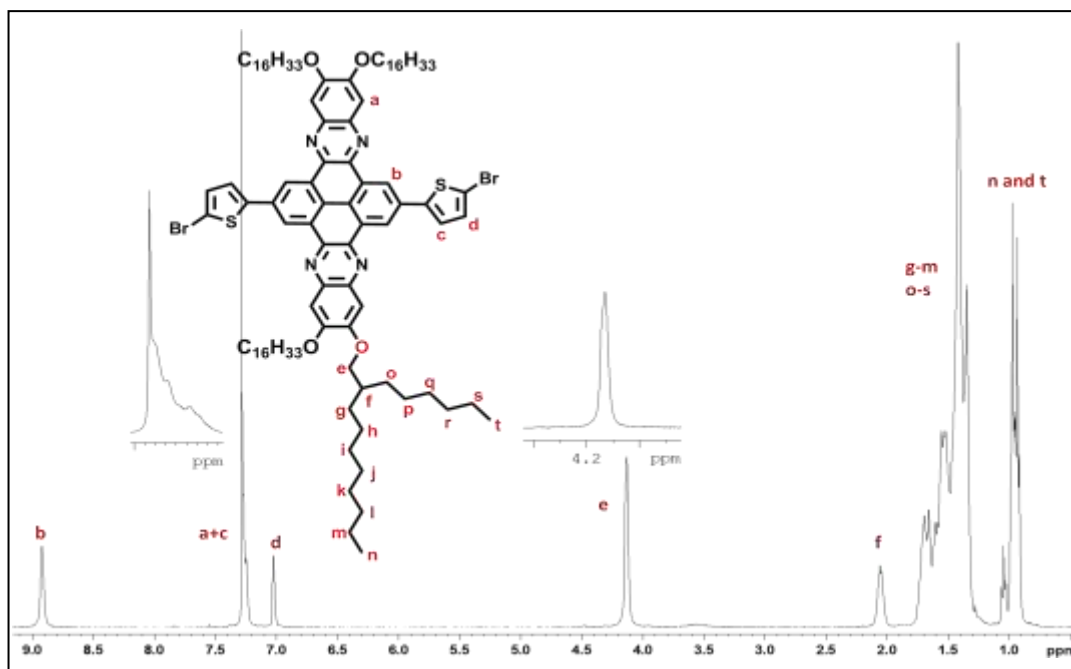
Figure 4-3: ^{1}H NMR spectrum of (**10**) after HPLC

The MALDI-TOF showed main integral peaks for this product between 1686, 1688 and 1690, which took into account the bromine isotopes. The elemental analysis was in agreement with the proposed structure. The ^{13}C NMR also confirmed the purity of (**10**) by having 12 peaks in the aromatic region between 154.3 to 106.5 ppm, which corresponds well with the proposed structure of (**10**).

4.3 Preparation and characterisation of P1 –P3

4.3.1 Synthesis of polymers P1, P2 and P3

A series of polymers which have low band gaps which were designed to harvest a wide wavelength range of sunlight have been synthesised. The synthesis of polymers **P1** and **P2** (**Scheme 4-10**) involved using Suzuki coupling reactions, which are the best methods to form C–C bonds effectively with environmentally friendly side products for large-scale usage.[22]
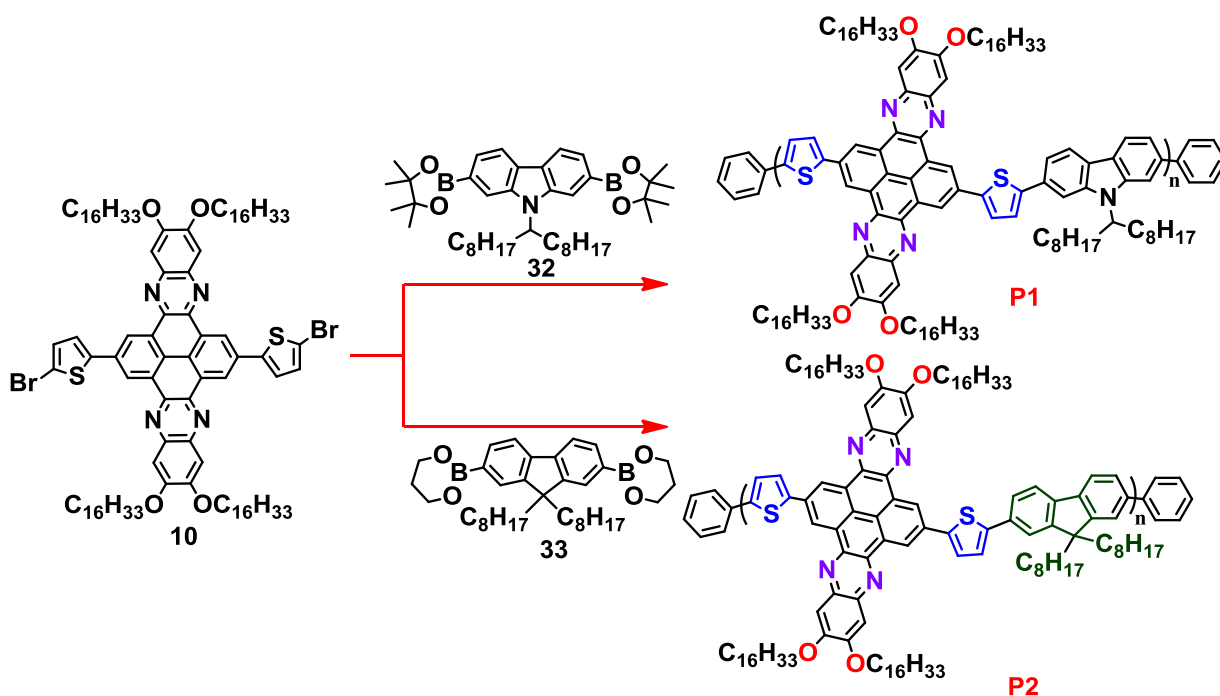
Scheme 4-10 Synthetic routes for polymers **P1** and **P2**

Polymerisation of the target polymers was performed in tetrahydrofuran (THF) with NaHCO$_3$ as a base. While the polymerisations proceeded the solutions became viscous, and more THF was added. At the end of the polymerisation, some more THF was added to solubilise the polymers, in which end-capping reagents, such as bromobenzene and phenyl boronic acid were used to end-cap the backbone of the polymers. This step is useful because the working time of devices and the efficiency of the operation could be improved.[151]

The proposed catalytic cycle for this reaction is illustrated in **Scheme 4-11**. In the first step, palladium (0) was converted to palladium (II) by aryl bromide, this step being an oxidative addition. The intermediate complex was formed after reaction with the base, which led the boronic ester of the second monomer to undergo transmetalation to form an organopalladium species. In the last step, the target polymer was obtained by reductive elimination, in which palladium (II) returned to its original form of palladium (0) and the cycle started again.

$$R_1\text{-Br} + R_2\text{-B}(OC_3H_6)_2 \longrightarrow R_1\text{-}R_2 + Br\text{-B}(OC_3H_6)_2$$
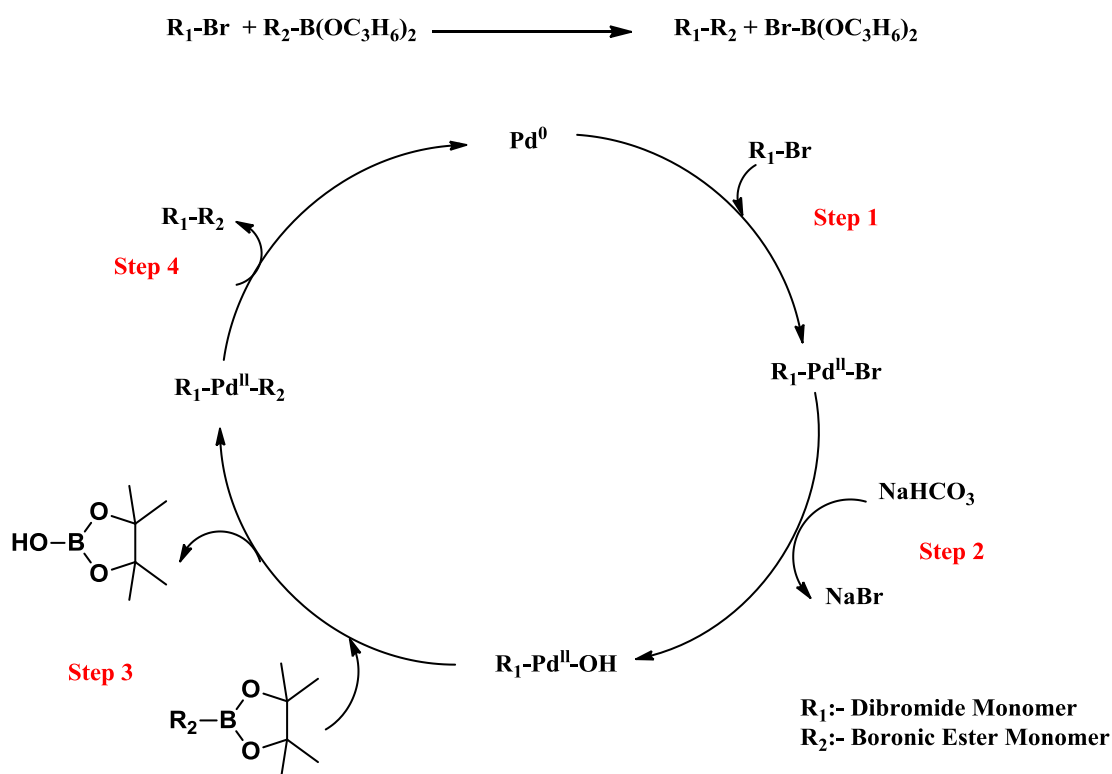
Scheme 4-11. Suzuki coupling catalytic cycle

Purification of the target polymers involved many steps; the crude product was stirred with ammonia to remove any traces of catalyst as well as other impurities.[152] The product was then washed with water to remove the ammonia, concentrated by rotary evaporation, and then precipitated in methanol. The crude product was collected by filtration on micropore membranes, which were transferred into a fibreglass thimble and washed in a Soxhlet apparatus with various solvents. These include methanol to eliminate any traces of catalyst or inorganic materials, followed by acetone, which was used to remove any remaining

impurities. Hexane was also used to clean off all small molecules, including oligomers, and toluene to extract the polymers followed by chloroform to dissolve the remaining polymers. Unlike toluene, chloroform extracted all polymer chains because of its high polarity. The polymer chains dissolved in chloroform were concentrated and precipitated in methanol and then collected by filtration using micropore membranes and dried under high vacuum. Polymers **P1** and **P2** were obtained as orange solids.

The synthesis of **P3** (**Scheme 4-12**) was performed using the Stille coupling polymerisation method, in toluene. At the end of the polymerisation, some toluene was added to solubilise the polymers; end-capping reagents, such as bromobenzene and 2-(tributylstannyl) thiophene, were added to end-cap the backbone of the polymer.
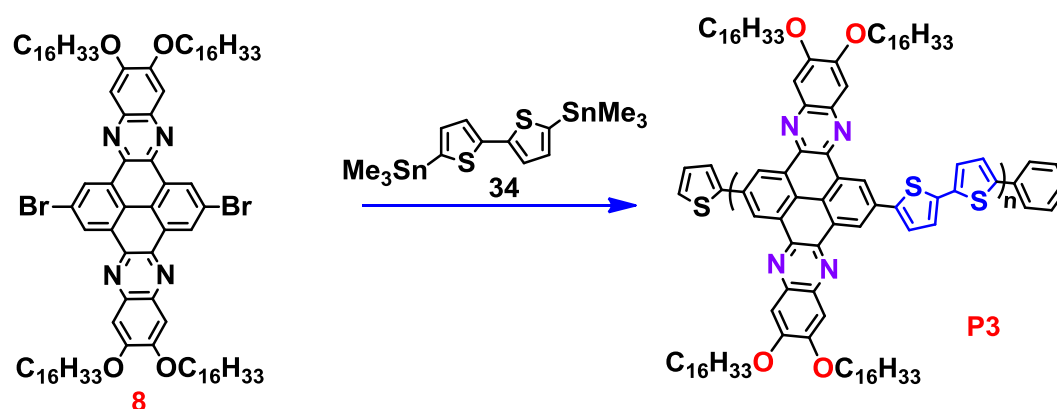
Scheme 4-12 Synthetic route for polymer **P3**

The proposed catalytic cycle for this reaction is illustrated in **Scheme 4-8**, which in the first step palladium (0) was converted to palladium (II) by reacting with P(o-tol)$_3$ to form the catalytically active complex (o-tol)$_3$P–Pd–P(o-tol)$_3$, this step being an oxidative addition. Second, the 2,11-bis(5-bromothiophen-2-yl)-6,7,15,16-tetra(hexadecyloxy)-tetrabenzo[a,c,d,e]phenazine reacts with Pd(P(o-tol)$_3$) to form a complex, which reacts with 5,5′-bis(trimethylstannyl)-2,2′-bithiophene to replace the phosphine by 2,2′-bithiophene, giving the intermediate. Then, nucleophilic attack of the Pd-coordinated bromine and electrophilic attack of Pd produce [3]. In summary, the coupling produced [4] and the

catalyst was eliminated to restart the cycle. Purification of the polymer followed a similar protocol to that for **P1** and **P2**.

4.3.2 Characterisation of polymers P1-P3

To characterise polymers **P1**-**P3**, some analytical instruments were involved, such as gel permeation chromatography (GPC) to calculate their molecular weights, ^{1}H NMR to determine the structure of these polymers, elemental analysis to determine the percentage weight of each element, and thermogravimetric analysis (TGA), which was used to examine the thermal stability of these polymers. Cyclic voltammetry was used for their electrochemical properties and for UV-vis spectroscopy their optical properties were analysed.

4.3.2.1 GPC data analysis for P1, P2 and P3

After Soxhlet extraction, the yield of these polymers was calculated and the GPC data were obtained in 1,2,4 trichlorobenzene (TCB) at 140 °C. This was because some difficulties were faced when doing the analysis at lower temperature, including aggregation and precipitation of the polymers inside the GPC columns. Polystyrene was used as a standard to calculate the molecular weight of the target polymers, as shown in **Table 4-1**.

Polymers	Soxhlet Fraction	Yield (%)	M_w	M_n	PDI	DP
P1	chloroform	88	67800	29300	2.31	15
P2	chloroform	92	50700	15300	3.31	8
P3	chloroform	39	16300	9900	1.6	7
	chlorobenzene	52	29800	21500	1.3	14

Table 4-1 The GPC analysis data for **P1**, **P2** and **P3**

 From **Table 4-1** it can be clearly seen that polymers **P1** and **P2** were obtained in good yields 88% and 92% respectively. In addition, **P3** was obtained in two fractions. The first fraction was in chloroform, 39%. The second fraction was in chlorobenzene, 52%. This reflects the low solubility of this polymer due to the thiophene segments having no

solubilising groups attached to them. The GPC analysis showed the degree of polymerisation for **P1** is roughly 15. Thus, **P1** has approximately 15 quinoxaline and carbazole units per polymer chain. GPC estimated the Mw and Mn of **P1** to be 67800 and 29300 Da respectively, with a polydispersity of 2.31. For polymer **P2** there are around 8 units of quinoxaline and fluorene units per polymer chain, (Mw = 50700, Mn = 15300, PDI = 3.31). Finally, polymer **P3** (chloroform fraction) has approximately 7 quinoxaline unit and 2,2'-bithiophene units per polymer chain with molecular weight Mw and Mn of 16300 and 9900 Da respectively. The low PDI of the chloroform fraction of **P3** (1.6) could be attributed to a fractionation effect limited to the solubility of different fraction of the polymer. Thus, only a small fraction of molecular weights are soluble in the chloroform fraction resulting in a low PDI. The chlorobenzene fraction of polymer **P3** (has approximately 14 quinoxaline unit and 2,2'-bithiophene units per polymer chain with a Mw and Mn of 29800 and 21500 Da respectively. This gives an even narrower PDI of 1.3.

4.3.2.2 ^{1}H NMR analysis for P1, P2 and P3

It is quite hard to observe well defined peaks using ^{1}H NMR analysis for these types of polymers because of aggregation of polymer chains. Broad peaks in the aromatic region are more likely to appear due to aggregation of the quinoxaline moieties. As a consequence of this phenomenon the structure of the polymer stiffens and hinders the breaking up of the polymer chains.[153] However, the aggregation could be broken by performing the ^{1}H NMR at 100 °C using 1,1,2,2-tetrachloroethane-d$_2$ ($C_2D_2Cl_4$), which could provide clearer spectra in the aromatic region.[154]

The ^{1}H NMR spectra for **P1** in $C_2D_2Cl_4$ at 100 °C is shown in **Figure 4-4**. There are broad peaks in the aromatic region, some of which could be identified. These include carbazole protons at positions a, b and c in which a singlet peak appeared at 7.87 ppm for proton a, however proton b has a doublet at 7.78 ppm and a signal observed at 7.53 ppm assigned to proton c. For the quinoxaline part, it has two aromatic peaks, one broad signal appeared at 9.55 ppm assigned to proton e and another one observed at 7.51 ppm belonged to proton d. Multiple peaks appeared between 7.18 and 7.30 ppm assigned to thiophene protons g and f. There are two peaks in the aliphatic region. The first one is a broad peak at 4.25 ppm

corresponding to the proton on the first carbon of the carbazole alkyl chain I, the second one is also a broad peak at 4.18 ppm assigned to the protons on the first carbon of the alkyl chain of the quinoxaline part.
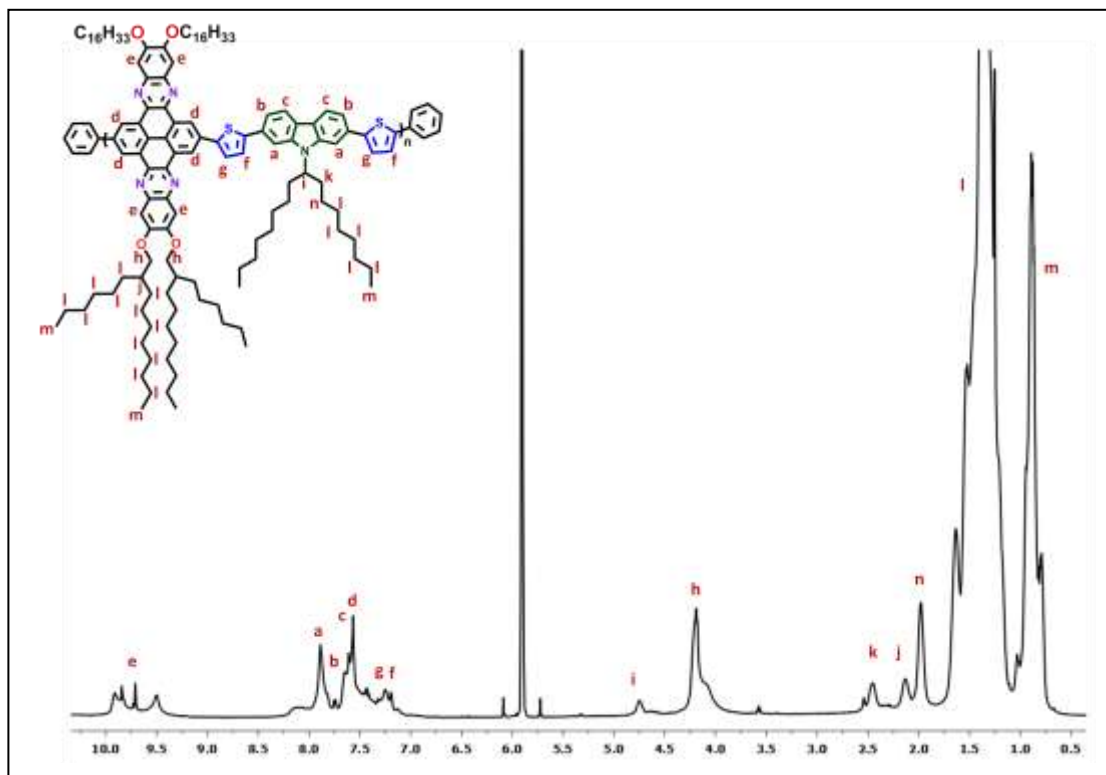
Figure 4-4. ^{1}H NMR spectrum of **P1** in $C_2D_2Cl_4$ at 100 °C

The ^{1}H NMR spectra for **P2** in $C_2D_2Cl_4$ at 100 °C in **Figure 4-5** shows one broad peak in the aromatic region, which makes it difficult to distinguish between the signal peaks; however, the ^{1}H NMR was performed at high temperature as stated above. The interpretation of this broad signal is based on the suggestion that there are multiple environments in the same region. The fluorene part has three aromatic peaks, the first one at 7.88 ppm assigned to the proton in position a, the proton in position b appearing at 7.71 ppm. Furthermore, the proton in position c has a signal at 7.60 ppm. In contrast, the quinoxaline part has two peaks belonging to the two protons in positions d and e at 7.52 ppm and 9.54 ppm respectively. The peaks in the aliphatic region for both parts are clearly observed as broad peaks; the proton on the carbon next to the oxygen in the alkyl chain of

the quinoxaline part appeared as a broad peak at 4.18 ppm. Another peak observed at 2.13 ppm corresponds to the proton on the carbon of the alkyl chain connected to the fluorene part, position i.
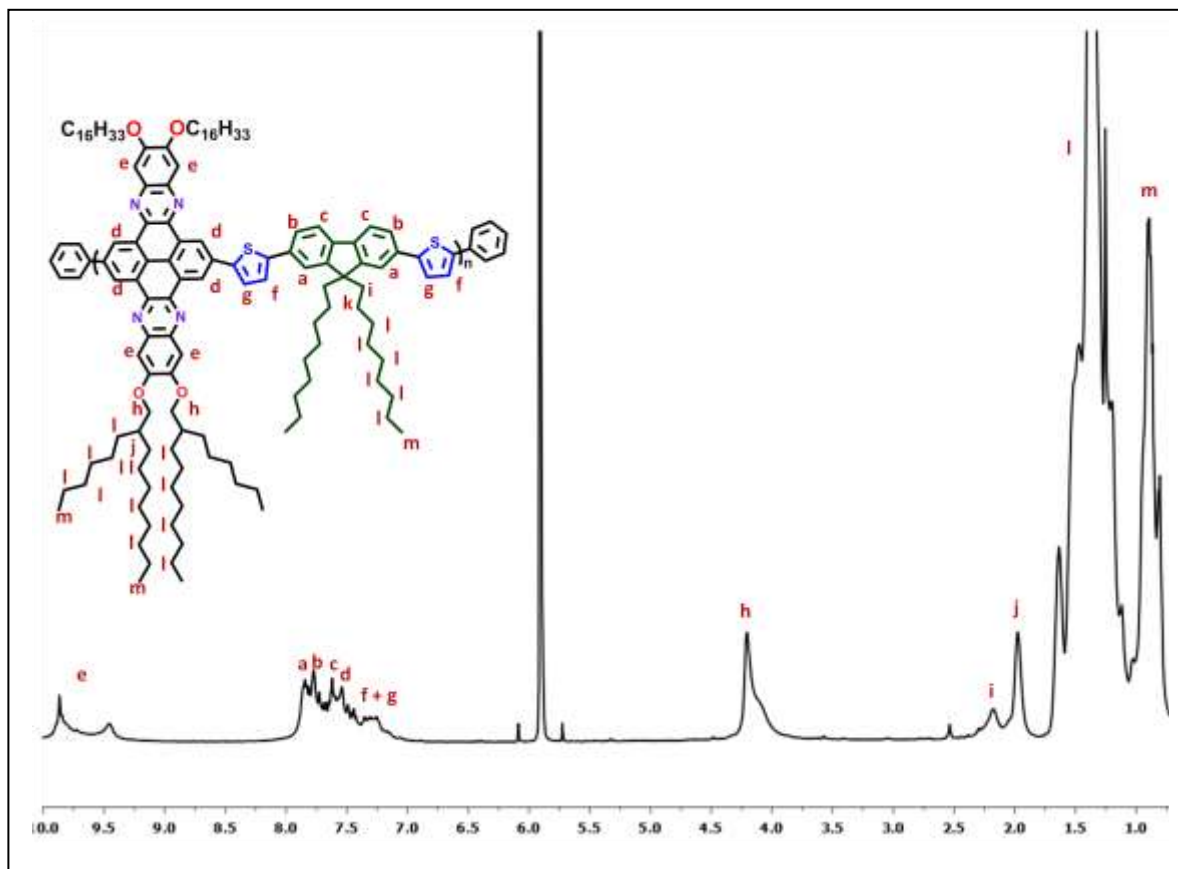
Figure 4-5. ^{1}H NMR spectrum of **P2** in C$_2$D$_2$Cl$_4$ at 100 °C

The ^{1}H NMR spectra for **P3** in C$_2$D$_2$Cl$_4$ at 100 °C, **Figure 4-6**, showed sharp peaks in the aromatic region, which are not usually easy to get with such aggregated molecules. The spectrum showed a broad peak at 9.52 ppm, which corresponds to the proton on the carbon of the quinoxaline part at position a. There is also a sharp peak at 7.70 ppm belonging to the proton on the carbon of the quinoxaline part at position b. The thiophene part has two broad peaks for both protons in positions c and d at 7.98 and 7.21 ppm respectively. The special peak appearing in the aliphatic region was assigned to the proton on the carbon next to the oxygen of the alkyl chain connected to the quinoxaline part at 4.18 ppm as a broad peak.
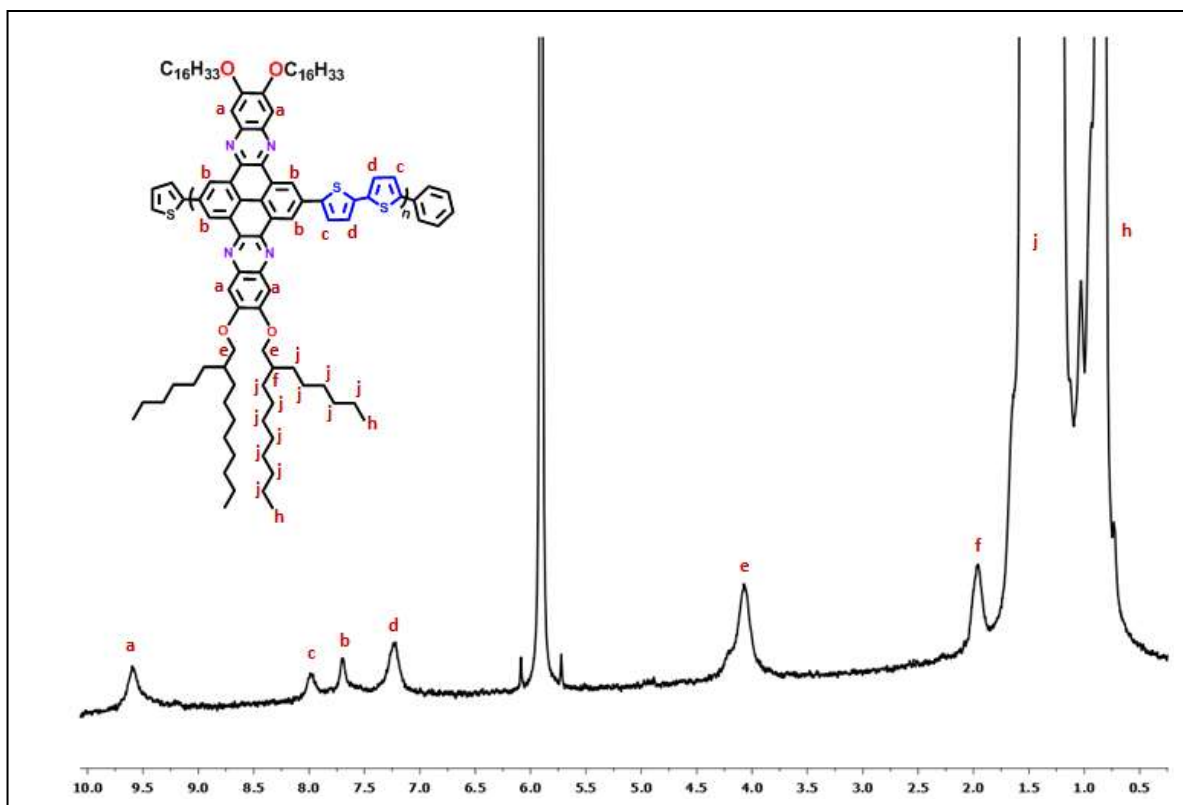
Figure 4-6. ^{1}H NMR spectrum of **P3** in $C_2D_2Cl_4$ at 100 °C

4.3.2.3 Elemental analysis for P1, P2 and P3

Elemental analysis is one of the techniques that was used to examine the target polymers, whether they are consistent with a given molecular formula and also to ensure the bromine atom is replaced with an end-capping molecule. The results shown in **Table 4-2** indicate that the elemental analysis of these polymers is in agreement with the proposed structures of **P1**, **P2** and **P3**, and also confirmed that they were end-capped with either bromobenzene or 2-(tributylstannyl)thiophene.

Polymers	Formula	Elemental analysis					
			C	H	N	Br	S
P1	$(C_{131}H_{189}N_5O_4S_2)_n$	Calculated	80.19	9.71	3.57	0	3.27
		Found	77.30	9.37	3.41	0	2.24
P2	$(C_{131}H_{188}N_4O_4S_2)_n$	Calculated	80.81	9.73	2.88	0	3.29
		Found	79.96	9.50	2.85	0	2.19
P3	$(C_{100}H_{146}N_4O_4S_2)_n$	Calculated	78.38	9.60	3.66	0	4.18
		Found	80.40	11.98	2.68	0	2.92

Table 4-2. Elemental analysis data for **P1**, **P2** and **P3**

4.3.2.4 Thermal analysis of P1, P2 and P3

Thermal stability is considered to be one of the requirements that must be fulfilled to employ any polymer in solar cells. Thus, **P1**, **P2** and **P3** were thermally studied using a TGA instrument, as can be seen in **Figure 4-7**, which confirmed the thermal stability of these polymers up to 400 °C; therefore, they can be used in solar cell applications. **P1** shows an onset of degradation at 382 °C due to degradation of the alkoxy chain and the main onset of degradation at 663 °C with a total weight loss of 45.78%. **P2** has the first onset of degradation at 366 °C due to degradation of the alkoxy chain and the main onset of degradation at 650 °C with a total weight loss of 43.12%. In addition, **P3** has the first onset of degradation at 431 °C due to degradation of the alkoxy chain and the main onset of degradation at 555 °C with a weight loss 47.22%.
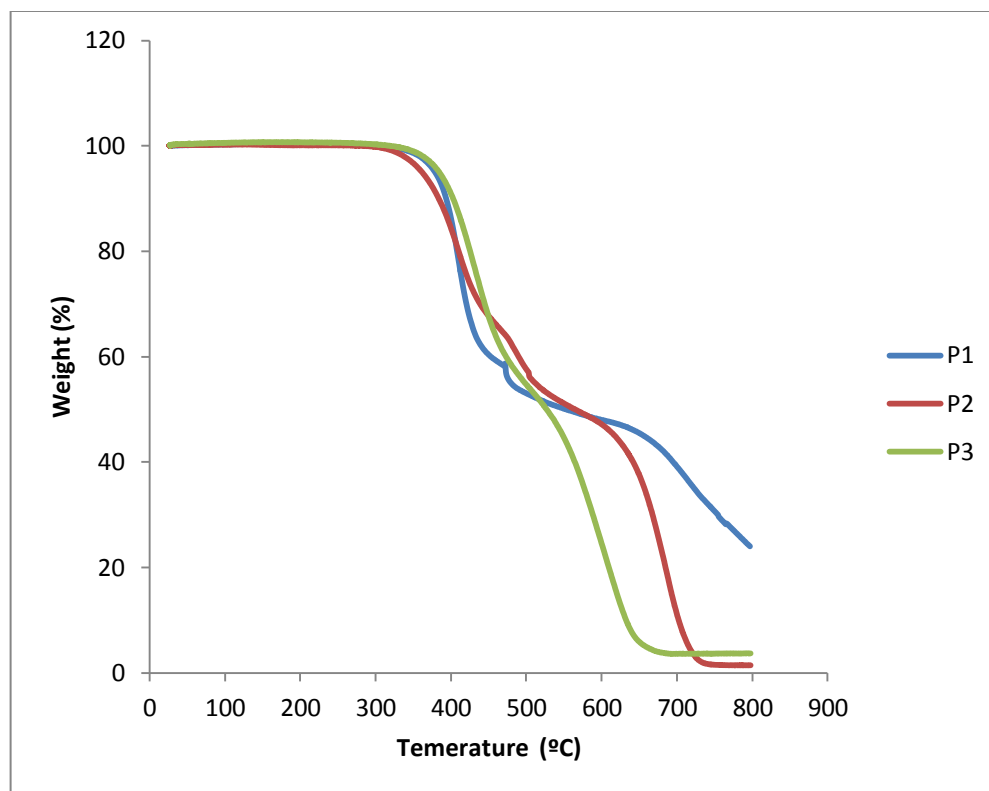
Figure 4-7. The TGA thermograms for **P1, P2 and P3**

4.3.3 Optical properties of P1, P2 and P3

Studies of the optical spectra of **P1**, **P2** and **P3** were performed in chloroform (**Figure 4-8**), and for films drop-cast on a quartz substrate (**Figure 4-9**). In solution and film states, all polymers display excellent electronic and vibronic structure with absorption bands located between 370 – 530 nm for polymers **P1**-**P3**. We speculate the improved electronic and vibronic resolution is a consequence of pyrene-quinoxaline extended π-system, planarity and rigidity. These properties should improve the stacking of the polymer in solid state. This phenomenon has been observed in pyrene-based small molecules as well as pyrene based polymers.[153,155] Such fine electronic and vibronic structure makes assigning specific bands (π-π* and ICT bands) difficult. However, we tentatively assign peak with the longest wavelength as the ICT band which will be referred to as the λ_{max}. The λ_{max} in chloroform solution appears at 471, 468 and 487 nm for **P1**, **P2** and **P3** respectively (**Figure 4-8**). When cast into films, the λ_{max} is red-shifted to 475, 470 and 489 nm for **P1**, **P2** and **P3** respectively (**Figure 4-9**). The red-shift between solution and film spectra is less

pronounced than for other conjugated polymers as very often there is a more planar structure in films than in solutions, which leads to a more extended conjugation. The red-shift is extremely small (between 2 and 5 nm). This indicates that there is little structural difference between the polymers conformation in solution and solid state.
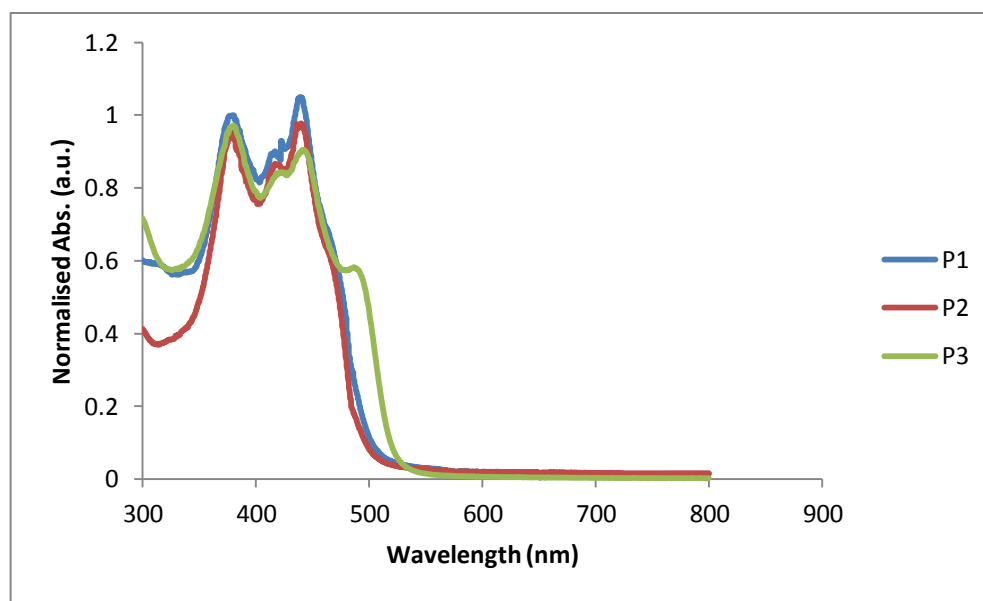
Figure 4-8. Normalised absorption spectra of **P1**, **P2** and **P3** in chloroform solutions

When comparing the solid state UV spectra of **P1**, **P2** and **P3** it can be seen that the λ_{max} of **P3** is more red-shifted relative to **P1** and **P2**. This can be attributed to the strength and architecture of the donor-moiety. Thiophene is a stronger donor, relative to carbazole and fluorene. We tentatively suggest this leads to improved intramolecular charge transfer along the polymer backbone. Unlike carbazole and fluorene, thiophene is not decorated with large, sterically demanding solubilising chains. This will allow **P3** to adopt a more planar and rigid structure in solid state when compared to **P1** and **P2**.
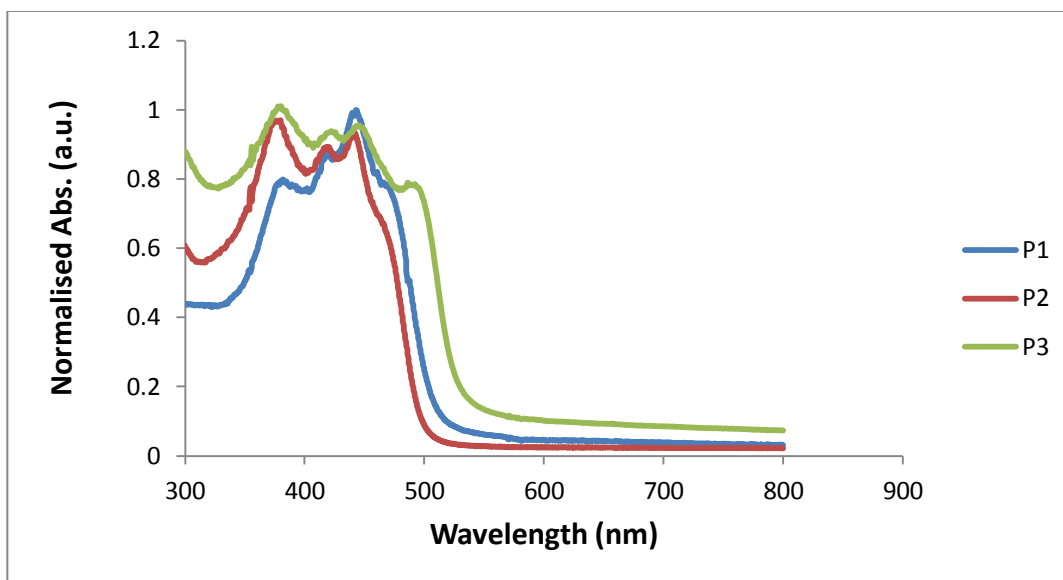
Figure 4-9 Normalised absorption spectra of **P1**, **P2** and **P3** as thin films

The optical band gaps of **P1**, **P2** and **P3** are 2.43, 2.49 and 2.34 eV respectively. A comparison between the band gap of these polymers and those of similar polymers designed in the literature (**Scheme 4-13**) with quinoxaline based repeat units indicated that polymers **P1**-**P3** have much wider band gaps which reflects the lack of intramolecular charge transfer in these polymers (**Table 4-3**).[114]
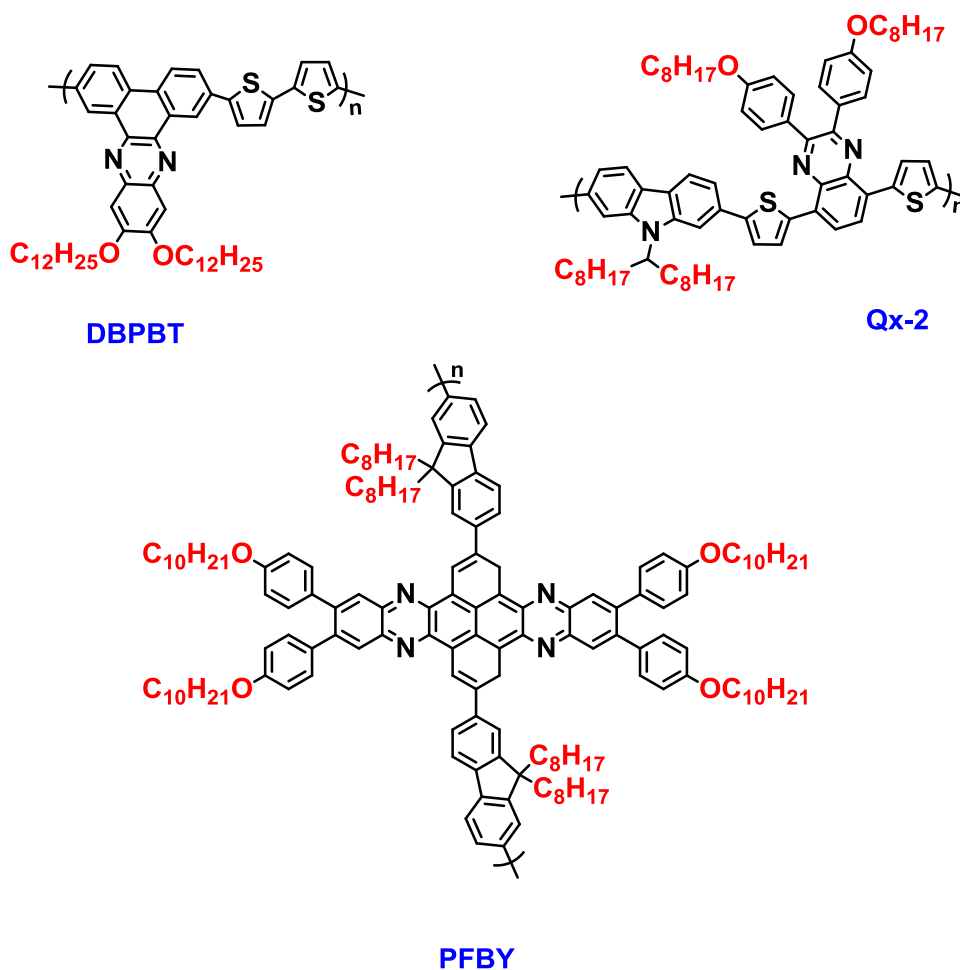
Scheme 4-13 The structures of Qx-2[114], PFBY[149] and DBPBT[153]

Lee and co-workers synthesised the polymer Qx-2 which has a similar structure to **P1**.[114] The authors only used quinoxaline as the acceptor unit in this D-A polymer. **P1** uses the pyrene-quinoxaline unit as an acceptor. A direct comparison between the two polymers will allow to assess the effects of extending the lateral π-system in **P1**. Qx-2 has a λ_{max} located at 535 nm and an optical band gap of 1.97 eV.[114] The λ_{max} is red-shifted when compared to that of **P1**. Furthermore, Qx-2 has a lower optical band gap relative to **P1**. This red-shift and lower optical band gap could be attributed to the stability of the quinoid structure of Qx-2 when compared to the quinoid structure of **P1**. Previous literature has shown that the fused rings in the pyrene-quinoxaline acceptor of **P1** may not be stable.[156] Although this reason has been previously reported, theoretical calculations need to be undertaken to see if this is the reason for the large band gap of **P1**. The optical properties of Qx-2 can be improved further when the octyloxy substituents on the phenyl-substituent are attached to

the *meta*-position instead of the *para*-position (TQ1).[88] When the octyloxy group is attached at the *para*-position its pushes electron density onto the quinoxaline unit making it less electron-accepting. However, when the octyloxy group is attached at the *meta*-position this effect is stopped and the quinoxaline unit is more electron-withdrawing. This increases the D-A characteristic of the polymer resulting in a lower optical band gap.

Ming and co-workers synthesised a series of conjugated copolymers (PFBY) that were composed of 9,9-dioctylfluorene and increasing amounts of pyrazine (**Scheme 4-13**).[157] These copolymers are structurally analogous to the polymer, **P2**, synthesised in this report. The UV-vis film absorption of PFBY displayed a λ_{max} at 446 nm, which is blue-shifted relative to **P2**. This can be attributed to the lack of a thiophene spacer of PFBY. Therefore, adjacent aromatics that possess large alkyl chains are in close proximity to each other and twist to minimise steric repulsion, which reduces the planarity of the backbone. Additionally, Ming and co-workers attached phenyl-decyloxy groups to the quinoxaline part of the pyrene-quinoxaline unit. We hypothesise that the solubilising group used by Ming *et al* possess an aromatic unit that does not lie in the same plane as the polymer backbone; it lies perpendicular to the planar polymer backbone.[157] We suspect that this disrupts the planarity of the conjugated system and inhibits π-π stacking between polymer backbones. The optical band gap of PFBY was estimated to 2.63 eV.[157] This is larger than the optical band gap of **P2** (2.49 eV). The smaller optical band gap of **P2**, relative to PFBY, indicates that **P2** has a more planar structure and extended π-delocalisation.

Dibenzo-[*a,c*]phenazine-*alt*-bithiophene (DBPBT) **Scheme 4-13** synthesised by Gautrot and co-workers is an analogous polymer to **P3**.[153] DBPBT possessed a large band located between 410-550 nm, which the authors attribute to ICT along the polymer backbone.[153] This is red-shifted when compared to **P3**. Furthermore, DBPBT possess an optical band gap of 2.25 eV which is smaller than **P3**.[153] DBPBT has a molecular weight of 26,600 Da.[153] **P3** has a molecular weight of 16,300Da. It is possible that the improved optical properties of DBPBT are a result of its higher molecular weight. A higher molecular weight will extend the conjugation along the polymer backbone, resulting in a more planar and rigid structure.[110]

Polymers	λ_{max} (nm) solution	λ_{max} (nm) film	λ_{onset} (nm) absorption	E_g Optical (eV)
P1	471	475	510	2.43
P2	468	470	497	2.49
P3	487	489	529	2.34
Qx-2	-	535	-	1.97
PFBY	-	446	-	2.63
DBPBT	-	550	-	2.25

Table 4-3. Summary of photophysical properties of **P1**, **P2**, **P3**, Qx-2, PFBY and DBPBT

4.3.4 Electrochemical properties of P1, P2 and P3

Electrochemical studies of **P1**, **P2** and **P3** were performed on drop-cast films in acetonitrile as a solvent with tetrabutylammonium perchlorate, which works as an electrolyte. In this examination, the highest occupied molecular orbital (HOMO) and lowest unoccupied molecular orbital (LUMO) were determined using CV (**Figure 4-10**)
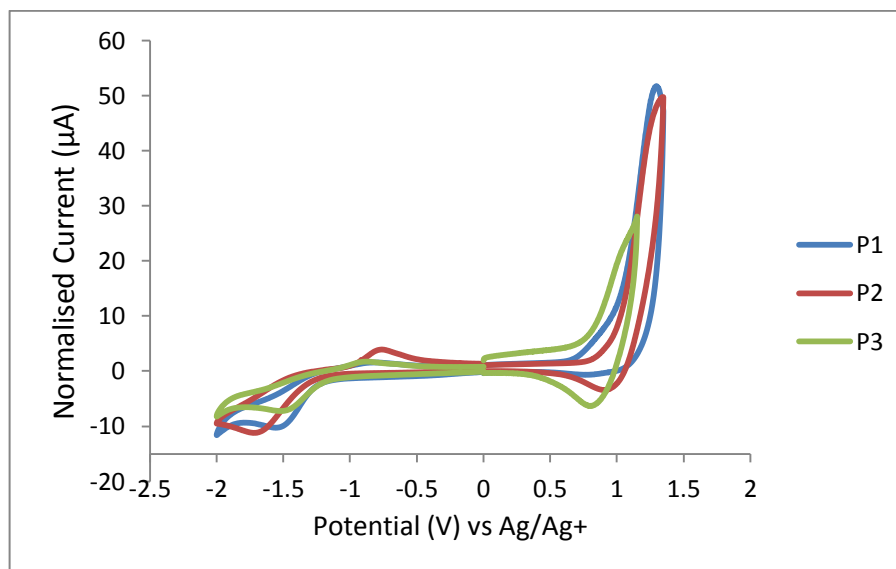
Figure 4-10. Normalised CV spectra of the **P1**, **P2** and **P3**

The onset potential of **P1** appeared at $E_{onset} = +0.98$ V for the oxidation and at $E_{onset} = -1.25$ V for the reduction, therefore the HOMO and LUMO levels of **P1** can be calculated as −5.69 eV and −3.46 eV respectively. The differences between the HOMO and LUMO level can be used to calculate the electrochemical band gap for **P1**, which is 2.23 eV.

Furthermore, **P2** has an onset potential observed at $E_{onset} = +1.02$ V for the oxidation and at $E_{onset} = -1.31$ V for the reduction. Therefore, the HOMO and LUMO levels of **P2** can be estimated as −5.73 eV and −3.40 eV respectively. The electrochemical band gap for **P2** is 2.33 eV. In addition, **P3** has an onset potential at $E_{onset} = +0.85$ V for oxidation and at $E_{onset} = -1.29$ V for reduction, therefore the HOMO and LUMO levels of **P3** can be calculated as −5.56 eV and −3.40 eV respectively. The differences between the HOMO and LUMO levels can be used to calculate the electrochemical band gap for **P3**, which is 2.14 eV.

In terms of comparing between the electrochemical band gap values of **P1**, **P2** and **P3**, it can be seen clearly that **P3** has a lower electrochemical band gap than **P1** and **P2**. This was also the case when the optical band gaps of **P1** and **P2** were compared to that of **P3**. This could be attributed to the donor unit of **P3**, which has stronger donating properties than the carbazole in **P1** and the fluorene unit in **P2**. In addition, a further comparison of electrochemical properties between the prepared polymers and polymers reported in the literature such as Qx-2, PFBY and BDPTB can be summarised in **Table 4-4**.

Polymers	HOMO (eV)	LUMO (eV)	E_{elect} (eV)
P1	−5.69	−3.46	2.23
P2	−5.73	−3.40	2.33
P3	−5.56	−3.40	2.14
Qx-2	−5.32	−3.35	1.97
PFBY	-5.77	-3.14	2.63
BDPTB	-5.3	-2.7	2.60

Table 4-4. Summary of electrochemical properties of **P1**, **P2**, **P3**, Qx-2, PFBY and BDPTB

From **Table 4-4** can be seen that **P1**, **P2** and **P3** have deep HOMOs (−5.69 eV for **P1**, −5.73 eV for **P2**, −5.56 eV for **P3**). The resulting polymers should exhibit good oxidative stability when fabricated into optoelectronic devices. **Qx-2** is an analogous polymer to **P1**. The HOMO level of **Qx-2** (-5.32 eV) is shallower than **P1**. Furthermore, the LUMO level of **P1** is deeper than **Qx-2** (-3.35 eV). It is thought that the deeper HOMO and LUMO levels of **P1** relative to **Qx-2** are a consequence of the extended lateral conjugation of the pyrene-quinoxaline system used in **P1**. Previous work has shown that the HOMO will be

diffused across the polymer backbone whilst the LUMO will be located on the acceptor unit. Thus, laterally extending the system will lower the LUMO for **P1**. The pyrene-quinoxaline has a longer longitudinal conjugation length relative to quinoxaline, which will explain the deeper HOMO level of **P1**.

PFBY is an analogous polymer to **P2**. The HOMO level of PFBY (-5.77 eV) is slightly deeper than **P2**. It should be noted that PFBY is not a true D-A copolymer. It is a random copolymer that has an average monomer ratio of 9 donor units (fluorene) to 1 acceptor unit (pyrene-quinoxaline). Thus, PFBY possesses more donor-character leading to a deep HOMO level. However, this leads to an extremely shallow LUMO level (-3.14 eV). Literature has shown the HOMO levels of pure polyfluorenes are extremely deep whilst the LUMO level remains relatively shallow,[158] a trend that is repeated in PFBY.

BDPTB, an analogous polymer to **P3**, possesses a HOMO level of -5.30 eV. This is significantly shallower than **P3**. The pyrene-quinoxaline acceptor used in **P3** has a laterally extended conjugated system that possesses more electron-withdrawing nitrogen atoms relative to the acceptor used in BDPTB. It is speculated the extended conjugation and incorporation of additional electron-withdrawing nitrogen atoms are responsible for the deeper HOMO level of **P3** relative to BDPTB. The electrochemical band gap of BDPTB was estimated to be 2.60 eV, which is significantly wider than **P3** (2.14 eV). The narrower electrochemical band gap of **P3** is a consequence of the laterally extended acceptor unit.

 Figure 4-11 shows the resonance structures of a *para*-substituted quinoxaline acceptor. From this it can be seen that positioning alkoxy substituents at the *para*-position can increase the electron density of neighbouring aromatic units. This will increase the electron density of the pyrene-quinoxaline unit resulting in poor electron acceptor unit; a result that has been confirmed in previous work.[88] This will lead to a decrease in the amount of D-A character, which will negatively impact the optical properties of the polymer and provide large band gaps.

It is believed that replacing the alkoxy substituent with a less electron-donating alkyl chain will prevent this effect and improve the optical properties of the resulting polymers. Therefore, a new class of monomer will be synthesised which position branched alkyl

chains at the *para*-position of the quinoxaline substituents. The lack of an electron dense oxygen atom should prevent electron density being pushed onto neighbouring aromatic units. [159]
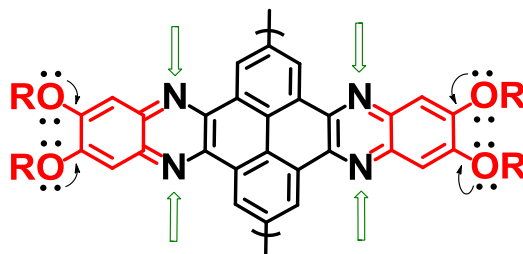
Figure 4-11. The effect of alkoxy group on the accepting properties of the molecule

4.4 Synthesis of polymers P4, P5 and P6

The benefits of using a pyrene-quinoxaline acceptor unit have been discussed in section 4.2. However, it was found that **P1**-**P3** suffered from several limitations. More specifically, the optical and electrochemical band gaps of these polymers were large, which limits the amount of incident radiation the polymer can harvest. It was believed the presence of a *para*-substituted quinoxaline unit increased the amount of electron density on neighbouring aromatics leading to an unfavourable electron-rich acceptor unit. This resulted in less D-A character and a poorly resolved ICT band.

It was believed that replacing the alkoxy substituents on the quinoxaline moieties with alkyl groups might prevent additional electron density being pushed onto neighbouring aromatics, thus, retaining the electron-deficient properties of the pyrene-quinoxaline acceptor unit. This should increase the amount of D-A character, resulting in a more pronounced ICT band. Consequently, the polymers should exhibit a lower optical and electrochemical band gap which will improve their spectral harvesting.

Previous literature has shown that placing the alkoxy chain at different positions on the quinoxaline unit is an effective method of reducing the problems stated above.[88] However, to the best of our knowledge no literature has directly compared the effect substituting -*para*-alkoxy groups with *para*-alkyl chains. Alkyl chains are less electron-donating when compared to alkoxy substituents. Therefore, the mesomeric effect will be reduced. This will allow the electron-withdrawing nitrogen atom to pull electron density from neighbouring donor units leading to formation of the highly favourable D-A system.[159]

The target polymers **P4**, **P5** and **P6** are shown in **Scheme 4-14**.
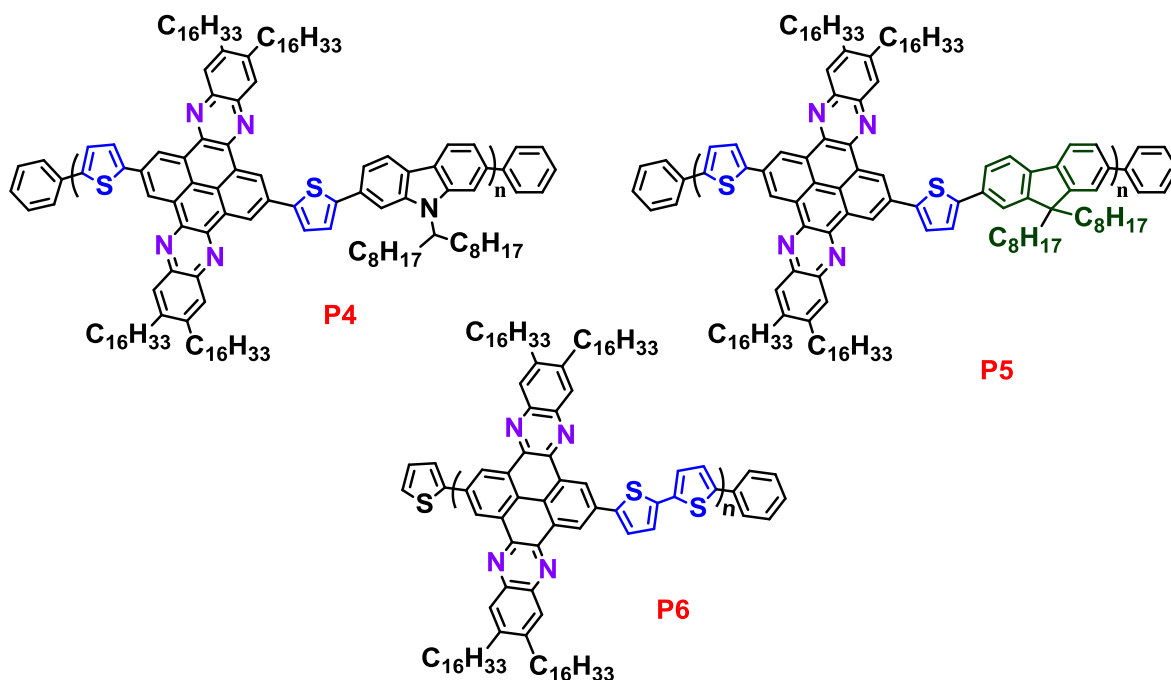
Scheme 4-14 Target polymers **P4**, **P5** and **P6**

4.5 Synthesis of monomers for polymers P4, P5 and P6

4.5.1 2,11-bis (5-bromothiophen-2-yl) -6,7,15,16-tetrakis (3-pentyl undecyl)quinoxalino[2′,3′:9,10]phenanthro[4,5-abc]phenazine (17)

The 2,11-bis (5-bromothiophen-2-yl) -6,7,15,16-tetrakis (3-pentylundecyl) quinoxalino [2′,3′:9,10]phenanthro[4,5-abc]phenazine (**17**) was prepared successfully in seven steps starting from 1,2-dibromo-4,5-dinitrobenzene (**11**) (**Scheme 4-15**). The structure and the purity of these intermediate monomers were examined and confirmed by ^{1}H NMR, ^{13}C NMR, FT-IR, mass spectrometry, melting point and elemental analysis.
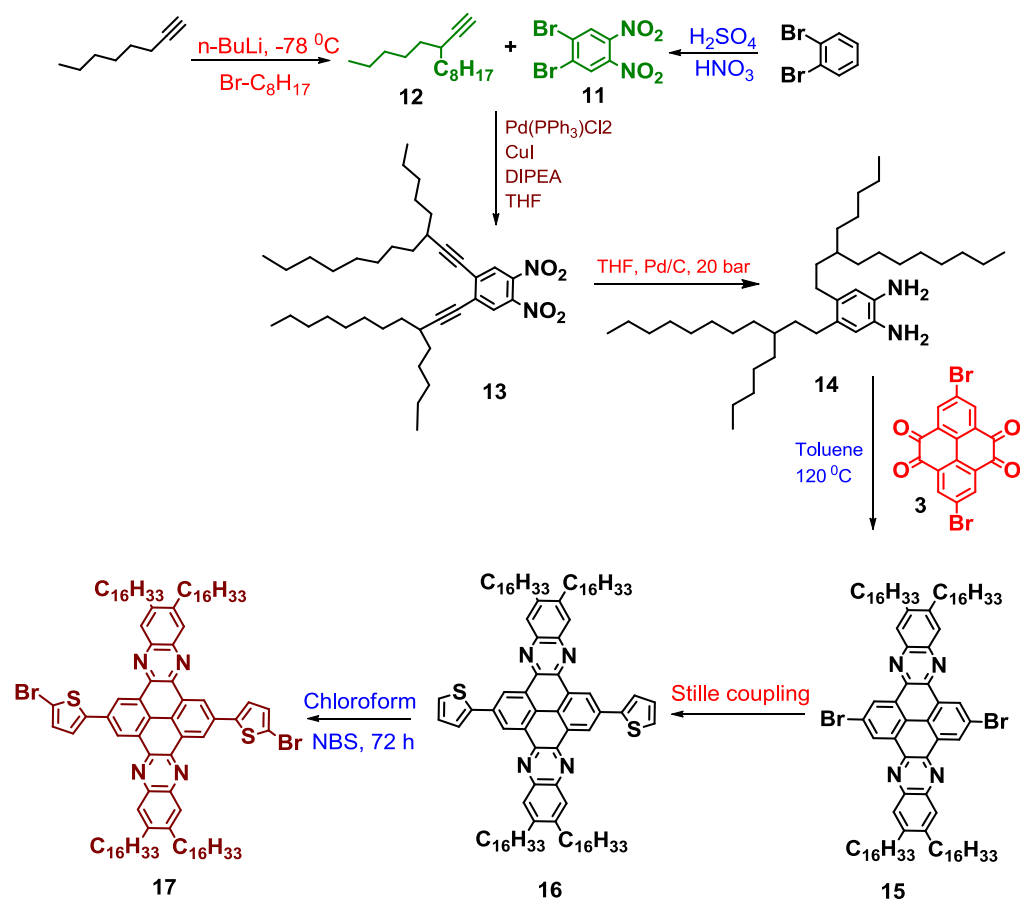
Scheme 4-15 The preparation route of (**17**)

The preparation of 1,2-dibromo-4,5-dinitrobenzene (**11**) involved using a modified method of Frode and co-workers.[124] 1,2-Dibromobenzene was nitrated using fuming nitric acid in concentrated sulphuric acid. The reactants were mixed in an ice bath for a couple of hours, after which the mixture was left stirring vigorously at reflux overnight. The crude product was recrystallised by acetic acid to remove any traces of acids or impurities. The mechanism of such a type of reaction involves two steps as discussed previously (**Scheme 4-6**). The first step is the generation of the nitronium cation (NO_2^+) using a proton from sulphuric acid to form H_2O. The second step is to introduce the nitro groups into the benzene ring at the para positions.

The product was characterised using ^1H NMR, where a singlet peak appeared at 8.20 ppm assigned to the hydrogens attached to the benzene ring. The mass spectrum of the pure product showed three peaks at m/z = 323.8, 325.8 and 327.8 (M^+) due to the bromine

isotopes. The elemental analysis also confirmed the purity of the product from the theoretically calculated composition. FT-IR spectra also confirmed the appearance of two bands at 1524 and 1353 cm^{-1} assigned to the nitro groups. The C–Br group has a band appearing at 739 cm^{-1}. The melting point of this molecule, which was observed at 159–161 °C, also confirmed its purity.[125]

The production of 3-pentylundec-1-yne (**12**) followed the modified method of Ding and co-workers,[126] in which oct-1-yne was placed in hexane at –78 °C under an inert gas. 1-Bromooctane was added after lithiation with *n*-butyl lithium. The resulting crude product was distilled under high vacuum to obtain the pure product of 3-pentylundec-1-yne.

n-Butyl lithium acted as a strong base to deprotonate the protons from oct-1-yne in C1 and C3. Although both positions C1 and C3 were deprotonated, C3 would be more favourable to react with 1-bromooctane. This is because C3 is more reactive than C1 (pKa C1 ~ 25; pKa C3 ~ 45).

Production of 3-pentylundec-1-yne (**12**) was confirmed using ^{1}H NMR, in which multiplet peaks appeared at 2.32 ppm assigned to the hydrogen located between the chiral C3. There is also a doublet peak at 2.05 ppm corresponding to the terminal hydrogen of C1. The remaining peaks have broad peaks at 1.61 and 0.90 ppm assigned to the hydrogens on internal carbons and the hydrogens at the end of aliphatic chains respectively.

^{13}C NMR was also used to confirm the production of this product, in which the terminal C1 signal appeared at 68.8 ppm. FT-IR spectroscopy was also involved in proving the production of 3-pentylundec-1-yne (**12**) by showing a band at 3313 cm^{-1} due to hydrogen on carbon 1. There was also a band at 2112 cm^{-1} observed for the triple bond between the carbons C1 and C2. The molecular weight of the product was determined *via* mass spectrometry and was found to be m/z = 222.2 (M$^+$), which is in agreement with the theoretical value.

1,2-Dinitro-4,5-bis(3-pentylundec-1-yn-1-yl)benzene (**13**) was synthesised using a modified method of Chi and co-workers,[127] in which Sonogashira coupling was used to form a carbon–carbon bond between 3-pentylundec-1-yne and 1,2 dibromo-4,5-

dinitrobenzene. The product was a yellow oil. The yield was reasonable, 71% compared with the literature values of 50%

The coupling of the aryl bromide with a terminal alkyne was catalysed by using palladium(0) as a catalyst and copper(I) iodide (CuI) as a co-catalyst. *N,N*-Diisopropylethylamine (DIPEA) was also used as a base for deprotonating the hydrogen on the terminal carbon. The catalytic cycle of this reaction started with the activation of the Pd catalyst, which was converted from Pd^{2+} to Pd^{0}. The oxidative addition of Pd^{0} was followed by the transmetalation step, in which the complex was formed. The cycle ended with reductive elimination, where the desired product formed and the Pd returned to Pd^{0} to start the cycle again,[160] as can be seen in **Scheme 4-16**.
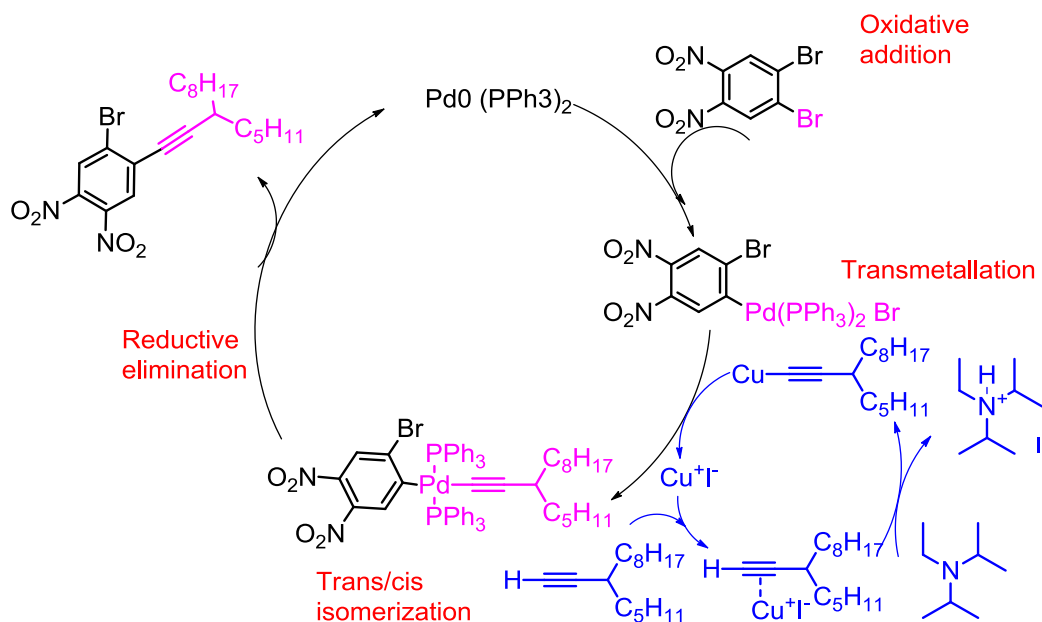
Scheme 4-16. Catalytic cycle for production of 1,2-dinitro-4,5-bis(3-pentylundec-1-yn-1-yl)benzene (**13**)

Production of the desired product was confirmed using ^{1}H NMR as a singlet peak appeared at 8.87 ppm, assigned to the hydrogen in the aromatic ring. There are also multiple peaks at 2.62 ppm assigned to the hydrogen located between the chiral C3. The doublet that appeared at 2.07 ppm for the terminal hydrogen was no longer present. This indicates that the product was successfully formed. ^{13}C NMR was also used to confirm the production of

the product, where the peak at 106.0 ppm corresponded to the carbon–carbon triple bond. The product was further analysed using mass spectrometry, giving a molecular weight of m/z = 609 (M$^+$). The FT-IR spectra showed a strong band between 1543 and 1358 cm^{-1} assigned to the nitro groups. The elemental analysis was in agreement with the theoretical composition for $C_{38}H_{60}N_2O_4$.

The synthesis of 4,5-bis(3-pentylundecyl)benzene-1,2-diamine (**14**) involved a hydrogenation in an autoclave at 10 bar and room temperature over two days. The surface of the palladium was provided to adsorb the organic compound and gaseous hydrogen. This would help to reduce the nitro groups to amino groups and also hydrogenate the triple bonds. Although using a hydrogenation autoclave should give a high yield, the crude product could not be further treated as (**14**) is not stable in view of the ease of oxidation of the compound. Therefore, the next reaction step was conducted as soon as the reduction reaction finished.

To prepare 2,11-dibromo-6,7,15,16-tetrakis(3-pentylundecyl)quinoxalino[2′,3′:9,10] [4,5-abc]phenazine, (**15**) a condensation reaction took place, which involved using both (**3**) and (**14**) under an inert atmosphere. The yield of the reaction was very high, 92%, as a yellow solid compound. The mechanism of this type of reaction was explained previously, **Scheme 4-7**, where the lone pair of the amine group attacked the carbonyl groups in the pyrene system, leading to reduction of the carbonyl to hydroxyl using the amino hydrogen. After forming a bond between the nitrogen in the amino group and the carbon at positions 4,5,9 and 10 of the pyrene system, the oxygen extracted another hydrogen from the amino group to leave as H_2O, forming the condensed molecule.

Purification of the resulting monomer was performed using column chromatography. To confirm the reaction was successful, ^{1}H NMR spectroscopy was used. Two peaks appeared in the aromatic region at 9.54 and 7.98 ppm which we tentatively assign to the aromatic protons at positions a and b, respectively. There were two triplet signals at 2.73 and 1.69 ppm which correspond to the protons on the first and second aliphatic carbon attached to the rings at the positions e and f, respectively. There were also multiple peaks between 1.45 and 1.21 ppm assigned to the aliphatic protons present on the alkyl chains (**Figure 4-12**).
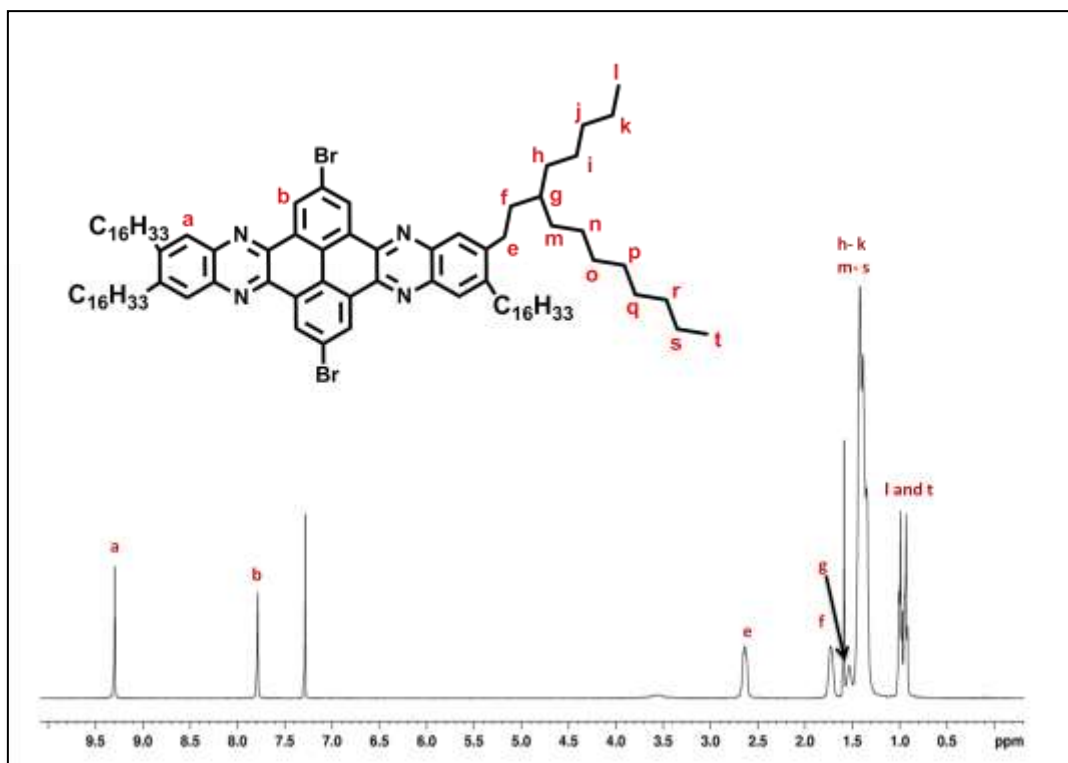
Figure 4-12. ^{1}H NMR for the target monomer (**15**)

^{13}C NMR also confirmed the production of the target monomer (**15**), where eight aromatic carbon environments were observed and no peak was seen for the carbon–carbon triple bonds. This means that the reduction reaction was ideally achieved.

FT-IR spectroscopy gave the desired spectra for the target monomer. There was a band at 3078 cm^{-1} assigned to the aromatic hydrogens, and three bands at 2955, 2924 and 2845 cm^{-1} corresponding to the aliphatic hydrogens. An observed band at 1623 cm^{-1} arose from the C=N double bond. Finally, the C–Br stretch gave a band at 729 cm^{-1}. The melting point of this monomer was 209 to 210 °C. The mass measurement for this molecule was performed using MALDI–TOF, which showed three values for (**15**) at m/z = 1460.4, 1462.3, 1464.3 (M^{+}) due to the isotopes of bromine.

The 6,7,15,16-tetrakis(3-pentylundecyl)-2,11-di(thiophen-2-yl)quinoxaline[2′,3′: 9,10] phenanthro[4,5-abc]phenazine (**16**) monomer was synthesised using Stille coupling, which was described earlier in this thesis. The reaction was performed under argon for 72 hours.

2.5 equivalents of 2-tributylstannyl thiophene were reacted with one equivalent of (**15**) to ensure that the bromines in both positions (2 and 11) of the pyrene phenazine system were replaced with thiophene. The mechanism of the reaction is the same as that discussed for the monomer earlier (**Scheme 4-8**).

The ^{1}H NMR spectra showed a singlet at 9.35 ppm which was assigned to the hydrogen on the quinoxaline molecule. Another singlet was observed at 7.76 ppm, which we tentatively assign to the hydrogen on the pyrene unit. There were three hydrogen environments assigned to the thiophene molecule: two doublets at 7.74 and 7.47 ppm, and one triplet at 7.22 ppm. Two triplet peaks were observed at 2.59 and 1.75 ppm, which correspond to the protons on the first and second aliphatic carbon atoms attached to the rings.

A further analysis was completed for this monomer to ensure that the formation and purity would be of high quality. A MALDI–TOF instrument was used to provide the molecular weight of the resulting monomer, as this monomer was quite large, so this instrument was ideal for calculating an accurate molecular weight. The mass spectrum as provided by MALDI–TOF, was m/z = 1468.1 (M$^+$), which was the same as the mass of the proposed structure. The elemental analysis of C, 78.33; H, 10; N, 3.56 was found, which was in agreement with the calculated values. The melting point of the molecule is quite high, 233 to 235 °C, which indicated the purity of the target product.

The preparation of 2,11-bis(5-bromothiophen-2-yl)-6,7,15,16-tetrakis(3-pentylundecyl) quinoxalino[2′,3′:9,10]phenanthro[4,5-abc]phenazine (**17**) followed a modified procedure of Qin et al.[123] The reaction was left for 72 hours at room temperature under an inert atmosphere and covered with foil all of the time to prevent bromine radicals from existing. Two equivalents of *N*-bromosuccinimide (NBS) were reacted with one equivalent of (**16**) to ensure that no tris-bromination could occur. The yield was as high as 87%, which was similar to the reported literature values.[123] The reaction followed the same mechanism described above (**Scheme 4-9**).

Purification of this monomer was performed using two techniques. Column chromatography eluted with hexane and toluene (7:3; v/v), which removed most of the

impurities. Recrystallisation from ethanol was used as a second manner of purification to give the pure product.

The production of pure target monomer was confirmed by many analytical instruments. The ^{1}H NMR spectrum showed two singlets at 8.92 and 7.70 ppm, which were tentatively assigned to the hydrogens in the quinoxaline (position a) and pyrene units (position b). Two doublets appeared at 7.28 and 7.04 ppm, which were assigned to the hydrogens in the thiophene segment. Another two triplet peaks appeared at 2.63 and 1.75 ppm, which correspond to the protons on the first and second aliphatic carbon atoms attached to the rings (**Figure 4-13**).
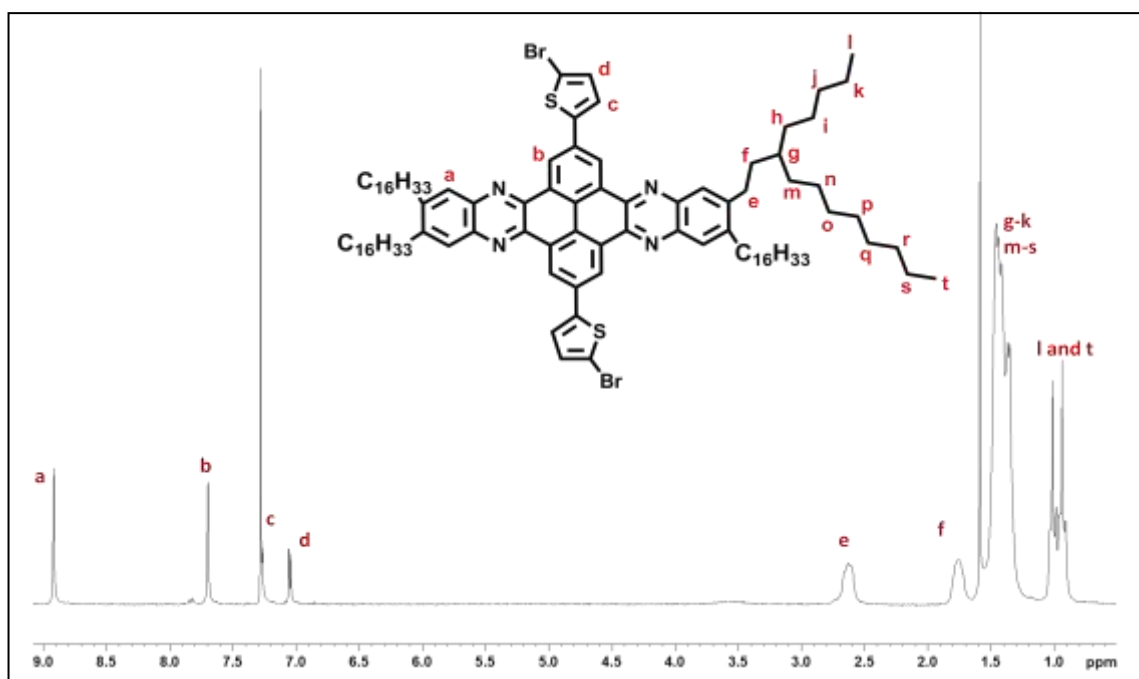
Figure 4-13 ^{1}H NMR for the target monomer (**17**)

4.6 Preparation and characterisation of polymers P4-P6

4.6.1 Synthesis of polymers P4, P5 and P6

The synthesis of **P4** and **P5** used Suzuki coupling, whereas for the synthesis of **P6** Stille coupling was used. Therefore, the synthesis of **P4** and **P5** will be discussed first followed

by the synthesis of **P6**, after which a comparative study for these polymers will be conducted.
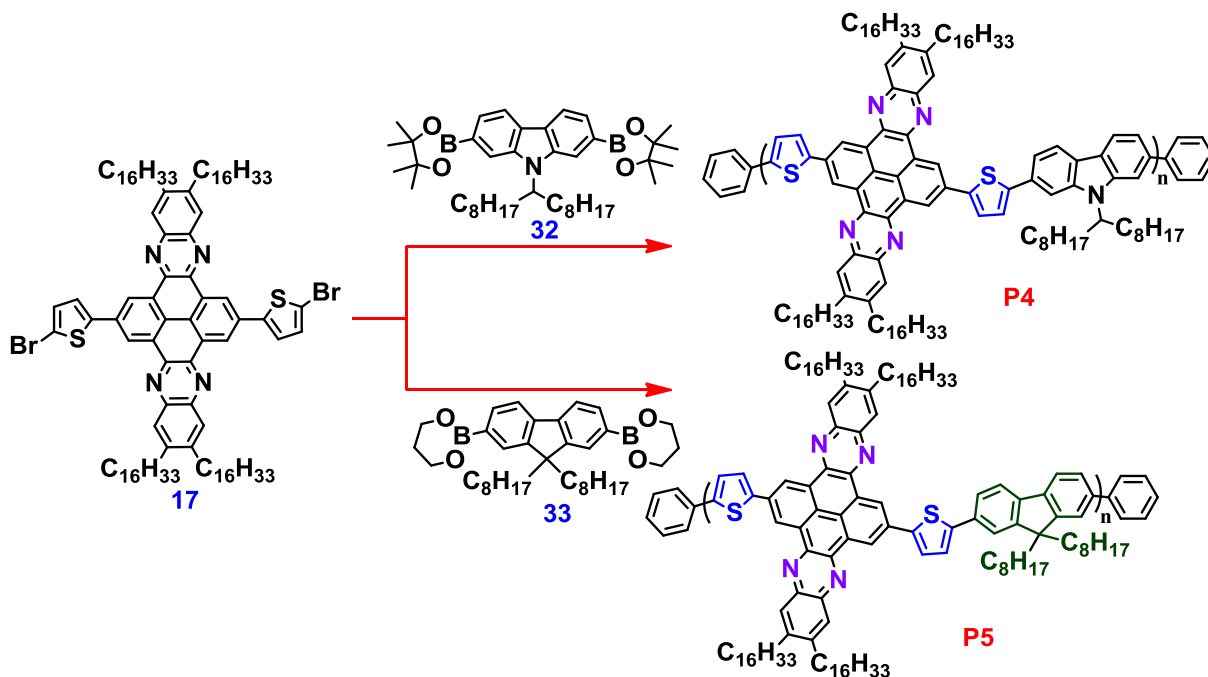
Scheme 4-17 The synthetic route for polymers **P4** and **P5**

Polymerisation of the target polymers **P4** and **P5** (**Scheme 4-17**) was performed in tetrahydrofuran (THF) using $NaHCO_3$ as a base. While the polymerisations proceeded the solutions became viscous, the polymerisations were stopped and further portions of THF were added. At the end of the polymerisation, some THF was added to solubilise the polymers, in which end-capping reagents, such as bromobenzene and phenyl boronic acid, were added to end-cap the backbone of the polymers. This step is useful because the working time of devices and the efficiency of the operation could be improved.[151] Polymers **P4** and **P5** were obtained as orange solids and their purifications followed similar procedures to that used to purify polymers **P1-P3**.
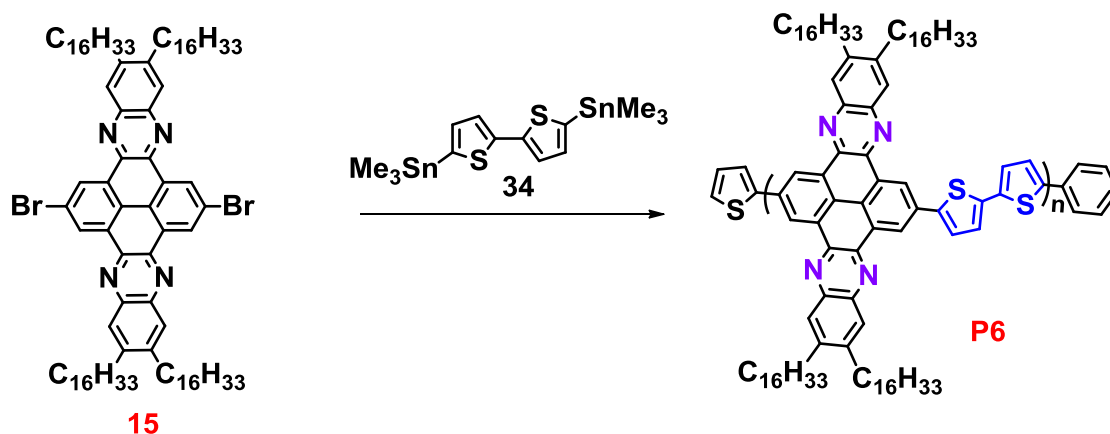
Scheme 4-18 The synthetic route for polymer **P6**

The synthesis of **P6**, **Scheme 4-18**, was performed using Stille coupling in toluene. At the end of the polymerisation, some toluene was added to solubilise the polymer with end-capping reagents, such as bromobenzene and 2-(tributylstannyl)thiophene added to end-cap the polymer's backbone. This step is useful because the working time of devices and the efficiency of the operation could be improved. The proposed mechanism for this reaction is illustrated in **Scheme 4-8**. Polymer **P6** was obtained as an orange powder and was purified in a similar protocol to that of polymers **P4** and **P5**.

4.6.2 Characterisation of polymers P4-P6

To characterise polymers **P1**-**P3**, some analytical instruments were involved, such as gel permeation chromatography (GPC) to calculate their molecular weights, ^{1}H NMR to determine the structure of these polymers, elemental analysis to determine the percentage weight of each element, and a thermogravimetric analysis (TGA), which was used to examine the stability of these polymers. Cyclic voltammetry was used for their electrochemical properties and for UV-vis spectroscopy their optical properties were analysed.

4.6.2.1 GPC data analysis for P4, P5 and P6

After Soxhlet extraction, the yield of these polymers was calculated and the GPC data were obtained in TCB at 140 °C. This was because some difficulties were faced when doing the

analysis at lower temperature, including aggregation and precipitation of the polymers inside the GPC column. Polystyrene was used as a standard to calculate the molecular weight of the target polymers, **P4**, **P5** and **P6**, as shown in **Table 4-5**.

Polymers	Soxhlet Fraction	Yield (%)	M_w	M_n	PDI	DP
P4	chloroform	75	46000	17800	2.5	10
P5	chloroform	67	26500	16800	1.5	9
P6	chloroform	23	11500	10400	1.1	7
	chlorobenzene	45	28500	19300	1.4	13

Table 4-5. GPC data of **P4**, **P5** and **P6**

From **Table 4-5** it can be clearly seen that polymers **P4** and **P5** were obtained in good yields, 75% and 67% respectively. In addition, **P6** was obtained in two fractions. The first fraction was in chloroform, 23%. The second fraction was in chlorobenzene, 45%. This reflects the low solubility of this polymer due to the thiophene units having no solubilising groups attached to them. The GPC analysis showed the degree of polymerisation for **P4** is roughly 10. Thus, **P4** has approximately 10 quinoxaline and carbazole units per the polymer chain. GPC estimated the Mw and Mn of **P4** to be 46000 and 17800 Da respectively, with a polydispersity of 2.5. For polymer **P5** there are around 9 units of quinoxaline and fluorene units per polymer chain, (Mw = 26500, Mn = 16800, PDI = 1.5). Finally, polymer **P6** (chloroform fraction) has approximately 7 quinoxaline units and 2,2'-bithiophene units per polymer chain with molecular weight Mw and Mn of 11500 and 10400 Da respectively. This fraction of **P6** has a narrow PDI of 1.1. The low PDI could be attributed to a fractionation effect. Thus, only a small fraction of molecular weights are soluble in the chloroform fraction resulting in a low PDI. The chlorobenzene fraction of polymer **P6** has approximately 13 quinoxaline units and 2,2'-bithiophene units per polymer chain with a Mw and Mn of 28500 and 19300 Da respectively. This gives a wider PDI of 1.4.

4.6.2.2 ^{1}H NMR analysis for P4, P5 and P6

As discussed previously, these types of polymers have low solubility due to the aggregation effect, which leads to stiffening of the polymer backbones and hence hinders the breaking up of the polymer chains. The ^{1}H NMR analysis for **P4** in C$_2$D$_2$Cl$_4$ at 100 °C, **Figure 4-14**, showed one broad signal in the aromatic region even though the analysis was done at high temperature. There are four peaks in the aromatic region, these include a broad peak at 8.17 ppm corresponding to the protons in positions a. Other overlapping peaks observed at 7.90 ppm are assigned for the protons in positions b and c. In addition, a singlet peak observed at 7.58 ppm corresponded to the proton in the position e. Moreover, the broad peak assigned for the protons in position d appeared at 9.55 ppm. For the thiophene protons at the positions g and f, a broad peak was observed at 7.16 ppm. There is a broad peak observed in the aliphatic region at 4.75 ppm assigned to the proton on the carbon that is connected to the nitrogen of the carbazole part. Furthermore, a broad peak is observed at 2.81 ppm corresponding to the protons in the positions k and h.
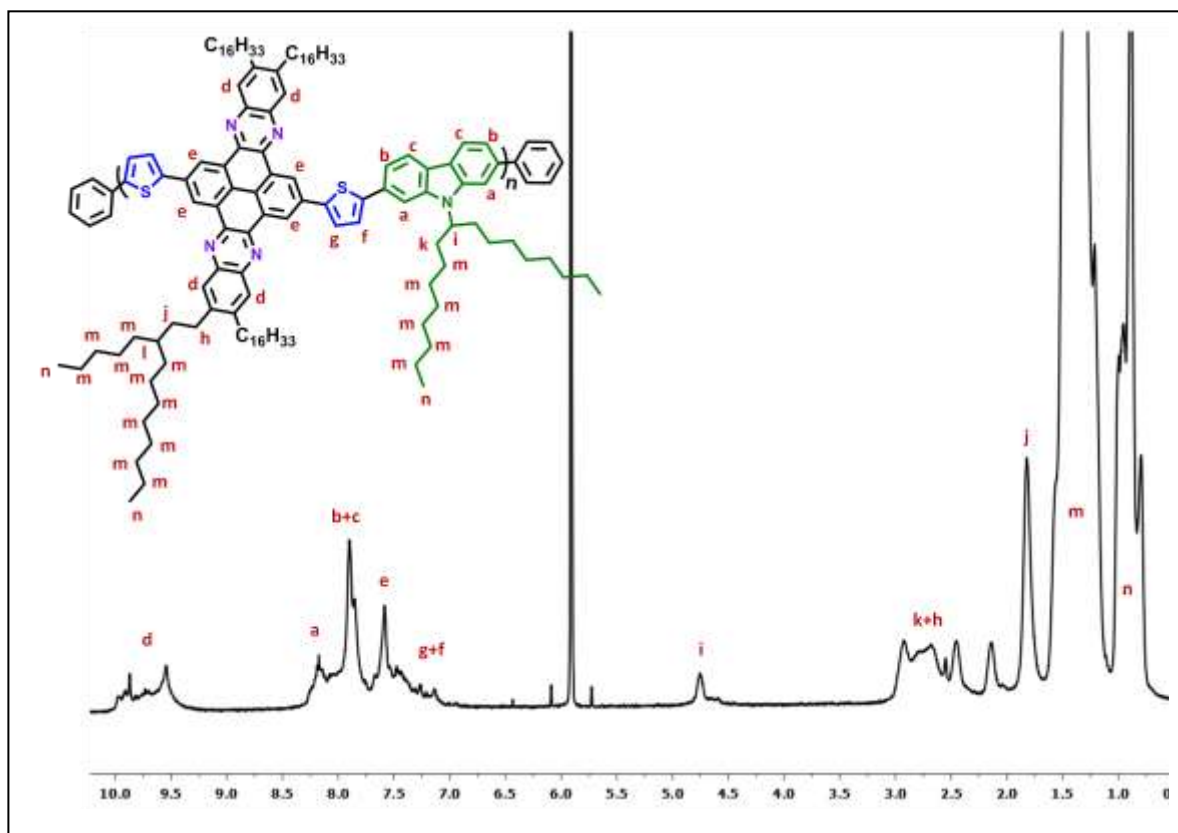
Figure 4-14. ^{1}H NMR analysis for **P4** in C$_2$D$_2$Cl$_4$ at 100 °C

The ^{1}H NMR spectra for **P5** in C$_2$D$_2$Cl$_4$ at 100 °C, **Figure 4-15**, showed one broad signal in the aromatic region, which makes it difficult to distinguish between the signal peaks; however, the ^{1}H NMR was done at high temperature as stated above. There is a broad peak at 8.10 ppm assigned to the protons on the carbons at position a of the fluorene part. In addition, two peaks appeared at 7.81 and 7.65 ppm assigned to the protons on the carbons at positions c and b respectively. The aromatic protons for the quinoxaline were observed at 9.56 and 7.53 ppm at positions d and e respectively. For the thiophene protons at positions g and f, a broad peak observed at 7.21 ppm. The peaks in the aliphatic region for both parts are observed as broad peaks. The proton (position h) on the first carbon connected directly to the fluorene part of the alkyl chain appeared as a broad peak at 2.78 ppm. Another two broad peaks observed at 2.22 and 1.85 ppm were assigned to the protons on the carbons at position i and j of the quinoxaline.
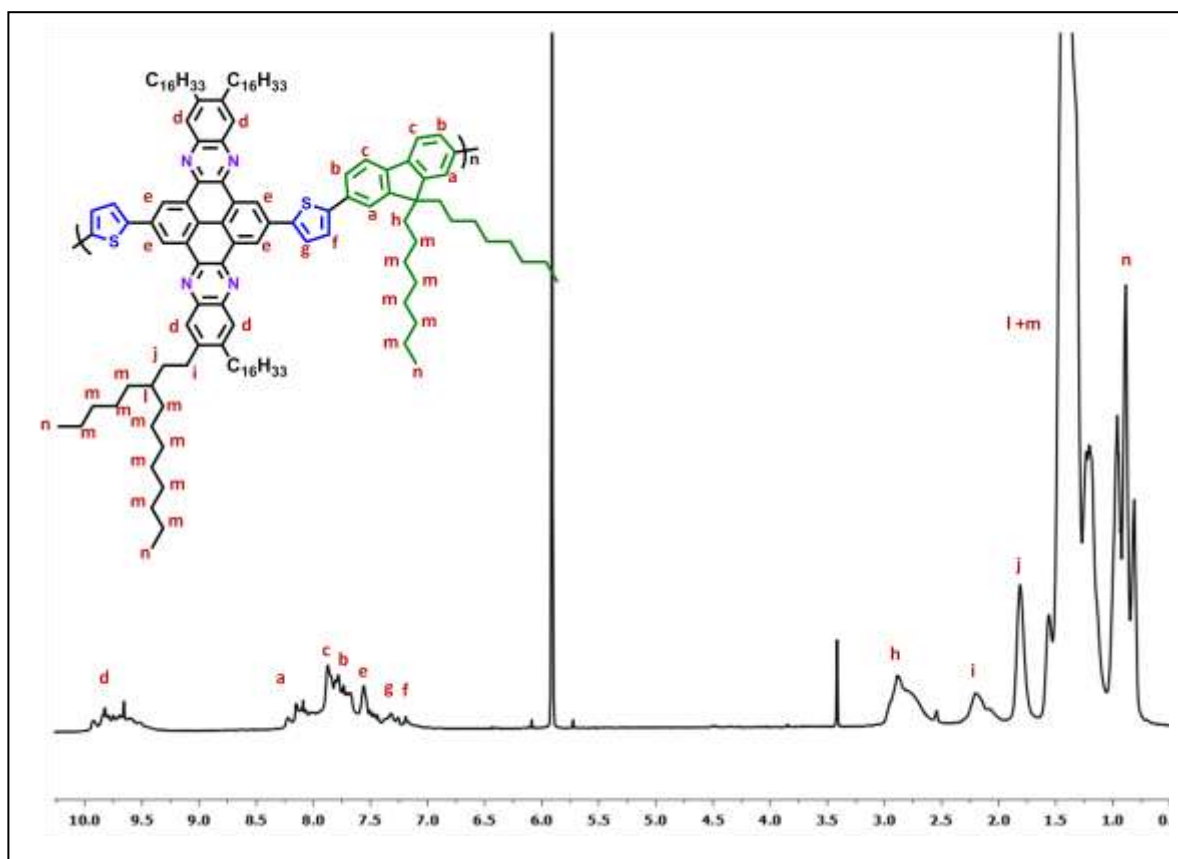
Figure 4-15. ^{1}H NMR analysis for **P5** in C$_2$D$_2$Cl$_4$ at 100 °C

eaks in the aromatic region. The peak for the protons of the quinoxaline in position a appeared at

9.50 ppm. In addition, the peak for the protons b, c and d are overlapped and appear as one broad peak at 7.92 ppm. The protons at position h on the first carbon connected directly to the quinoxaline part of the alkyl chain appeared as a broad peak at 2.78 ppm.
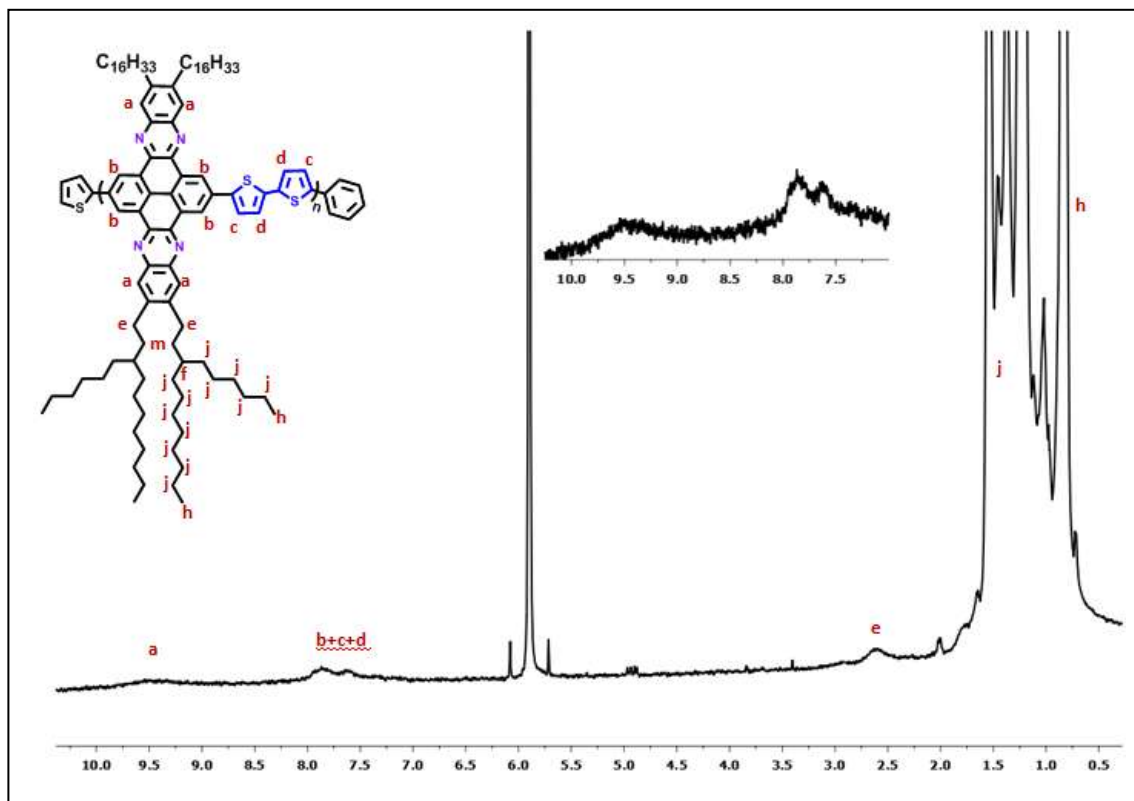
Figure 4-16. ^{1}H NMR analysis for **P6** in C$_2$D$_2$Cl$_4$ at 100 °C

4.6.2.3 Elemental analysis for P4, P5 and P6

Elemental analysis was used to examine the target polymers, whether they are consistent with a given molecular formula and also to ensure the bromine atom is replaced with an end-capping molecule. The result shown in **Table 4-6** indicate that the elemental analysis of these polymers is in agreement with the proposed structures of **P4**, **P5** and **P6** and also confirmed that **P4** and **P5** were end-capped with either bromobenzene or phenylboronic acid, whereas **P6** was end-capped with bromobenzene or 2-(tributylstannyl)thiophene.

Polymers	Formula		Elemental analysis				
			C	H	N	Br	S
P4	$(C_{129}H_{187}N_5S_2)_n$	Calculated	82.76	10.07	3.74	0	3.43
		Found	82.83	9.62	3.63	0	2.97
P5	$(C_{129}H_{186}N_4S_2)_n$	Calculated	83.43	10.10	3.02	0	3.45
		Found	81.60	9.63	3.12	0	3.21
P6	$(C_{100}H_{146}N_4S_2)_n$	Calculated	81.80	10.02	3.82	0	4.37
		Found	80.10	11.32	2.17	0	2.76

Table 4-6. Elemental analysis data for **P4**, **P5** and **P6**

4.6.2.4 Thermal analysis of P4, P5 and P6

Thermal analysis of polymers **P4**, **P5** and **P6** was undertaken in order to see if these polymers can be employed in solar cells. As can be seen in **Figure 4-7**, the diagram confirms the thermal stability of these polymers up to 400 °C; therefore, they can be used in solar cell applications. **P4** has the first onset of degradation at 420 °C due to degradation of the alkyl chain and the main onset of degradation at 590 °C with a weight loss 59.44%. **P5** has the first onset of degradation at 414 °C due to degradation of the alkyl chain and the main onset of degradation at 559 °C with a weight loss of 48.09%. **P6** has the first onset of degradation at 401 °C due to degradation of the alkyl chain and the main onset of degradation at 550 °C with a weight loss 46.36%.
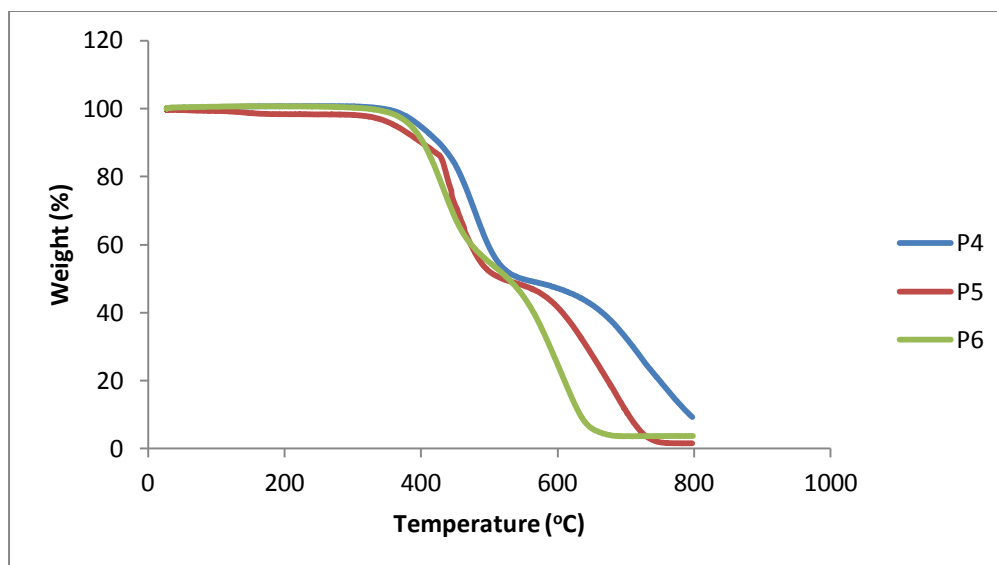
Figure 4-17. The TGA thermograms for **P4**, **P5** and **P6**

4.6.3 Optical properties of P4, P5 and P6

Studies of the UV-vis spectra of **P4**, **P5** and **P6** were performed in chloroform (**Figure 4-18**), and on films drop-cast on quartz substrates (**Figure 4-19**). In solution and film states, all polymers display excellent electronic and vibronic structure with absorption bands located between 370 – 550 nm for polymers **P4**-**P6**. We speculate the improved electronic and vibronic resolution is a consequence of pyrene-quinoxaline extended π-system, planarity and rigidity. These properties should improve the stacking of the polymer in solid state. This phenomenon has been observed in pyrene-based small molecules as well as for polymers.[153,155] Furthermore, similar features were observed for polymers **P1-P3** described earlier in this chapter. Such fine electronic and vibronic structure makes assigning specific bands (π-π* and ICT bands) difficult. However, we tentatively assign peak with the longest wavelength as the ICT band. As with previous polymers, this absorption band will be referred to as the λ_{max}. The λ_{max} in chloroform solutions appear at 476, 470 and 500 nm for **P4**, **P5** and **P6** respectively, (**Figure 4-18**). When cast into films, the λ_{max} is red-shifted to 487, 482 and 504 nm for **P4**, **P5** and **P6** respectively (**Figure 4-19**). The red-shift between solution and film is relatively small (between 4-12 nm), as was observed in the previous series of polymers (**P1-P3**) which indicates there is little structural difference between the polymers conformation in solution and solid state.
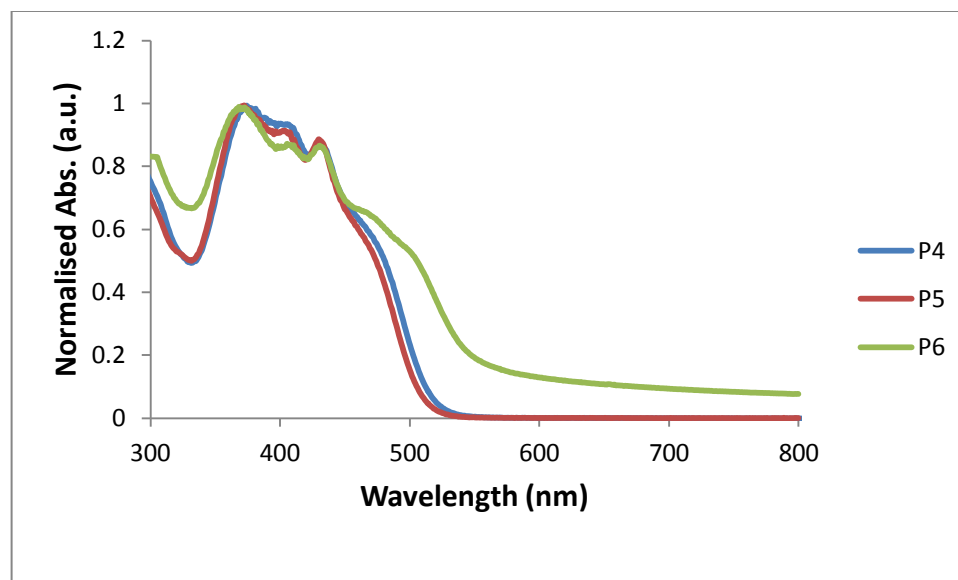
Figure 4-18. UV-vis analysis for **P4**, **P5** and **P6** in chloroform solution

P4-P6 are analogous polymers to **P1-P3**. The electron-donating alkoxy chains in **P1-P3** have been replaced with less electron-donating alkyl chains in **P4**-**P6**. It was hoped this would decrease the amount of electron density pushed onto neighbouring molecules resulting in improved optical properties. When comparing the UV-vis absorption spectra of **P1-P3** with **P4**-**P6** (**Table 4-7**) it can be seen that the λ_{max} of **P4**-**P6** is red-shifted by ~15 nm relative to the λ_{max} in **P1-P3**. Furthermore, **P4**-**P6** demonstrates lower optical band gaps relative to **P1-P3**. The results support our hypothesis that replacing the electron donating alkoxy chains with a less electron-donating alkyl chain will improve the optical properties of the polymer. It is known that alkoxy groups are electron-donating.[88] When these groups are attached to the *para*-position of the pyrene-quinoxaline unit electron density is pushed onto neighbouring aromatics through the mesomeric effect. This will decrease the electron-accepting properties of the electron-accepting pyrene-quinoxaline unit. Thus, the polymer will exhibit less D-A character. Alky chains are less electron-donating when compared to alkoxy chains. Thus, less electron density is pushed onto neighbouring aromatic substituents. Therefore, **P4**-**P6** exhibits more D-A character relative to **P1-P3**, which is reflected in their red-shifted λ_{max}. Whilst the optical properties of **P4**-**P6** are improved relative to **P1-P3**, the improvement is negligible. Despite the red-shifted ICT and narrower

optical band gaps, it is believed that **P4**-**P6** will still suffer from poor spectral harvesting, which will limit their application in organic solar cells.
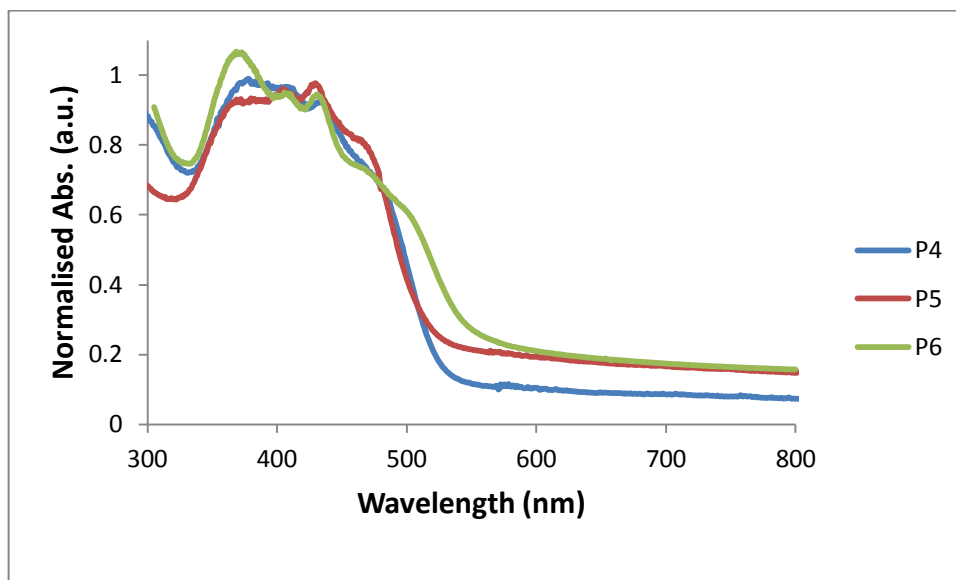
Figure 4-19. UV-vis analysis for **P4**, **P5** and **P6** as thin films

The results obtained from the UV-vis spectroscopy indicate that the *para*-substituted alkoxy chains were not responsible for the poor performance of these polymers. Replacing the alkoxy chain with a less electron-donating alkyl chain should have yielded a far larger improvement in terms of the polymers optical properties. With this in mind, it is believed that the pyrene-quinoxaline system is a poor electron-accepting unit and would prosper if used as an electron-donating unit instead.

Polymers	λ_{max} (nm) solution	λ_{max} (nm) film	λ_{onset} (nm) absorption	E_g Optical (eV)
P1	471	475	510	2.43
P2	468	470	497	2.49
P3	487	489	529	2.34
P4	476	487	528	2.34
P5	470	482	519	2.38
P6	500	504	545	2.27

Table 4-7 Photophysical properties of **P1**-**P6**

4.6.4 Electrochemical properties of P4, P5 and P6

Electrochemical studies of **P4**, **P5** and **P6** were performed on drop-cast films in dried acetonitrile solvent with tetrabutylammonium perchlorate, which works as an electrolyte. In this examination, the HOMO and LUMO were determined using CV (**Figure 4-20**).
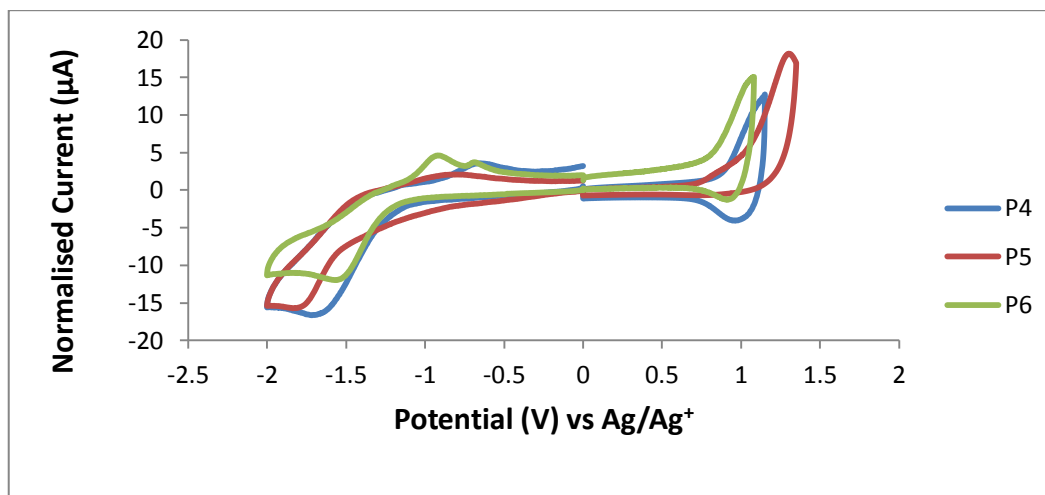
Figure 4-20. Normalised CV spectra of **P4**, **P5** and **P6**

The onset oxidation potential of **P4** appeared at $E_{onset} = +0.91$ V for the oxidation and at $E_{onset} = -1.22$ V for the reduction, therefore the HOMO and LUMO levels of **P4** can be calculated as –5.62 eV and –3.49 eV respectively. The differences between the HOMO and LUMO level can be used to calculate the electrochemical band gap for **P4**, which is 2.13 eV. Furthermore, **P5** has an onset potential observed at $E_{onset} = +1.01$ V for the oxidation and at $E_{onset} = -1.25$ V for the reduction. Therefore, the HOMO and LUMO levels of **P5**

can be estimated as –5.72 eV and –3.46 eV respectively. The electrochemical band gap for **P5** is 2.23 eV. In addition, **P6** has an onset potential at E_{onset} = +0.87 V for the oxidation and at E_{onset} = –1.24 V for the reduction, therefore the HOMO and LUMO levels of **P6** can be calculated as –5.58 eV and –3.47 eV respectively. The difference between the HOMO and LUMO level can be used to calculate the electrochemical band gap for **P6**, which is 2.11 eV.

P4-P6 are analogous polymers to **P1-P3**. The electron-donating alkoxy chains in **P1-P3** have been replaced with less electron-donating alkyl chains in **P4**-**P6**. It was hoped this would decrease the amount of electron density pushed onto neighbouring molecules resulting in improved electrochemical properties. The HOMO levels of **P4-P6** are similar to their analogous polymer **P1-P3** suggesting that replacing alkoxy chains for less electron-donating alkyl chains has little impact upon the resulting HOMO level. However, P4-P6 possess deeper LUMO levels relative to the analogous polymers, **P1-P3**, a result which suggests replacing the alkoxy chains with alkyl solubilising groups improves the accepting properties of the pyrene-quinoxaline unit. This results agrees with optical data which shows **P4-P6** possess improved intramolecular charge transfer between donor and acceptor units (**Table 4-8**).

Polymers	HOMO (eV)	LUMO (eV)	E_{elect} (eV)
P1	–5.69	–3.46	2.23
P2	–5.73	–3.40	2.33
P3	–5.56	–3.42	2.14
P4	–5.62	–3.49	2.13
P5	–5.72	–3.46	2.23
P6	–5.58	–3.47	2.11

Table 4-8. Summary of the electrochemical properties of **P1**, **P2**, **P3**, **P4**, **P5** and **P6**

4.7 Conclusion

In conclusion, the monomer 2,11-bis(5-bromothiophen-2-yl)-6,7,15,16-tetra(hexadecyloxy) -tetrabenzo[a,c,d,e]phenazine (**10**) was successfully synthesised in nine steps, which was then polymerised as an acceptor *via* Suzuki coupling using various donors. **10** was

polymerised with 9-(heptadecan-9-yl)-2,7-bis(4,4,5,5-tetramethyl-1,3,2-dioxaborolan-2-yl)-9H-carbazole (**32**) and 9,9-dioctylfluorene-2,7-diboronic acid bis(1,3-propanediol) ester (**33**) to obtain **P1** and **P2** respectively. Polymer **P3** was made by polymerising 2,11-dibromo-6,7,15,16-tetrakis(2-hexyldecyloxy) quinoxalino [2',3':9,10]phenanthro[4,5-abc]phenazine (**8**) with 5,5'-bis(trimethylstannyl)-2,2'-bithiophene monomer (**34**). GPC results for these polymers showed that the molecular weight of **P1** has approximately 15 quinoxaline- *alt*-carbazole repeat units per polymer chain. The Mw and Mn of **P1** were estimated to be 67800 and 29300 Da respectively. This equates to a polydispersity of 2.31. For polymer **P2** there are around 8 repeat units of quinoxaline-*alt*-fluorene parts per polymer chain. The Mw and Mn of **P2** were estimated to be the 50700 and 15300 Da respectively, with a polydispersity of 3.31. Finally, polymer **P3** has approximately 7 quinoxaline-*alt*-2,2'-bithiophenes units per polymer chain with a molecular weight of 16300 Da and a number-average molecular weight of 9900 Da. This yields a polydispersity of 1.6. **P3** has a lower molecular weight when compared to **P1** and **P2** which is a consequence of having no solubilising chain attached to the bithiophene donor unit.

Polymers **P4**, **P5** were prepared successfully by synthesising 2,11-bis (5 bromothiophen-2-yl) -6,7,15,16-tetrakis (3-pentylundecyl) quinoxalino[2′,3′:9,10] phenanthro[4,5-abc]phenazine (**17**) in seven steps. **17** was then polymerised as an acceptor *via* Suzuki coupling using various donors. Polymerising **17** with 9-(heptadecan-9-yl)-2,7-bis(4,4,5,5-tetramethyl-1,3,2-dioxaborolan-2-yl)-9H-carbazole (**32**) and 9,9-dioctylfluorene-2,7-diboronic acid bis(1,3-propanediol) ester (**33**) yielded **P4** and **P5**. In addition, polymer **P6** has been prepared by polymerising 2,11-dibromo-6,7,15,16-tetrakis(3-pentylundecyl)quinoxalino[2′,3′:9,10] [4,5-abc]phenazine, (**15**) with 5,5'-bis(trimethylstannyl)-2,2'-bithiophene monomer (**34**). GPC results for polymers **P4** to **P6** showed that the molecular weight of **P4** has approximately 10 quinoxaline-*alt*-carbazole repeat units per polymer chain (Mw = 46000 Da, Mn = 17800 Da, polydispersity = 2.5). For polymer **P5** there are around 9 repeat units of quinoxaline-*alt*-fluorene per polymer chain. The Mw and Mn of **P5** were estimated to be 26500 and 16800 Da respectively. This yields a polydispersity of 1.5. Finally, polymer **P6** has approximately 7 quinoxaline-*alt*-2,2'-bithiophene units per polymer chain. The molecular weight and number-average

molecular weight of **P6** were estimated to be 11500 and 10400 Da respectively, with a polydispersity of 1.1. Again, **P6** had a lower molecular weight when compared to **P4** and **P5**, which is due to the lack of solubilising chains on the bithiophene donor-unit.

All polymers display excellent electronic and vibronic structure with distinct absorption bands located between 370 – 550 nm for polymers **P1**-**P6**. We speculate the improved electronic and vibronic resolution is a consequence of pyrene-quinoxaline extended π-system, planarity and rigidity. The λ_{max} of **P4-P6** are red-shifted when compared to **P1-P3**. Substituting the electron-donating alkoxy group in **P1-P3** for the less electron-donating alkyl chain is responsible for this. Furthermore, **P4-P6** display narrower optical band gaps relative to **P1-P3**. Despite this, all polymers display optical band gaps in excess of 2.0 eV, which will result in poor spectral harvesting.

When comparing the solid state UV spectra of **P1**, **P2** and **P3** it can be seen that the λ_{max} of **P3** is more red-shifted relative to **P1** and **P2**. Furthermore, **P3** displays a lower optical band gap relative to **P1** and **P2**. This can be attributed to the strength and architecture of the donor-moiety. Thiophene is a stronger donor, relative to carbazole and fluorene. We tentatively suggest this leads to improved intramolecular charge transfer along the polymer backbone. Unlike carbazole and fluorene, thiophene is not decorated with large, sterically demanding solubilising chains. This will allow **P3** to adopt a more planar and rigid structure in solid state when compared to **P1** and **P2**. A similar result is observed when comparing **P4-P6**.

Electrochemical studies of **P1** to **P6** showed that the calculated HOMO and LUMO levels of **P1** (–5.69 eV *vs* –3.46 eV), (–5.73 eV *vs* –3.40 eV) for **P2** and (–5.56 eV *vs* –3.40 eV) for **P3**, (-5.62 *vs* -3.49 eV) for **P4**, (-5.72 *vs* -3.46 eV) for **P5**, (-5.58 *vs* -3.47 eV) for **P6**. The electrochemical band gaps for **P1** to **P6** are (2.23 *vs* 2.33, 2.14, 2.13, 2.23 and 2.11 eV) respectively. **P3** and **P6** have lower electrochemical band gaps when compared to **P1**, **P2**, **P4** and **P5**. This can be attributed to use of 2,2'-bithiophene as an electron donating unit. When compared with fluorene and carbazole, 2,2'-bithiophene is a stronger electron donor resulting in the polymer displaying more D-A character.

The LUMO levels of **P4-P6** are deeper than their analogous polymers, **P1-P3**. Substituting the alkoxy chains on the pyrene-quinoxaline unit for alkyl chains is responsible for this. Alky chains are less electron-donating when compared to alkoxy chains. Therefore, when alkyl chains are used less electron density is pushed on neighbouring aromatics resulting in the polymer having more donor-acceptor character. This result is consistent with the red-shifted intramolecular charge transfer observed in the UV-vis spectra.

TGA revealed that all polymers possessed excellent thermal stability with degradation temperatures in excess 360 °C. This should allow for thermal annealing of organic solar devices, if needed.

From the results, it can be concluded that **P1**, **P2** and **P3** were affected by the alkoxy chain. Oxygen pushed electron density towards the quinoxaline groups which decreased their accepting properties. Therefore, the decision was made to replace the alkoxy chain with an alkyl chain to neutralise the effect of the oxygen. This gave **P4**, **P5** and **P6**, which showed improvement in their optical and electrochemical properties. However, they still have large band gaps, which will limit the use of these polymers in organic solar cells. The work done in this chapter indicates that the pyrene-quinoxaline unit is perhaps better suited to the role of a donor-unit rather than acceptor unit. Therefore, further work will investigate the pyrene-quinoxaline unit as a donor and copolymerise it with alternate benzothiadiazole acceptor units, to generate a new class of low band gap laterally extended two dimensional polymers. This will allow us to determine whether the pyrene-quinoxaline unit is best used as an electron-donating repeat unit.

5 Chapter 5: Synthesis of laterally extended two-dimensional quinoxaline based polymers with alternating benzothiadiazole acceptors

5.1 Introduction

As discussed in the previous chapter, polymers **P1** to **P6** were synthesised based on laterally extended two-dimensional structures. It was discovered that **P1-P3** suffered from large band gaps and poor spectral light harvesting. This was a consequence of using *para*-alkoxy quinoxaline, which increased the electron density of neighbouring aromatics. Attempts were made to rectify this and the alkoxy groups were substituted for alkyl chains. It was hoped that the lack of an electron rich oxygen atom would reduce the mesomeric effect and lead to more D-A character in the polymer. However, optical and electrochemical studies conducted on **P4**-**P6** revealed that the improvement they displayed over their analogous polymers (**P1**-**P3**) was minimal. **P6** showed the largest increase in performance over its analogous polymer, **P3** (**Table 4-7**). The ICT in **P3** was located at 489 nm and the polymer was estimated to have an optical band gap of 2.34 eV. Substituting the alkoxy chains for alkyl chains gave **P6** which possessed an ICT band located at 504 nm and an optical band gap of 2.27 eV. Whilst an improvement is definitely observable, it is not significant. The band gap for **P6** is larger than that of P3HT.[161] It is known that the performance of P3HT is limited by its optical band gap and limited spectral harvesting.[162] The band gap of **P6** is larger than P3HT. Therefore, it will suffer from the same fate.

It is thought that the use of *para*-alkoxy/*para*-alkyl quinoxaline means the resulting pyrene-quinoxaline system functions more as a donor than an acceptor. To test this theory a new class of polymers will be synthesised in which monomer (**8**) and (**15**) will be used as electron donating units. The monomers (**8** and **15**) will be polymerised with various benzothiadiazole acceptor units (**Scheme 5-1**).
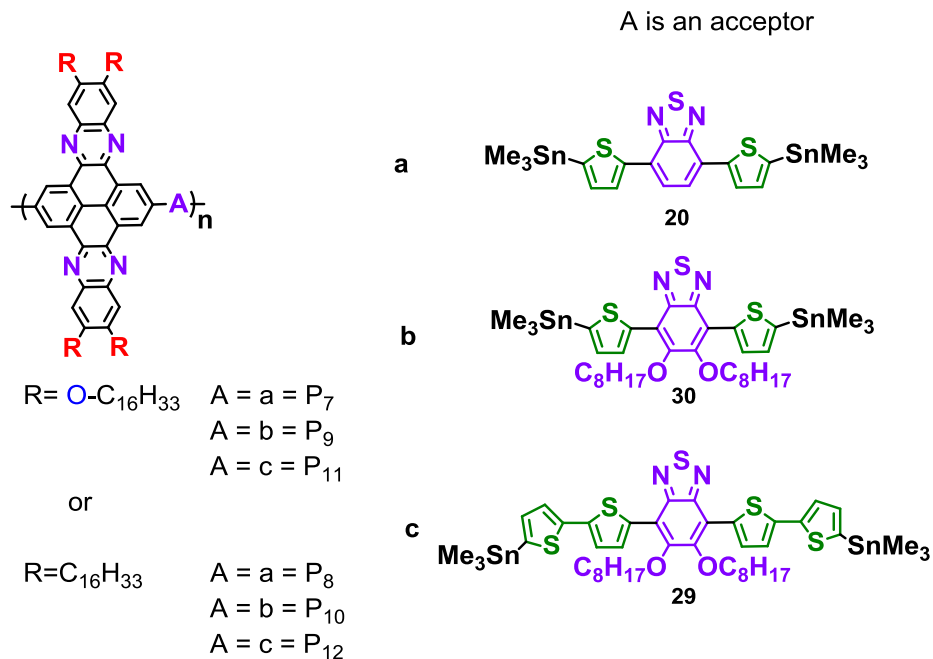
Scheme 5-1 The chemical structures of the target polymers

Benzothiadiazole has interesting properties which allows this molecule to be used in many optoelectronic applications.[163,164] Benzothiadiazole is a heterocyclic molecule that has multiple nitrogen atoms and a hypervalent sulphur, which are linked together. This allows benzothiadiazole to exhibit conducting behaviour with various resonance structures [(=N-S-N=) and (-N=S=N-)].[165] The lone-pair on nitrogen does not participate in the π-aromatic system owing to its hybridisation state and position. Therefore, the electronegative nitrogen atom withdraws electron-density from the benzene ring. Thus, benzothiadiazole is an electron-withdrawing unit which is shown to possess high electron mobilities when used in organic semiconductor devices.[166] Furthermore, the high polarisability of (-N=S=N-) gives rise to strong intermolecular interactions which allow benzothiadiazole based molecules to exhibit high crystallinity.[167] All these features are highly attractive, which makes benzothiadiazole a highly advantageous molecule for use in organic electronic devices. Literature has shown that benzothiadiazole based polymers have low optical band gaps and efficiencies in excess of 7%. For example, PBnDT-DTffBT (**Scheme 5-2**) has good spectral harvesting with a low band gap (1.7 eV) and power conversion efficiency that exceeds 7%.[168]
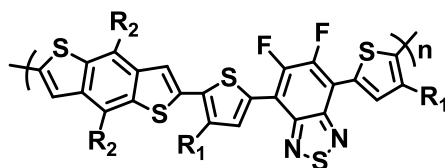
R₁ = 2-ethylhexyl
R₂ = 3-butlnonyl

Scheme 5-2 The chemical structure of PBnDT-DTffBT

5.2 Synthesis of monomers for polymers P7-P12

In order to prepare polymers **P7** and **P8**, monomer (**20**) was prepared successfully in three steps as shown in **Scheme 5-3**. Moreover, monomer (5,6-bis(octyloxy)-4,7-bis(5-(trimethylstannyl)thiophen-2-yl)benzo[c][1,2,5]thiadiazole) (**30**) **Scheme 5-1** was synthesised by S. Alesae of the Iraqi group, and was used for preparing polymer **P9** and **P10** (**Scheme 5-1**).
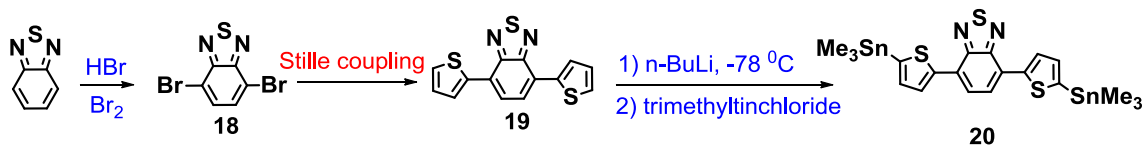
Scheme 5-3 The preparation route for monomer (**20**)

5.2.1 Synthesis of 4,7-bis(5-(trimethylstannyl)thiophen-2-yl)benzo[c][1,2,5] thiadiazole (20)

The synthesis of monomer (**20**) started by synthesising 4,7-dibromobenzo [c][1,2,5]thiadiazole (**18**), as shown in **Scheme 5-3**, which was prepared using a modified method of Zoombelt et al.[128] In this reaction, 1,2,5-benzothiadiazole was heated at 110 °C with hydrogen bromide and bromine added dropwise. Another portion of hydrogen bromide was also added to ensure the complete bromination on both sides of the molecule. The yield was approximately 97% with a white solid product.

The mechanism of the reaction involved electrophilic substitution, in which positions 4 and 7 were activated by nitrogen atoms. Although positions 5 and 6 have lower electron density, the bromines in positions 4 and 7 could activate them, and some trace of tris and tetrakis bromine may have been produced. These traces can be removed easily by recrystallisation.

Production of the target monomer was confirmed by ^{1}H NMR, where a singlet peak appeared at 7.76 ppm assigned to the protons on the aromatic rings. ^{13}C NMR showed three signals at 152.9, 132.3 and 113.9 ppm, which corresponded to the three carbons in the target molecule. The melting point was also used to confirm the purity of the product, which is in agreement with the literature value 186–187 °C.[129] The elemental analysis also was in agreement with the proposed structure and the mass spectrum gave three peaks at 292, 294 and 296 due to the isotopes of bromine.

4,7-Di(thiophen-2-yl)benzo[c][1,2,5]thiadiazole (**19**) was prepared using a modified procedure of Palama and co-workers.[130] This reaction is known as the Stille coupling reaction, which is used to form a carbon–carbon bond by using catalysts such as palladium with tri-o-tolylphosphine. The mixture was heated at 110 °C under dry conditions for 48 hours. The purification was performed using two different methods. First, by column chromatography with a mixture of DCM and hexane (1:1; v/v). Then, recrystallisation from ethanol was also conducted to purify the product. The production of the product was confirmed by ^{1}H NMR, where doublet peaks appeared at 8.13, 7.48 and 7.23 ppm assigned to the protons on the thiophene rings. There was also a singlet recorded at 7.89 ppm corresponding to the protons of the aromatic rings. The melting point also confirmed the purity of the molecule, which was in agreement with the literature value 123–124 °C.[131] The mass spectra showed a signal at 300 (M$^+$), which is in agreement with the theoretical calculation. The FT-IR spectra and elemental analysis also confirmed production of the product.

The synthesis of 4,7-bis(5-(trimethylstannyl)thiophen-2-yl)benzo[c][1,2,5] thiadiazole (**20**) was performed according to a modified procedure by Reichmanis and co-workers.[132] This reaction was performed overnight under an inert gas, which involved using n-butyllithium

as a strong base with 2,2,6,6-tetramethylpiperidine (TMP) to form the complex lithium 2,2,6,6-tetramethylpiperidide (LTMP) at low temperature, –78 °C. This was then used to lithiate (**19**) then, trimethyltin chloride was added dropwise to functionalise position 5 of the thiophene rings on both sides with trimethylstannyl groups. The target monomer was purified by recrystallisation from ethanol to afford orange needle-like crystals with 90% yield.

^{1}H NMR spectra of (**20**) showed doublets at 8.20 and 7.32 ppm assigned to the thiophene ring protons. Also, there was a singlet at 7.88 ppm corresponding to the aromatic protons (**Figure 5-1**). The mass spectrum for this molecule was in agreement with the proposed structure, 626 (M[+]). Elemental analyses were also in agreement with its proposed structure. The FT-IR showed a stretching vibration peak at 536 cm^{−1} assigned to the C–Sn bond. The melting point of the product was between 170 and 171 °C, which confirmed the purity of the product.
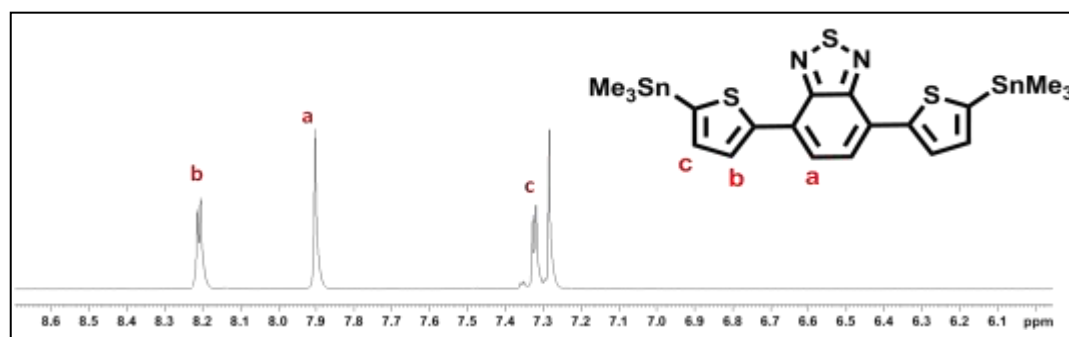
Figure 5-1 The ^{1}H NMR for (**20**)

5.2.2 Synthesis of 5,6-bis(octyloxy)-4,7-bis(5′-(trimethylstannyl)-[2,2′-bithiop hen]-5-yl)benzo[c][1,2,5]thiadiazole (29)

For the preparation of polymers **P11** and **P12**, monomer (**29**) was prepared successfully in nine steps as shown in **Scheme 5-4**. The structure and the purity of these intermediate monomers were checked and examined by ^{1}H NMR, ^{13}C NMR, FT-IR, mass spectrometry, melting point and elemental analysis.
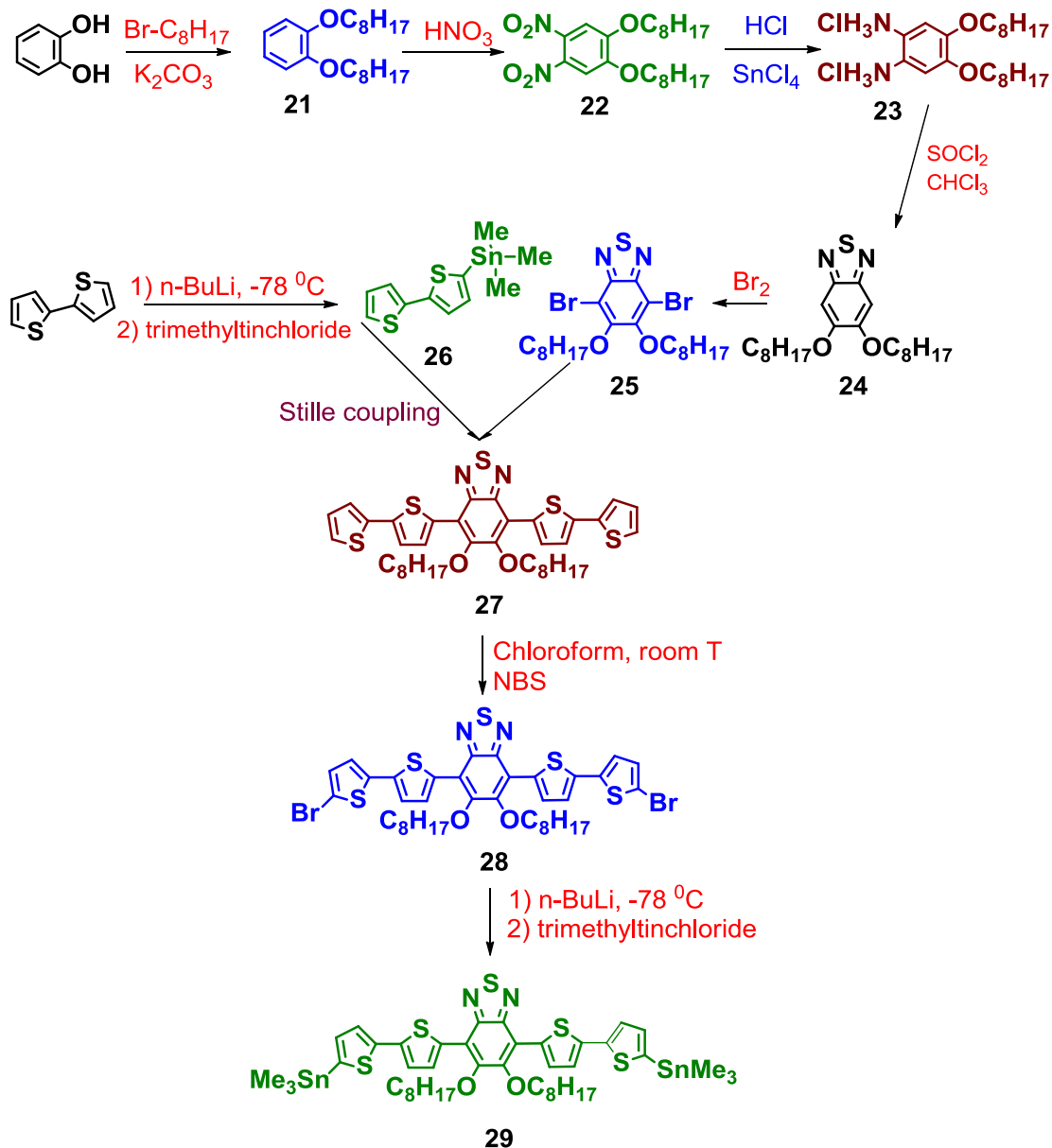
Scheme 5-4 The preparation route for (**29**)

To prepare 1,2-bis(octyloxy)benzene (**21**),[118] a modified method of Janssen and co-workers was used.[133] This reaction was performed by mixing catechol, potassium carbonate and 1-bromooctane together under inert gas for 48 hours at 100 °C. The crude product was purified using recrystallisation from ethanol to afford a white needle-like crystal product with 78% yield. The mechanism of this reaction was discussed earlier, which involved an S_N2 mechanism.

Production of the product was confirmed using ^{1}H NMR, which gave a singlet at 6.94 ppm assigned to the aromatic protons. There was also a triplet at 4.01 ppm corresponding to the hydrogen on the carbon next to the oxygen. The aliphatic protons gave multiple peaks between 1.93 and 0.89 ppm. Mass spectrometry also confirmed the production of the desired product, which recorded the molecular weight at 334 (M^+). Elemental analysis results were in agreement with the theoretical calculation. FT-IR also was used to examine the OH band at 3100–3700 cm^{-1}, which disappeared; a new band between 2953 and 2850 cm^{-1} appeared for the aliphatic chain. The bending vibrations at 1466 and 1387 cm^{-1} belong to carbon–oxygen in the aromatic region. The melting point was observed at between 24 and 25 °C.[134]

The preparation of 1,2-dinitro-4,5-bis(octyloxy)benzene (**22**) involved using a modified method of Janssen and co-workers.[133] The reaction started by stirring 1,2-bis(octyloxy)benzene in dichloromethane with acetic acid and nitric acid (65%) being added dropwise at 0 °C. After allowing the mixture to stir at room temperature, it was cooled again to 0 °C and fuming nitric acid was added dropwise. Upon completion of the reaction, the crude product was purified by recrystallisation from ethanol to give a yellow powder with 90% yield.

^{1}H NMR gave a deshielded singlet at 7.31 ppm assigned to the aromatic protons. There was a triplet peak at 4.12 ppm corresponding to the proton on the carbon next to the oxygen. For the aliphatic region, multiple peaks between 1.96 to 0.90 ppm appeared. The melting point was also used to confirm the purity of the product, where a recorded melting point between 88 and 89 °C was observed.[134] The mass spectrum for this molecule was in agreement with proposed structure, 424 (M^+). The FT-IR spectra showed bands assigned to the aromatic nitro groups at 2023 and 1354 cm^{-1}. The elemental analysis was also in agreement with the theoretical calculation.

The synthesis of 4,5-bis(octyloxy)benzene-1,2-diaminium chloride (**23**) was performed according to a modified method of Janssen and co-workers.[133] The reactants, 1,2-dinitro-4,5-bis(octyloxy)benzene, ethanol as a solvent, $SnCl_2$ as a reducing agent and HCl were mixed and refluxed overnight. The crude product was washed with H_2O and methanol and

dried under nitrogen, before being used directly for the next reaction. Thus is due to the instability of the product. No analytical analysis was done for this product due to its sensitivity to oxygen, which might oxidise the amino group back to the nitro group.

To synthesise 5,6-bis(octyloxy)benzo[c][1,2,5]thiadiazole (**24**), a modified method of Janssen and co-workers was used.[133] To 4,5-bis(octyloxy)benzene-1,2-diaminium chloride in dry chloroform with triethylamine was added thionyl chloride. The mixture was heated to reflux overnight. Recrystallisation was used to purify the target product to obtain a white solid powder with 92% yield.

The mechanism of this reaction involved first, generating the diamine by abstracting the HCl with triethylamine and second, the diamines on the benzene ring worked as nucleophiles and attacked the sulphur atom in the thionyl chloride to provide a closed ring compound with HCl and H_2O as side products.

Production of the target product was confirmed using many techniques. These include ^{1}H NMR which gave a singlet peak at 7.14 ppm assigned to the aromatic protons. There was also a triplet peak at 4.10 ppm corresponding to the protons on the carbon next to the oxygen of the aliphatic alkyl chain. Multiple peaks appeared between 1.99 and 0.91 ppm from the alkyl chain protons. The FT-IR also confirmed the existence of an N–C bond at 1195 and 1065 cm^{-1} and N–S bond at 724 cm^{-1}. The elemental analysis was also in agreement with the theoretical value of the monomer. The melting point of the product was between 100 and 101 °C, which is in agreement with the literature value.[134] The mass spectrum showed the main peak at 392 (M^+), which is as the calculated mass of the target product.

To synthesise 4,7-dibromo-5,6-bis(octyloxy)benzo[c][1,2,5]thiadiazole (**25**), a modified method of Janssen and co-workers was used.[133] In this reaction, bromine was utilised with acetic acid under an inert gas in the dark for 72 hours to achieve the desired product. There were two purification steps for this monomer, column chromatography followed by recrystallisation from ethanol as the second step. The reaction was successful and gave (**25**)

white needles with 77% yield. The mechanism of this reaction involves an electrophilic substitution on the aromatic ring, as described previously.

The production of the target product was confirmed by ^{1}H NMR, where there was no peak observed in the aromatic region. The triplet of the carbon proton next to the oxygen shifted from 4.10 to 4.17 ppm, which indicated the production of the desired product. The mass spectrum also showed the main integer masses of the product, which gave peaks at 548, 550, 552 (M$^+$) assigned to the bromine isotopes. The FT-IR spectra showed stretching peaks at 1285 and 1059 cm^{-1} corresponding to aromatic C–N, 797 cm^{-1} due to the C–Br and 724 cm^{-1} due to the N–S bonds. The elemental analysis was in agreement with the proposed structure, and the melting point was between 44 and 45 °C.[134]

5-Trimethylstannyl-2,2-bithiophene (**26**) was synthesised according to a modified procedure by Jakle and co-workers.[135] This reaction was performed under inert gas overnight, and involved using n-butyllithium as a strong base at –78 °C. Trimethyltin chloride was then added dropwise to functionalise position 5 of the bithiophene with the trimethylstannyl group. Column chromatography was performed to purify the product, which was eluted with hexane and triethylamine (8:2; v/v). The target product was obtained as a colourless oil with 87% yield.

The mechanism of this reaction involved using *n*-butyllithium as a strong base to deprotonate the bithiophene at position 5, then trimethyltin chloride was added to quench the reaction and achieve the desired product, as can be seen in **Scheme 5-5**.
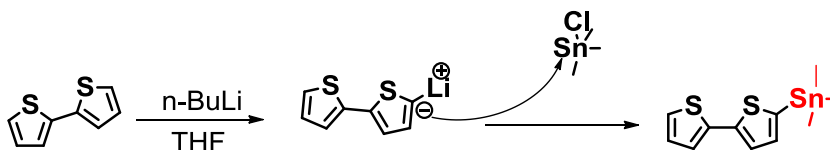
Scheme 5-5. The proposed scheme for producing (**26**)

Production of the desired monomer was confirmed using many analytical techniques. ^{1}H NMR confirmed the structure by giving four different environments in the aromatic region: a doublet at 7.32 ppm, a multiplet between 7.23 and 7.19 ppm, a doublet at 7.11 ppm and another doublet at 7.01 ppm. The molecular weight was confirmed by mass spectrometry, which gave an integer mass peak at 329 (M^{+}). The FT-IR showed the stretching vibration peak at 816 cm^{-1} for the C–S bond and a peak at 533 cm^{-1} assigned to the C–Sn bond. The elemental analysis was also in agreement with the proposed structure of the desired product.

The synthesis of 4,7-di(2,2′-bithiophen-5-yl)-5,6-bis(octyloxy)benzo[c][1,2,5] thiadiazole (**27**) followed the modified method of Iraqi and co-workers.[136] In this reaction a Stille coupling reaction was conducted between 5-trimethylstannyl-2,2-bithiophene (**26**) and 4,7-dibromo-5,6-bis(octyloxy)benzo[c][1,2,5]thiadiazole (**25**) under an inert gas for 72 h. The palladium acetate [Pd(OAc)$_2$] catalyst was used with co-catalyst tri-o-tolylphosphine [P(o-tol)$_3$] to form a carbon–carbon bond and eliminate trimethyltin bromide in the form of a salt. Purification of the target product was performed using column chromatography eluting with hexane and chloroform as a gradient (5:1; v/v). Recrystallisation was also used to remove any remaining impurities, resulting in an orange solid crystal being obtained with 84% yield.

For characterisation of the pure product, many analytical techniques were used. ^{1}H NMR spectra showed doublets at 8.52, 7.32, 7.29 and 7.09 ppm assigned to the protons of the thiophene rings. Also, there was a triplet at 4.19 ppm corresponding to the protons on the carbon next to the oxygen in the aliphatic alkyl chain. Mass spectrometry was also used to assess the purity of the product, which gave a main peak at 721 (M^{+}). Elemental analyses were in agreement with the proposed structure. The melting point of the product was between 89 and 91 °C, which confirmed the purity of the product.

The synthesis of 4,7-bis(5′-bromo-2,2′-bithiophen-5-yl)-5,6-bis(octyloxy)benzo[c][1,2,5]thiadiazole (**28**) was performed using a modified method of Iraqi and co-workers.[136] In this reaction, NBS with dried chloroform under an inert gas were left to stir for 48 hours. The target monomer was obtained after purification using column chromatography eluted

with hexane and toluene (8:2; v/v) to give the desired product as a dark red crystal with 82% yield.

The mechanism of this reaction involved electrophilic substitution at position 5 on the thiophene rings. The reaction is very sensitive to light, therefore it was performed in the dark. The amount of NBS added to the reaction was crucial at 1 to 2 eq exactly, because any additional NBS could lead to formation of tri- and tetra-brominated products.

For characterisation of the pure product, many analytical techniques were used. ^{1}H NMR spectra showed doublets at 8.51, 7.25 and 7.04 ppm assigned to the thiophene rings protons. Also, there was a triplet at 4.17 ppm corresponding to the protons on the carbon next to the oxygen in the aliphatic alkyl chain. Mass spectrometry was also used to assess the purity of the product, which gave multiple peaks at 876, 878, 880 assigned to the bromine isotopes. Elemental analyses were in agreement with the proposed structure. The melting point of the product was between 92 and 94 °C, which confirmed the purity of the product.

The synthesis of 5,6-bis(octyloxy)-4,7-bis(5′-(trimethylstannyl)-[2,2′-bithiophen]-5-yl)benzo[c][1,2,5] thiadiazole (**29**) was done according to a modified procedure by Jin et al.[100] This reaction was performed under an inert gas overnight, which involved using n-butyllithium as a strong base and a very low temperature of –78 °C. Trimethyltin chloride was added dropwise to functionalise position 5 of the thiophene rings on both sides with the trimethylstannyl group. The target monomer was washed with ethanol passed over a basic alumina to remove any traces of acidity, and the product was dried under high vacuum due to the low stability of the trimethylstannyl groups. The product was used directly without further purification and kept in the fridge all of the time.

For characterisation of the pure product, many analytical techniques were used. ^{1}H NMR spectra showed doublets at 8.51, 7.42, 7.31 and 7.16 ppm assigned to the protons of the thiophene rings. Also, there was a triplet at 4.17 ppm corresponding to the protons on the carbon next to the oxygen in the aliphatic alkyl chain (**Figure 5-2**). Mass spectrometry was also used to assess the purity of the product, which gave an integer mass peak at 1048.

Elemental analyses were in agreement with the proposed structure. The FT-IR spectra showed the stretching vibration peak at 538 cm^{-1} assigned to the C–Sn bond.
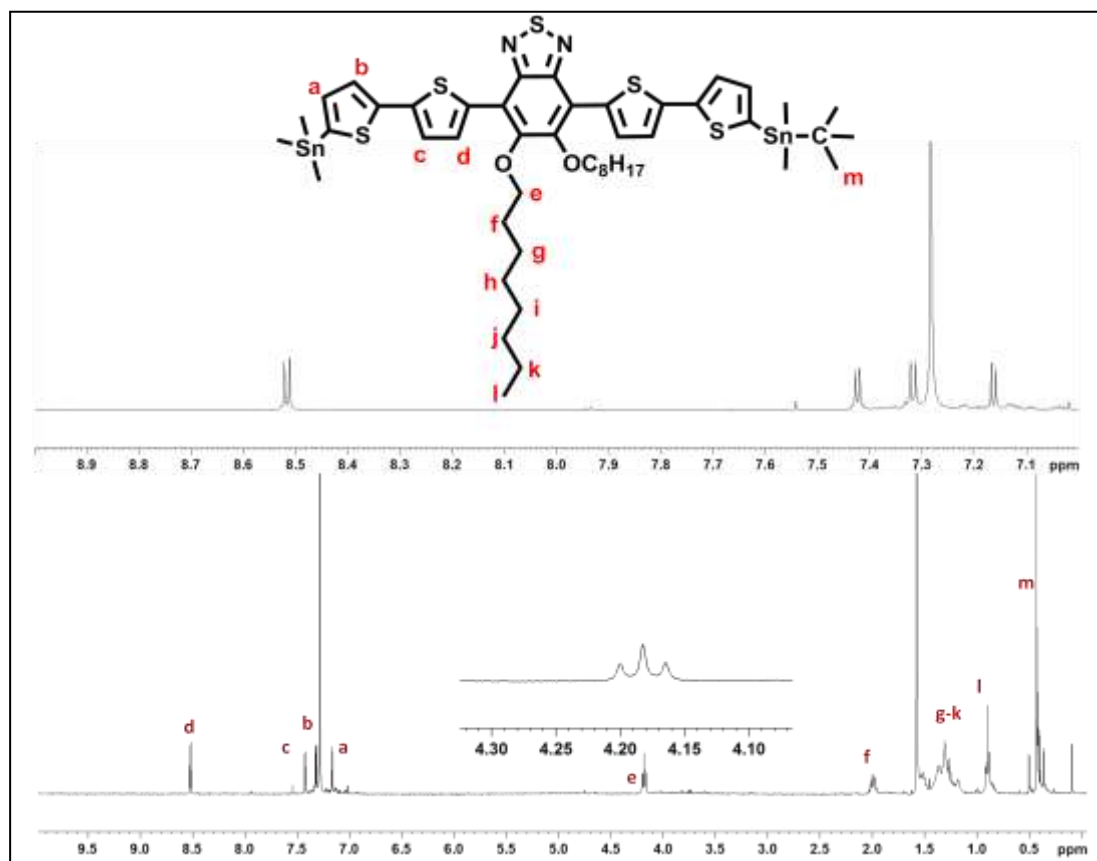
Figure 5-2 ^{1}HNMR spectra for (**29**)

5.3 Preparation and characterisation of Polymers P7-P12

A series of laterally extended two-dimensional pyrene-quinoxaline based polymers has been designed to have low band gaps that could lead to harvesting of light with a wide wavelength range of sunlight. The synthesis of polymers **P7**-**P12** involved using Stille coupling methods that can effectively form C–C bonds by having a homogeneous solution during the polymerisation. The characterisation of these polymers involved using some analytical techniques such as ^{1}H NMR, which was utilised to determine the structure of these polymers, GPC to calculate their molecular weight, elemental analysis to determine the percentage weight of each element, and thermal analysis, which was used to examine

the stability of these polymers. For the electrochemical and optical properties, cyclic voltammetry and a UV-vis spectroscopy were used respectively.

5.3.1 Synthesis of polymer P7 and P8

The synthesis of **P7** and **P8** was performed using the Stille coupling polymerisation method in toluene (**Scheme 5-6**). At the end of the polymerisation, some toluene was added to solubilise the polymers using end-capping reagents, such as bromobenzene and 2-(tributylstannyl)thiophene, added to end-cap the backbone of the polymer. The proposed mechanism for this reaction was illustrated in **Scheme 4-8**. Polymers **P7** and **P8** were both obtained as purple solids and were purified in a similar protocol to that of polymers **P1**-**P6**.
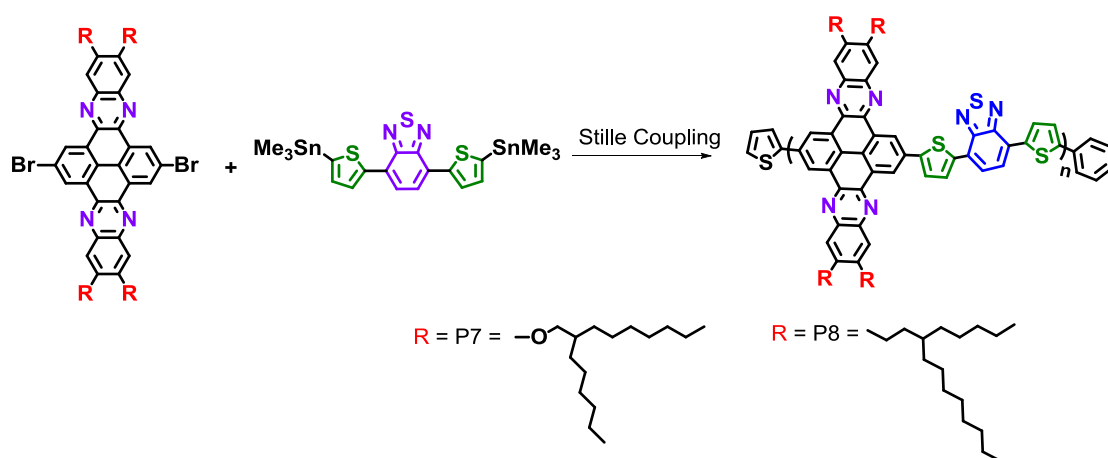
Scheme 5-6 The preparation route for polymers **P7** and **P8**

5.3.2 Characterisation of P7 and P8

5.3.2.1 GPC data analysis for P7 and P8

After Soxhlet extraction, the yield of these polymers was calculated and the GPC data were obtained in 1,2,4-trichlorobenzene at 140 °C. This was because some difficulties with the solubility of the polymers were faced when doing the analysis at lower temperature, including aggregation and precipitation of the polymers inside the column. Polystyrene was

used as a standard to calculate the molecular weight of the target polymers, **P7** and **P8**, as shown in **Table 5-1**.

Polymers	Soxhlet Fraction	Yield (%)	M_w	M_n	PDI	DP
P7	chloroform	26.6	20200	10500	1.9	7
	chlorobenzene	52.3	25500	14900	1.7	9
P8	chloroform	19.54	15520	9700	1.6	6
	chlorobenzene	60.33	23200	16500	1.4	11

Table 5-1 GPC data of **P7** and **P8**

From **Table 5-1** it can be clearly seen that polymers **P7** and **P8** were obtained in two fractions. The first fraction was extracted in chloroform and had yields of 26% and 9% for **P7** and **P8** respectively. The second fraction was extracted in chlorobenzene with yields of 52% for **P7** and 60% for **P8**. Small amounts of polymer were extracted in the chloroform fraction. However, large amounts were extracted in the chlorobenzene fraction. Furthermore, the PDI of all fractions is low, a result attributed to the fractionation process. This limits the molecular weight of soluble polymers which could explain the narrow PDI. GPC analysis showed the number average and weight average molecular weight of the chloroform fraction of **P7** to be 10500 and 20200 Da respectively. This equates to approximately 7 quinoxaline-*alt*-benzothiadiazole repeat unit per polymer chain. In contrast, the chloroform fraction of **P8** has approximately 6 repeat units of quinoxaline-*alt*-benzothiadiazole per polymer chain (Mw = 15520 Da, Mn = 9700 Da, PDI = 1.6). The chlorobenzene fraction of **P7** has around 9 quinoxaline-*alt*-benzothiadaizole units per polymer chain (Mw = 25500 Da, Mn = 14900 Da, PDI = 1.7). In contrast, GPC analysis on the the chlorobenzene fraction of **P8** has a Mn and Mw of 16500 and 23200 respectively. This equates to a degree of polymerisation of 11.

5.3.2.2 ^{1}H NMR analysis for P7 and P8

The ^{1}H NMR spectrum for **P7** in C$_2$D$_2$Cl$_4$ at 100 °C, **Figure 5-3**, showed some broad peaks in the aromatic region. However, the benzothiadiazole part has no solubilising group, which makes it difficult for the solvent to dissolve the polymer chains, even at high temperature. As a result, the aggregation phenomenon stiffens the structure of the polymer backbone and limits the movement of the polymer chains at elevated temperature. Therefore, it is not easy to identify and distinguish between the proton peaks. The peaks for the protons of the quinoxaline in positions a and b appeared as broad peaks at 9.54 and 7.31 ppm respectively. In addition, the protons on the carbons at position c of the benzothiadiazole are observed as one broad peak at 7.87 ppm. There are two protons at positions e and d corresponding to the thiophene molecule whose peaks appeared at 8.31 and 7.13 ppm respectively. Furthermore, the aliphatic region has a broad peak at 4.18 ppm due to the proton on the first carbon connected directly to the quinoxaline part of the alkyl chain (position f).
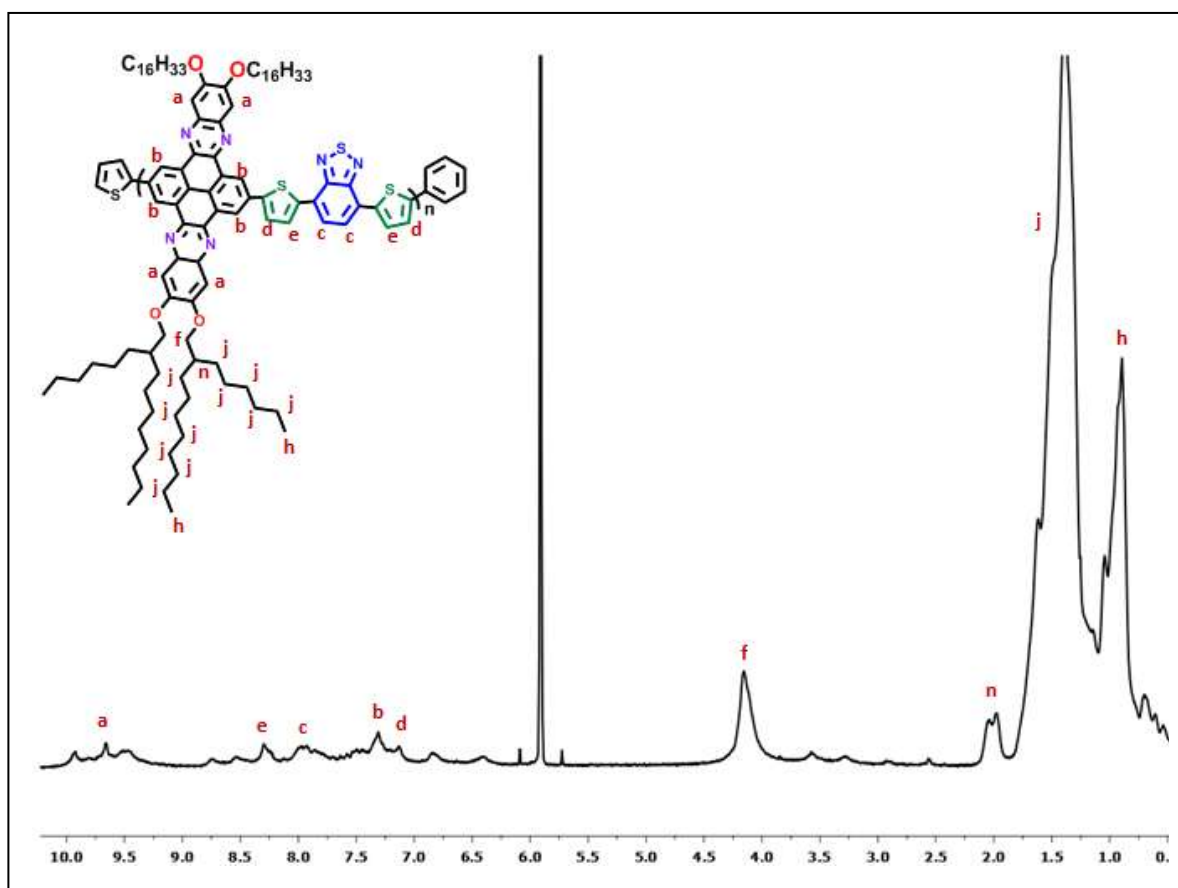
Figure 5-3. ^{1}H NMR analysis for **P7** in C$_2$D$_2$Cl$_4$ at 100 °C

The ^{1}H NMR spectrum for P8 in $C_2D_2Cl_4$ at 100 °C, **Figure 5-4**, revealed two broad peaks and also sharp peaks in the aromatic region. As discussed previously, the result of the benzothiadiazole part having no solubilising group is that aggregation makes it difficult for the solvent to dissolve the polymer chains even at high temperature. Therefore, the polymer chains have a limitation of movement even at elevated temperature. The peaks for the protons in positions a and e appeared as broad peaks at 9.30 and 7.80 ppm respectively. There is also a peak due to the proton on pyrene at position b that appeared as a sharp peak at 7.36 ppm. In addition, the protons on the carbons at position c of the benzothiadiazole appeared as one sharp singlet peak at 7.49 ppm. There is also a proton at positions d corresponding to the thiophene molecule whose peak appeared at 7.15 ppm. Furthermore, the aliphatic region has a broad peak at 2.70 ppm due to the proton on the first carbon connected directly to the quinoxaline part of the alkyl chain (position f).
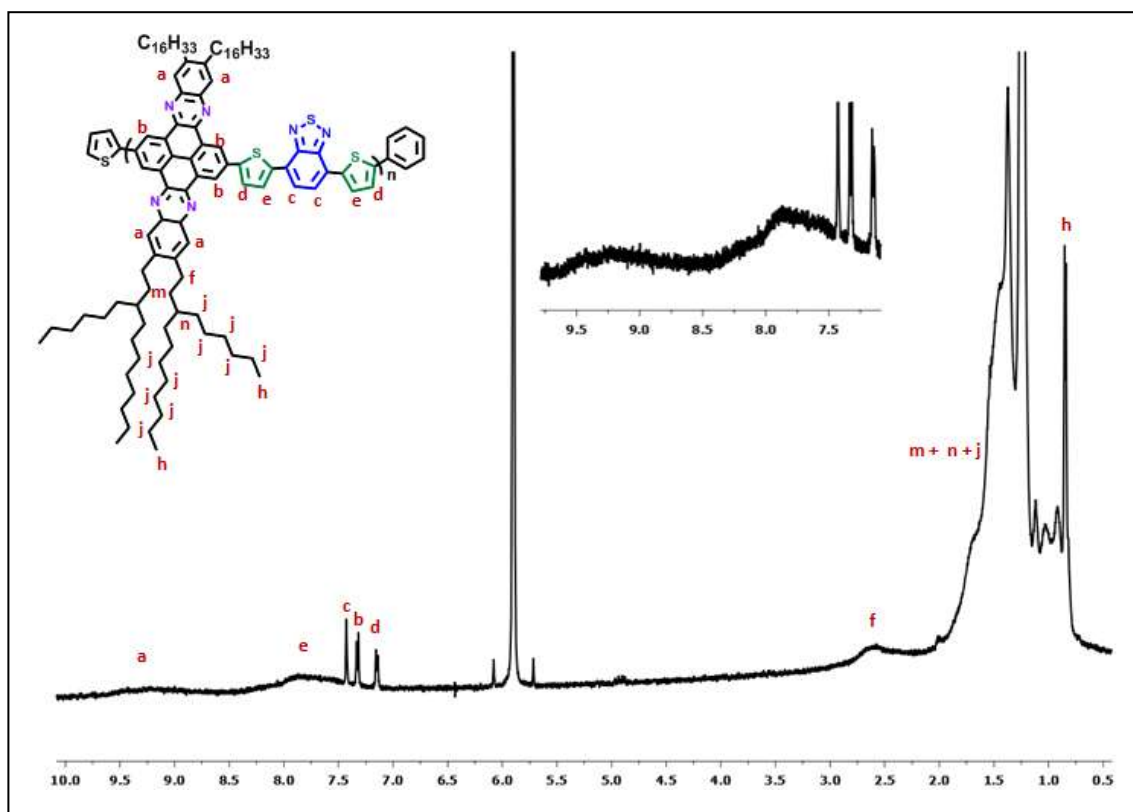
Figure 5-4. ^{1}H NMR analysis for **P8** in $C_2D_2Cl_4$ at 100 °C

5.3.2.3 Elemental analysis for P7 and P8

Elemental analysis is one of the techniques that were used to examine the target polymers, whether they are consistent with a given molecular formula and also to ensure the bromine atom is replaced with an end-capping molecule. The results shown in **Table 5-2** indicate that the elemental analysis of these polymers is in agreement with the proposed structures of **P7** and **P8** and also confirmed that they were end capped with either bromobenzene or 2-(tributylstannyl) thiophene.

Polymers	Formula		Elemental analysis				
			C	H	N	Br	S
P7	$(C_{106}H_{148}N_6O_4S_3)_n$	Calculated	76.39	8.95	5.04	0	5.77
		Found	77.10	10.03	3.97	0	4.53
P8	$(C_{106}H_{148}N_6S_3)_n$	Calculated	79.44	9.31	5.24	0	6.00
		Found	80.50	10.60	4.49	0	5.04

Table 5-2. Elemental analysis data for **P7** and **P8**

5.3.2.4 Thermal analysis of P7 and P8

To use polymers **P7** and **P8** in solar cell devices they must be thermally stable. A TGA instrument examination of the polymers can indicate whether **P7** and **P8** could be employed in these cells. As can be seen in **Figure 5-5**, the diagram confirmed the thermal stability of these polymers up to 400 °C, therefore, they can be used in solar cell applications. **P7** has the first onset of degradation at 386 °C due to degradation of the alkyl chain and the main onset of degradation at 608 °C with a weight loss of 49.38%. **P8** has the first onset of degradation at 356 °C due to degradation of the alkyl chain and the main onset of degradation at 549 °C with a weight loss of 55.36%.
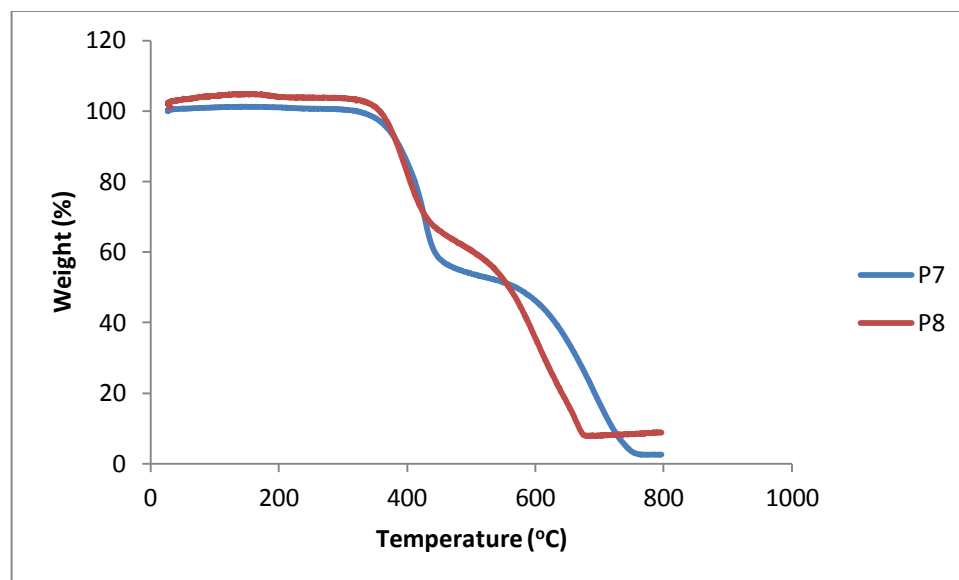
Figure 5-5. The TGA thermograms for **P7** and **P8**

5.3.3 Optical properties of P7 and P8

The UV-vis spectrum of **P7** was obtained in chloroform solution and thin films which were cast on quartz plates. **Figure 5-6** shows that polymer **P7** has two main absorption bands in chloroform solution. Previous literature has shown that the band located at the shorter wavelength (368 nm) corresponds to π–π* transition. The peak located at the longer wavelength (540 nm) corresponds to intramolecular charge transfer between donor and acceptor units along polymer chains. This band will be referred to as the λ_{max}. These bands are red-shifted to 372 and 620 nm when cast into films, which can be attributed to a more coplanar structure in solid state. These results indicate a net improvement in the light harvesting properties of this class of polymers and where the pyrene flanked by quinoxaline units is used as an electron-donor rather than an electron-acceptor in the previous polymers series (**P1-P6**).
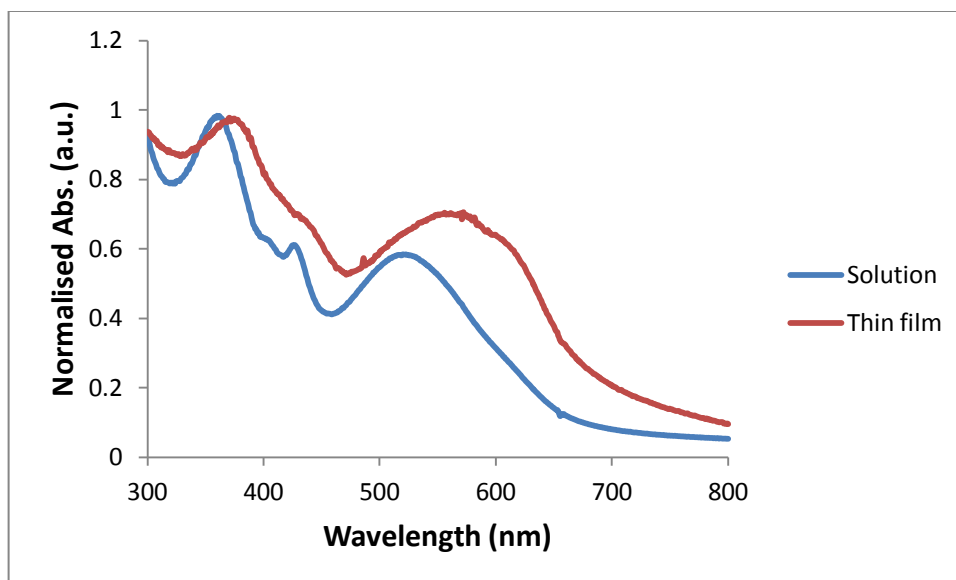
Figure 5-6. Normalised absorption spectra of **P7** as a thin film and chloroform solution

Figure 5-7 shows that polymer **P8** has two main absorption bands in chloroform solution with the band located at the shorter wavelength (360 nm) corresponding to a π–π* transition, and at the longer wavelength (520 nm), to intramolecular charge transfer between donor and acceptor units and will be referred to as the λ_{max}. These are red-shifted to 370 and 610 nm when cast into films, which can be attributed to a more coplanar structure of polymer chains in solid state.
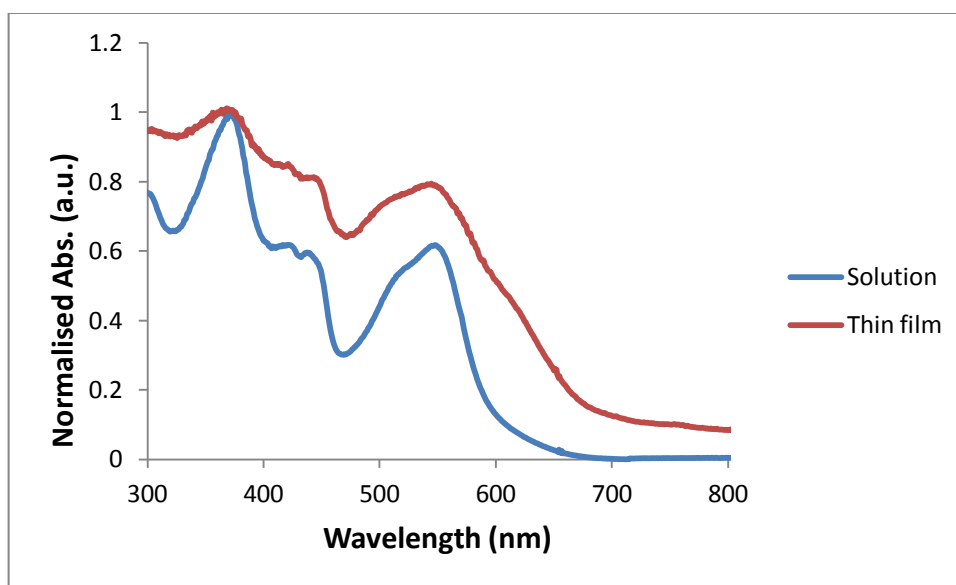
Figure 5-7. Normalised absorption spectra of **P8** as a thin film and as a solution in chloroform

The optical band gaps of **P7** and **P8** were estimated to be 1.75 and 1.84 eV (**Table 5-3**). The results suggest that D-A copolymers based on alternate benzothiadiazole pyrene-quinoxaline units are affected by the solubilising chain attached to the pyrene-quinoxaline unit. More specifically, changing the alkoxy chain in **P7** for the alkyl chain in **P8** yields an increase in the optical band gap (**Figure 5-8**). This can be explained by the fact that alkoxy groups attached to the pyrene-quinoxaline release more electron density into these units making them more electron-donating and, as a result, leading to strong ICT along polymer chains and lower band gaps.

Polymers	λ_{max} (nm) solution	λ_{max} (nm) film	λ_{onset} (nm) absorption	E_g Optical (eV)
P7	540	620	708	1.75
P8	520	610	674	1.84

Table 5-3. Summary of photophysical properties of **P7** and **P8**
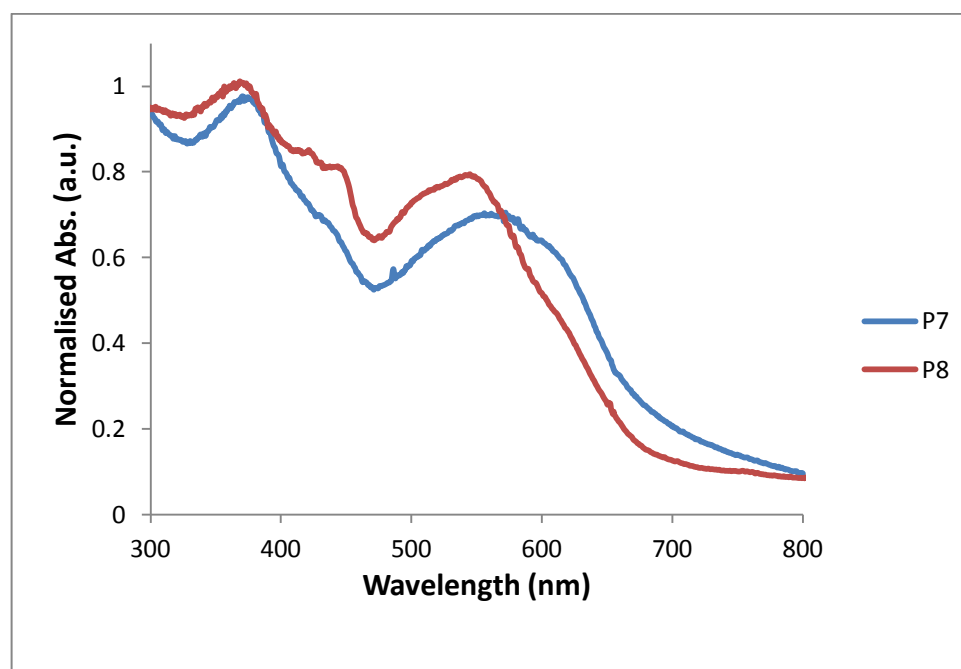
Figure 5-8. Normalised absorption spectra of **P7** and **P8** as thin films

PCDTBT is an analogous polymer to **P7** and **P8** (**Scheme 5-7**).[136] The electron donating unit in PCDTBT is carbazole whereas the electron-donating unit in **P7** and **P8** is pyrene-quinoxaline. The absorption bands for PCDTBT are located at 396 and 570 nm in film states.[136] The optical band gap of PCDTBT is estimated to be 1.88 eV, which is wider than both **P7** and **P8**. It is believed that the laterally extended conjugation of pyrene-quinoxaline allows polymers that use this unit to demonstrate lower optical band gaps relative to carbazole based polymers.

PF10TBT is an analogous polymer to **P7** and **P8** (**Scheme 5-7**).[169] The electron donating unit in PF10TBT is fluorene whereas the electron-donating unit in **P7** and **P8** is pyrene-quinoxaline. PF10TBT has a red-shifted onset of absorption (689 nm) when compared to **P7** and **P8**. Thus, PF10TBT has a lower optical band gap when compared to **P8** but higher than that of **P7**. This indicates a close similarity in the electronic properties of PF10TBT to those of **P7** and **P8**.
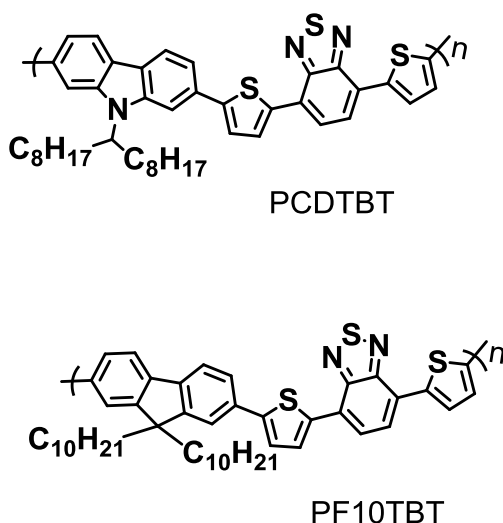
Scheme 5-7 The chemical structures of PCDTBT and PF10TBT

5.3.4 Electrochemical properties of P7 and P8

Electrochemical studies of **P7** and **P8** were performed on drop-cast films in anhydrous acetonitrile solvent with tetrabutylammonium perchlorate as the electrolyte. The HOMO

and LUMO energy levels were determined using CV (**Figure 5-9**). The electrochemical band gap for the polymer can be obtained from the cyclic voltammograms.
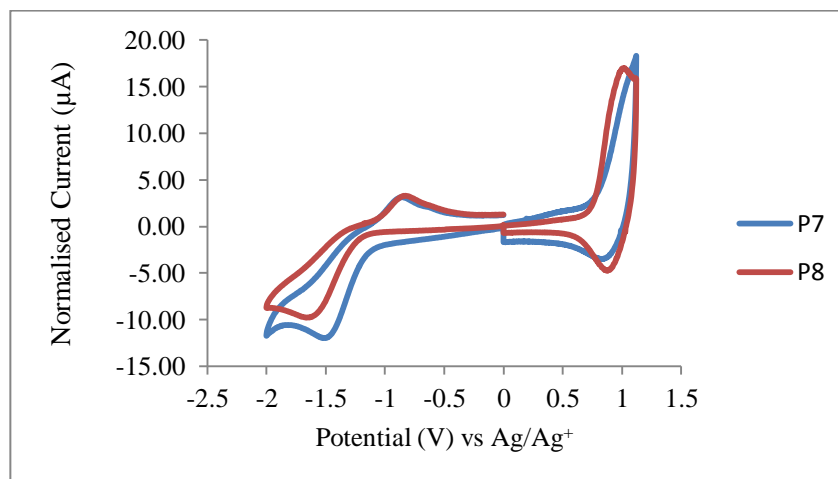
Figure 5-9. Normalised CV spectra of **P7** and **P8**

The onset oxidation potential of **P7** appeared at $E_{onset} = +0.70$ V for the oxidation and at $E_{onset} = -1.05$ V for the reduction. Therefore, the HOMO and LUMO levels of **P7** can be calculated as −5.41 eV and −3.66 eV respectively. The difference between the HOMO and LUMO is known as the electrochemical band gap. **P7** has an electrochemical band gap of 1.75 eV which is the same as the optical band gap. **P8** has an onset oxidation potential observed at $E_{onset} = +0.74$ V for the oxidation and at $E_{onset} = -1.10$ V for the reduction. Therefore, the HOMO and LUMO levels of **P8** can be estimated as −5.45 eV and −3.61 eV respectively. The electrochemical band gap for **P8** is 1.84 eV which is the same value obtained for its optical band gap.

Comparing the electrochemical properties of **P7** and **P8**, it can be clearly seen that the HOMO levels of these polymers are comparable (**P7**, −5.41 eV and **P8**, −5.45 eV). However, **P7** has a slightly lower electrochemical band gap than **P8.** This is a result of the alkoxy chains where the oxygen atoms attached to the quinoxaline groups in **P7**, push electron density towards the nitrogen atoms, thus, neutralising the accepting properties of quinoxaline group (**Figure 5-10**) making pyrene-quinoxaline a stronger donor.

The resonance direction
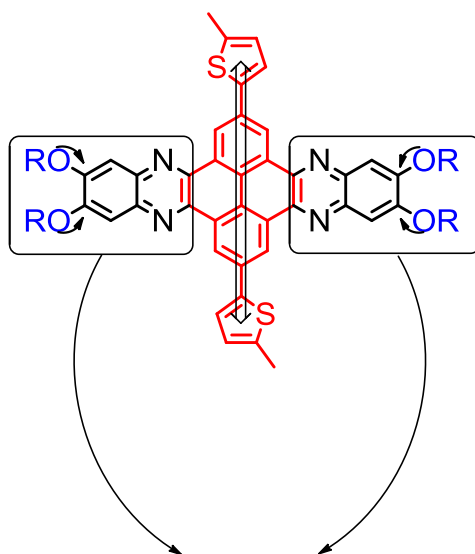
The quinoxaline groups pulling the electron density
toward them from the oxygen so they are neutralized

Figure 5-10. The neutralisation of quinoxaline groups by oxygen atoms

We compare the redox behaviour of **P7** and **P8** with analogous polymers in the literature, such as PCDTBT (**Scheme 5-7**), which has been reported by Iraqi and co-workers[136] and PF10TBT, which has been reported by Slooff and co-workers.[169] It is worth noting that PCDTBT (-5.35 eV) and PF10TBT (-5.30 eV) have shallower HOMO levels relative to **P7** (**-**5.41 eV**)** and **P8** (**-**5.45 eV**)**. This result suggests that pyrene-quinoxaline is a weaker donor relative to carbazole and fluorene. When compared with PCDTBT and PF10TBT, both **P7** and **P8** have large solubilising groups which dilute the chromophore density. This could lead to a decrease in the ICT resulting in **P7** and **P8** displaying deeper HOMO energy levels. In contrast, the LUMO levels of these polymers are comparable.

5.3.5 Preparation of polymer P9 and P10

The solubilities of **P7** and **P8** are low. The need for inserting an alkyl chain in the benzothiadiazole part is important as this could increase the solubility and hence increase the molecular weight of the polymers.

Scheme 5-8 Preparation route for **P9** and **P10**

The syntheses of **P9** and **P10**, **Scheme 5-8**, were performed using Stille coupling in toluene. At the end of the polymerisations, some toluene was added to solubilise the polymer with end-capping reagents, such as bromobenzene and 2-(tributylstannyl)thiophene, to end-cap the polymer's backbone. This step is useful because the working time of devices and the efficiency of the operation could be improved. The proposed mechanism for this reaction is illustrated in **Scheme 4-8**. Polymers **P9** and **P10** were obtained as a dark red powder and were purified in a similar protocol to that of polymers **P1** and **P6**.

5.3.6 Characterisation of P9 and P10

5.3.6.1 GPC data analysis for P9 and P10

After Soxhlet extraction, the yield of these polymers was calculated and the GPC data were obtained in TCB at 140 °C. This was because some difficulties were faced when doing the analysis at lower temperature, including aggregation and precipitation of the polymers inside the column. Polystyrene was used as a standard to calculate the molecular weight of the target polymers, **P9** and **P10** as shown in **Table 5-4**.

Polymers	Soxhlet Fraction	Yield (%)	M_w	M_n	PDI	DP
P9	toluene	21	13200	10100	1.3	5
P10	toluene	15	16300	13300	1.2	7

Table 5-4. GPC data of **P9** and **P10**

From **Table 5-4** it can be clearly seen that polymers **P9** and **P10** were obtained in low yields 21% and 15% respectively. The low yield of these two polymers **P9** and **P10** could be attributed to the purity of the 5,6-bis(octyloxy)-4,7-bis(5-(trimethylstannyl)thiophen-2-yl)benzo[c][1,2,5]thiadiazole (**31**) as it was used without purification. GPC estimated the Mw and Mn of **P9** to be 13200 and 10100 Da respectively, with a polydispersity of 1.3. For polymer **P9** there are around 5 units of quinoxaline and octyloxybenzothiadiazole units per polymer chain Finally, polymer **P10** has approximately 7 quinoxaline units and octyloxybenzothiadiazole units per polymer chain with molecular weight Mw and Mn of 16300 and 13300 Da respectively. This gives a wider PDI of 1.2. The low PDI of **P9** and **P10** could be attributed to the polymerisation method used. These polymers used a Stille coupling procedure. The Stille coupling method uses a homogeneous solvent system that allows the polymer to remain in solution for longer.

5.3.6.2 ^{1}H NMR analysis for P9 and P10

The ^{1}H NMR spectrum for **P9** in $C_2D_2Cl_4$ at 100 °C is shown in **Figure 5-11**. Some solubilising groups were introduced into the benzothiadiazole part, improving the characterisation of this type of polymer. Some peaks could be identified and distinguished more easily than for polymers **P7** and **P8**. The peak for the proton of the quinoxaline in position a appeared as a broad signal at 9.98 ppm. In addition, the protons on the carbons at position b of the pyrene appeared as a broad signal at 7.87 ppm. The protons on the carbons at position c of the thiophene were observed at 7.21 ppm. There is also a proton at position d due to the thiophene molecule whose peak appeared at 8.58 ppm. It is believed that the proton in position d experiences a strong electron-withdrawing effect of the benzothiadiazole, therefore this proton is deshielded further to 8.58 ppm. Furthermore, the aliphatic region has a broad peak at 4.31 ppm due to the proton on the first carbon connected directly to the quinoxaline part of the alkyl chain (position f). In addition, a broad peak appeared at 4.22 ppm due to the proton in position e, which is the first carbon next to the oxygen of the alkyl chain of benzothiadiazole.
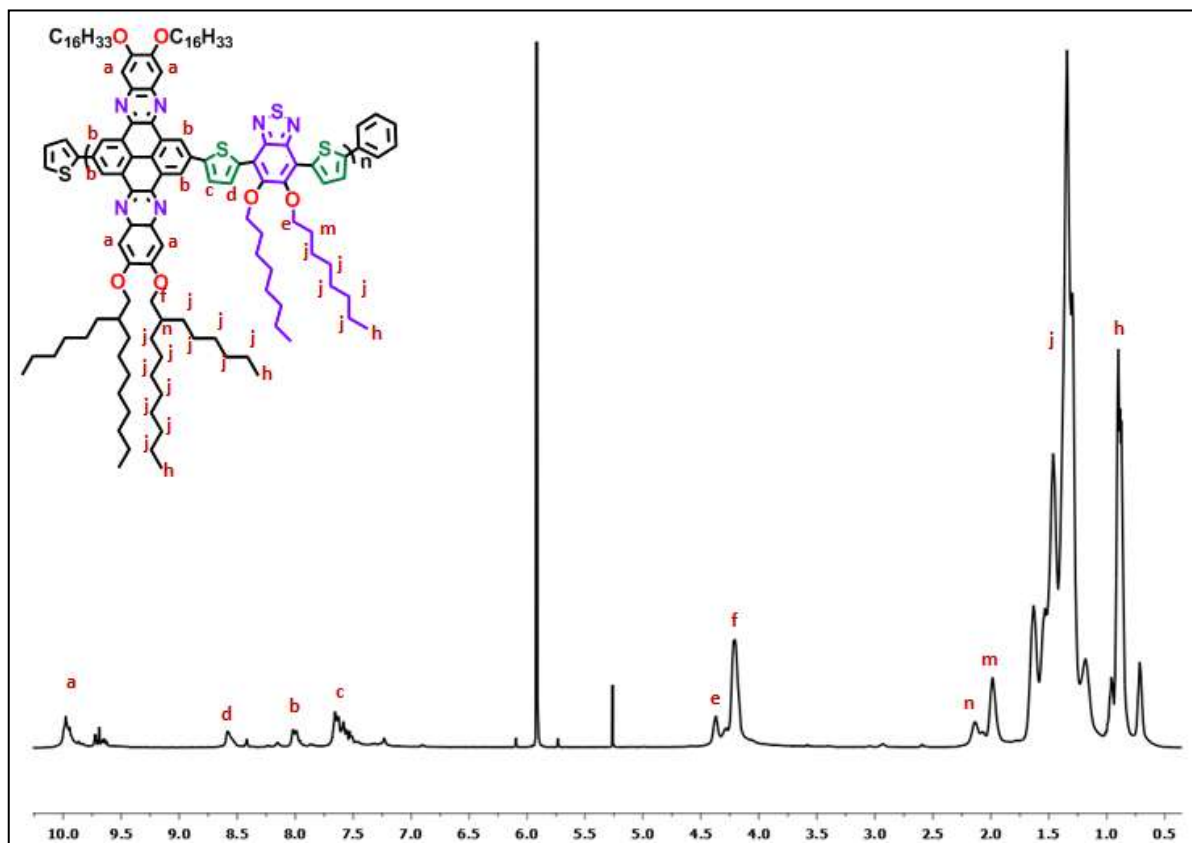
Figure 5-11. ^{1}H NMR spectra for **P9** in $C_2D_2Cl_4$ at 100 °C

The ^{1}H NMR spectrum for **P10** in $C_2D_2Cl_4$ at 100 °C, **Figure 5-12**, showed some improvement in the sharpness of the peaks, especially after adding some solubilising groups to the benzothiadiazole part. This addition decreases the aggregation and hence increases the solubility of this type of polymer. There are also some peaks that could be identified and distinguished more easily than for polymers **P7** and **P8**. The peak for the proton of the quinoxaline in position a appeared as a sharp singlet peak at 9.95 ppm and another proton in position b appeared at 7.51 ppm as a sharp singlet peak. In addition, the protons on the carbons at position c of the thiophene were observed as a doublet at 7.21 ppm. There is also a proton at position d due to the thiophene molecule, whose peak appeared at 8.58 ppm. It is believed that the proton in position d experiences the strong pulling properties of benzothiadiazole, therefore this proton is deshielded further to 8.58 ppm. Furthermore, the aliphatic region has a broad peak at 2.82 ppm due to the proton on

the first carbon connected directly to the quinoxaline part of the alkyl chain (position f). In addition, a broad peak appeared at 4.22 ppm due to the proton in position e, which is the first carbon next to the oxygen of the alkyl chain of benzothiadiazole.
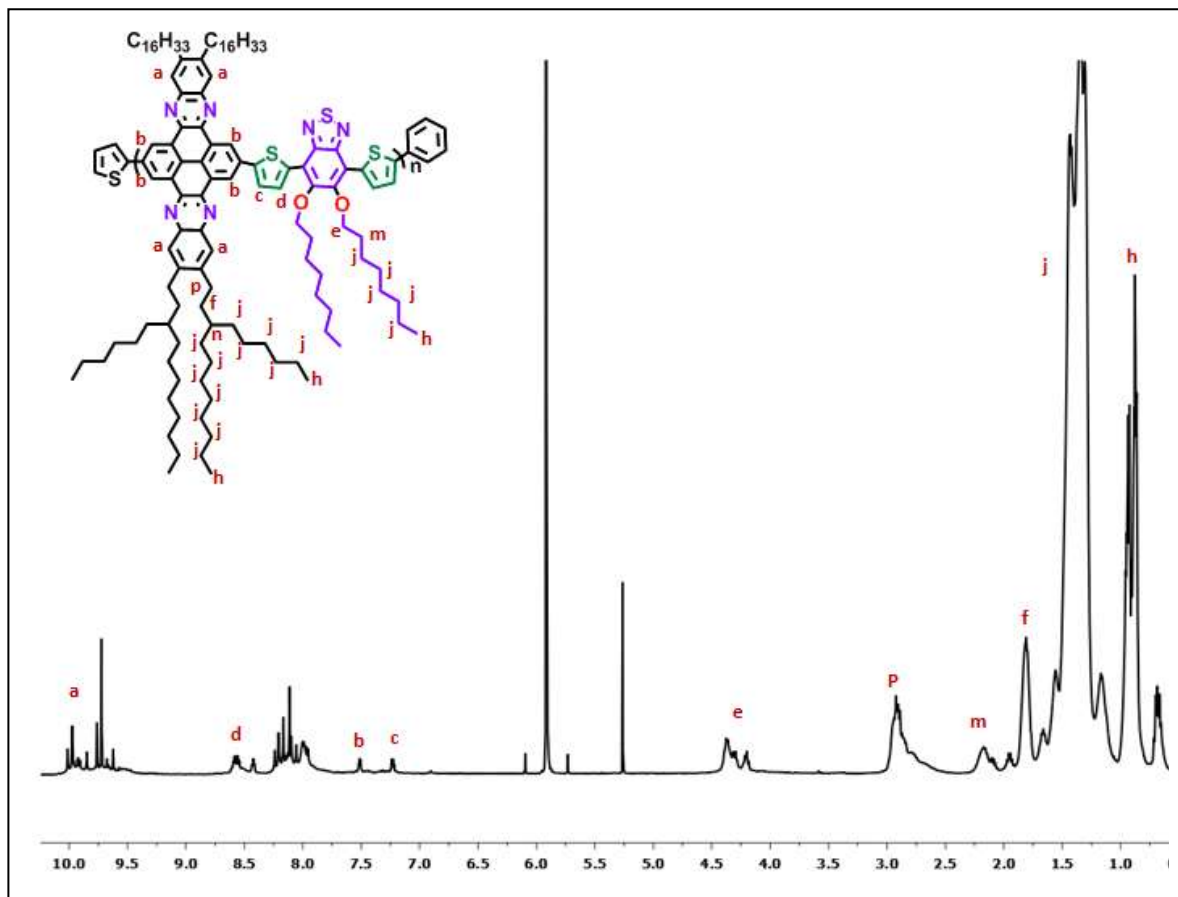
Figure 5-12. ^{1}H NMR spectra for **P10** in $C_2D_2Cl_4$ at 100 °C

5.3.6.3 Elemental analysis for P9 and P10

Elemental analysis is one of the techniques that were used to examine the target polymers, whether they are consistent with a given molecular formula and also to ensure the bromine atom is replaced with an end-capping molecule. The results shown in **Table 5-2** indicate that the elemental analysis of these polymers is in agreement with the proposed structures of **P9** and **P10**, and also confirmed that they were end-capped with either bromobenzene or 2-(tributylstannyl)thiophene.

Polymers	Formula	Elemental analysis					
			C	H	N	Br	S
P9	$(C_{122}H_{180}N_6O_6S_3)$ n	Calculated	76.20	9.43	4.37	0	5.00
		Found	74.18	9.03	4.29	0	4.38
P10	$(C_{122}H_{180}N_6O_2S_3)$ n	Calculated	78.82	9.76	4.52	0	5.17
		Found	74.02	9.13	3.88	0	4.23

Table 5-5. Elemental analysis data for **P9** and **P10**

5.3.6.4 Thermal analysis of P9 and P10

To use polymers **P9** and **P10** in solar cell devices they should be thermally stable. Using a TGA instrument the examination of the polymers can indicate whether **P9** and **P10** could be employed in these cells. As can be seen in **Figure 5-5**, the diagram confirmed the thermal stability of these polymers up to 400 °C, therefore, they can be used in solar cell applications. **P9** has the first onset of degradation at 323 °C due to degradation of the alkyl chain and the main onset of degradation at 551 °C with a weight loss of 50.29%. **P10** has the first onset of degradation at 311 °C due to degradation of the alkyl chain and the main onset of degradation at 540 °C with a weight loss of 54.26%.
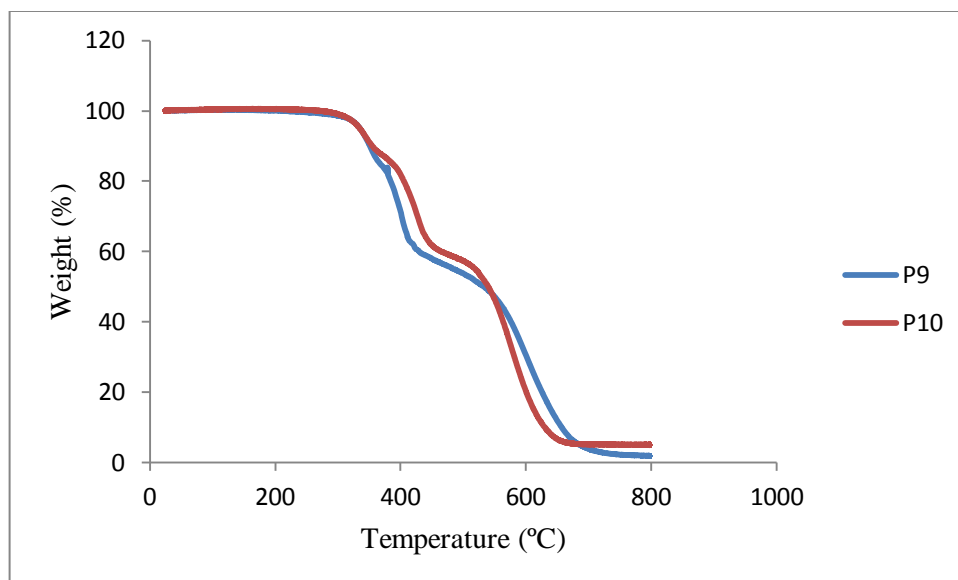
Figure 5-13. The TGA thermograms for **P9** and **P10**

5.3.7 Optical properties of P9 and P10

The UV-vis spectrum of **P9** was obtained in chloroform solution and thin films which were cast on quartz plates. **Figure 5-14** shows that polymer **P9** has two main absorption bands in chloroform solution. Previous literature has shown that the band located at the shorter wavelength (364 nm) corresponds to a π–π^* transition. The peak located at the longer wavelength (504 nm) corresponds to intramolecular charge transfer between donor and acceptor units and will be classified as the λ_{max}. These are red-shifted to 366 and 520 nm when cast into films, which can be attributed to a more coplanar structure in solid state.
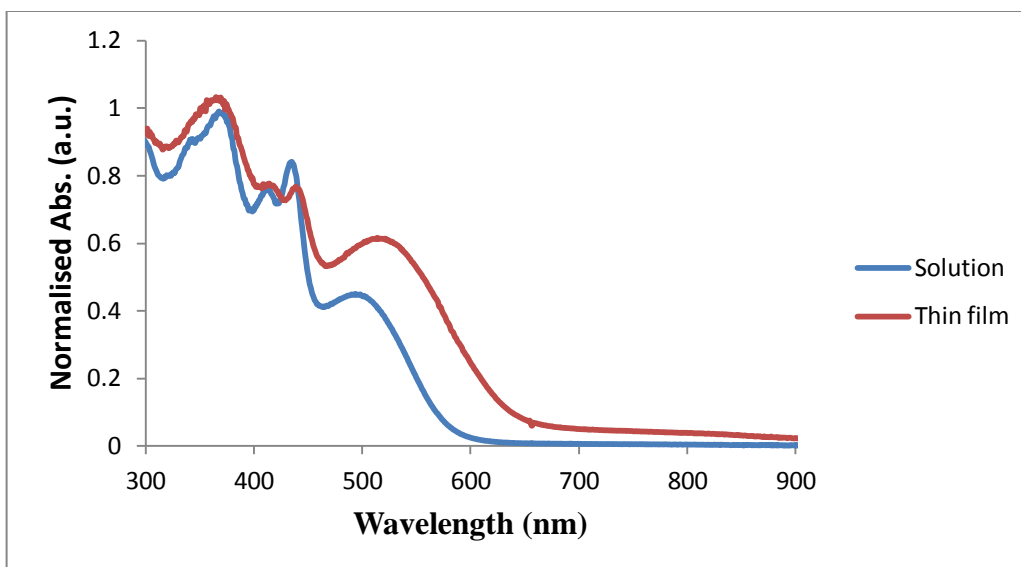
Figure 5-14. Normalised absorption spectra of **P9** as a thin film and chloroform solution

Figure 5-15 shows that polymer **P10** has two main absorption bands in chloroform solution. Previous literature has shown that the band located at the shorter wavelength (360 nm) corresponds to π–π* transition. The peak located at the longer wavelength (500 nm) corresponds to intramolecular charge transfer between donor and acceptor units.
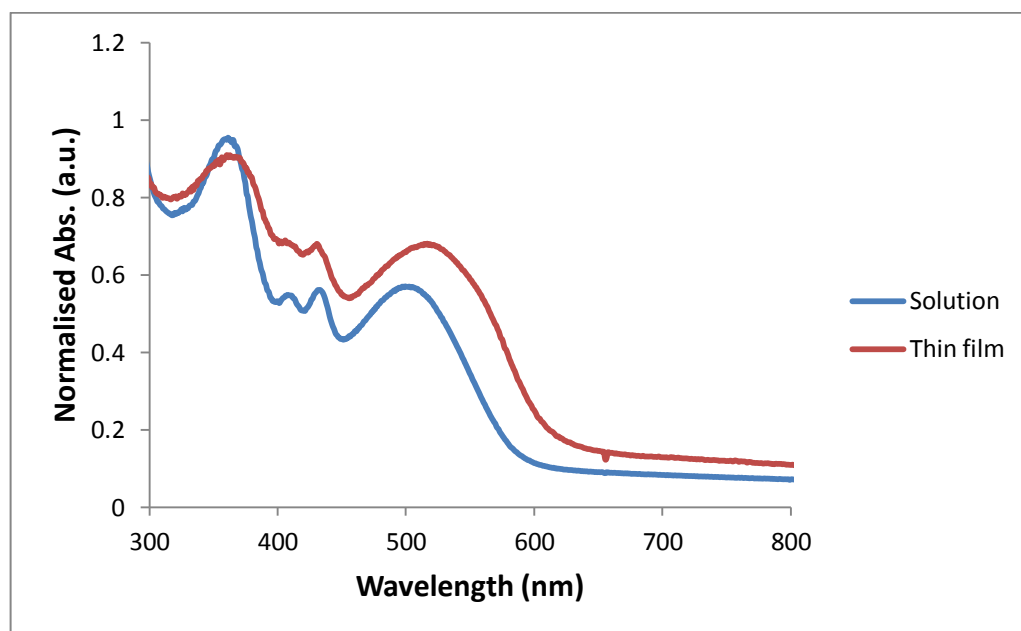
Figure 5-15. Normalised absorption spectra of **P10** as a thin film and as a solution in chloroform

These λ_{max} values are red-shifted to 364 and 517 nm when cast into films, which can be attributed to a more coplanar structure in solid state. The optical band gaps of **P9** and **P10** were estimated to be 1.95 and 2.01 eV (**Table 5-9**). The results suggest that D-A copolymers based on alternate benzothiadiazole pyrene-quinoxaline units are affected by the solubilising chain attached to the pyrene-quinoxaline unit. More specifically, changing the alkoxy chain in **P9** for the alkyl chain in **P10** yields a small increase in the optical band gap, **Figure 5-16** in a similar fashion to the observation for polymers **P**7 and **P8**.

Polymers	λ_{max} (nm) solution	λ_{max} (nm) film	λ_{onset} (nm) absorption	E_g Optical (eV)
P9	504	520	633	1.95
P10	500	517	614	2.01

Table 5-6. Summary of the photophysical properties of **P9** and **P10**

The optical band gaps of **P9** and **P10** were estimated to be 1.95 and 2.01 eV respectively. These are larger than the optical band gaps of **P7** and **P8**, which is due to the introduction of solubilising octyloxy chains at the 5,6-positions of the benzothiadiazole unit. These are electron donating units, which increase the electron density of the benzothiadiazole acceptor. Consequently, the polymer exhibits less D-A character resulting in larger optical band gaps. Furthermore, the optical band gap of **P10** was wider than **P9**; a consequence of substituting the alkoxy chains on pyrene-quinoxaline in **P9** for alkyl chains in **P10**. Alkoxy substituents are more electron-donating than their alkyl counterparts. The alkoxy substituent will push electron density onto the quinoxaline-unit, negating the withdrawing effect of the nitrogen atoms, making alkoxy functionalised pyrene-quinoxaline a more efficient electron donor than alkyl functionalised pyrene-quinoxaline.
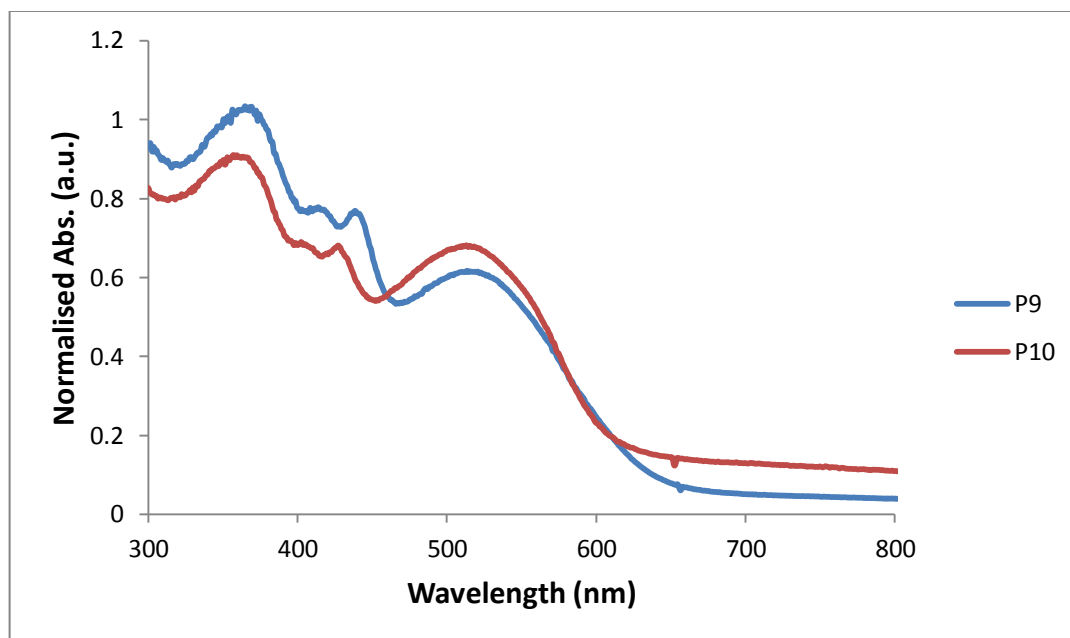
Figure 5-16. Normalised absorption spectra of **P9** and **P10** as thin films

PCDTOBT is an analogous polymer to **P9** and **P10** (**Scheme 5-9**). The electron donating unit in PCDTOBT is carbazole whereas the electron-donating unit in **P9** and **P10** is pyrene-quinoxaline. PCDTOBT has a red-shifted λ_{max} (536 nm) when compared to **P9** (520 nm) and **P10** (517 nm). This could be attributed to the higher molecular weight of PCDTOBT relative to **P9** and **P10**. PCDTOBT has a molecular weight of 15,000 Da.[153] **P9** and **P10** have molecular weights of 10,000 and 13,000 Da respectively. It is possible that the improved optical properties of PCDTOBT are a result of its higher molecular weight. A higher molecular weight will extended the conjugation along the polymer backbone, resulting in a more planar and rigid structure.[110]
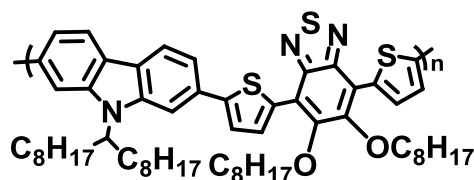
PCDTOBT

Scheme 5-9 The chemical structure of PCDTOBT

5.3.8 Electrochemical properties of P9 and P10

Electrochemical studies of **P9** and **P10** were performed on drop-cast films in anhydrous acetonitrile as a solvent with tetrabutylammonium perchlorate as the electrolyte. In this investigation, the HOMO and LUMO energy levels were determined using CV. The electrochemical band gaps of the polymers were obtained from the onsets of their oxidation and reduction (**Figure 5-17**).
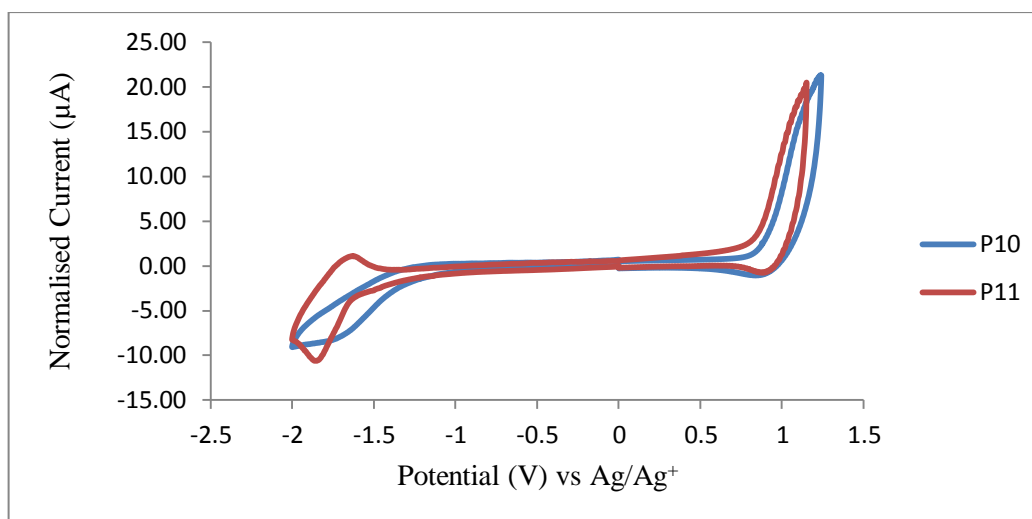
Figure 5-17. Normalised CV spectra of **P10** and **P11**

The onset oxidation potential of **P9** appeared at $E_{onset} = +0.90$ V. The onset reduction potential of **P9** occurred at $E_{onset} = -1.13$ V. Using this, the HOMO and LUMO levels of **P9** can be calculated as -5.61 eV and -3.58 eV respectively. The differences between the HOMO and LUMO levels can be used to calculate the electrochemical band gap for **P9**, which is 2.03 eV. **P10** has an oxidation onset potential observed at $E_{onset} = +0.88$ V. The onset reduction potential of **P10** appeared at $E_{onset} = -1.21$ V. Using these values, the HOMO and LUMO levels of **P10** can be estimated as -5.59 eV and -3.47 eV respectively. The electrochemical band gap for **P10** is 2.09 eV.

Comparing the electrochemical band gap values of **P9** and **P10**, it can be seen clearly that **P9** has a lower electrochemical band gap than **P10**. This could be attributed to the oxygen atoms attached directly to the quinoxaline groups in **P9**, which push the electron density

towards the nitrogen atom and hence decrease the accepting properties of the nitrogen atoms located on the quinoxaline. This may limit the withdrawing effect of the quinoxaline groups, as can be seen in **Figure 5-10**. It is interesting to compare **P9** and **P10** with analogous polymers from the literature, such as PCDTOBT which has been reported by Iraqi and co-workers. Although the HOMO levels of **P9** and **P10** are comparable (–5.61 eV *vs.*–5.59 eV) the HOMO level of PCDTOBT is shallower (–5.20 eV). This could be attributed to the strong donor properties of carbazole. Additionally, carbazole only has one solubilising chain whereas the pyrene-quinoxaline system used in **P9** and **P10** has multiple chains. It is possible that the additional solubilising chains present in pyrene-quinoxaline dilute the chromophore density, which reduces the ICT along the polymer backbone.

5.3.9 Preparation of polymer P11 and P12

Although the solubilities of **P9** and **P10** are quite high, they did not show improvement of absorbing a wide portion of sun light; therefore, inserting two additional thiophene units in the backbone of the polymer is important as this could increase the conjugation along the polymer chains and hence increase the absorption spectrum of these polymers and lower their band gaps.

Scheme 5-10 The preparation route for **P11** and **P12**

The synthesis of **P11** and **P12**, **Scheme 5-10**, was performed using Stille coupling in toluene. At the end of the polymerisations, toluene was added to solubilise the polymer

with end-capping reagents, such as bromobenzene and 2-(tributylstannyl)thiophene which were added to end-cap the polymer's backbone. This step is useful because the working time of devices and the efficiency of the operation could be improved. The proposed mechanism for this reaction is illustrated in **Scheme 4-8**. Polymers **P11** and **P12** were obtained as purple powders and were purified in a similar protocol to that of polymers **P1** and **P6**.

5.3.10 Characterisation of P11 and P12

5.3.10.1 GPC data analysis for P11 and P12

After Soxhlet extraction, the yield of these polymers was calculated and the GPC data were obtained in TCB at 140 °C. This was because some difficulties were faced when doing the analysis at lower temperature, including aggregation and precipitation of the polymers inside the column. Polystyrene was used as a standard to calculate the molecular weight of the target polymers, **P11** and **P12**, as shown in **Table 5-7**.

Polymers	Soxhlet Fraction	Yield (%)	M_w	M_n	PDI	DP
P11	chloroform	67	16000	11000	1.4	6
P12	chloroform	70	14000	10000	1.4	5

Table 5-7 GPC data of **P11** and **P12**

From **Table 5-7** it can be clearly seen that polymers **P11** and **P12** were obtained in good yields, 67% and 70% respectively. This could be attributed to the additional thiophene spacer. This increases the distance between the alkyl chains on the donor and acceptor units, which reduces the steric hindrance and leads to a greater degree of polymerisation. GPC estimated the Mw and Mn of **P11** to be 16000 and 11000 Da respectively, with a polydispersity of 1.4. For polymer **P11** there are around 6 units of quinoxaline and octyloxybenzothiadiazole units per polymer chain. Finally, polymer **P12** has approximately 5 quinoxaline unit and octyloxybenzothiadiazole units per polymer chain with molecular weight Mw and Mn of 14000 and 10000 Da respectively. This gives a low PDI of 1.4. The

low PDI of **P3**, **P6**, **P7**, **P8**, **P9**, **P10**, **P11** and **P12** could be attributed to the polymerisation method used. These polymers used a Stille coupling procedure. **P1**, **P2**, **P4** and **P5** used a biphasic Suzuki coupling. It is assumed that the use of water in Suzuki coupling promotes early precipitation of the polymer leading to a range of molecular weights. The Stille coupling method uses a homogeneous solvent system that allows the polymer to remain in solution for longer.

5.3.10.2 ^{1}H NMR analysis for P11 and P12

The ^{1}H NMR spectra for **P11** in $C_2D_2Cl_4$ at 100 °C, **Figure 5-18**, showed some identified and distinguished peaks in the aromatic region. The peak for the proton of quinoxaline in position a appeared as a broad signal at 9.90 ppm and also another broad peak in position b was observed at 7.49 ppm. In addition, the protons on the carbons at positions c, d and e of thiophene were observed at 7.25, 7.55 and 7.71 ppm respectively. There is also a proton at position f due to the thiophene molecule whose peak appeared at 8.45 ppm. It is believed that the proton in position f experiences the strong pulling effect of benzothiadiazole; therefore, this proton was deshielded further to 8.45 ppm. Furthermore, the aliphatic region has an overlapped broad peak between 4.16 and 4.31 ppm due to the proton on the first carbon connected directly to the quinoxaline part of the alkyl chain (position g), and also the proton on the carbon next to the oxygen in position h.
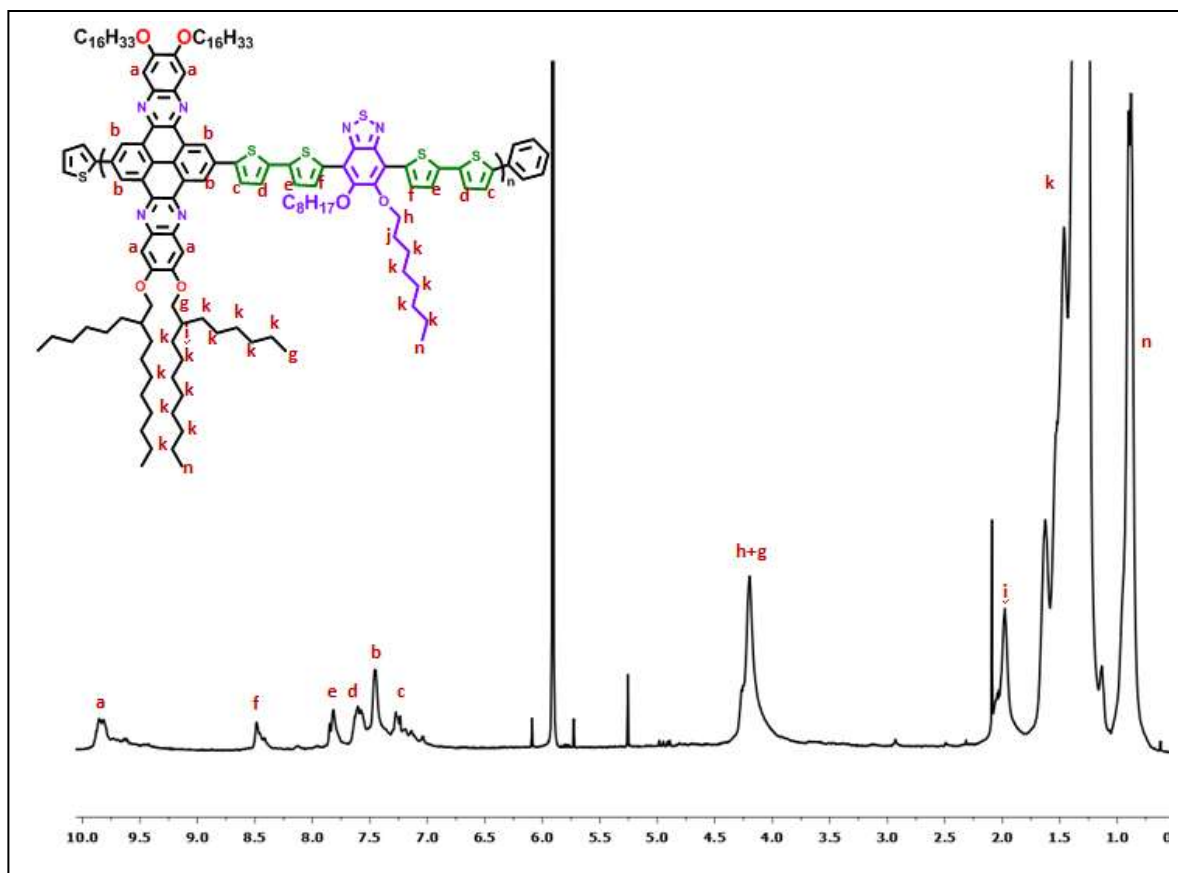
Figure 5-18. ^{1}H NMR spectra for **P11** in $C_2D_2Cl_4$ at 100 °C

The ^{1}H NMR spectrum for **P12** in $C_2D_2Cl_4$ at 100 °C, **Figure 5-19**, revealed some identified and distinguished peaks in the aromatic region. The peak for the proton of quinoxaline in position a appeared as a broad peak at 9.88 ppm and also another broad peak in position b was observed at 7.75 ppm. In addition, the protons on the carbons at positions c and d of thiophene overlapped to give a broad peak between at 7.25 ppm. Moreover, the protons at position e of the thiophene were observed as a doublet at 7.89 ppm. There is also a proton at positions f due to the thiophene molecule whose peak appeared at 8.40 ppm. It is believed that the proton in position f experiences a strong pulling effect of the benzothiadiazole, therefore this proton was deshielded further to 8.40 ppm. In addition, a broad peak appeared at 4.21 ppm due to the proton in position h, which is the first carbon next to the oxygen of the alkyl chain of benzothiadiazole. Furthermore, the aliphatic region has an overlapped broad peak between 2.93 and 2.16 ppm due to the proton on the first

carbon connected directly to the quinoxaline part of the alkyl chain (position m), and also the proton on the second carbon next to the oxygen in position j.
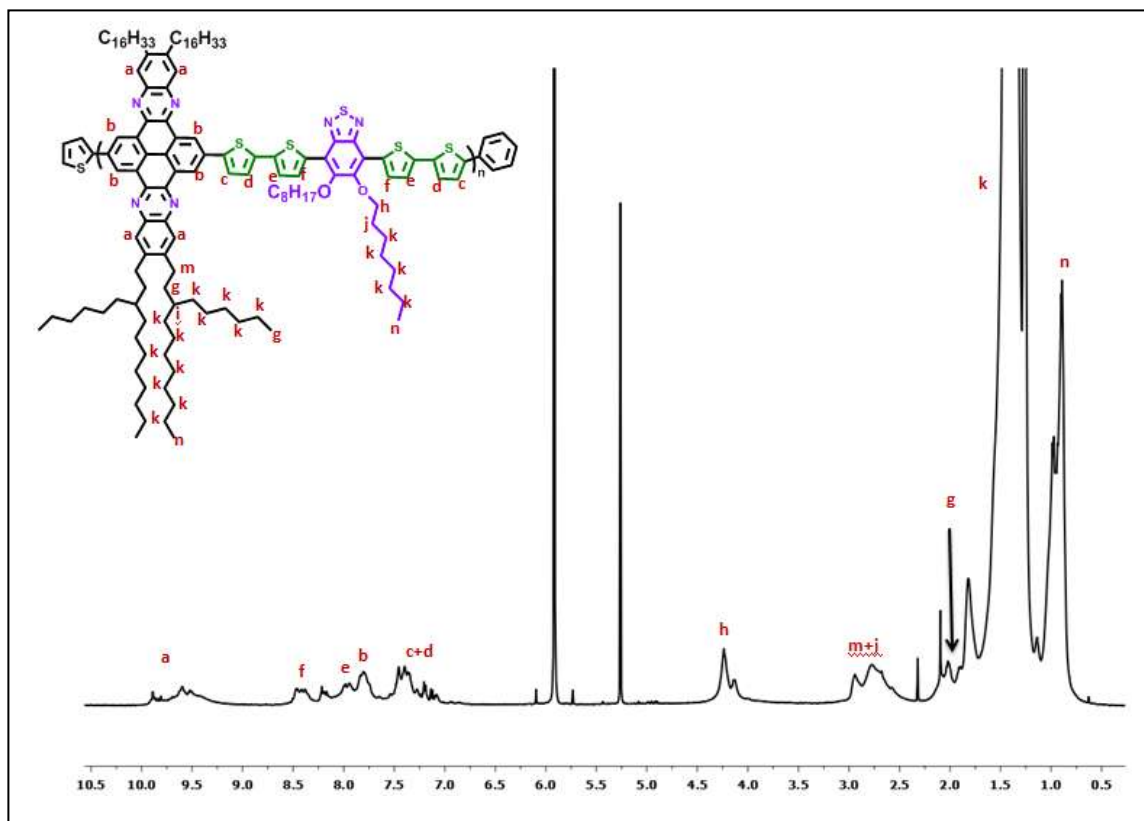
Figure 5-19. ^{1}H NMR spectra for P12 in $C_2D_2Cl_4$ at 100 °C

5.3.10.3   Elemental analysis for P11 and P12

Elemental analysis is one of the techniques that were used to examine the target polymers, whether they are consistent with a given molecular formula and also to ensure the bromine atom is replaced with an end-capping molecule. The results shown in **Table 5-2** indicate that the elemental analysis of these polymers is in agreement with the proposed structures of **P11** and **P12**, and also confirmed that they were end capped with either bromobenzene or 2-(tributylstannyl)thiophene.

Polymers	Formula		Elemental analysis				
			C	H	N	Br	S
P11	$(C_{130}H_{184}N_6O_6S_5)_n$	Calculated	74.81	8.89	4.03	0	7.68
		Found	76.69	10.15	3.21	0	5.90
P12	$(C_{130}H_{184}N_6O_2S_5)_n$	Calculated	77.17	9.17	4.15	0	7.92
		Found	79.17	10.47	3.19	0	6.94

Table 5-8. Elemental analysis data for **P11** and **P12**

5.3.10.4 Thermal analysis of P11 and P12

To use polymers **P11** and **P12** in solar cell devices, they should be thermally stable. Using a TGA instrument can indicate if **P11** and **P12** could be employed in these cells. As can be seen in **Figure 5-20**, the diagram confirmed the thermal stability of these polymers up to 400 °C, therefore, they can be used in solar cell applications. **P11** has a first onset of degradation at 351 °C due to degradation of the alkyl chain and the main onset of degradation at 553 °C with a weight loss of 40.98%. **P12** has the first onset of degradation at 381 °C due to degradation of the alkyl chain and the main onset of degradation at 559 °C with a weight loss of 62.26%.
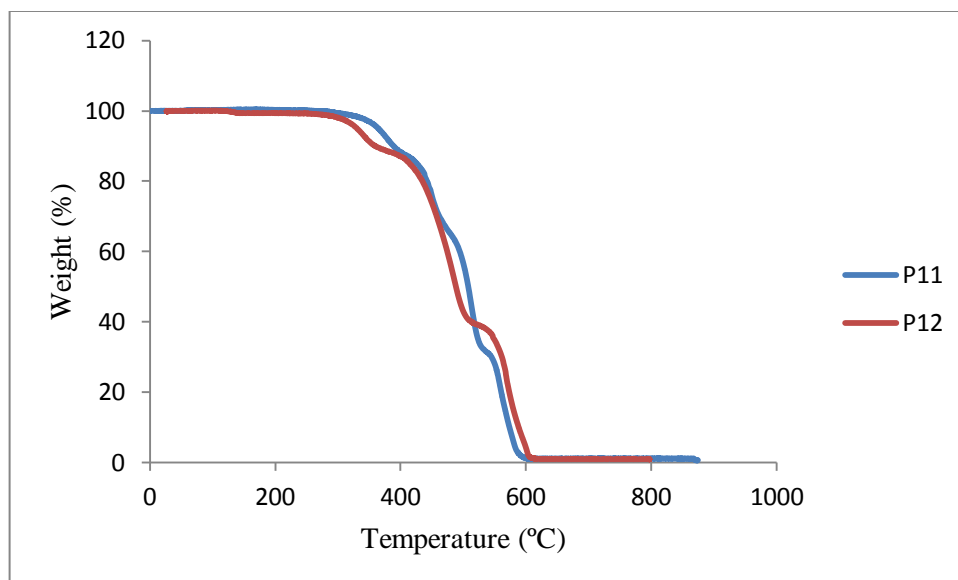
Figure 5-20. The TGA thermograms for **P11** and **P12**

5.3.11 Optical properties of P11 and P12

The UV-vis spectrum of **P11** was obtained in chloroform solution and thin films which were cast on quartz plates. **Figure 5-21** shows that **P11** has a λ_{max} located at 530 nm in chloroform solution. This λ_{max} is red-shifted to 605 nm in film. The red-shifted can be attributed to a more planar structure in solid state. **P11** shows an additional peak at a shorter wavelength. This occurs at 380 nm and 387 nm in solution and film states respectively. The absorption at the shorter wavelength can be attributed to a $\pi-\pi^*$ transition whereas the band at the longer wavelength corresponds to charge transfer between donor and acceptor units.
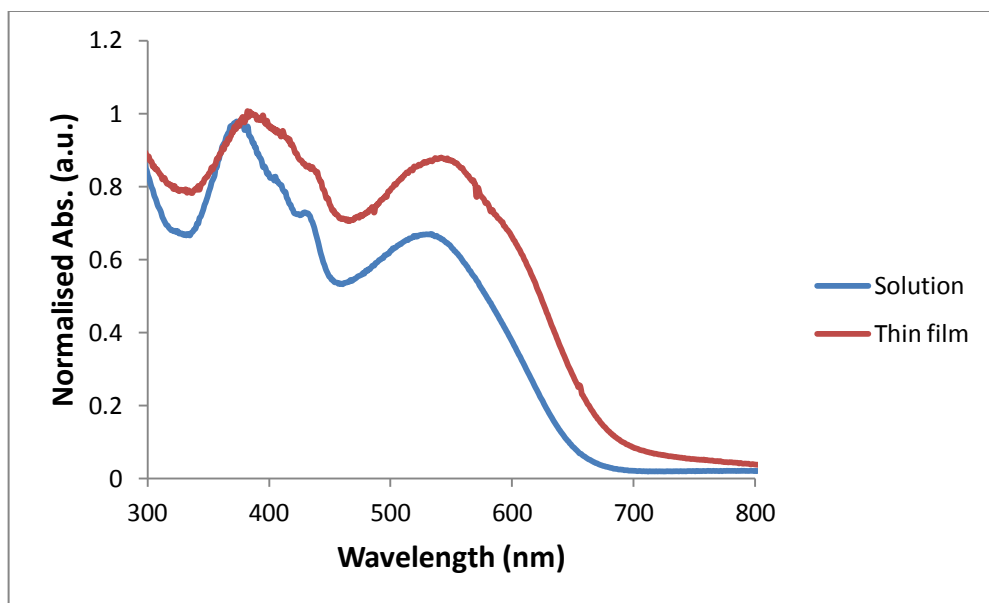
Figure 5-21. Normalised absorption spectra of **P11** as a thin film and as a solution in chloroform

Figure 5-22 shows that **P12** has a λ_{max} located at 528 nm in chloroform solution. This λ_{max} is red-shifted to 600 nm in film. The red-shift can be attributed to a more planar structure in solid state. **P12** shows additional peaks at shorter wavelength in chloroform solution. These occur between 380 - 430 nm. However, when cast into a film, these peaks merge to form one continuous, broad absorption band. It is speculated that the improved vibronic structure demonstrated in chloroform solution is a result of aggregates in solution. When cast into films, the amorphous nature of the polymer leads to a variety of local environments that result in poor vibrational overlap resulting in poor spectral resolution.[170]
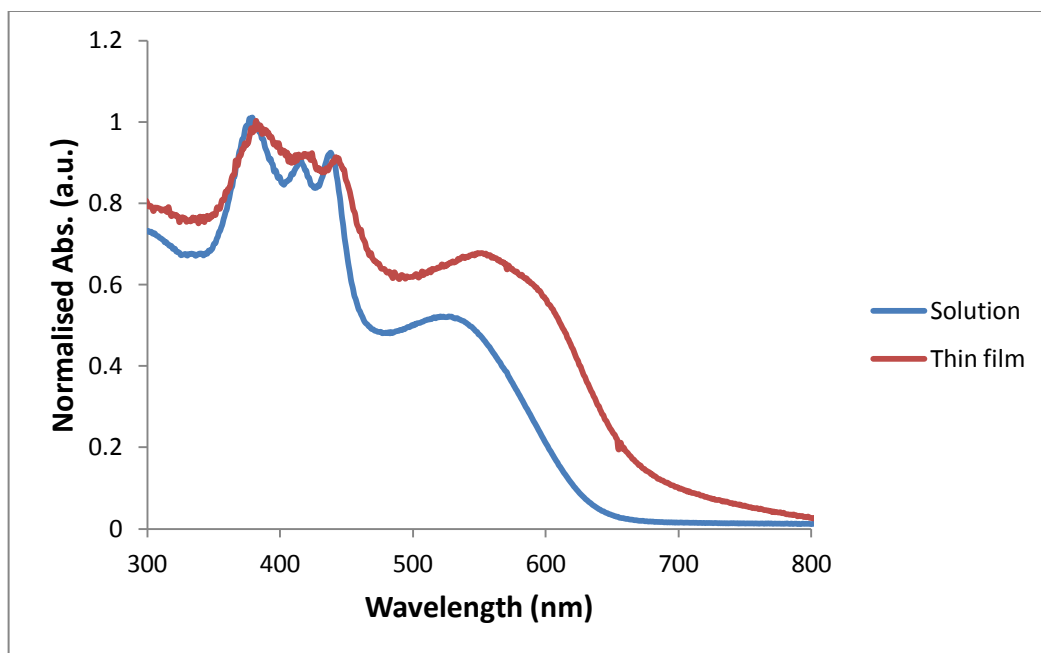
Figure 5-22. Normalised absorption spectra of **P12** as a thin film and as a solution in chloroform

The optical band gaps of **P11** and **P12** were estimated to be 1.84 and 1.85 eV respectively (**Table 5-9**). The results support earlier suggestions that D-A copolymers based on alternate benzothiadiazole pyrene-quinoxaline units are affected by the solubilising chain attached to the pyrene-quinoxaline donor.

Polymers	λ_{max} (nm) solution	λ_{max} (nm) film	λ_{onset} (nm) absorption	E_g Optical (eV)
P11	530	605	673	1.84
P12	528	600	670	1.85

Table 5-9. Summary of photophysical properties of **P11** and **P12**
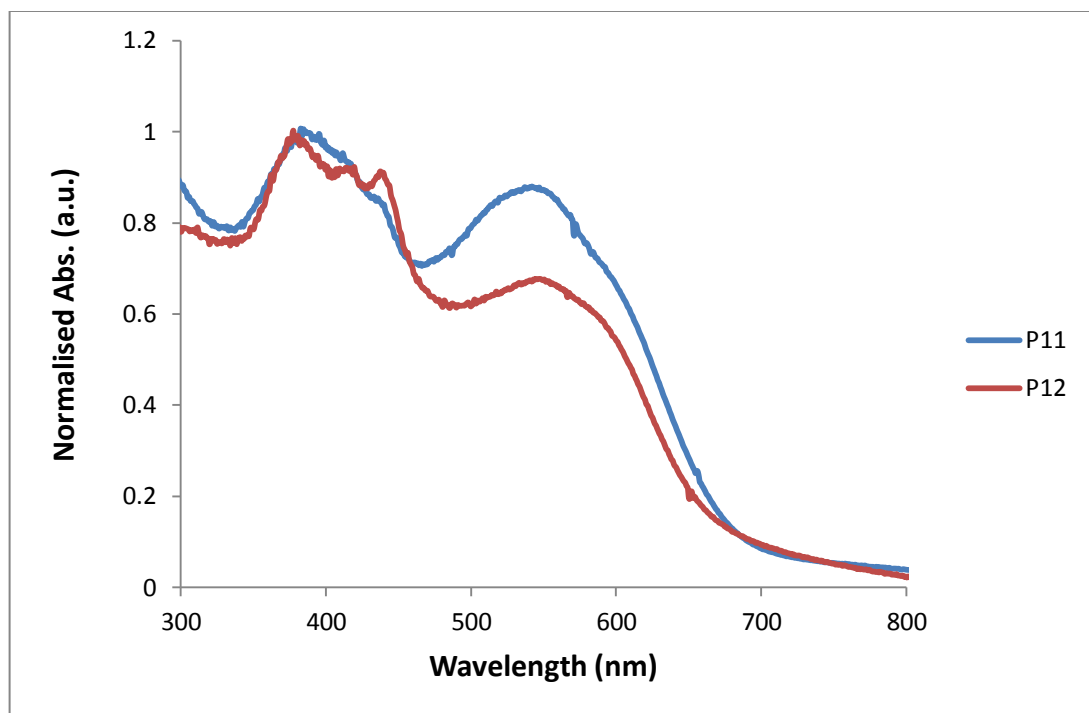
Figure 5-23. Normalised absorption spectra of **P11** and **P12** as thin films

P7, **P9** and **P11** are analogous polymers. However, **P9** and **P11** have solubilising octyloxy chains attached to the benzothiadiazole moiety. Consequently, **P7** displays enhanced ICT between the donor and acceptor unit resulting in a red-shifted λ_{max} and a lower optical band gap. The octyloxy groups present in **P9** and **P11** have electron-donating oxygen atoms, which push the electron density towards the nitrogen atom and decrease the accepting properties of the benzothiadiazole unit. This could decrease the ICT along the polymer chain, which could explain the wider optical band gaps of **P9** and **P11**. It is also interesting to note that, unlike **P9**, polymer **P11** has an additional thiophene spacer. This increases the distance between the alkyl chains on the donor and acceptor units, which reduces the steric hindrance and promotes backbone planarity. As a consequence, **P11** has a narrower optical band gap than **P9**, **Table 5-10**. The same phenomenon is observed when comparing **P8**, **P10** and **P12**, which supports the conclusions made (**Table 5-11**).

Polymers	λ_{max} (nm) solution	λ_{max} (nm) film	λ_{onset} (nm) absorption	E_g Optical (eV)
P7	540	620	708	1.75
P9	504	520	633	1.95
P11	530	605	673	1.84

Table 5-10 Summary of UV-vis spectra for **P7**, **P9** and **P11**

It is also worth mentioning the comparison between **P7**, **P9** and **P11** with previously prepared polymers **P1**, **P2** and **P3**. It can be clearly seen that **P7**, **P9** and **P11** have more red-shifted λ_{max} and narrower optical band gaps when compared with **P1**, **P2** and **P3**. The decreased optical band gaps of **P7**, **P9** and **P11** can be attributed to the electron density of the pyrene-quinoxaline monomer units. In **P1**, **P2** and **P3** the pyrene-quinoxaline system was used as an electron-accepting group. In **P7**, **P9** and **P11** it was used as a donating unit. The results show that the pyrene-quinoxaline unit functions better as a donor than an acceptor. It is speculated that this is a result of pyrenes fused ring system, which makes it electron rich. Theoretical calculations would help confirm this. It is recommended that these calculations are done in future work. The same phenomenon is observed when comparing **P8**, **P10** and **P12** with their analogous polymers **P4**, **P5** and **P6**, which supports the conclusions made.

Polymers	λ_{max} (nm) solution	λ_{max} (nm) film	λ_{onset} (nm) absorption	E_g Optical (eV)
P8	520	610	674	1.84
P10	500	517	614	2.01
P12	528	600	670	1.85

Table 5-11. Summary of UV-vis spectra for **P8**, **P10** and **P12**

P11 and **P12** can be also compared with the reported PCDT2OBT, which has two thiophene units on either side of the benzothiadiazole (**Scheme 5-11**).[136] The λ_{max} for **P11** is located at 605 nm, while the λ_{max} for **P12** is located at 600 nm. In contrast, the λ_{max} for PCDT2OBT is located at 548 nm. **P11** and **P12** have a more red-shifted λ_{max} relative to PCDT2OBT. Furthermore, the band gap of **P11** (1.84 eV) and **P12** (1.85 eV), are narrower

than PCDT2OBT (1.88 eV). It is thought that both of these results are a consequence of the laterally extended conjugated system present in the pyrene-quinoxaline donor unit.
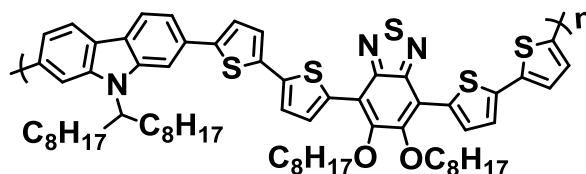
Scheme 5-11 The chemical structure of PCDT2OBT with additional thiophenes

5.3.12 Electrochemical properties of P11 and P12

Electrochemical studies of **P11** and **P12** were performed on drop-cast films in anhydrous acetonitrile as a solvent with tetrabutylammonium perchlorate as the electrolyte. In this investigation, the HOMO and LUMO were determined by CV, as can be seen in **Figure 5-17**, from which the electrochemical band gaps of the polymers can be obtained.
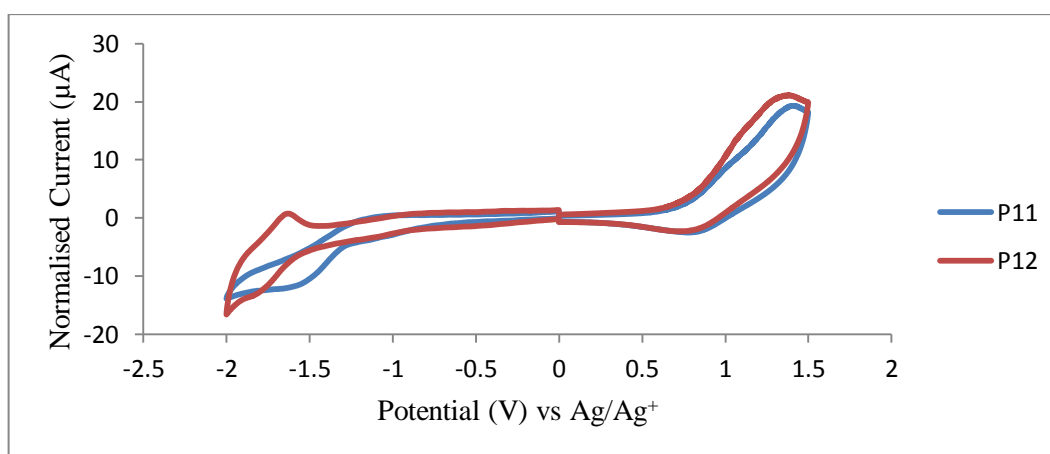
Figure 5-24 Normalised CV spectra of **P11** and **P12**

The onset potential of **P11** appeared at $E_{onset} = +0.76$ V for the oxidation and at $E_{onset} = -1.01$ V for the reduction. The HOMO and LUMO levels of **P11** can be calculated as -5.47 eV and -3.70 eV respectively. The differences between the HOMO and LUMO levels can be used to calculate the electrochemical band gap for **P11**, which is 1.77 eV. **P12** has an onset potential observed at $E_{onset} = +0.73$ V for the oxidation and at $E_{onset} = -1.16$ V for the

reduction. Therefore, the HOMO and LUMO levels of **P12** can be estimated as –5.44 eV and –3.55 eV respectively. The electrochemical band gap for **P12** is 1.89 eV.

Comparing **P11** and **P12**, it can be seen that **P11** has a narrower electrochemical band gap than **P12**, a result which is analogous to that deduced from comparing polymers **P7** to **P8** and **P9** to **P10** as explained earlier. A comparison between **P7**, **P9** and **P11** is important. The HOMO level of **P9** (-5.61 eV) is deeper than **P7** (-5.41 eV) and **P11** (-5.47 eV). Furthermore, the LUMO level of **P9** (-3.58 eV) is shallower than the LUMO levels of **P7** (-3.66 eV) and **P11**(-3.70 eV). The deeper HOMO level and shallower LUMO level of **P9** could be attributed to the large solubilising groups positioned on both the donor and the acceptor units of **P9.** It is possible that these dilute the chromophore density and reduce charge transfer between the donor and acceptor units. Additionally, **P9** and **P11** have octyloxy substituents on the benzothiadiazole moiety. This group pushes electron density onto the benzothiadiazole moiety and reduces its accepting properties. It is believed that this phenomenon is overcome by the incorporation of an additional thiophene unit (**P11**), which would explain why the HOMO and LUMO levels of **P7** and **P11** are comparable.[136] This would explain why the electrochemical band gaps of **P7** (1.75 eV) and **P11** (1.77 eV) are narrower than **P9** (2.03 eV). As expected, the same result is repeated in **P8**, **P10** and **P12**.

Comparing **P7**, **P9** and **P11** with previous prepared polymers **P1**, **P2** and **P3**, It can be clearly seen that the HOMO levels of **P1**, **P2** and **P3** (-5.69, -5.73 and -5.56) are deeper than **P7**, **P9** and **P11** (-5.41, -5.61 and -5.47 eV respectively) which indicates that the HOMO levels of **P7**, **P9** and **P11** are almost comparable to the ideal value of the HOMO level (-5.40 eV).[103] Consequently, when **P7**, **P9** and **P11** are blended with PC$_{70}$BM and fabricated into BHJ devices the polymers should exhibit improved exciton dissociation properties. The same trend is observed when comparing the analogous polymers **P8**, **P10** and **P12** with **P4**, **P5** and **P6**.

It is worth comparing **P11** and **P12** with analogous polymers in the literature, such as PCDT2OBT which has two thiophene units on both sides of the benzothiadiazole (**Scheme 5-11**). The HOMO levels of **P11** (–5.47 eV) and **P12** (-5.44 eV) are comparable. The

HOMO level of PCDT2OBT (–5.20 eV) is shallower than those of **P11** and **P12**. Furthermore, the electrochemical band gap of PCDT2OBT (1.91 eV) is higher than those for **P11** (1.77 eV) and **P12** (1.89 eV). It is thought that both of these results are a consequence of two properties: (1) the laterally extended conjugated system present in the pyrene-quinoxaline donor unit; and (2) the strong donor properties of carbazole and the small alkyl chain attached to it, which may increase the ICT along the backbone of the polymer.

5.4 Conclusion

In conclusion, polymers **P1** to **P6** were synthesised. The polymers were based on two-dimensional structures. However, they have large band gaps and poor spectral harvesting. Therefore, we synthesised a new series of polymers in which monomers (**8**) and (**15**) were used as electron donor units to give **P7**-**P12**. The series of acceptors used in this investigation includes benzothiadiazole derivatives. The monomer 4,7-bis(5-(trimethylstannyl)thiophen-2-yl)benzo[c][1,2,5] thiadiazole (**20**) was prepared successfully in three steps in order to prepare polymers **P7** and **P8**. In addition, the monomer 5,6-bis(octyloxy)-4,7-bis(5′-(trimethylstannyl)-[2,2′-bithiophen]-5-yl)benzo[c][1,2,5]

thiadiazole (**29**) was successfully synthesised in nine steps to give **P11** and **P12**. GPC analysis showed the molecular weight of the chloroform fractions of **P7** and **P8 to** have approximately 7 and 6 quinoxaline-*alt*-benzothiadaizole units per polymer chain respectively. The molecular weight of **P7** is 20200 Da and the number-average molecular weight is 10500 Da. This gives a PDI of 1.9. The Mw and Mn of **P8** were estimated to be 15520 and 7900 Da respectively. This yields a polydispersity of 1.6. **P9** has approximately 5 quinoxaline-*alt*-octyloxybenzothiadiazole repeat units per polymer chain (Mw = 13200 Da, Mn = 10100 Da, polydispersity = 1.3). For polymer **P10** there are roughly 7 repeat units of quinoxaline-*alt*-octyloxybenzothiadiazole per polymer chain. The Mw and Mn of **P10** were estimated to be 16300 and 13300 Da respectively. This yields a polydispersity of 1.2. Finally, polymers **P11** and **P12** have approximately 6 and 5 quinoxaline-*alt*-2,2'-bithiophene-benzothiadiazole units per polymer chain respectively. The Mn of **P11** and **P12** were estimated to be 11000 and 10000 Da respectively. The Mw of **P11** and **P12** were

estimated to be 16000 and 14000 Da respectively. From these values, the polydispersity of **P11** and **P12** were calculated to be 1.40.

The thermal stability of these polymers was studied using TGA. It is important that the polymers are stable under the conditions in which they will be applied in solar cell devices. These temperatures do generally not exceed 100 °C when used in solar cells. Polymers **P7** to **P12** showed good thermal stability with degradation temperatures exceeding 310 °C. All polymers revealed two onsets of degradation. The first onset occurred at temperature between 311 and 381 °C for (**P7- P12**). This was attributed to degradation of the alkyl chain. The second was located at a higher temperature and represented the main onset of degradation. This occurred between 540 and 608 °C for (**P7- P12**). The results from these studies indicate that these materials will not be affected by thermal degradation when used in solar cell devices.

UV-visible absorption spectroscopy (UV-vis) in chloroform solution showed the λ_{max} occurred at 540, 520, 504, 500, 530 and 528 nm for **P7**, **P8**, **P9**, **P10**, **P11** and **P12** respectively. When cast into films, these are red-shifted to 620, 610, 520, 517, 605 and 600 nm for **P7**, **P8**, **P9**, **P10**, **P11** and **P12** respectively. The blue-shifted absorption maxima present in solution are due to polymer-solvent interactions which disrupt the planarity of the polymer backbone and limit the conjugation length. The optical band gaps of **P7**, **P8**, **P9**, **P10**, **P11** and **P12** were estimated to be 1.83, 184, 1.95, 2.01, 1.84 and 1.85 eV respectively.

Cyclic voltammetry was used to calculate the HOMO and LUMO levels of the polymers. From the onset of oxidation it was found that the HOMO levels of **P7**, **P8**, **P9**, **P10**, **P11** and **P12** were located at -5.41, -5.45, -5.61, -5.59, -5.47 and -5.44 eV. From the onset of reductions it was found that the LUMO levels of **P7**, **P8**, **P9**, **P10**, **P11** and **P12** were located at -3.66, -3.61, -3.58, -3.50, -3.70 and -3.55 eV. From the HOMO and LUMO levels it is possible to calculate the electrochemical band gap. This was calculated to be 1.75, 1.84, 2.03, 2.09, 1.77 and 1.89 eV for **P7**, **P8**, **P9**, **P10**, **P11** and **P12** respectively.

From the results it can be seen that **P7**, **P8**, **P11** and **P12** demonstrate the best photophysical properties. **P9** and **P10** demonstrate wider optical and electrochemical band

gaps relative to other polymers synthesised within this chapter. **P9**, **P10**, **P11** and **P12** have solubilising octyloxy chains attached to the benzothiadiazole moiety. The octyloxy groups have electron-donating oxygen atoms, which push the electron density towards the nitrogen atom and decrease the accepting properties of the benzothiadiazole unit. This decreases charge transfer along the polymer chain for **P9** and **P10**. Thus, **P9** and **P10** have a blue shifted λ_{max} when compared to other polymers synthesised within this chapter. It is also possible that the additional octyloxy chains dilute the chromophore density decreasing intramolecular charge transfer along the polymer backbone. **P11** and **P12** have two thiophene units on either side of the benzothiadiazole in comparison to the one thiophene unit in **P9** and **P10**. This additional thiophene unit increases the distance between the alkyl chains on the donor and acceptor units, which reduces the steric hindrance and promotes backbone planarity. This allows **P11** and **P12** to demonstrate comparable properties to **P7** and **P8**.

6   Chapter 6: Conclusion and future work

6.1   Conclusion

The aim of this project was to prepare and characterise laterally extended conjugated polymers for solar cell application. The synthesis of laterally extended two-dimensional polymers based on pyrene-quinoxaline derivatives has been achieved. The pyrene molecule was successfully inserted between two quinoxaline groups to increase the planarity as well as the charge mobility of the system. The successful synthesis of pyrene-quinoxaline monomers was confirmed *via* ^{1}H NMR, ^{13}C NMR, MALDI-TOF mass spectrometry, elemental analysis and FT-IR spectroscopy.

All of the polymers **P1** to **P12** were synthesised using either Suzuki or Stille cross-coupling reactions. The polymers were fully characterised and examined using different techniques. The structure of these polymers was confirmed using ^{1}H NMR spectroscopy. The number-average and weight-average molecular weights were investigated using gel permeation chromatography (GPC). GPCs were carried out using 1,2,4-trichlorobenzene as the eluent. The optical and electronic properties of **P1** to **P12** were examined using UV-vis absorption spectroscopy and cyclic voltammetry respectively. Thermogravimetric analysis (TGA) was used to investigate the thermal stability of the polymers.

P1-P6 used the laterally extended pyrene-quinoxaline monomer as an acceptor unit. In **P1-P3** alkoxy chains were attached to the pyrene-quinoxaline unit in order to promote solubility and provide high molecular weight polymers. **P3** exhibited the lowest molecular weight (16300 Da) whilst **P1** demonstrated the highest molecular weight with a value of 67800 Da. The difference was due to the type of donor-monomer used. **P3** used a simple, unfunctionalised bithiophene spacer whereas **P1** used a carbazole-donor that was decorated with a branched C17 chain. The addition of a large solubilising chain in **P1** (and **P2**) allowed the synthesis of high molecular weight polymers. Despite **P3** having the lowest molecular weight it possessed the lowest optical band gap of 2.34 eV in film states. In contrast, **P1** and **P2** possessed optical band gaps of 2.43 and 2.49 eV respectively, in film states. This due to the fact that **P3** uses a stronger donor (thiophene) relative to **P1** (carbazole) and **P2** (fluorene). It is possible that this leads to improved intramolecular

charge transfer along the polymer backbone. Additionally, the thiophene donor in **P3** is not decorated with large, sterically demanding solubilising chains. This allows **P3** to exhibit a more planar structure in solid state, which accounts for its reduced optical band gaps. The electrochemical band gaps of **P1**, **P2** and **P3** were estimated to be 2.23, 2.33 and 2.14 eV respectively. All polymers display high molecular weights and good thermal stability. However, they have wide optical and electrochemical band gaps, which make them unsuitable for application in organic solar cells.

It was believed that the presence of an electron-donating oxygen atom pushed electron density onto the quinoxaline group, which decreased the accepting properties of pyrene-quinoxaline units. It was thought that replacing the alkoxy chain with an alkyl chain would negate the impact of the oxygen atom. This yielded **P4**, **P5** and **P6**, which showed an improvement in their optical and electrochemical properties. **P4**, **P5** and **P6** demonstrate molecular weights of 46000, 26500 and 11500 Da respectively. Again, the different molecular weights were a consequence of using different donor-units. **P4** used carbazole whilst **P5** and **P6** used fluorene and 2,2'-bithiophene respectively. Replacing the alkoxy substituents with alkyl chains had little impact on the molecular weight of the resulting polymers. The optical bands gaps of **P4**, **P5** and **P6** were estimated to be 2.34, 2.38 and 2.27 eV respectively. The λ_{max} of **P4-P6** are red-shifted by ~12 nm when compared to their analogous polymers **P1-P3**. Furthermore, the optical band gaps of **P4-P6** are lower when compared to their analogous polymers **P1-P3**. Clearly, changing the alkoxy groups for alkyl chains had a positive impact on the optical properties of the resulting polymers. However, the improvement is not significant and **P4-P6** still suffer from wide optical band gaps. This is not good as it is thought this will limit their spectral harvesting, which will limit their applications in organic solar cells. The electrochemical band gaps of **P4**, **P5** and **P6** were estimated to be 2.13, 2.23 and 2.11 eV respectively. The HOMO levels of **P4**, **P5** and **P6** were calculated to be -5.62, -5.72 and -5.58 eV. These are deeper than the ideal HOMO level of -5.40 eV.[103] The deep HOMO levels of **P4**, **P5** and **P6** will result in excellent oxidative stability. However, when **P4**, **P5** and **P6** are blended with $PC_{70}BM$ and put into organic solar cells the deep HOMO levels will result in poor exciton dissociation. This will have a negative impact on the efficiency of the solar device.

From the results, it can be concluded that **P1**, **P2** and **P3** were affected by the alkoxy chain. Oxygen pushed electron density towards the quinoxaline groups which decreased their accepting properties. Therefore, the decision was made to replace the alkoxy chain with an alkyl chain to neutralise the effect of the oxygen. This gave **P4**, **P5** and **P6**, which showed improvement in their optical and electrochemical properties. However, they still have large band gaps, which will limit the use of these polymers in organic solar cells. The work indicates that the pyrene-quinoxaline unit is not a good electron-accepting species and it is better suited to the role of a donor-unit. Therefore, further work was undertaken to investigate the suitability of pyrene-quinoxaline as a donor species.

The alkoxy functionalised pyrene-quinoxaline monomer was therefore polymerised with 4,7-bis(5-(trimethylstannyl)thiophen-2-yl)benzo [c][1,2,5] thiadiazole (**20**), 5,6-bis(octyloxy)-4,7-bis(5-(trimethylstannyl)thiophen-2-yl)benzo[c][1,2,5]thiadiazole (**30**) and 5,6-bis(octyloxy)-4,7-bis(5'-(trimethylstannyl)-[2,2'-bithiophen]-5-yl)benzo[c][1,2,5] thiadiazole (**29**) to give **P7, P9** and **P11** respectively. All polymers have degradation temperatures above 320 °C which makes them well within the temperature range for application in solar cell devices. Therefore all polymers have good thermal stability. **P7, P9** and **P11** gave molecular weights of 20500, 13200 and 16000 Da respectively. The uv-vis spectra **P7, P9** and **P11** display two absorption bands. The first band is due to a π-π* transition. The second absorption band, the λ_{max}, is due to intramolecular charge transfer along the polymer backbone. The λ_{max} of **P7, P9** and **P11** were located at 620, 520 and 605 nm. The optical band gaps of **P7, P9** and **P11** were estimated to be 1.75, 1.95 and 1.84 eV respectively. The blue-shifted λ_{max} and wider optical band gap displayed by **P9** is a consequence of the octyloxy groups attached to the benzothiadiazole unit, which disrupt the planarity of the polymer backbone and dilute the chromophore density. Additionally, these substituents are electron-donating and push electron density onto the benzothiadiazole acceptor making it more electron rich. These factors decrease the amount of intramolecular charge transfer along the polymer backbone resulting in a wider optical band gap. This decrease in intramolecular charge transfer is confirmed with cyclic voltammetry as the HOMO level of **P9** (-5.61 eV) is deeper than that of **P7** (-5.41 eV) and **P11** (-5.47 eV). Although **P11** does have octyloxy substituents, it also has two flanking thiophene units

compared to the one flanking thiophene unit present in **P9**. It is thought that the presence of the additional thiophene unit reduces steric hindrance resulting in a more planar polymer backbone which increases intramolecular charge transfer along the polymer backbone. As a result, the optical and electrochemical properties of **P11** are comparable to those of **P7**.

The alkyl functionalised pyrene-quinoxaline monomer was polymerised with 4,7-bis(5-(trimethylstannyl)thiophen-2-yl)benzo [c][1,2,5] thiadiazole (20), 5,6-bis(octyloxy)-4,7-bis(5-(trimethylstannyl)thiophen-2-yl)benzo[c][1,2,5]thiadiazole (**30**) and 5,6-bis(octyloxy)-4,7-bis(5'-(trimethylstannyl)-[2,2'-bithiophen]-5-yl)benzo[c][1,2,5]

thiadiazole (**29**) to give **P8**, **P10** and **P12** respectively. These are analogous polymers to **P7**, **P9** and **P11**. The molecular weights of **P8**, **P10** and **P12** were estimated to be 15500, 16300 and 14000 Da respectively. These molecular weights are comparable to **P7**, **P9** and **P11**. Any large differences are due to the inaccuracies and limitations of GPC. The optical band gaps of **P8**, **P10** and **P12** were estimated to be 1.84, 2.01 and 1.85 eV respectively. These are slightly wider when compared to the alkoxy-functionalised pyrene-quinoxaline polymers, **P7**, **P9** and **P11**. The difference is due to the solubilising chain attached to the pyrene-quinoxaline monomer. The alkyl chain in **P8**, **P10** and **P12** is less electron-donating than the alkoxy chain in **P7**, **P9** and **P11**. The oxygen atom in **P7**, **P9** and **P11** pushes electron density onto the pyrene-quinoxaline unit, which increases its electron density. This results in a stronger donor unit which increases the amount of intramolecular charge transfer along the polymer backbone resulting in **P7**, **P9** and **P11** demonstrating lower optical band gaps. The electrochemical band gaps of **P8**, **P10** and **P12** were estimated to be 1.84, 2.09 and 1.89 eV respectively.

The aim of this thesis was to use laterally extended pyrene-quinoxaline as both a donor unit and an acceptor unit in conjugated donor-acceptor polymers. **P1-P6** investigated the use of pyrene-quinoxaline as an acceptor. In comparison, **P7-P12** investigated the use of pyrene-quinoxaline as a donor unit. The smallest optical band gap in this series of polymers was **P6** (2.27 eV). The smallest electrochemical band gap in this series of polymers was **P6** (2.11 eV). Unfortunately, the band gap of **P6** is considered large and should limit the application of this material in organic solar cells. **P3** demonstrates the shallowest HOMO level with a value of -5.56 eV. This is considered too deep and will result in poor exciton dissociation

when fabricated into organic solar cells. Using these 'best' values it can be assumed the other polymers in this series are also unsuitable for application in organic solar cells. The optical band gaps of **P7-P12** are reduced when compared with **P1-P6**. The results suggest that polymers that use pyrene-quinoxaline as a donor are more promising than polymers that use pyrene-quinoxaline as an acceptor. It is speculated that this is a result of pyrene fused rings, which make it electron rich. Theoretical calculations would help confirm this. It is recommended that these calculations are done in future work. The lower optical and electrochemical band gaps of **P7-P12** should result in better spectral harvesting, which should increase the efficiency of the device.

Of all polymers synthesised, **P7** demonstrates the most promising photophysical properties. It demonstrates the lowest optical band gap (1.75 eV) and electrochemical band gap (1.75 eV). Furthermore, the HOMO level of this polymer (-5.41 eV) is located near the ideal HOMO value of -5.40 eV. This should result in improved exciton dissociation when fabricated into solar cells. However, further work is needed to confirm this and it is recommended that organic solar cells are made from polymers **P7-P12**.

6.2 Future work

It would be interesting to study the planarity of the pyrene-quinoxaline monomers and oligomers using single x-ray crystallography. This would determine whether the pyrene-quinoxaline monomer is planar. It is assumed that the poor photophysical properties of **P1-P6** are a result of the electron-rich pyrene-quinoxaline. It would be helpful to determine the electron density of pyrene-quinoxaline using density functional theory (DFT) calculations. It is strongly recommended that these calculations be conducted in the near-future.

It would be interesting to undertake differential scanning calorimetry and powder x-ray diffraction studies on all polymers synthesised in this thesis. This will give an analysis of the polymers' crystallinity in solid state. It is possible there is a link between the optical properties of the polymer and its crystallinity. Specifically, it is possible that a crystalline polymer will result in a planar backbone and a lower optical band gap. Additionally, a more crystalline polymer should result in improved charge transfer properties.

Organic solar cells should be fabricated from polymers **P7-P12** as these show the most promising photophysical properties of all polymers synthesised in this thesis. Optimisation of polymer:fullerene blend ratios, casting solvent, active layer thickness and thermal annealing are required to obtained organic solar cells with the highest efficiencies.

When optimum solar devices have been fabricated from **P7-P12** a thorough analysis on each cell should be undertaken. External quantum efficiency (EQE), hole mobility measurements and atomic force microscopy (AFM) measurements of the active layer should be obtained in order to understand the varied photovoltaic performance of devices fabricated from polymers **P7-P12**.

Polymers **P1-P6** have demonstrated that when pyrene-quinoxaline is used as an acceptor it produces polymers with poor photophysical properties. Work done within this thesis has suggested this is a consequence of pyrene-quinoxalines electron-rich nature. Further work could be conducted in order to make the pyrene-quinoxaline unit a more electron-withdrawing monomer. It is suggested that an imide functional group is added above the quinoxaline unit (**M36**). Previous literature has shown that the imide group could work as an electron-withdrawing species.[171] It is hoped that by incorporating this additional electron-withdrawing unit, electron density will be pulled away from the fused ring system making it electron deficient. Polymerising 2,12-bis(5-bromothiophen-2-yl)-7,17-dihexadecylpyrrolo[3,4-i]pyrrolo [3'',4'':6',7']quinoxalino[2',3':9,10]phenanthro[4,5-abc] phenazine-6,8,16,18(7H,17H)-tetraone (**M36**) with various donor-units would be successful in ascertaining whether the accepting properties of pyrene-quinoxaline units can be improved further (**Scheme 6-1**).
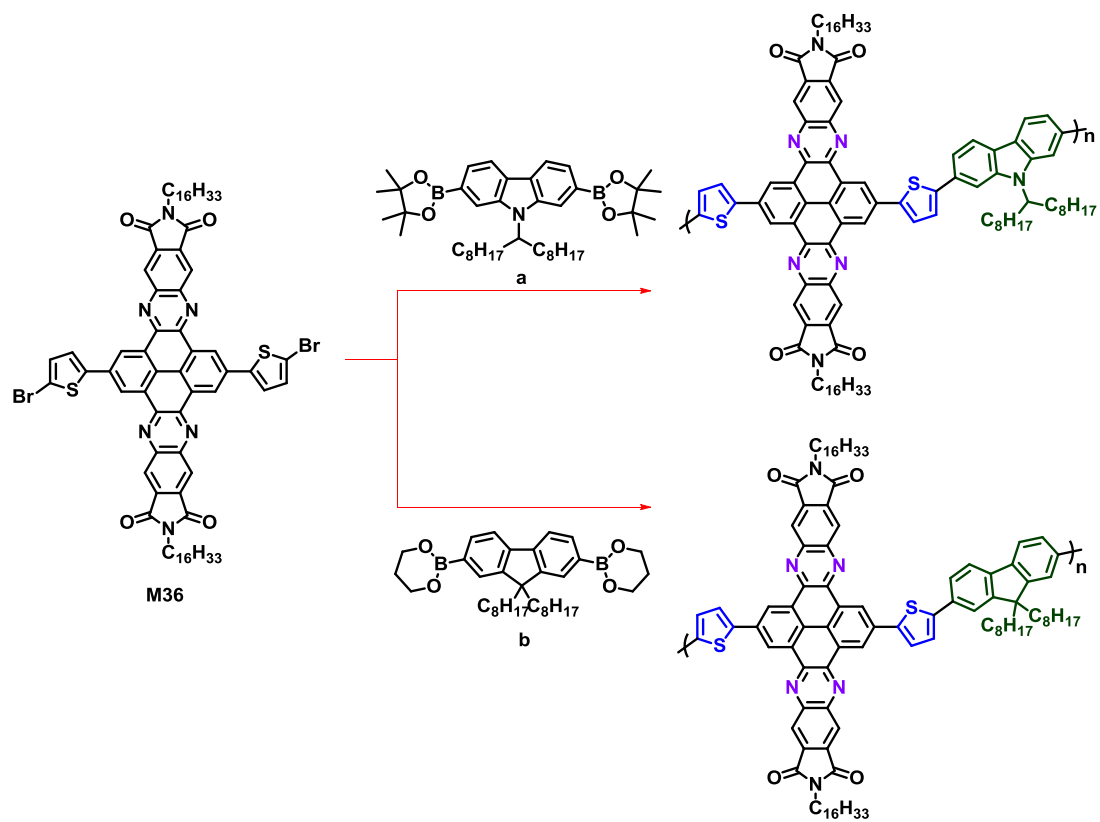
Scheme 6-1 The preparation scheme for new polymers

References

(1) Heeger, A. J. *Angewandte Chemie-International Edition* **2001**, *40*, 2591.
(2) Shirakawa, H.; Louis, E. J.; Macdiarmid, A. G.; Chiang, C. K.; Heeger, A. J. *J Chem Soc Chem Comm* **1977**, 578.
(3) Chiang, C.; Gau, S.; Fincher Jr, C.; Park, Y.; MacDiarmid, A.; Heeger, A. *Applied Physics Letters* **1978**, *33*, 18.
(4) Cheng, C. H.; Lonergan, M. C. *Journal of the American Chemical Society* **2004**, *126*, 10536.
(5) Glenis, S.; Tourillon, G.; Garnier, F. *Thin Solid Films* **1986**, *139*, 221.
(6) Heeger, A. J.; Kivelson, S.; Schrieffer, J. R.; Su, W. P. *Reviews of Modern Physics* **1988**, *60*, 781.
(7) Brédas, J.-L.; Norton, J. E.; Cornil, J.; Coropceanu, V. *Accounts of Chemical Research* **2009**, *42*, 1691.
(8) Heeger, A. J. *Chemical Society Reviews* **2010**, *39*, 2354.
(9) Hendriks, K. H.; Li, W.; Wienk, M. M.; Janssen, R. A. *Journal of the American Chemical Society* **2014**, *136*, 12130.
(10) Günes, S.; Neugebauer, H.; Sariciftci, N. S. *Chemical Reviews* **2007**, *107*, 1324.
(11) Morita, S.; Kiyomatsu, S.; Yin, X. H.; Zakhidov, A. A.; Noguchi, T.; Ohnishi, T.; Yoshino, K. *Journal of Applied Physics* **1993**, *74*, 2860.
(12) Hoppe, H.; Sariciftci, N. S. *Journal of Materials Research* **2004**, *19*, 1924.
(13) Morita, S.; Zakhidov, A. A.; Yoshino, K. *Solid State Communications* **1992**, *82*, 249.
(14) Bredas, J.; Themans, B.; Andre, J.; Chance, R.; Silbey, R. *Synthetic Metals* **1984**, *9*, 265.
(15) Gerard, M.; Chaubey, A.; Malhotra, B. *Biosensors and Bioelectronics* **2002**, *17*, 345.
(16) Toshima, N.; Hara, S. *Progress in Polymer Science* **1995**, *20*, 155.
(17) Sadki, S.; Schottland, P.; Brodie, N.; Sabouraud, G. *Chemical Society Reviews* **2000**, *29*, 283.
(18) Leclerc, M. *Journal of Polymer Science Part A: Polymer Chemistry* **2001**, *39*, 2867.
(19) Cheng, Y. J.; Luh, T. Y. *Journal of Organometallic Chemistry* **2004**, *689*, 4137.
(20) Grigore, L.; Petty, M. C. *Journal of Materials Science-Materials in Electronics* **2003**, *14*, 389.
(21) Babudri, F.; Colangiuli, D.; Farinola, G. M.; Naso, F. *European Journal of Organic Chemistry* **2002**, 2785.
(22) Miyaura, N.; Suzuki, A. *Chemical Reviews* **1995**, *95*, 2457.
(23) Miura, Y.; Oka, H.; Morita, M. *Macromolecules* **1998**, *31*, 2041.
(24) Stanforth, S. P. *Tetrahedron* **1998**, *54*, 263.
(25) Lee, A. S. Y.; Dai, W. C. *Tetrahedron* **1997**, *53*, 859.
(26) Genies, E.; Lapkowski, M. *Synthetic Metals* **1987**, *21*, 117.
(27) Cao, J.; Curtis, M. D. *Chemistry of Materials* **2003**, *15*, 4424.
(28) Winder, C.; Sariciftci, N. S. *Journal of Materials Chemistry* **2004**, *14*, 1077.
(29) Nechtschein, M.; Devreux, F.; Genoud, F.; Vieil, E.; Pernaut, J.; Genies, E. *Synthetic Metals* **1986**, *15*, 59.

(30)   Scott, J.; Bredas, J.; Yakushi, K.; Pfluger, P.; Street, G. *Synthetic Metals* **1984**, *9*, 165.

(31)   Samuelson, L. A.; Druy, M. A. *Macromolecules* **1986**, *19*, 824.

(32)   Roncali, J. *Chemical Reviews* **1992**, *92*, 711.

(33)   Coakley, K. M.; McGehee, M. D. *Chemistry of Materials* **2004**, *16*, 4533.

(34)   Liew, W. H.; Mirshekarloo, M. S.; Chen, S.; Yao, K.; Tay, F. E. H. *Scientific Reports* **2015**, *5*.

(35)   Wang, Y.; Jing, X. *Polymers for Advanced Technologies* **2005**, *16*, 344.

(36)   Sirringhaus, H.; Wilson, R.; Friend, R.; Inbasekaran, M.; Wu, W.; Woo, E.; Grell, M.; Bradley, D. *Applied Physics Letters* **2000**, *77*, 406.

(37)   Shah, A.; Torres, P.; Tscharner, R.; Wyrsch, N.; Keppner, H. *Science* **1999**, *285*, 692.

(38)   Mazzio, K. A.; Luscombe, C. K. *Chemical Society Reviews* **2015**, *44*, 78.

(39)   Lin, Y.; Wang, J.; Zhang, Z. G.; Bai, H.; Li, Y.; Zhu, D.; Zhan, X. *Advanced Materials* **2015**, *27*, 1170.

(40)   Weerasinghe, H. C.; Watkins, S. E.; Duffy, N.; Jones, D. J.; Scully, A. D. *Solar Energy Materials and Solar Cells* **2015**, *132*, 485.

(41)   Green, M. A.; Emery, K.; Hishikawa, Y.; Warta, W.; Dunlop, E. D. *Progress in Photovoltaics: Research and Applications* **2015**, *23*, 1.

(42)   Scharber, M. C.; Muhlbacher, D.; Koppe, M.; Denk, P.; Waldauf, C.; Heeger, A. J.; Brabec, C. J. *Advanced Materials* **2006**, *18*, 789.

(43)   Qi, B.; Wang, J. *Journal of Materials Chemistry* **2012**, *22*, 24315.

(44)   Clarke, T. M.; Durrant, J. R. *Chemical Reviews* **2010**, *110*, 6736.

(45)   Pivrikas, A.; Sariciftci, N.; Juška, G.; Österbacka, R. *Progress in Photovoltaics: Research and Applications* **2007**, *15*, 677.

(46)   Stoessel, M.; Wittmann, G.; Staudigel, J.; Steuber, F.; Blässing, J.; Roth, W.; Klausmann, H.; Rogler, W.; Simmerer, J.; Winnacker, A. *Journal of Applied Physics* **2000**, *87*, 4467.

(47)   Moses, D.; Dogariu, A.; Heeger, A. J. *Synthetic Metals* **2001**, *116*, 19.

(48)   Mihailetchi, V.; Koster, L.; Hummelen, J.; Blom, P. *Physical Review Letters* **2004**, *93*, 216601.

(49)   Blom, P. W.; Mihailetchi, V. D.; Koster, L. J. A.; Markov, D. E. *Advanced Materials* **2007**, *19*, 1551.

(50)   Kuik, M.; Wetzelaer, G. J. A.; Nicolai, H. T.; Craciun, N. I.; De Leeuw, D. M.; Blom, P. W. *Advanced Materials* **2014**, *26*, 512.

(51)   Yang, X.; Zhou, G.; Wong, W.-Y. *Journal of Materials Chemistry C* **2014**, *2*, 1760.

(52)   (a) Labuz, M.; Wal, A.; Wisz, G.; Kuzma, M. *Journal of Physics: Conference Series* **2006**, *30*, 325(b) Zaumseil, J.; Sirringhaus, H. *Chemical Reviews (Washington, DC, United States)* **2006**, ACS ASAP.

(53)   Tsumura, A.; Koezuka, H.; Ando, T. *Applied Physics Letters* **1986**, *49*, 1210.

(54)   Bendikov, M.; Houk, K. N.; Duong, H. M.; Starkey, K.; Carter, E. A.; Wudl, F. *Journal of the American Chemical Society* **2004**, *126*, 7416.

(55)   Garnier, F.; Peng, X.; Horowitz, G.; Fichou, D. *Molecular Engineering* **1991**, *1*, 131.

(56)   (a) Hohnholz, D.; MacDiarmid, A. G. *Synthetic Metals* **2001**, *121*, 1327(b) Okuzaki, H.; Ishihara, M.; Ashizawa, S. *Synthetic Metals* **2003**, *137*, 947(c) Horowitz, G.; Hajlaoui, R.; Bourguiga, R.; Hajlaoui, M. *Synthetic Metals* **1999**, *101*, 401.

(57)   Tang, C. W. *Applied Physics Letters* **1986**, *48*, 183.

(58)   Hummelen, J. C.; Knight, B. W.; Lepeq, F.; Wudl, F.; Yao, J.; Wilkins, C. L. *Journal of Organic Chemistry* **1995**, *60*, 532.

(59)   Sariciftci, N. S.; Smilowitz, L.; Heeger, A. J.; Wudl, F. *Science* **1992**, *258*, 1474.

(60)   Hiramoto, M.; Fujiwara, H.; Yokoyama, M. *Journal of Applied Physics* **1992**, *72*, 3781.

(61)   Yu, G.; Gao, J.; Hummelen, J. C.; Wudl, F.; Heeger, A. J. *Science* **1995**, *270*, 1789.

(62)   (a) Brabec, C. J.; Shaheen, S. E.; Winder, C.; Sariciftci, N. S.; Denk, P. *Applied Physics Letters* **2002**, *80*, 1288(b) Wienk, M. M.; Kroon, J. M.; Verhees, W. J. H.; Knol, J.; Hummelen, J. C.; van Hal, P. A.; Janssen, R. A. J. *Angewandte Chemie-International Edition* **2003**, *42*, 3371.

(63)   Padinger, F.; Rittberger, R. S.; Sariciftci, N. S. *Advanced Functional Materials* **2003**, *13*, 85.

(64)   Peet, J.; Kim, J. Y.; Coates, N. E.; Ma, W. L.; Moses, D.; Heeger, A. J.; Bazan, G. C. *Nature Materials* **2007**, *6*, 497.

(65)   Blouin, N.; Michaud, A.; Leclerc, M. *Advanced Materials* **2007**, *19*, 2295.

(66)   (a) Liang, Y. Y.; Wu, Y.; Feng, D. Q.; Tsai, S. T.; Son, H. J.; Li, G.; Yu, L. P. *Journal of the American Chemical Society* **2009**, *131*, 56(b) Chen, H. Y.; Hou, J. H.; Zhang, S. Q.; Liang, Y. Y.; Yang, G. W.; Yang, Y.; Yu, L. P.; Wu, Y.; Li, G. *Nature Photonics* **2009**, *3*, 649.

(67)   Price, S. C.; Stuart, A. C.; Yang, L. Q.; Zhou, H. X.; You, W. *Journal of the American Chemical Society* **2011**, *133*, 4625.

(68)   Zhou, H. X.; Yang, L. Q.; Stuart, A. C.; Price, S. C.; Liu, S. B.; You, W. *Angewandte Chemie-International Edition* **2011**, *50*, 2995.

(69)   Subbiah, J.; Purushothaman, B.; Chen, M.; Qin, T.; Gao, M.; Vak, D.; Scholes, F. H.; Chen, X.; Watkins, S. E.; Wilson, G. J. *Advanced Materials* **2015**, *27*, 702.

(70)   Chakravarthi, N.; Gunasekar, K.; Kim, C. S.; Kim, D.-H.; Song, M.; Park, Y. G.; Lee, J. Y.; Shin, Y.; Kang, I.-N.; Jin, S.-H. *Macromolecules* **2015**, *48*, 2454.

(71)   (a) Hou, J.; Tan, Z. a.; Yan, Y.; He, Y.; Yang, C.; Li, Y. *Journal of the American Chemical Society* **2006**, *128*, 4911(b) Zhang, S.; Ye, L.; Zhao, W.; Liu, D.; Yao, H.; Hou, J. *Macromolecules* **2014**, *47*, 4653.

(72)   Li, W.; Li, Q.; Liu, S.; Duan, C.; Ying, L.; Huang, F.; Cao, Y. *Science China Chemistry* **2015**, *58*, 257.

(73)   Lee, Y.; Nam, Y. M.; Jo, W. H. *Journal of Materials Chemistry* **2011**, *21*, 8583.

(74)   Li, Y.; Zou, Y. *Advanced Materials* **2008**, *20*, 2952.

(75)   Hou, J.; Huo, L.; He, C.; Yang, C.; Li, Y. *Macromolecules* **2006**, *39*, 594.

(76)   Figueira-Duarte, T. M.; Mullen, K. *Chemical Reviews* **2011**, *111*, 7260.

(77)   Kalyanasundaram, K.; Thomas, J. K. *Journal of the American Chemical Society* **1977**, *99*, 2039.

(78)   Rutkaite, R.; Swanson, L.; Li, Y.; Armes, S. P. *Polymer* **2008**, *49*, 1800.

(79)   Kawano, S. I.; Baumgarten, M.; Müllen, K.; Murer, P.; Schäfer, T.; Saleh, M.; WO Patent 2,010,006,852, **2010**.

(80)   Figueira-Duarte, T. M.; Müllen, K. *Chemical Reviews* **2011**, *111*, 7260.

(81) Wu, J. S.; Cheng, S. W.; Cheng, Y. J.; Hsu, C. S. *Chemical Society Reviews* **2015**, *44*, 1113.

(82) Iraqi, A.; Barker, G. W.; Pickup, D. F. *Reactive and Functional Polymers* **2006**, *66*, 195.

(83) Jaso, A.; Zarranz, B.; Aldana, I.; Monge, A. *Journal of Medicinal Chemistry* **2005**, *48*, 2019.

(84) Bailly, C.; Echepare, S.; Gago, F.; Waring, M. J. *Anti-Cancer Drug Design* **1999**, *14*, 291.

(85) Obrien, D.; Weaver, M.; Lidzey, D.; Bradley, D. *Applied Physics Letters* **1996**, *69*, 881.

(86) Justin Thomas, K.; Velusamy, M.; Lin, J. T.; Chuen, C.-H.; Tao, Y.-T. *Chemistry of Materials* **2005**, *17*, 1860.

(87) Yamamoto, T.; Lee, B. L.; Kokubo, H.; Kishida, H.; Hirota, K.; Wakabayashi, T.; Okamoto, H. *Macromolecular Rapid Communications* **2003**, *24*, 440.

(88) Wang, E.; Hou, L.; Wang, Z.; Hellström, S.; Zhang, F.; Inganäs, O.; Andersson, M. R. *Advanced Materials* **2010**, *22*, 5240.

(89) Xu, T.; Yu, L. *Materials Today* **2014**, *17*, 11.

(90) Lee, W.; Kim, G.-H.; Ko, S.-J.; Yum, S.; Hwang, S.; Cho, S.; Shin, Y.-H.; Kim, J. Y.; Woo, H. Y. *Macromolecules* **2014**, *47*, 1604.

(91) Liu, C.; Yi, C.; Wang, K.; Yang, Y.; Bhatta, R. S.; Tsige, M.; Xiao, S.; Gong, X. *ACS Applied Materials Interfaces* **2015**, *7*, 4928.

(92) Cui, C.; Wong, W.-Y.; Li, Y. *Energy & Environmental Science* **2014**, *7*, 2276.

(93) Huo, L.; Zhang, S.; Guo, X.; Xu, F.; Li, Y.; Hou, J. *Angewandte Chemie* **2011**, *123*, 9871.

(94) Ouyang, D.; Xiao, M.; Zhu, D.; Zhu, W.; Du, Z.; Wang, N.; Zhou, Y.; Bao, X.; Yang, R. *Polymer Chemistry* **2015**, *6*, 55.

(95) Ye, L.; Zhang, S.; Zhao, W.; Yao, H.; Hou, J. *Chemistry of Materials* **2014**, *26*, 3603.

(96) Lee, O. P.; Yiu, A. T.; Beaujuge, P. M.; Woo, C. H.; Holcombe, T. W.; Millstone, J. E.; Douglas, J. D.; Chen, M. S.; Fréchet, J. M. *Advanced Materials* **2011**, *23*, 5359.

(97) Colladet, K.; Fourier, S.; Cleij, T. J.; Lutsen, L.; Gelan, J.; Vanderzande, D.; Huong Nguyen, L.; Neugebauer, H.; Sariciftci, S.; Aguirre, A. *Macromolecules* **2007**, *40*, 65.

(98) Chen, H.-Y.; Hou, J.; Zhang, S.; Liang, Y.; Yang, G.; Yang, Y.; Yu, L.; Wu, Y.; Li, G. *Nature Photonics* **2009**, *3*, 649.

(99) Zhang, Z.-G.; Li, Y. *Science China Chemistry* **2015**, *58*, 192.

(100) Zhang, Z.-G.; Min, J.; Zhang, S.; Zhang, J.; Zhang, M.; Li, Y. *Chemical Communications* **2011**, *47*, 9474.

(101) Meager, I.; Ashraf, R. S.; Mollinger, S.; Schroeder, B. C.; Bronstein, H.; Beatrup, D.; Vezie, M. S.; Kirchartz, T.; Salleo, A.; Nelson, J. *Journal of the American Chemical Society* **2013**, *135*, 11537.

(102) Kirchartz, T.; Taretto, K.; Rau, U. *The Journal of Physical Chemistry C* **2009**, *113*, 17958.

(103) Zhou, H.; Yang, L.; You, W. *Macromolecules* **2012**, *45*, 607.

(104) Scharber, M. C.; Muhlbacher, D.; Koppe, M.; Denk, P.; Waldauf, C.; Heeger, A. J.; Brabec, C. J. *Advanced Materials* **2006**, *18*, 789.

(105) Vandewal, K.; Tvingstedt, K.; Gadisa, A.; Inganäs, O.; Manca, J. V. *Nature Materials* **2009**, *8*, 904.

(106) Yang, L.; Zhou, H.; You, W. *The Journal of Physical Chemistry C* **2010**, *114*, 16793.

(107) Thompson, B. C.; Frechet, J. M. *Angewandte Chemie International Edition* **2008**, *47*, 58.

(108) Kroon, R.; Lenes, M.; Hummelen, J. C.; Blom, P. W.; De Boer, B. *Polymer Reviews* **2008**, *48*, 531.

(109) Qi, B.; Wang, J. *Physical Chemistry Chemical Physics* **2013**, *15*, 8972.

(110) Cheng, Y. J.; Yang, S. H.; Hsu, C. S. *Chemical Reviews* **2009**, *109*, 5868.

(111) Shim, C.; Kim, M.; Ihn, S.-G.; Choi, Y. S.; Kim, Y.; Cho, K. *Chemical Communications* **2012**, *48*, 7206.

(112) Zhang, J.; Cai, W.; Huang, F.; Wang, E.; Zhong, C.; Liu, S.; Wang, M.; Duan, C.; Yang, T.; Cao, Y. *Macromolecules* **2011**, *44*, 894.

(113) Fan, Q.; Liu, Y.; Xiao, M.; Tan, H.; Wang, Y.; Su, W.; Yu, D.; Yang, R.; Zhu, W. *Organic Electronics* **2014**, *15*, 3375.

(114) Lee, S. K.; Lee, W.-H.; Cho, J. M.; Park, S. J.; Park, J.-U.; Shin, W. S.; Lee, J.-C.; Kang, I.-N.; Moon, S.-J. *Macromolecules* **2011**, *44*, 5994.

(115) Hu, J.; Zhang, D.; Harris, F. W. *Journal of Organic Chemistry* **2005**, *70*, 707.

(116) Kawano, S.-I.; Baumgarten, M.; Müllen, K.; Murer, P.; Schäfer, T.; Saleh, M.; Google Patents, 2014.

(117) Lee, S.; Gallegos, J. R.; Klein, J.; Curtis, M. D.; Kanicki, J. Proceedings of SPIE, **2003**; p 123.

(118) Zhang, D. M.; Tessier, C. A.; Youngs, W. J. *Chemistry of Materials* **1999**, *11*, 3050.

(119) Sessler, J. L.; Callaway, W. B.; Dudek, S. P.; Date, R. W.; Bruce, D. W. *Inorganic Chemistry* **2004**, *43*, 6650.

(120) Hui, J. K. H.; Yu, Z.; Mirfakhrai, T.; MacLachlan, M. J. *Chemistry-A European Journal* **2009**, *15*, 13456.

(121) Hu, J.; Zhang, D.; Jin, S.; Cheng, S. Z. D.; Harris, F. W. *Chemistry of Materials* **2004**, *16*, 4912.

(122) Helgesen, M.; Sørensen, T. J.; Manceau, M.; Krebs, F. C. *Polymer Chemistry* **2011**, *2*, 1355.

(123) Qin, R. P.; Li, W. W.; Li, C. H.; Du, C.; Veit, C.; Schleiermacher, H. F.; Andersson, M.; Bo, Z. S.; Liu, Z. P.; Inganas, O.; Wuerfel, U.; Zhang, F. L. *Journal of the American Chemical Society* **2009**, *131*, 14612.

(124) Morkved, E. H.; Neset, S. M.; Bjorlo, O.; Kjosen, H.; Hvistendahl, G.; Mo, F. *Acta Chemica Scandinavica* **1995**, *49*, 658.

(125) Woolley, D.; Pringle, A. *Journal of Biological Chemistry* **1952**, *194*, 729.

(126) Li, Z.; Lu, J.; Tse, S.-C.; Zhou, J.; Du, X.; Tao, Y.; Ding, J. *Journal of Materials Chemistry* **2011**, *21*, 3226.

(127) Tong, C.; Zhao, W.; Luo, J.; Mao, H.; Chen, W.; Chan, H. S. O.; Chi, C. *Organic Letters* **2012**, *14*, 494.

(128) Zoombelt, A. P.; Fonrodona, M.; Wienk, M. M.; Sieval, A. B.; Hummelen, J. C.; Janssen, R. A. *Organic Letters* **2009**, *11*, 903.

(129) Mancilha, F. S.; DaSilveira Neto, B. A.; Lopes, A. S.; Moreira, P. F.; Quina, F. H.; Gonçalves, R. S.; Dupont, J. *European Journal of Organic Chemistry* **2006**, *2006*, 4924.

(130) Palama, I.; Di Maria, F.; Viola, I.; Fabiano, E.; Gigli, G.; Bettini, C.; Barbarella, G. *Journal of the American Chemical Society* **2011**, *133*, 17777.

(131) Alesi, S.; Di Maria, F.; Melucci, M.; Macquarrie, D. J.; Luque, R.; Barbarella, G. *Green Chemistry* **2008**, *10*, 517.

(132) Fu, B.; Baltazar, J.; Hu, Z.; Chien, A.-T.; Kumar, S.; Henderson, C. L.; Collard, D. M.; Reichmanis, E. *Chemistry of Materials* **2012**, *24*, 4123.

(133) Helgesen, M.; Gevorgyan, S. A.; Krebs, F. C.; Janssen, R. A. *Chemistry of Materials* **2009**, *21*, 4669.

(134) Ding, P.; Chu, C. C.; Liu, B.; Peng, B.; Zou, Y.; He, Y.; Zhou, K.; Hsu, C. S. *Macromolecular Chemistry and Physics* **2010**, *211*, 2555.

(135) Parab, K.; Venkatasubbaiah, K.; Jäkle, F. *Journal of the American Chemical Society* **2006**, *128*, 12879.

(136) Yi, H.; Al-Faifi, S.; Iraqi, A.; Watters, D. C.; Kingsley, J.; Lidzey, D. G. *Journal of Materials Chemistry* **2011**, *21*, 13649.

(137) Li, Y. Y. *Advanced Materials* **2010**, *22*, 380.

(138) He, Y.; Li, Y. *Physical Chemistry Chemical Physics* **2011**, *13*, 1970.

(139) Lee, Y.; Russell, T. P.; Jo, W. H. *Organic Electronics* **2010**, *11*, 846.

(140) Müller, C.; Wang, E.; Andersson, L. M.; Tvingstedt, K.; Zhou, Y.; Andersson, M. R.; Inganäs, O. *Advanced Functional Materials* **2010**, *20*, 2124.

(141) Zeng, G.; Yu, W.-L.; Chua, S.-J.; Huang, W. *Macromolecules* **2002**, *35*, 6907.

(142) Abbel, R.; Schenning, A. P.; Meijer, E. *Journal of Polymer Science Part A: Polymer Chemistry* **2009**, *47*, 4215.

(143) Jo, J.; Chi, C.; Hoger, S.; Wegner, G.; Yoon, D. Y. *Chemistry* **2004**, *10*, 2681.

(144) Zhang, Z. G.; Wang, J. *Journal of Materials Chemistry* **2012**, *22*, 4178.

(145) Ku, J.; Lansac, Y.; Jang, Y. H. *The Journal of Physical Chemistry C* **2011**, *115*, 21508.

(146) Yue, W.; Zhao, Y.; Shao, S.; Tian, H.; Xie, Z.; Geng, Y.; Wang, F. *Journal of Materials Chemistry* **2009**, *19*, 2199.

(147) Min, J.; Zhang, Z.-G.; Zhang, S.; Zhang, M.; Zhang, J.; Li, Y. *Macromolecules* **2011**, *44*, 7632.

(148) Pryor, K. E.; Shipps, G. W.; Skyler, D. A.; Rebek, J. *Tetrahedron* **1998**, *54*, 4107.

(149) Wang, M.; Li, Y.; Xie, Z. Y.; Wang, L. X. *Science China Chemistry* **2011**, *54*, 656.

(150) Trippett, S. *Journal of the Chemical Society* **1962**, 2337.

(151) Park, J. K.; Jo, J.; Seo, J. H.; Moon, J. S.; Park, Y. D.; Lee, K.; Heeger, A. J.; Bazan, G. C. *Advanced Materials* **2011**, *23*, 2430.

(152) Perzon, E.; Wang, X.; Admassie, S.; Inganäs, O.; Andersson, M. R. *Polymer* **2006**, *47*, 4261.

(153) Gautrot, J. E.; Hodge, P. *Polymer* **2007**, *48*, 7065.

(154) Catellani, M.; Luzzati, S.; Lupsac, N.-O.; Mendichi, R.; Consonni, R.; Famulari, A.; Meille, S. V.; Giacalone, F.; Segura, J. L.; Martín, N. *Journal of Materials Chemistry* **2004**, *14*, 67.

(155) Gao, B.; Wang, M.; Cheng, Y.; Wang, L.; Jing, X.; Wang, F. *Journal of the American Chemical Society* **2008**, *130*, 8297.

(156) Li, S.; He, Z.; Yu, J.; Zhong, A.; Tang, R.; Wu, H.; Qin, J.; Li, Z. *Journal of Materials Chemistry* **2012**, *22*, 12523.

(157) Wang, M.; Li, Y.; Xie, Z.; Wang, L. *Science China Chemistry* **2011**, *54*, 656.

(158) Brabec, C. J.; Gowrisanker, S.; Halls, J. J.; Laird, D.; Jia, S.; Williams, S. P. *Advanced Materials* **2010**, *22*, 3839.

(159) Livi, F.; Zawacka, N. K.; Angmo, D.; Jørgensen, M.; Krebs, F. C.; Bundgaard, E. *Macromolecules* **2015**.

(160) Chinchilla, R.; Najera, C. *Chemical Society Reviews* **2011**, *40*, 5084.

(161) Dennler, G.; Scharber, M. C.; Brabec, C. J. *Advanced Materials* **2009**, *21*, 1323.

(162) Mayer, A. C.; Scully, S. R.; Hardin, B. E.; Rowell, M. W.; McGehee, M. D. *Materials Today* **2007**, *10*, 28.

(163) Li, W.; Du, C.; Li, F.; Zhou, Y.; Fahlman, M.; Bo, Z.; Zhang, F. *Chemistry of Materials* **2009**, *21*, 5327.

(164) Neto, B. A. D.; Lopes, A. S. A.; Ebeling, G.; Gonçalves, R. S.; Costa, V. E.; Quina, F. H.; Dupont, J. *Tetrahedron* **2005**, *61*, 10975.

(165) Miranda, M. S.; Matos, M. A. R.; Morais, V. M.; Liebman, J. F. *The Journal of Chemical Thermodynamics* **2012**, *50*, 30.

(166) Lee, J.; Jung, B. J.; Lee, S. K.; Lee, J. I.; Cho, H. J.; Shim, H. K. *Journal of Polymer Science Part A: Polymer Chemistry* **2005**, *43*, 1845.

(167) Tsuzuki, S.; Sato, N. *The Journal of Physical Chemistry B* **2013**, *117*, 6849.

(168) Zhou, H.; Yang, L.; Stuart, A. C.; Price, S. C.; Liu, S.; You, W. *Angewandte Chemie* **2011**, *123*, 3051.

(169) Slooff, L.; Veenstra, S.; Kroon, J.; Moet, D.; Sweelssen, J.; Koetse, M. *Applied Physics Letters* **2007**, *90*, 143506.

(170) Cartwright, L.; Iraqi, A.; Zhang, Y.; Wang, T.; Lidzey, D. G. *RSC Advances* **2015**, *5*, 46386.

(171) Li, C.; Wonneberger, H. *Advanced Materials* **2012**, *24*, 613.